Population Dynamics in the Late Glacial Refugium of Southwest France

C.M. Collins

PhD

November 2012

University of Sheffield

Acknowledgements

I would first of all like to thank my supervisor Andrew Chamberlain for advising me throughout my PhD. In addition many people aided me throughout the three years of my PhD. I am grateful to Pierre-Yves Demars for giving me access to his archaeological database. I am also grateful to Matt Grove for allowing me to utilize his method for working with radiocarbon dates and assisting me in doing so. As well as providing help with Matlab and LaTeX, James Hook also joined me in many interesting conversations. I would also like to thank the following people for general useful discussions and advice: Jean-Pierre Bocquet-Appel, Paul Mellars, Michael White, Caitlin Buck, Rob Dinnis, Jenni French, Tom O'Mahoney, Tom Booth and Isabelle Heyerdahl-King. Tom Hannan was kind enough to read a draft of my thesis and provide detailed feedback. I am also grateful to Bob Johnston for taking me on as a PhD student after the departure of Andrew from Sheffield in my final weeks of study.

The University of Sheffield provided me with a scholarship that supported this endeavour.

Thanks also go to my parents and friends for supporting me over the past years.

Abstract

In this thesis I explore population processes in the Upper Palaeolithic of Southwest France. Traditionally, prehistorians have regarded the region as a 'refugium' during the Last Glacial Maximum, into which populations contracted during periods of climatic deterioration in Europe. This refuge zone status has been used to explain the proliferation of artworks and diverse archaeological traces found in the region.

Innovation and demography have been theoretically linked for some time. High population densities are thought to lead to high innovation rates. Two possible mechanisms link these two variables. In the first scenario, high population densities cause intra-species competition, which leads to a pressure to innovate. The second scenario is a simple 'numbers game'; high population density increases the probability of innovation occurring and being transmitted from person to person.

In this thesis I explore population processes in the Upper Palaeolithic of Southwest France using the proxies of radiocarbon dates and intra-site lithic densities. I demonstrate that there are several peaks in population in the region, including ones coinciding with the onset and end of the LGM. Based on this data, I argue that the region served as a refugium during the LGM and also at several other points during the Upper Palaeolithic. I demonstrate that there is a negative relationship between climate and population in the region. This contrasts with the situation for modern hunter-gatherers. The cold conditions of the Pleistocene create a 'unique situation', where usual rules linking population and environment are interrupted as populations contract into refugia.

I also test the relationship between demography and innovation, using lithic assemblage diversity data as a proxy for innovation. I demonstrate that population and innovation are positively correlated. This relationship is unchanged in modern hunter-gatherers. I argue that the mechanism linking demography and innovation has changed from prehistory to the present day.

Environment, demography and innovation all interact in a complex manner during the Upper Palaeolithic and I shed some light on wider patterns of human behaviour through exploring these processes in this fascinating period.

Contents

List of Tables

List of Figures

Chapter 1

Aims and Objectives

§ 1.1 Aims and Objectives

This thesis is a study into population processes in French prehistory, with an emphasis on the Last Glacial Maximum and the impact that this extreme climatic phase had upon human demography. The Southwest region of France forms the study area, as it is the only area of France continuously occupied throughout the Upper Palaeolithic, and is one of the few regions in Europe not abandoned in the bracing conditions of the LGM. The Palaeolithic demography of this corner of France is ripe for study; if the region served as a refuge zone, as examined in this thesis, then populations surviving in the area will represent a precursor to modern European populations. The unique archaeology of the region, which includes a wealth of parietal art and technological developments, suggests that the area was a vibrant, cultural centre; incredible given the dearth of activity elsewhere. It is posited that technological developments in the refuge zone are the result of population pressure in the region, as other areas are abandoned due to inhospitable climatic conditions, leading to the wealth of innovations and cultural activities found in Southwest France. This thesis will examine the theoretical link between population pressure and human innovation; population processes will be explored using data from radiocarbon dates and intra-site lithic densities, whilst innovation will be measured

using diversity measures taken from lithic assemblages. The link between demography and innovation has not been explicitly tested using actual archaeological data before, although there have been many attempts to model it.

The original contributions to archaeology made in this thesis can be essentially divided into five broad groups:

- Methodological developments.
- Conclusions drawn regarding population processes in the study region and period.
- Conclusions drawn about the nature of human innovation in the study region and period.
- Conclusions drawn about wider human behaviour
- Finally, some additional interesting results came to light along the way. These include the nature of transitions between some technocomplexes and the level of sedentism observed in the Palaeolithic

Methodological developments made in this thesis are largely related to the use of radiocarbon dates as a proxy for human activity. I have outlined some possible developments to the 'dates as data' approach to prehistoric demography. An approach which includes Bayesian modelling as a part of the dates as data process is pioneered and tested. I have also rigorously tested the use of 'summed probability distributions' to obtain a demographic signal; finding that the approach produces demographic results. I hope that the methods developed here will be useful for future generations of prehistoric demographers.

There have been many previous attempts to quantify population dynamics in prehistory in general, and in the region specifically. However, in combining radiocarbon dates as a proxy for human activity with lithic data and site count data, the multi-proxy approach used here will yield more reliable results than can be achieved in single proxy studies.

There is an abundance of models linking demography and innovation. However, there is a distinct lack of studies that test this relationship with empirical data. This thesis addresses this lack of empirical examinations of this hypothesized relationship. I am able to confirm that this relationship exists and show that it impacted on human cultural evolution during a vulnerable stage in our prehistory, during the LGM.

The aims of this thesis are the following:

- To develop a methodology for exploring prehistoric demography.
- To explore population processes in French prehistory, focusing on the LGM.
- To test the LGM refugium model.
- To examine the link between population parameters and human innovation, using archaeological data.

These aims are achieved through the following objectives:

- Elaboration of the 'dates as data' methodology through

  - refinement of radiocarbon chronology for the region through the use of Bayesian modelling

  - testing of a 'chronometric hygiene' approach, placing differential value on radiocarbon dates according to perceived reliability

  - testing of the 'summed probability' approach to 'dates as data'

- Production of a 'dates as data' dataset following elaboration of the methodology
- Collation of intra-site lithic density data
- Collation of diversity measures on lithic artefacts from assemblages
- Production of simulated datasets for comparative purposes

- Analysis of all population-proxies to build a picture of population dynamics in the study region and period
- Analysis of diversity measures and population-proxies to answer questions about interrelatedness of these variables

In addition, through addressing the aims and objectives set out here, some further matters of interest came to light. These included the nature of transitions between technocomplexes and the degree of sedentism occurring in various phases of the Upper Palaeolithic. Questions were also raised about the nature of relations between France and Spain during the Upper Palaeolithic. Further areas of interest will come to light with any academic study and I hope that I have the opportunity to address the new issues raised in future. In particular, further study regarding the relationship between southern France and the Iberian peninsula during the LGM will be necessary before demographic events at this time can be truly understood.

Chapter 2

Theoretical Background

§ 2.1 Demography and Innovation

The interest of demography for the archaeologist lies in the hypothesis that population pressure can lead to cultural, technological and social innovation. Prior to the emergence of this theory, social and biological theorists spent many years working in the shadow of Thomas Malthus. The concept of a finite and arithmetically increasing resource reservoir that would provide an immovable ceiling to population growth (Malthus, 1798) constrained theories of social change. Malthus, writing in the late 18th Century, believed that when population overtook resources population would crash as a result of 'positive checks' invariably involving death. To avoid the misery of positive checks 'preventative checks' are evident in all societies, typically involving delayed marriage or social incentives against marriage. This idea is echoed in the champagne and caviar hypothesis of Douglas (1966); where men must concede a reduction in lifestyle with every child produced. Ultimately, Malthusian theory places resources as an immobile limit to population growth that cannot be surpassed; viewing any increase in population as resulting from a change in production. Following this, any population increase must follow an agricultural or technological revolution of some description and the reverse is not possible. The dominance of Malthusian theory created an obvious

intellectual barrier, preventing demographic factors from being posited as potential causes in archaeological explanation.

The emergence of Boserupian theory in the 1960s and its swift adoption by archaeologists, allowed theories of demographic growth to be incorporated into explanations of cultural change. Esther Boserup, a Danish economist and agronomist, writing in the 1960s, argued that agricultural methods and degree of intensification varied globally and according to population pressure (Boserup, 1965). At one extreme lies extensive agriculture, whereby one or two years' use would be followed by a fallow period of decades; at the other extreme, intensive agriculture sees land harvested twice yearly. Clearly, between these two extremes lies a host of intermediate agricultural practices, with a sliding scale that can be adjusted according to need. The importance of Boserup's argument to demography is that it implies changes in agricultural practice are the result of population pressure; human innovation allows the adoption of a practice which can support the necessary population level and incites movement along the sliding scale of agricultural intensification. The implication is that human populations are capable of intrinsic growth, in turn leading to technological innovation to support the new, augmented population densities. The very notion of intrinsic population increase prior to a technological advance, not following and resulting from such an advance, is opposed to the doctrine of Malthus.

The impact of Boserupian theory upon archaeological explanations has been immense and since the 1960s a proliferation of theories citing demography as an explanation for change in archaeology occurred. Notable among these theories is Mark Nathan Cohen's theory of high intrinsic Mesolithic population growth resulting in the Neolithic Revolution (Cohen, 1979). This theory is clearly closely related to the work of Boserup herself, concerning as it does agricultural developments necessitated by intrinsic population growth. Indeed, Cohen argued that the only advantage of agriculture over a hunter-gatherer lifestyle is that the former is able to support high population densities, a notion echoed in the anti-agriculturalist backlash of recent years eg (Diamond, 1997)

(Diamond, 1987).

Since Boserup, numerous authors have taken up the argument that intrinsic population growth can lead to human innovation. Kent Flannery (1969) linked dietary shifts in the Late Upper Palaeolithic to population growth, with the 'Broad Spectrum Revolution' , whereby small, nutritionally inferior game were adopted into the diet. Such game exploited in the Late Upper Palaeolithic included tortoises and lagomorphs (Stiner and Munro, 2002); animals one would assume to be last resorts, given the low nutritional value of these animals. As well as broadening of game animals, Weiss et al. (2009) demonstrated that the Broad Spectrum Revolution also included a shift to a broader selection of plant foods. The Broad Spectrum Revolution theory is clearly linked to the Boserupian world view, whereby population growth can be intrinsic and incite human adaptation. The shift from resources of high nutritional value, to less nutritious food stuffs, seen in the Late Upper Palaeolithic, closely parallels the shift in agricultural methods described by Boserup in her classic treatise on farming methods, albeit in regards to hunter-gatherer economy.

Smith (1972) linked technological developments in the Solutrean to demographic processes coinciding with this technocomplex, considering whether the shouldered points that characterize the Late Solutrean were an adaptation to population pressure in the Périgord region. At the opposite end of material culture from hunting technology, the proliferation of parietal art in the Upper Palaeolithic of southern Europe is equally linked to population pressure in the Late Upper Palaeolithic. The 'art as information' theory as championed by many authors tends to have a strong demographic component (Jochim, 1983) (Conkey, 1980) (Barton and G.A. Clark, 1994).

It must be noted that the demography of refugia is unique. A strong component of the Malthus/Boserup debate, as it is played out in archaeology, hinges upon whether *intrinsic natural population growth* is possible amongst hunter-gatherers. Hunter-gatherers are often regarded as living in equilibrium with their environments, maintaining population at a level well below carrying capacity. While this may be a slightly romanticized

and unrealistic view, it remains unlikely that hunter-gatherer population will dramatically increase without being accompanied by a change in lifestyle, be it of landuse patterns or of subsistence organization. Within a refuge zone, however, population increase is likely to occur as a result of migration, as people move from inhospitable zones into the refugia. Thus, given the constraints placed upon hunter-gatherer fertility and their tendencies to regulate population, it is likely that any dramatic population increase observed in an area identified as a refugium is likely to be the result of inward migration into the zone. There is a strong case for the Southwest France region serving as a refugium in the Upper Palaeolithic, on the basis of palaeoclimatic data. It therefore seems likely that any population growth occurring in the region at this time is the result of inward migration, rather than of intrinsic natural population growth. Equally, associations between environmental variables and population density amongst hunter-gatherers have been noted and are explored below. Generally, warmer temperatures are associated with greater population density. In the case of a climatic refugium that is experiencing inward migration from climate refugees, we will expect to see a negative correlation between temperature and population.

The examples invoked above are all instances where an increase in population density elicits a positive change in human cultural innovation. However, we can also find examples where the inverse has occurred. A notorious example is that of technological regression in prehistoric Tasmania. With the onset of the Holocene, Tasmania is separated from mainland Australia by rising sea levels. Archaeologists observe a steady loss of technology in Tasmania from the end of the Pleistocene to the arrival of Europeans in Australasia. Bone tools, cold weather clothing and fishing technology are all lost from the Pleistocene to the late Holocene on Tasmania, an astounding loss of culture that does not occur on the mainland (Henrich, 2004). The separation of Tasmania from the mainland severely disrupted networks of cultural transmission and substantially reduced the effective population of the island. Networks for cultural transmission were subsequently disrupted and the result was the loss of technology that archaeologists

observe.

Having examined several diverse case studies linking population dynamics to a variety of archaeological 'firsts', we come to examine the two possible mechanisms linking the variables of population pressure and innovation. The two mechanisms are ostensibly very similar and are almost indistinguishable in the archaeological traces that they leave. The first mechanism states that population pressure increases resource stress, and thus overall stress within a population, to a level where innovation is necessary for survival. The link between necessity and invention in this theory is apparent and we shall therefore refer to this argument throughout as the 'mother of invention' theory. This theory links demography and innovation through the medium of resource-stress in high-density populations. This theory is favoured by Richerson et al. (2009) who state that if per capita income is below a threshold value innovation will occur, above the threshold and the pressure to innovate is removed and deinnovation occurs. The alternative mechanism proposed states that population pressure merely increases the number of individuals within a group and, subsequently, the probability of an innovation occurring. This idea will be referred to throughout as the 'numbers game' theory. This theory is favoured by researchers such as Bocquet-Appel (Bocquet-Appel, 2010). Obviously, both processes are density-dependent but the former theory suggests that increases in population density elicit some sort of response in the human brain, leading to enhanced creativity. The latter theory, by contrast, does not imply any change in the individuals' capacity for invention, and instead it is simply a mathematical process.

In the 'mother of invention' process, population increase leads to greater intra-species competition. This elicits a change in individuals' behaviour, and the result is increased innovation rates. In the 'numbers game' process, no such change in human behaviour occurs. Instead, the larger local population simply leads to a greater frequency of 'new ideas'. Likewise, the larger population now contains a greater number of interpersonal networks, along which these innovations can be transmitted. The result of both processes is an increased innovation rate, but we see that in the former scenario there is a

change in individual behaviour, whereas in the latter case there is not.

There are certain obvious barriers to the study of innovation levels in the past. Innovation and individual 'creativity' are inextricably linked and difficult to separate. Creative flashes by individuals are essential for the process of innovation and consequently it is easy to imagine that changing innovation rates can be attributed to *individuals*, rather than the societies at large that prehistorians are predominantly interested in. However, innovation itself is also inherently a social and statistical activity. While an individual may be responsible for the actual moment of invention, that the novelty passes into society at large and is sustained in the society for long enough to leave archaeological traces is indicative of group dynamics. As such, the role of individual creativity does not create a barrier to the analysis of innovation in archaeology and we may hope to uncover evidence for changing innovation rates in prehistory. This is summarized nicely by Colin Renfrew:

An innovation involves not only the formulation of the novel, but also its adoption: innovation is a property not of the individual but of the community. For it is the community that adopts an innovation, even if it may be the genius who formulates it. Creativity is thus a social phenomenon. It involves persuasion, teaching and communication as much as ingenuity. (Renfrew, 1998, p192)

A further barrier to the study of innovation in prehistory is the importance of genuine 'novelty' in invention. Margaret Boden distinguishes between psychological and historical creativity, with the former being any incidence of ideogenesis that is new to the individual for whom the thought has occurred. Historical creativity, however, can only occur when an idea is new to both its progenitor and the world in general (Boden, 1998). Now, of course, if we were only interested in completely 'novel' technological innovations in prehistory we would have a very difficult task ahead of us. Tool forms wax and wane in popularity throughout the span of the Upper Palaeolithic, with many disappearing completely in phases, only to reappear at a later date. However, as we are treating innovation as a social and statistical phenomenon, it does not matter for our

purposes whether an innovation in prehistory has occurred for the very first time; we are instead concerned with the wider social phenomenon of creativity and transmission of ideas and the notion of human societies as composed of multitudes of 'vessels' for the containment of knowledge. To this extent, it is possible to analyse human innovation in prehistory and methods for doing so are discussed in Chapter Four. When the concepts of innovation and novelty are deconstructed it is apparent that they are social phenomena that can be reconstructed from archaeological data.

§ 2.2 Cultural Evolution and Transmission

Culture is broadly analogous to behaviour, but for humans also includes a strong material component; objects are both a part of culture and are used as teaching aids in its transmission. Culture is a broad beast, difficult to define and encompassing most aspects of human behaviour. In archaeology, and in prehistory in particular, we tend to regard all artefacts as 'cultural', while in the modern world technological items are seldom regarded as a part of culture. Archaeologists frequently use technology to identify ethnic groups in prehistory, eg (Bordes and de Sonneville-Bordes, 1970). I find this approach slightly absurd, given that I do not define myself by modern technology and I am therefore wary of approaches that 'identify' ethnic groups on the basis of lithics. However, I accept that technology is affected by cultural transmission and that it therefore can be used as a proxy for human innovation. Equally, though I reject that ethnic identity can be centred on technology, processes of cultural transmission could lead to the association of technology with particular groups.

Before delving into a discussion of cultural transmission and the role that this plays on the spread of innovation, we should probably be clear on what we mean by 'innovation'. As with any such term, definitions vary wildly. However, following Henrich (2010), we shall clearly separate 'inventions' from 'innovations', with the former defined as 'useful or adaptive novelties' and the latter the 'spread of those inventions through the

population' (Henrich, 2010). Thus the invention may be regarded as the new idea, while the innovation only exists once it has diffused somewhat through the population. In archaeological terms, it is very unlikely that we will see inventions, whereas innovations by definition will have spread through a population and are therefore much more likely to be visible archaeologically.

Following Cavalli-Sforza and Feldman (1981) biological evolution is frequently used as a model for cultural evolution. Indeed the principles of natural and sexual selection do appear to constrain cultural evolution. The novelty is the agent of cultural change and corresponds to the genetic mutation, which is the agent of biological evolution. Natural selection may operate on the cultural trait in exactly the same manner as it operates on a genetic mutation; traits which increase fitness are likely to survive, whereas deleterious traits are likely to disappear.

Sexual selection may also play a role in cultural evolution, an idea posited by Darwin and taken up by Miller (1999), with the latter author regarding all human cultural traits as a form of courtship ritual, explaining the dominance of young males in cultural spheres such as popular music and visual art.

Random processes analogous to genetic drift will also impact on cultural traits. Genetic drift is the change in allele frequency in a population due to random sampling and it is particularly potent in small populations. In just such a way, we can imagine that random sampling will impact on the frequency of a cultural trait in a population. Shennan and Edinborough (2007) developed a model illustrating the negative effects of cultural drift upon small populations, with deleterious traits retained to the detriment of the society, something which is less likely to occur in large populations. The model is outlined below.

Cultural transmission may occur vertically from parents to offspring, obliquely inter-generationally between the younger generation and members of the older generation other than their parents such as is seen in educational institutes, or horizontally within

generations (Cavalli-Sforza and Feldman, 1981). The innovation itself may arise during the transmission process, in much the same way as a genetic mutation arises during transcription and translation, as a result of copying error. However, cultural transmission and genetic transmission differ somewhat. Cultural transmission can occur through a number of routes, while only vertical transmission is possible in biological evolution. It is worth noting that humans are inherently conservative and tend towards mimicry rather than novelty (Larson, 2010). Any innovation is likely to occur as a by-product of faulty replication during the copying process.

Given the similarities between cultural and genetic evolution, it is unsurprising that many attempts have been made to reconstruct cultural evolutionary trees using the phylogenetic techniques commonly used in the biological sciences, whereby shared traits between 'species' are used to suggest common evolutionary pathways. Phylogenetic trees were constructed to analyse the evolution of basket weaving practices among Iranian tribes (Tehrani and Collard, 2002), indicating that vertical transmission is likely to have been the predominant mode of cultural transmission among the tribes studied, with very little ethnogenesis evident. O'Brien et al. (2001) also applied cladistics to the problem of relations between various Palaeoindian points. Some caution is urged though in the direct application of genetic methods to cultural evolution. While the similarities between the processes are undoubted, the difficulty in determining what constitutes a 'meme' when compared to the tangibility of genes means that identical approaches are not ideal. Likewise, cladistics may not be able to sufficiently control for the degree of horizontal transmission occurring (Tëmkin and Eldridge, 2007), something which is not a factor in genetic evolution, though the dominance of vertical and oblique transmission among hunter-gatherer societies has been demonstrated (Hewlett and Cavalli-Sforza, 1986) and suggests that horizontal transmission may have been of equally low importance in the Palaeolithic.

§ 2.3 Cultural Transmission and Population Densities

Several models exist linking population density to cultural transmission processes. One model, based on cultural drift and developed by Shennan (2000) demonstrated that in small populations random drift can lead to the transmission of maladaptive traits. By contrast large populations are relatively immune to such deleterious cultural drift.

An alternative model, developed by Henrich (2004) depicts a population of adults each possessing a level of skill, z as well as a probability of being selected as a teacher, f. The model is described in the following equation:

$$\Delta\bar{z} = -\alpha + \beta(\varepsilon + ln(N)) \tag{2.1}$$

where $\bar{z}$ is the average z score in the population, β is the dispersal parameter and α is the difference between the z score of the teacher and of the pupil, a value drawn from a Gumbel distribution. ε is the constant 0.577. The model suggests that the size of the population will affect the cumulative evolution within the group. The model was developed by Powell et al. (2010) into a simulation, whereby parent generations are replaced by a succession of offspring generations. The adapted model also took account of migration and the fact that the most skilled member of a group is not always the one to teach a skill.

Both the Shennan, and Henrich and Boyd/Powell *et al* models suggest that population size is positively correlated with cultural innovation, though in slightly different ways. In the Shennan model population size positively correlates with beneficial traits. By contrast the alternative models consider just the number of cultural traits in the population, regardless of whether they are beneficial.

Henrich (2010) demonstrated that the *inventiveness* of a population can be of little importance to the overall *innovation* level of the group, providing that the population is of sufficiently large size. In fact the 'percentage of adopters' in the population is

identical, regardless of the 'likelihood of invention' of the population when the number of associates reaches 16. This is shown in Figure 2.1, where λ corresponds to the effectiveness of cultural transmission and ϵ is the likelihood of individual invention.

Figure 2.1: Henrich's model of cultural transmission. From (Henrich, 2010)

This model is important for this study. We see that when the number of learning ties reaches 16, the percentage of adopters is the same, regardless of the level of inventiveness within the population. It demonstrates further that innovation is a social, rather than individual, phenomenon that leaves archaeological traces and can be studied in prehistory.

§ 2.4 Population, innovation and human evolution

We have already considered the relationship between population and innovation and potential causes of this relationship. This relationship has been invoked as a potential explanation in human evolution. In general, the Lower and Middle Palaeolithic are regarded as periods of immense stasis in material culture. Neanderthal technology in particular is traditionally regarded as exceptionally unchanging over vast amounts of time (Mellars, 1995), and this has been further demonstrated by Bocquet-Appel and Truffeau (2009). The apparent rapid adoption of Upper Palaeolithic culture after the

arrival of Anatomically Modern Humans in Europe is widely viewed as evidence for their lack of creativity, yet apparent ability to 'copy' others. Could it be the case that Neanderthals were in fact held back by low population numbers? Recent research by Mellars and French (2011) has suggested that Neanderthals were numerically disadvantaged in Europe in comparison to the newly arrived *Homo sapiens sapiens*. It could conceivably be the case that low population size amongst Neanderthals, rather than intellectual incapacity, could be the cause of apparent stasis in Middle Palaeolithic technology, though, of course, some variability and innovation is still evident amongst Neanderthals.

Likewise, the 'sapient paradox', has perplexed researchers for some time (Renfrew, 1996). This term describes the enormous hiatus that is observed between the origins of biologically modern *H. sapiens sapiens* and the advent of 'modern' behaviour and a variety of explanations have been advanced for this strange situation eg (Spikins, 2009). However, again, it may simply be the case that low population densities in Africa reduced innovation and the transmission of ideas. This notion has been put forward by Powell et al. (2009) and seems to provide a reasonable explanation, particularly having examined the strong relationship between population density and innovation in general.

§ 2.5 Hunter-gatherer demography

Prehistoric demographers frequently make recourse to hunter-gatherer populations as a data source. In many instances this is a logical step; modern and ancient hunter-gatherers share life-ways and are constrained by similar limits to population growth. Obvious barriers to population growth in hunter-gatherer societies include; the necessity to carry young infants, high infant mortality and low life-expectancy. However, the use of ethnography as a data source for prehistoric demography may also be decried on the basis that modern hunter-gatherer populations, marginalized by modern, industrialized

society, will bear little resemblance to their Palaeolithic forebears and as such cannot be used as a model (Graburn and Strong, 1973). Likewise, a pre-formed ethnographic model can lead to researchers seeking to fit archaeological data to the model, and leading to the perpetuation of current beliefs. Indeed, Wobst (1978) challenged the 'tyranny of the ethnographic record', arguing that it imposes modern hunter-gatherer lifestyles onto the archaeological record.

Hunter-gatherers as living, moving sources of data for prehistorians really came to the fore in the late 1960s, with the *Man the Hunter* conference organized by Richard Lee and Irven Devore (Lee and DeVore, 1968). Largely taking a romanticized view of hunter-gatherers, there is also a strong, environmentally-deterministic current flowing through the conference proceedings, with many attempts to find universal, predictive 'laws' to which all hunter-gatherers could be fitted, a popular approach at the time. Among such laws, the concept of 'magic numbers', around which hunter-gatherer group size fluctuates, was a strong theme at the time. This is exemplified by Birdsell's study into tribal size regulation amongst aboriginal Australians (Birdsell, 1953). Though later vindication for these 'magic numbers' came from the simulations of Wobst (1974), they still largely fell out of favour. However a later renaissance occurred through biological studies of cranial anatomy and primate group size, in the form of 'Dunbar's number', a biologically determined upper limit to the number of active relationships an individual may possess simultaneously. Dunbar (1989) observed a relationship between the size of the neocortex in primates and the sizes of group composition. Dunbar proposed that there is a limit to the number of individuals that an animal may hold relationships with, and that for humans this limit is set at around 150. 'Dunbar's number' as it has become known, may provide further support for the older sets of 'magic numbers' provided by Birdsell and Wobst, with the latter's size for the viable breeding unit set at around 175 individuals. Thus, studies of the relationship between physiology and central tendencies in human group size can potentially provide evolutionary explanations for hunter-gatherer social organization.

Ethnographic studies have highlighted the fluid nature of hunter-gatherer settlements, and this is something that any study of prehistoric demography should be aware of; the nature of mobile hunter-gatherer lifestyles, utilizing a range of sites simultaneously, will require separate demographic methods to studies of farming peoples. Ethnographic studies have highlighted the variety of functional sites utilized by hunting peoples. Binford (1980)'s comparison of the Nunamiut and San identified an organizational spectrum from *foragers* to *collectors* (Binford, 1980). The former can generally be characterized as 'moving people to resources', whilst the latter 'move resources to people'. Consequently foragers have simpler organization, with just two types of site, a *base* and a, more temporary *location*. In addition to these types of sites collectors, for whom storage is a central part of subsistence organization will also utilize *field camps* and *stations* for short-term missions, as well as *caches* for the storage of food. While these categories are by no means set in stone and a degree of overlap is likely to exist between both site types and hunter-gatherer types, they do highlight the fluid nature of prehistoric life and also raise questions about whether hunter-gatherers can truly be characterized as fully nomadic.

Having alerted ourselves to the importance of land-use patterns to hunter-gatherer archaeology, we are aware of two main challenges in identifying hunter-gatherer demographic patterns, brought to our attention through ethnographic evidence. First, ephemeral sites for specific purposes, such as the processing of carcasses may leave scant archaeological trace and be difficult to identify. Secondly, the occupation of multiple, functional sites simultaneously can lead to confusion for palaeodemographers. A change in land-use that involves a shift in the number of sites required concurrently could be erroneously interpreted as demographic decline. Equally, the fluctuating size of hunter-gatherer groups, varying yearly and prone to self-regulation, are likely to complicate the calculation of prehistoric population on the basis of material culture. However, it has been pointed-out (Straus, 1991b) that as the majority of Upper Palaeolithic sites are cave and shelter dwellings, unlikely to have been used for short-term functional

sites, the focus on *dwellings* in the archaeological record is likely to be a constant for the region and may ameliorate some of the difficulties of hunter-gatherer archaeology. Likewise, as this study is largely focused on sites for which multiple radiocarbon dates are available and for which Bayesian calibration was possible (see Chapter Four), the unintentional focus on sites used over long periods of time as living centres, rather than merely for specific tasks such as carcass processing, is likely to be even stronger. Thus, ironically, we are faced with a situation where one form of archaeological bias has removed another.

From an environmentally deterministic, and therefore decidedly 1960s, anthropological approach, universal laws can be formulated linking demographic and environmental factors. The approach is seen by some as an outdated methodology, eg (Judkins et al., 2008) but strong correlations *are* visible linking climate and population. The graphs below display the relationship between *effective temperature* (ET) and population density for 340 modern hunter-gatherer populations, in data taken from Binford (2001)'s tome. The variable is given by:

$$ET = \frac{(18 \times MWM) - (10 \times MCM)}{(MWM - MCM + 18)}$$

Where MWM is the mean temperature of the warmest month and MCM is the mean temperature of the coldest month. ET is more informative as a variable than simply using average temperatures.

To test the strength of the correlation between ET and population density amongst modern hunter-gatherers the Pearson correlation coefficient was calculated in PASW statistics, using data obtained from Binford (2001), which is included in the appendix. A weak positive correlation was observed between these two variables for the entire dataset.

However, it appears that two separate linear trends are visible in the dataset. When the data is separated into two groups, one with ETs greater than 15, and another with ETs less than 15, this positive correlation becomes very strong ($0.356, p < 0.01$ for the first

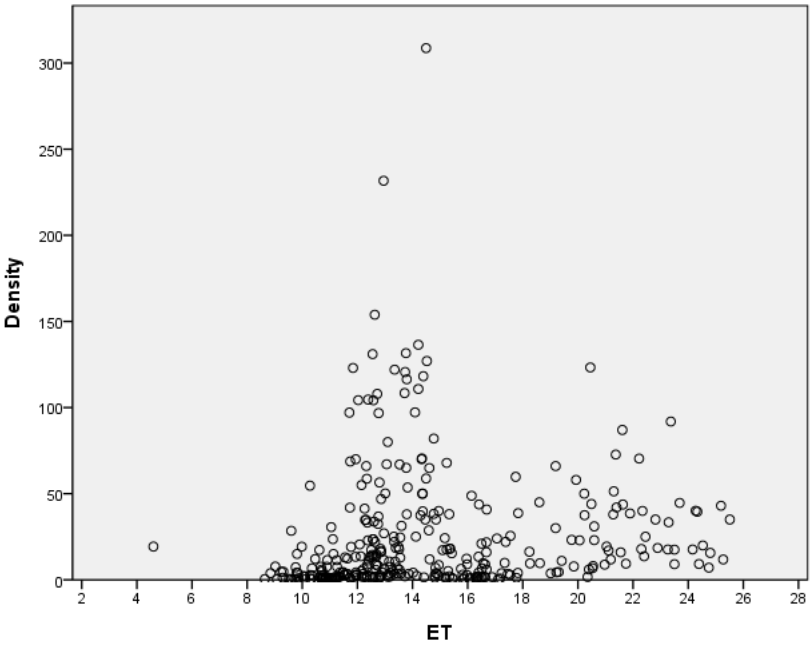

Figure 2.2: ET and population density amongst modern hunter-gatherers. An apparent 'break' at ET 15 is visible

Correlations

		Density	ET
Density	Pearson Correlation	1	.109*
	Sig. (2-tailed)		.045
	N	338	338
ET	Pearson Correlation	.109*	1
	Sig. (2-tailed)	.045	
	N	338	339

*. Correlation is significant at the 0.05 level (2-tailed).

Table 2.1: Pearson correlation coefficient for ET and population density

group and $0.357, p < 0.01$ for the second group). In short, there is a positive correlation between ET and population density, up to ET values of 15, where there is then a break in this relationship and another positive correlation, for values above 15, begins. These two groups broadly agrees with the division between 'warm hunter-gatherers' and 'cold hunter-gatherers' that is recognized in the anthropological literature, though the break between the two groups is usually placed at ET 13 eg (Marlowe, 2005).

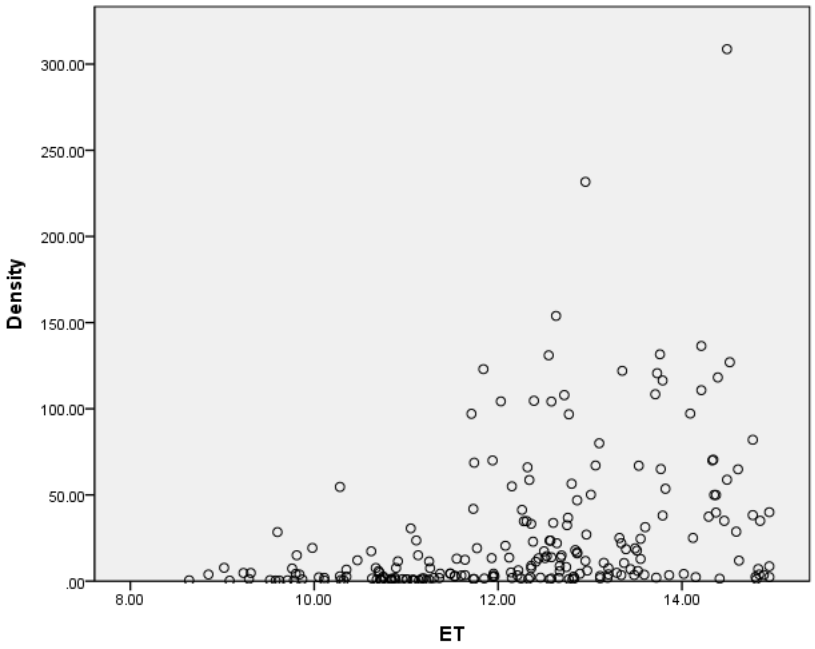

Figure 2.3: ET and population density amongst modern hunter-gatherers up to ET15

Correlations

		Density	ET
Density	Pearson Correlation	1	.356**
	Sig. (2-tailed)		.000
	N	220	220
ET	Pearson Correlation	.356**	1
	Sig. (2-tailed)	.000	
	N	220	220

**. Correlation is significant at the 0.01 level (2-tailed).

Table 2.2: Pearson correlation coefficient for ET and population density, up to ET 15

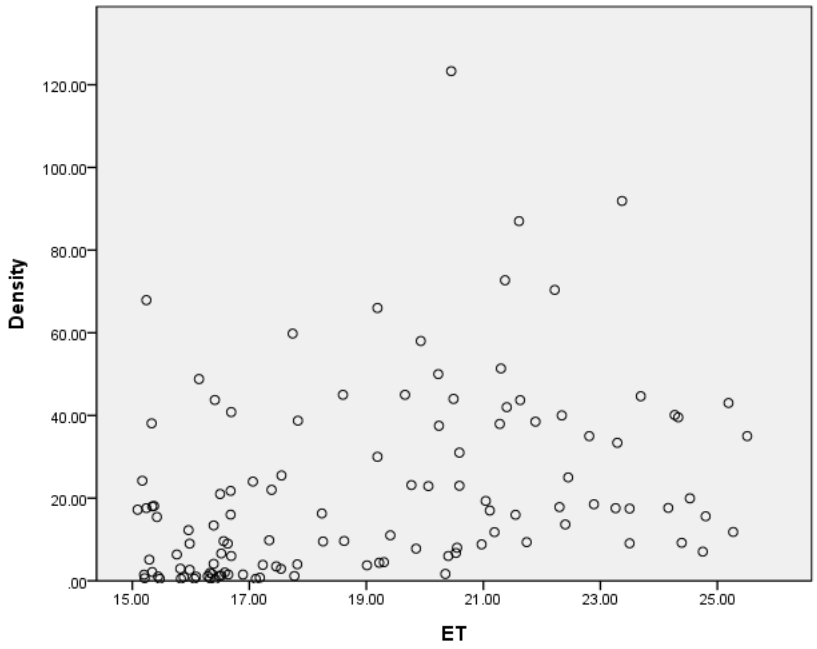

Figure 2.4: ET and population density amongst modern hunter-gatherers over ET 15

Correlations

		Density	ET
Density	Pearson Correlation	1	.356**
	Sig. (2-tailed)		.000
	N	220	220
ET	Pearson Correlation	.356**	1
	Sig. (2-tailed)	.000	
	N	220	220

**. Correlation is significant at the 0.01 level (2-tailed).

Table 2.3: Pearson correlation coefficient for ET and population density, over ET 15

Thus, the influence of the environment on demographic variables cannot be precluded simply because it is an unfashionable approach. Climatic variables and population are interlinked, at least in the modern world, and are likely to have been in the Palaeolithic also. This is not to say that population is entirely environmentally prescribed; social behaviour can still impact on demographic processes, even in a system where the environment and population dynamics are strongly linked. Likewise, one must always expect an exception and we can anticipate anomalous situations where normal rules linking population and effective temperature in a positive relationship do not apply. As will be seen in Chapter Three, the Upper Palaeolithic of France is just such a unique situation, where the 'normal' positive relationship between climate and population density is interrupted due to shrinking of the habitable world and migration into *refuge zones*.

§ 2.6 Previous Studies into Archaeological Demography

At the simplest level, site counts alone are indicative of population size, and regional site censuses provide indicators of relative changes in population pressure. This approach has been utilized in a number of regions and time periods (Sbonius, 1999). However, it is important to be aware that archaeological information is lost over time, and any perception of prolonged population growth from the distant past to the present may in fact be simply due to taphonomic processes (Surovell et al., 2009). Some attempts have been made to model these processes and it may be the case that calibration of site counts may be necessary, rather than merely accepting the apparent evidence of simple censuses. However, site counts are certainly a starting point and like the evidence of ethnography cannot be ignored.

2.6.1 Ethnography

The ethnographic record itself has been used to 'back-project' population densities into the past. A key example of this approach is David's study of the Noaillian phase of the Gravettian in Southwest France (David, 1973). Suitable ethnographic analogues were selected on the basis of appropriate environmental variables and the subsistence regimes employed by the modern populations. The environmentally deterministic approach to using ethnographic data is a useful approach, if one accepts the validity of overarching 'rules' governing human ecology, as previously discussed. However we are acutely aware that there is no absolute analogue for the environment of Pleistocene France; the sun would have stood higher in the sky than it does in the present day Arctic and subarctic latitudes, resulting in a longer growing season. The use of the variable *Effective Temperature* (Binford, 2001), see previous section, allow as appropriate analogues as possible to be selected, as this variable is computed through consideration of mean temperatures in both winter and summer.

In our study here, where we are dealing with a potentially unique situation due to

the Last Glacial Maximum, it is unlikely that the approach utilized by David will be helpful. Refugia conditions are likely to lead to populations exceeding the group sizes observed in the modern world. Likewise, the approach is not helpful for estimating population change over long periods of time, as population density data obtained from modern reindeer-hunting groups would lead to an image of static, unchanging population densities over time. Of course an understanding of hunter-gatherer group dynamics and adaptations can still be helpful for developing demographic models for prehistory.

Upper Palaeolithic European population sizes were estimated by (Bocquet-Appel et al., 2005) through utilizing hunter-gatherer density data, principally from North American hunter-gatherer groups, in conjunction with archaeological data. These demographic densities were then projected onto estimates of hunter-gatherer ranges in Europe, obtained through climatic simulations. The estimated population sizes for various phases of the Upper Palaeolithic are shown in Table 2.4. Their estimates are interesting, given the increase in population seen during the LGM, a phase when one would expect overall population decline in Europe. The estimated *increase* in the European metapopulation size, in conjunction with the predicted reduction in size of human habitat during the LGM would lead to very high population density within the remaining occupied territories. The suggestion clearly is that people were migrating into the southern refuges, rather than simply dying out in more northern latitudes.

Table 2.4: Population estimates from Bocquet-Appel et al. (2005)

Phase	Average Population Estimate
Aurignacian	4424
Gravettian	4776
Glacial Maximum	5885
Late Glacial	28,736

The same approach, of combining archaeological and ethnographic data was utilized by (Demars, 1996), with specific reference to the Southwest France region during the Upper Palaeolithic and Mesolithic. This study will be fully outlined in Chapter Three,

as the results are of central importance to this study. However, a key finding of this research was the contraction of French populations upon the Dordogne region during the Solutrean and subsequent and rapid expansion across the whole of the nation in the Magdalenian.

2.6.2 Dates as Data

The 'dates as data' approach to modelling population growth and expansion is based on the same principle as the site-count method; material remains are assumed to be correlated with human activity. This particular approach, however, exploits the abundance of radiometric data; data which contains temporal, spatial and frequency dimensions. Thus population expansion can be modelled geographically with ease. Potential sources of bias, as introduced above, include the loss of material over time, although it has been noted that charcoal, one of the most dated materials, is of a durable constitution (Rick, 1987). Further biases through uneven archaeological interest may also exist. Funding issues, for instance, may mean that areas abundant in archaeology lack radiocarbon dates. Likewise, where multiple dates are provided for site phases, further biases can arise. There have been many claims that the region of Southwest France has been unduly studied and that subsequently a disproportionate mass of data exists for this region (Rigaud and Simek, 1987). Whilst rejected by many authors (largely Southwest France specialists), the issue becomes moot when dealing with radiocarbon dates, as the technique did not exist prior to 1949 and therefore any Antiquarian influence will be eliminated. In latter years, archaeological pressure in France has been exerted far more evenly (Bocquet-Appel and Demars, 2000) than in the days of the 'Gentleman Archaeologist'.

The 'dates as data' approach was first used by Rick (Rick, 1987) in a study of Peruvian preceramic population. It has been applied to the Palaeolithic of Europe on several occasions. Bocquet-Appel and Demars Bocquet-Appel and Demars (2000) used the distribution of dates associated with *Homo neanderthalensis* and *Homo sapiens* to

model the interaction of the two species at the Middle/Upper Palaeolithic transition. The Stage Three Project, which modelled European climate, environment and demographics, also utilized the radiocarbon database as the primary source of demographic evidence (van Andel et al., 2003).

These are just a few examples of the the use of the radiocarbon record for modelling archaeological demography. In short, the ^{14}C record provides an extensive and readily accessible source of information on the extent of human presence throughout history and it will be employed in this project.

The actual application of the 'dates as data' method will be outlined further in the methods chapter, as it is heavily used in this thesis. I attempt to further develop the method and consequently it will be referred to throughout this document.

Many radiocarbon calibration programmes facilitate the production of 'summed probability distributions'. This function is generally provided to allow the summing of multiple dates from the same phases. However, some researchers have applied this method to observing demographic processes in prehistory. Shennan and Edinborough (Shennan and Edinborough, 2007) collated ^{14}C dates for Central and Northern Europe from the Mesolithic to the late Neolithic, creating summed probability distribution graphs for the entire period and utilizing this as the main source of demographic information. Likewise, Tallavaara *et al* (Tallavaara et al., 2010) applied this approach to Fennoscandia, and Buchanan *et al* (Buchanan et al., 2008) to Palaeoindian demography. Whilst calibration software readily facilitates this approach, and radiocarbon dates can be regarded as good proxies for past human activity, there are some statistical issues with the use of summed probability distributions derived from radiocarbon dates. Averaging multiple dates from single phases at a site is statistically valid, as the determinations theoretically originate from the same 'event'. However, the averaging of multiple dates from multiple phases, at multiple sites is more problematic, as determinations are from distinct events. The popular approach of combining determinations has therefore been challenged on statistical grounds (Blackwell and Buck, 2003). The approach is further

outlined in Chapter Four and as we shall see after testing of the method is Chapter Five, the approach does seem to produce genuine demographic signals.

However, with regard to previous studies into archaeological demography, the summed probability approach is incredibly popular and it has been applied to prehistoric Europe many times in the past. Gamble et al. (2005)'s study looking at demographic processes across Europe during the period 25,000 to 11,000 BP also took radiocarbon dates as the chief point of departure. Summed probability plots based on the S2AGES database of radiocarbon dates were produced and 5 chief demographic events in Europe during this period were identified by the authors. These are outlined in table 2.5.

Table 2.5: Demographic events identified in Gamble et al. (2005)

Population event	Phylogeography	GRIP Ice-core years BP
1. Refugium	Low population size	25-19.5 BP
2. Initial Demic Expansion	Low population size	19.5 - 16 BP
3.1 Main demic expansion	Low population size	16 - 14.7 BP
3.2 Main demic expansion	Founder effect and expansion	14.7-14 BP
4. Population stasis	Founder effect and expansion	14-12.9 BP
5. Population contraction		12.9 - 11.5 BP

2.6.3 Genetic Evidence

Evidence from modern DNA is an invaluable source of information about past population expansions and contractions. The degree of genetic diversity in a modern population will be a product of past demographic events and, unlike archaeological data, genetic data is simple to collect and does not degrade with time. Data can also be collected by proxy information from phenotypes, such as blood groups. Construction of gene trees, through mismatch analysis of modern samples, can allow analysis of the past population histories of our species; indicating whether a population has undergone past expansion, contraction, or remained stable. Coalescent events should be frequent just prior to a population expansion, and fewer after such an expansion (Harpending et al., 1998). Among the most renowned genetic studies into archaeolog-

ical problems are those involving the 'control region' of mitochondrial DNA, such as the 1980s mtDNA analyses which essentially put paid to the multiregional hypothesis of human origins (Cann et al., 1987), though controversies still exist. Mitochondrial studies have also been used to assess population processes. However, mtDNA research only utilizes a single locus, that of the mtDNA control region and subsequently the reliability of the results may be questioned. The coalescence timing of a single gene only provides information about the origins of that particular gene, rather than a species as a whole. It is therefore preferable to observe the frequencies of coalescence times in order to ascertain when speciation occurred, or when population events took place, and only studies of nuclear DNA can allow such observations to be made. Coalescent events will cluster around periods of population expansion, or display dispersed timings in stable populations.

Genetic data has been called-upon on several occasions in attempts to solve the problem of Neolithic origins . Ammerman and Cavalli-Sforza produced a genetic map of Europe with a strong East-to-West cline, indicative of a European Neolithic created by Near Eastern migrants (Ammerman and Cavalli-Sforza, 1984). Such a cline was supported by the temporal distribution of radiocarbon dates. However mtDNA samples from several localities in Europe and the Near East were interpreted by Richards et al. (1996) as evidence for a Palaeolithic ancestry for most modern Europeans, arguing for a Near Eastern origin, albeit an ancient one corresponding to the Upper Palaeolithic transition, rather than the Neolithic one. Genetic evidence is not definitive, and the usual controversies will prevail.

A multi-locus analysis by Reich and Goldstein demonstrated that an expansion had occurred in Africa, between 44,000 and 570,000 BP (Reich and Goldstein, 1998), but found no evidence of expansions outside of Africa. However, all archaeological evidence informs us that population growth has occurred outside of Africa. Mismatch analysis of mitochondrial DNA has placed the expansion of human populations into a similar timeframe of 66,000 to 150,000 BP (Rogers, 1995); an enormous window of time. It is

apparent that the resolution of the genetic data is currently not sufficient to provide all of the demographic answers sought. However, it is an additional avenue of inquiry that can reach phases of human evolution that are off-limits to archaeological demographic research.

Several genetic studies are particularly pertinent to understanding the demography of the Pleniglacial. Achilli et al. (2005) analysed mtDNA samples from modern populations and observed that certain subhaplogroups of haplogroup H had frequencies centred on Southwestern Europe, with declining frequencies as one moves northward. This provides genetic evidence of a population expansion out of Southern Europe, supporting the Southern European refugium concept. A similar trend was observed by Pereira et al. (2005) on the basis of genetic data; they suggest that haplogroup H arrived in Europe from the Near East during the Last Glacial Maximum. They also corroborate the notion of demic expansion from Southern Europe following the LGM, as noted by Achilli et al. (2005). The idea of groups arriving from the Near East during the LGM is a little troubling, given that other lines of evidence point to population contractions upon southern refugia in Europe at this time. However, overall genetic studies utilizing modern mtDNA samples support the idea of demic contraction and subsequent expansion into southern European refuge zones during the LGM, as evidenced by other lines of enquiry.

Some authors have used non-human genetic evidence to explore population events. Population events experienced by all animals will be written in their genes, in the same way as the human genome. Given the close relationships between humanity and certain species of animals, notably game animals such as *Rangifer tarandus*, examination of the genetics of these species can support human population models, such as the glacial refugium concept. Glacial refugia have been noted for several species on the basis of phylogeny, with a refuge zone in Eastern Europe posited for the common grasshopper, hedgehog and the brown bear (Hewitt, 2000). Likewise examination of mtDNA of *Rangifer tarandus*, a species with strong ties to Palaeolithic man, have revealed refugial

origins for this animal as well (Flagstad and Røed, 2003)

2.6.4 Dietary shifts: The Broad Spectrum Revolution

In the late 1960s, Binford and Flannery, in separate studies, drew attention to evidence for resource diversification in the Late Pleistocene of Eurasia. Flannery argued that such diversification was a means of increasing carrying capacity and was an essential precursor to the Neolithic revolution, terming this shift in dietary patterns the 'Broad Spectrum Revolution'. The notion of shifts in dietary behaviour as a potential *indicator* of population change, particularly when focussing on small game, was later picked up by Mary Stiner and colleagues, and utilized alongside foraging theory to produce demographic studies into the Mediterranean in prehistory. Several key premises are central to this approach, utilized by Stiner and colleagues. First, it is assumed that the 'principle of least effort' will apply and that humans will preferentially select larger individual animals for hunting; more buck for your dollar, literally in the case of lagomorph hunting. Secondly, it is assumed that species will be hunted at a relatively sustainable level. Thus species which are slow to reproduce and cannot survive intensive hunting are unlikely to be hunted by large populations. A preference for easily-captured species is also likely to be in effect. Based on these assumptions, Stiner et al. (2000) argued that Middle Palaeolithic demographic densities in the Mediterranean were low; species with very low resilience to intensive hunting are significantly represented in faunal assemblages. By contrast, demographic increase was noted at several points in Mediterranean prehistory due to the decreasing average size of limpets and tortoise shells found in assemblages. Not only are smaller individuals less preferred by hunter-gatherers, but average individual size is likely to decrease in the prey population in general under conditions of intensive hunting. The increased occurrence of avian fauna in assemblages studied by Stiner et al. (2000) also suggests population pressure was causing humans to seek-out increasingly lower-ranked species for sustenance; birds are regarded as particularly hard to hunt.

Overall, the application of the Broad Spectrum model to demographic studies is a useful approach and the logic behind the preferential selection of certain prey animals certainly seems to make sense. Of course, the possibility remains that the switch to including a wider choice of animals in the diet may not be entirely down to demography. For instance, imagine the wealth of cultural accoutrements ascribed to diet; religious proscriptions in both modern and traditional societies and the effects of totemic and moiety systems on patterns of consumption. Though, certainly, that necessity caused by demographic growth is likely to be a prime mover in such social changes seems highly probable. From a strictly archaeological perspective, there may be preservation issues affecting the recovery and identification of small animal remains, potentially resulting in the appearance of a demographic 'upswing' simply due to taphonomic effects. Likewise, routine sieving during excavation would be necessary for the recovery of small animal remains. However, some evidence for increasing dietary breadth in the Upper Palaeolithic of Southwest France will be considered in Chapter Three, as we consider the background data for demographic trends in the region and period of interest to us here.

2.6.5 'Bottom-up' approaches: carrying capacity

The approaches to prehistoric demography that we have examined so far are all approaches where population size is inferred from the traces that population events leave behind; anthropogenic carbon, faunal remains and gene frequencies in living populations. These are all 'top down' approaches where the archaeological and genetic remains are used to make inferences about population size. A contrasting approach is to reconstruct the environment of the society you are studying and to estimate how many individuals could be supported by this environment. Jochim (1998) was able to build an exceptionally detailed model for prehistoric Germany and predict population size on the basis of this model. Mithen (1990) also utilized predictive modelling to this effect, estimating population size in prehistoric Iberia on the basis of environmental models.

I trialled the resource-centred approach in my masters thesis (Collins, 2008). I estimated the Palaeolithic reindeer population of the Dordogne from modern analogues and used this to estimate food availability in the region. However, this approach was not ideal. While reindeer are a dominant food source throughout the Upper Palaeolithic, they are not the only food source. Basing models solely on reindeer consumption produces a biased result. Equally, basing resource estimates on modern analogues is akin to using a modern reindeer hunting society as a direct analogue, so we might as well go straight to the ethnographic source. Equally, this approach is not adequate for understanding *change* in prehistoric population size, presenting instead a static picture of population. Still, it is interesting to try to estimate prehistoric carrying capacity and the more complete models built by Jochim (1998) and Mithen (1990) are more realistic.

§ 2.7 Previous studies into Innovation in Prehistory

We have previously outlined the possible link between demography and innovation, which has been recognized for sometime. Several investigations into innovation rates in prehistory have already been conducted, although many have not considered the role of demography, even in some cases where it would provide a good explanation for the phenomena observed.

Soffer (2000) considers evidence for technological innovation at very large Gravettian sites in Moravia, where the survival of a considerable quantity of perishable material provides evidence for basket making and the production of netting, amongst other 'innovations'. The author here focusses on the notion that these technological processes are newly developed, on account of their scarcity at other sites. Of course, an obvious possibility is that such organic materials simply do not *survive* elsewhere. Soffer argues that these aggregation sites see an increase in consumption, which requires innovation to meet the demands of the large groups congregated at these sites; the 'mother of invention' hypothesis. However, as outlined above, the possibility also remains that it

is not necessity, but the simple 'numbers game' mathematical process, which is driving innovation in these sites. However, the evidence for high innovation rates at these sites remains unconvincing, given that it is based on perishable remains likely to be absent elsewhere for simple taphonomic reasons. Likewise, as outlined above, it is unclear whether searching for the very first example of an artefact is actually useful for the study of innovation in prehistory, or indeed if it is remotely feasible.

Likewise, other studies have recognized the possible link between climate and innovation, something that we are explicitly interested in here as a result of the perceived demographic response to climatic variables in Southwest France during the pleniglacial. Rigaud (2000) attempted to relate the typology of various Upper Palaeolithic technocomplexes to the climate and environment of these phases. However, no attempt was actually made to directly quantify tool frequencies or climatic variables and any reference to 'correlations' in the paper are purely subjective and qualitative. Rigaud (2000) focusses on identifying unique tool types that correspond to particular climatic situations, identifying only a 'correlation' between Noailles and Raysse burins and climatic amelioration. The notion that tool forms are affected by climatic events is an interesting one, and a worthwhile subject for investigation. However, greater attempts to actually quantify both technology and climatic variables would improve the study. To some extent, it is a very similar study to that presented here, although, as outlined in Chapter Four, we are attempting to quantify tool diversity. We have also extended the logic of climate-technology relations slightly, by placing demographic processes between climatic change and technological change, as the driving force for such change.

Chapter 3

Archaeological Background

§ 3.1 Geography and Environmental Background

The study region is comprised of the southwest corner of France, which for the most part corresponds to the region of Aquitaine. However parts of Midi-Pyrénées, Poitou-Charentes and Limousin are also included, as I feel that restricting the region according to administrative lines is a false distinction; such administrative lines are clearly not relevant to our prehistoric subjects. Aquitaine is comprised of five *départments*: The Dordogne, Lot-et-Garonnes, Landes, Gironde and Pyrénées-Atlantiques. The study region is flanked to the south by the Pyrénées mountains and to the west by the further montagne range of the *Massif Central*. Hunter-gatherer groups only occupied these upland regions in more temperate phases of the Upper Palaeolithic. The low valleys of the Dordogne, carved from Jurassic limestone, feature an abundance of caves and rock shelters, attractive to Palaeolithic man and, indeed, archaeologists thousands of years later. Aquitaine, and especially the Dordogne département , is one of the only regions of France, and indeed Europe as a whole, which sees continuous occupation throughout the entire Upper Palaeolithic sequence and this is the rationale behind its central role in the study here.

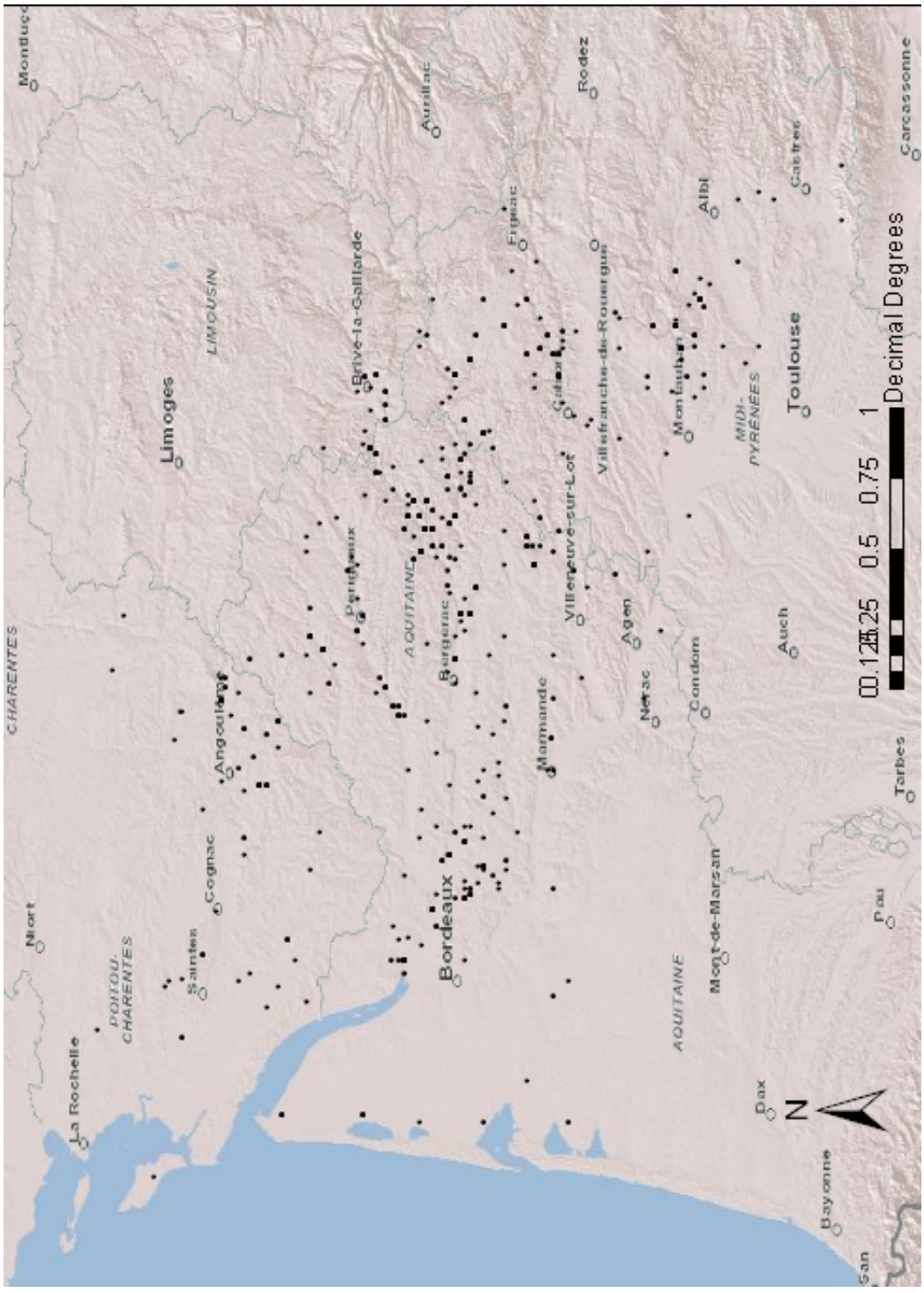

Figure 3.1: The study region of Southwest France, showing Upper Palaeolithic sites. Sites are taken from P-Y Demars' database (Demars, 1996)

3.1.1 Climate

The Upper Palaeolithic occupation of Europe occurs against a backdrop of rapidly changing climate, which sees the inhabited territory expanding and contracting in accordance with this climatic change. Variations in global climate are likely to result from regular 'wobbles' in the earth's orbit known as Milankovitch cycles. Currently we are still in an ice age, though we have been enjoying warm, interglacial conditions for the past 10,000 years or so. The scheme for dealing with geological and climatic phases is extremely complex and inter-nested. The broad geological period, which encompasses both the present day and the entirety of the Palaeolithic, is the Quaternary period. Within this period are two epochs; the Pleistocene and the Holocene. We could potentially add the Anthropocene to the end of this sequence, though the existence of this latter epoch is disputed (Gale and Hoare, 2012). These two/three epochs together form the latest ice age or glacial period and a multitude of cooling and warming events have occurred throughout this ice age. Interglacial and glacial periods within an ice age tend to be of the order of tens of thousands of years, whilst briefer, stadial (cold) and interstadial (warm) events are likely to be of the order of thousands of years. The glacial period of interest to the Upper Palaeolithic is that of the last glaciation, known as the Würm glaciation in the Alps and the Weicheselian glaciation in Northern Europe with a multitude of local synonyms the world over, stretching from approximately 110,000 years ago up until the onset of the Holocene at about 10,000 years ago. Within this glaciation we are also aware of a plethora of stadials and interstadials, from a variety of scientific sources, including stable isotope ratios in marine and ice cores (Andersen et al., 2006), pollen cores eg (Woillard, 1978), biostratigraphy (Bouchud, 1975) and sedimentology eg (Farrand, 1995). In many instances, these climatic proxies coalesce, but there are some contradictions between local datasets.

Climatic information is obtained from deep sea cores on the basis of oxygen isotope ratios in foraminifera; the oxygen isotope method is also the basis behind those of

ice cores in palaeoclimatology, introduced presently. There are three stable isotopes of oxygen; ^{16}O, ^{17}O and ^{18}O and numerous radioactive isotopes. Many processes result in 'fractionation'; a change in ratios of stable isotopes. During cold phases large amounts of ^{16}O will be locked-up in ice, meaning that global sea water will be 'heavier', containing proportionally larger amounts of ^{18}O. The ratio of ^{16}O to ^{18}O is reported as a $\delta^{18}O$ value, where the proportion of the heavier isotope present is compared to a laboratory standard, Standard Mean Ocean Water. In simple terms, larger $\delta^{18}O$ values correspond to cooler phases, and vice versa. As well as providing climatic information, marine cores have widely been used to produce chronology, as, climatically, various 'stages' can be seen in the changing ratios of oxygen isotopes. The stages of relevance to the Upper Palaeolithic are stages 1, 2 and 3. Stage 1 begins at the end of the Younger Dryas (see below) and includes the present day. Stage 2 begins around 24,000 years ago and encompasses the Last Glacial Maximum (see below). Stage 3 begins around 60,000 years ago and includes an important section of early human history, including the arrival of modern humans into Europe and the Neanderthal extinction.

Icecore data from places such as Greenland is widely used to provide climatic data for the Upper Palaeolithic; researchers are able to sample the annual layers within these ice cores for stable isotope analysis. Oxygen isotope analysis on these annual layers works in a similar manner to that described for marine cores, with one important exception. Due to the various processes at work leading to fractionation, layers which are enriched in ^{18}O are provenanced from *warmer* phases. This can be seen from Figure 3.2; the onset of the Holocene around 10,000 years ago is plainly apparent from the NGRIP ice core data (dating group, 2008), due to the sharp increase in $\delta^{18}O$ values with the onset of this era.

At present the Greenland Ice Core Chronology GICC05 provides high resolution climatic data back to 60,000 b2k (before 2000 AD) and is based on data from three ice core records; GRIP, NGRIP and DYE-3 (Blockley et al., 2012). We can observe a number of interstadials in the Greenland climatic data. Shown in Table 3.1, taken from

Andersen et al. (2006). These high-frequency warm oscillations observable in ice core data and referred to as Dansgaard-Oeschger events, after their discoverers (Dansgaard et al., 1993).

Table 3.1: Greenland Interstadials. From (Andersen et al., 2006)

GI	Year B2K
GI-1	14,680 +/- 93
GI-2	23,340 +/- 298
GI-3	27,780 +/- 416
GI-4	28,900 +/- 449
GI-5	32,500 +/- 566
GI-6	33,740 +/- 606
GI-7	35,480 +/- 661
GI-8	38,220 +/- 724
GI-9	40,160 +/- 790
GI-10	41,460 +/- 817

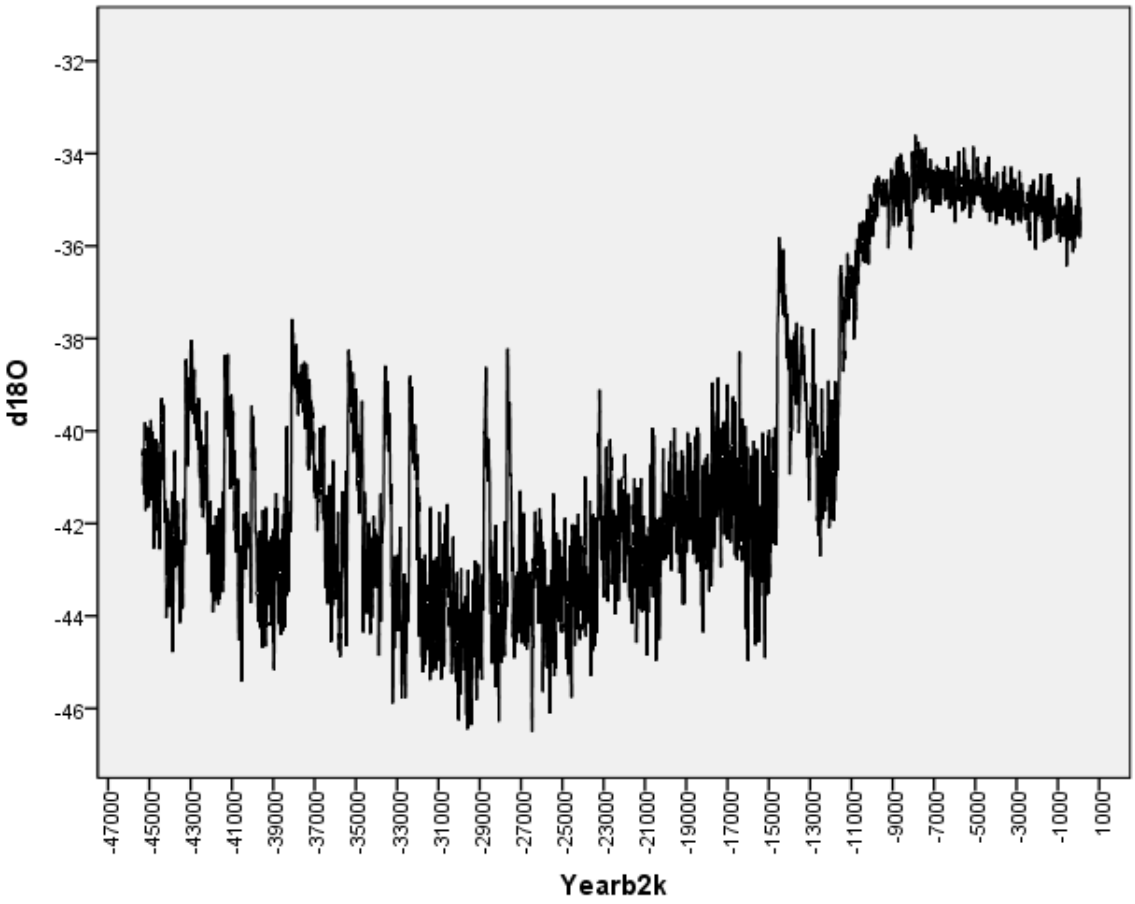

Figure 3.2: $\delta^{18}O$ data from the NGRIP icecore GICC05 model. Years are in B2K (before 2000), so there is a 50-year difference from calibrated radiocarbon years. Data from NGRIP dating group (2008)

While the Greenland Ice Core Chronology is obviously constructed based on data from Greenland, it is widely used to provide proxy climatic data for other global regions and when used in conjunction with other climatic proxies, such as pollen cores, can be used to construct climate chronologies for local regions. There is, however, some debate as to whether climatic events seen in Greenland reflect events on continental Europe and whether we can make inferences about global climate trends from Arctic data. (Larsen et al., 1995), for example, observed that Holocene environmental changes observed in Northwest Europe do not appear in the Summit ice core. It may therefore, be useful to refer to both icecore data and pollen profiles where possible.

Palynologists construct pollen profiles from pollen cores, basing climatic reconstruction on their knowledge of the modern day ranges and preferences of individual plant species. In this way, pollen data can reveal floral recolonization events and contractions. Many stadials and interstadials observed on the basis of pollen data are named after the sites where pollen cores were taken from, or after individual plant species. For example, the various Dryas stadial phases are named for the *Dryas* species of thermophobic plant. Ice cores are able to corroborate some of the interstadials observed through pollen analysis, although we can see that Greenland Interstadials far outnumber those observed in pollen cores. This could, however, potentially be a result of the high resolution data available from the ice-cores when compared to pollen profiles.

Table 3.2: Major interstadials observed through pollen profiles

Interstadial	Age cal BP
Oerel	58-54
Glinde	51-48
Moershoofd	46-44
Hengelo	38-36
Denekamp	30-25

Additional climatic events of note are Heinrich events; discharges of ice-caps into the north Atlantic, of which there are six covering the period of study here. Heinrich event 0, at 12,900 BP, corresponds to the Younger Dryas period in Europe (Burroughs, 2005), a brief return to glacial conditions that punctuates the general Late Glacial trend towards improving climatic conditions.

As part of the Stage Three Project examining Neanderthal and AMH lifeways in Upper Palaeolithic Europe (van Andel and Davies, 2003), climatic simulations were performed to examine the magnitude of D/O events. The authors used Global Circulation Models (GCMs) as the basis for models, which were then tested using palynological evidence (Barron et al., 2003). They also ran simulations for the present day to test the models' validity, observing these to be sufficiently accurate. The authors produced models for

several temporal phases, with the LGM simulation based on orbital parameters, a large ice-sheet, sea level and sea-surface temperatures. Observe the temperature simulations for LGM summer and winter months (Figure 3.3).

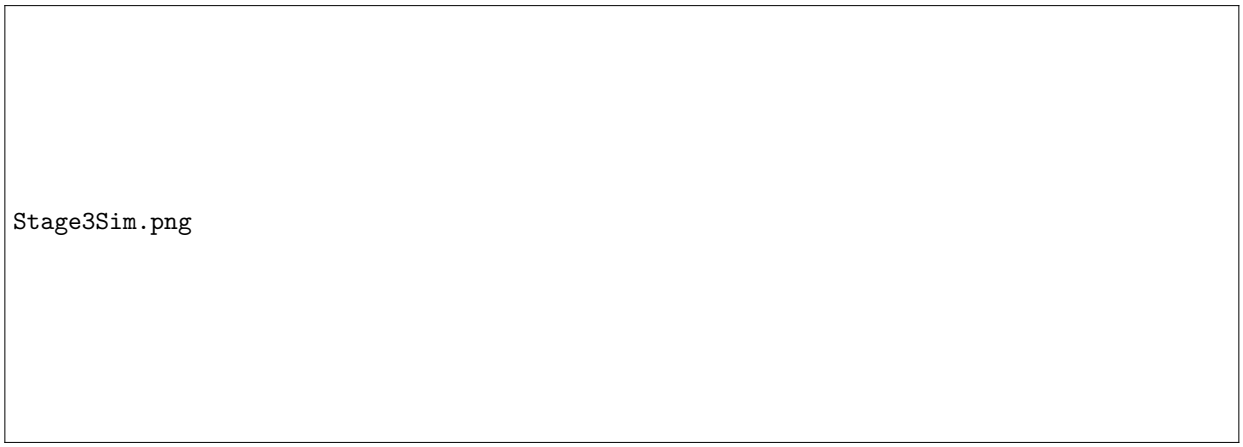

Figure 3.3: Climatic simulations for LGM Europe in summer(right) and winter (left). From (Barron et al., 2003)

The more hospitable temperatures projected for southern Europe during the LGM and, in particular, during the coldest months of the LGM provide environmental support for the refuge zone concept. The reasons why populations have been thought to have retreated into this region during the LGM are obvious, once climate is considered.

Overall, based on the various climatic data sources available, we are aware of a variety of both warm and cool events covering the Upper Palaeolithic period. The range of human adaptability required to survive the Pleistocene is quite remarkable. That human populations would increase and decrease their ranges in response to climatic change only seems logical when we consider the extreme variability of the Upper Palaeolithic environment. Table 3.3, taken from Burroughs (2005), displays the composite climatic events for the period of interest.

Of particular note is the Last Glacial Maximum phase, where the ice sheets were at their greatest extent. Various dates have been put forth for this all-important phase and there does not seem to be a great deal of consensus on the issue. Generally, most definitions encompass a 'core range' of 21-18,000 BP (uncalibrated), or roughly 20-

Table 3.3: Major Climatic Events. From (Burroughs, 2005)

Age (kya)	DO events	Heinrich events	Interstadials and Stadials
0-10			
10-20	1 (14.5)	H0 (12.9)	Younger Dryas (12.9-11.6 kya)
		H1 (16.5)	Bolling warm stage (14.5 kya)
20-30	2 (23.4)	H2(23.5)	Denekamp interstadial (30-25 kya)
	3(27.4)		
	4 (29)		
30-40	5 (32.3)	H3(32)	Hengelo interstadial (38-36 kya)
	6(33.4)	H4 (39.5)	
	7(35.3)		
	8(38)		

23,000 calendar years, with some variations on the timing of the start of this major climatic event. A recent attempt to constrain the LGM using data on relative sea level change was able to identify the period between 26.5 and 19,000 ka (calendar years) as witnessing the fullest spatial extent of global ice sheets, though local ice sheets will have varied in the specific timings of this event (Clark et al., 2009). We shall use this definition here, as it corresponds to the phase where the majority of global ice sheets were at their greatest extent, thereby corresponding most closely to a true definition of 'Last Glacial Maximum'.

§ 3.2 Southwest France as a Refugium

The interest in Southwest France for a demographic study stems from the continuity of the archaeological record throughout the Upper Palaeolithic trajectory, including throughout the LGM. As discussed above, southwest France was less dramatically affected by the climatic events surrounding the LGM and for this reason several authors have proffered the concept of this region as a refugium for animals and people (Jochim, 1987). Such a refuge zone would be a region into which groups retreated into, as other areas became inhospitable. The region supported diverse animal species in great densities and this is likely to be the primary cause of the regions importance to prehistoric populations. The distribution of site numbers over time for Southwest France supports this refugium concept, as inhabitations dwindle at higher latitudes during the LGM. Northern Spain also sees the continuation of populations throughout the harshest periods of the last glaciation and subsequently some archaeologists argue that the Franco-Cantabrian region was a single refuge zone (Straus, 1991b). In addition, some researchers have also proposed an Eastern European refugium, though evidence for continuity of human populations in the East is more equivocal (Soffer, 1987).

Several faunal refuge zones are identifiable in Europe. A phylogeographic study by (Taberlet et al., 1998) demonstrated that Northern Europe was recolonized from a refuge zone in Iberia. A later palaeontological study confirmed and refined the proposed southern European refugia; demonstrating mammalian refugia in the Dordogne, Iberia, Italy and the Balkans, all dating to between 23000 and 16000 BP (Sommer and Nadachowski, 2006). The coincidence of the proposed mammalian and human refugia in Europe is pleasing, but unsurprising. It is highly likely that human groups would follow the fauna when migrating to avoid the cold.

In addition to the continuity of the archaeological record in the refuge zone throughout the Upper Palaeolithic, the archaeology is also unique in the density and diversity of cultural and archaeological remains. Palaeolithic parietal and portable art is incredibly

beautiful and no study into the prehistory of Southwest France would miss the chance to include some beautiful images of this ancient artwork. However, the artworks themselves are also of great relevance to the questions we are seeking to answer here. We have already touched on the claims for the 'rich archaeology' of the region and along with the abundance of sites, enormous assemblages of lithics and faunal remains and, crucially, the evidence for continuous occupation of the region throughout the *entire* Upper Palaeolithic sequence, the wealth of beautiful artistic depictions can be added to this pantheon of archaeological activity.

Cave art in the region is predominantly Magdalenian, though some sites date to earlier ages (Valladas et al., 2001). Depictions are mostly of animals; bison, mammoth, horse, rhinoceros, though some humanoid and anthropomorphic figures are also known, for example the 'sorcerer' character from Trois Frères. Abstract signs also appear in parietal art and these have become significant for some interpretations of the meaning behind Palaeolithic art, while what have been interpreted as 'sexual signs' are also common. Early interpretations of the 'meaning' behind the art were simple and fell into the 'art for art's sake' explanation, a deeply unpopular approach in modern times (Halverson et al., 1987). Later explanations tended to focus on the notion of sympathetic hunting magic, supported somewhat by depictions of animals with apparent 'spear marks' around them. Fertility magic explanations found similar support in the apparent depictions of genitals, some vague images of possible copulation and the depictions of fuller-figured ladies interpreted as *en grossesse*. Structuralist interpretations similarly found validation in the co-occurrence of particular images and the layout of figures within the architecture of the cave (by A. Michelson, 1986). Shamanistic interpretations have found support in the abstract signs and symbols; signs which in many cases reflect the images seen cross-culturally under the influence of hallucinogenic drugs (Lewis-Williams, 2002). Likewise, the cramped, awkward placing of several images in inaccessible locales suggests an esoteric element to the artwork. In all cases, interpretations of cave art tend to, at least partially, reflect something of the society and time

of the researchers.

Figure 3.4: Sorceror figure from Trois Frères. Drawing by the Abbé Breuil

An alternative explanation for the production of cave art is directly relevant to this thesis; several researchers have proffered the notion that high population pressure led to the production of cave art. According to (Conkey, 1980), high population density would have required the development of new social structures to maintain peace between groups, which would otherwise have recourse to violence. Parietal art would have been part of a mechanism for the relief of tensions, which would otherwise lead to interpersonal conflict in the refuge zone (Conkey, 1980). However, as outlined in Chapter Two, the link between increased population density and cultural endeavours may not necessarily involve conflict at all, though of course warfare could be a part of the mechanism linking the variables of population and innovation. Warfare could conceivably be a part of the mother of invention mechanism, but is not required at all for the numbers game process to be at work.

The Franco-Cantabrian region sees the greatest density of parietal art found anywhere in the world for this period (Mellars, 1985). We can see evidence for artistic endeavours

throughout the Upper Palaeolithic but parietal art develops rapidly in the LGM and is markedly concentrated in the Franco-Cantabrian region (Barton and G.A. Clark, 1994). However, other forms of material culture also display high levels of apparent innovation. Lithic assemblages from the LGM contain unique tool forms; the foliate points that define the Solutrean are geographically restricted to the refuge zone and temporally restricted to the Solutrean era. We can see from a cursory summary of the regions archaeology that the people living in the refuge zone were creative and innovative. As outlined in Chapter Two, we can model cultural innovation in the region as a function of increased population, and both population dynamics and innovation rates in the study region are quantified in Chapter Five in order to test this relationship.

§ 3.3 Lithic Technology of Southwest France

The technocomplexes of Southwest France have taken a great deal of unravelling over time; a great deal of typological wrangling has taken place throughout the years and we are still by no means certain of chronology. Peyrony was of the opinion that the Aurignacian and what he termed the Périgordian technocomplexes were contemporaneous, representing two separate 'tribes' coexisting in the region (Peyrony, 1933). He termed the Châtelperronian industry which is now widely regarded as a separate, Neanderthal-produced technocomplex as the Lower Périgordian, and saw evidence for local evolution of this industry into the Upper Périgordian, which we would now call the Gravettian. Nowadays, archaeologists have largely abandoned Peyrony's system, and despite some disagreements over the current typological systems, we can be sure of the broad sequence of: Châtelperronian, Aurignacian, Gravettian, Solutrean, Magdalenian and finally, leading into the Mesolithic, the Azilian. The Badegoulian period, whose existence some dispute, can be added into this sequence prior to the onset of the Magdalenian proper. The Protomagdalenian, proposed by Peyrony as an early form of the Magdalenian, is only known at the Abri Pataud and Laugerie-Haute (Laville et al., 1980) and bears no actual relationship to the Magdalenian. As the Châtelperronian is a

Neanderthal produced industry, it will not be explored in detail in this thesis, as we are chiefly concerned with population processes amongst *H. sapiens*. Technocomplexes are summarized in table 3.4 and individual technocomplexes are outlined in the following sections.

It is important to introduce some further terminology here, which I will use throughout this thesis. The Upper Palaeolithic is broadly divided into Early, Middle and Late phases, with further subdivisions according to technocomplexes. The Early Upper Palaeolithic refers to the Châtelperronian and Aurignacian phases. The Mid-Upper Palaeolithic typically refers to the Gravettian and The Late Upper Palaeolithic refers to the period following the LGM, generally corresponding to the Magdalenian.

3.3.1 The Aurignacian

The Aurignacian is the first undisputed, non-transitional Upper Palaeolithic industry in Europe and the starting point for the analysis in this thesis. There is a modicum of debate as to which hominid species manufactured the Aurignacian (Conard et al., 2004), although consensus holds that AMH manufactured the industry. A number of transitional industries between the Middle Palaeolithic and Aurignacian are known in Europe, including the Uluzzian in Italy, the Szeletian in Eastern Europe and the Châtelperronian from France and Spain. Incidences of Neanderthal remains associated with Châtelperronian industries, as at Saint-Cesaire (aka La Roche à Pierrot) have led to the characterization of this industry as produced by Neanderthals. There is some debate as to whether the Châtelperronian predates the Aurignacian, or is contemporaneous with it. Some evidence for interstratification of Châtelperronian and Aurignacian levels, as at the site of Arcy-sur-Cure in Northern France (Gravina et al., 2005), suggests that the two industries are contemporaneous. However, the validity of these interstratified sections has been questioned by some (Zilhao et al., 2006) and the debate rages on. Such debates about the production of these industries have serious implications for our view of Neanderthal intelligence; if they independently were able to

produce Upper Palaeolithic technology, rather than simply copying, or appropriating AMH-produced tools, then it would follow that this species had more creativity and intelligence than they are otherwise given credit for. However, given the lengthy period of technological stasis that is the Middle Palaeolithic, the occurrence of a technological revolution amongst the Neanderthals in the very same period as modern humans arrive into Europe has been described as an 'impossible coincidence' by Paul Mellars (Mellars, 2005), a view that I am inclined to agree with.

Due to the complications that would arise in performing a demographic study into two species, the Châtelperronian has therefore been excluded from this study and our analysis will begin with the Aurignacian. This technocomplex is named for the type site of Aurignac, excavated by Lartet in 1860. However since the first definition of the Aurignacian, the technocompexes has been divided into a number of subphases, Lower, Middle and Upper, by Breuil based on the stratigraphic sequences noted at Laussel, La Ferrassie and Roc de Combe-Capelle. Breuil's scheme was seriously complicated by Peyrony in the 1930s, with the introduction of the term Périgordian to the system, apportioning the Lower and Upper phases of the Aurignacian to this new technocomplex, regarding the Périgordian and Aurignacian to represent two competing tribes rather than chronological phases (Peyrony, 1933). Peyrony also subdivided the Aurignacian into phases I to IV. The term Périgordian is now all but dead in the typological literature, with the Lower Périgordian now known as the Châtelperronian and the Upper Périgordian denoted by Gravettian.

Peyrony's four phases have been grouped into the Early Aurignacian and the Evolved Aurignacian, corresponding to the first stage and last three stages of the old system respectively (Demars and Laurent, 1992). The Early Aurignacian is generally dominated by scrapers, compared to burins, and features the split-base bone point as a type fossil and the subphase also features numerous Aurignacian blades and retouched blades (Demars and Laurent, 1992). The Evolved Aurignacian by contrast features increasing numbers of burins and lacks split-base bone points. Thus, the key distinctions between

the Early and Evolved Aurignacian are the ratio of burins to scrapers and the presence of split-base bone points.

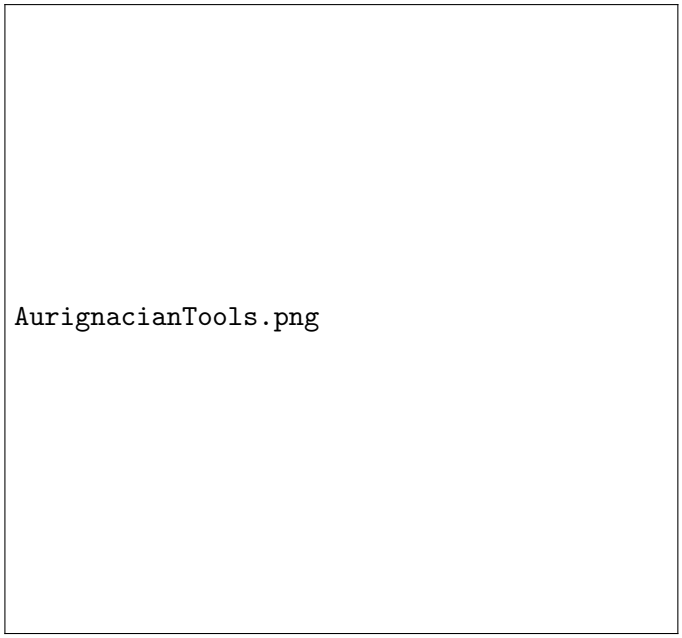

Figure 3.5: Typical Aurignacian Tools, from (Mellars, 2006). *1,2* Aurignacian blades, *3* burin and end-scraper *4* split-base antler point *5* scaled piece, *6,7* carinate scrapers, *8* nosed scraper

As well as the distinctive tool forms that characterize this phase there are a number of other accoutrements of the period which are worth considering. In Southeast France, the famous painted cave of Chauvet dates to the Aurignacian age (Sadier et al., 2012), making it considerably older than the majority of painted caves in France. However, this is not to say that it is the only example of artistic endeavour dating from this period; engraved rocks are numerous. Many portable artworks in the form of statuettes also date from this period, such as the incredible lion-headed man from Hohlenstadel, Germany. Some 'Venus' figurines date from this period, although the great majority are Gravettian. Jewellery in the form of beads is also very common at Aurignacian archaeological sites. 157 distinct type of Aurignacian beads have been recorded in Europe (Vanhaeren and d'Errico, 2006) and hundreds of beads are known from the sites of Castanet and Abri Blanchard in Southwest France. The abundance of Aurignacian

artwork points to a great deal of social complexity amongst Aurignacian society, an image that is compounded by the evidence for long-distance trade and exchange in raw materials in this phase.

Dating the Aurignacian

In order to summarize the temporal distribution of Aurignacian assemblages in Southwest France, a summed probability distribution was produced using data from 19 sites. The summed probability method is outlined fully in the methods section, but essentially the radiocarbon data is averaged first within sites, and then across the landscape, and a normalized distribution is produced. Peaks and troughs in the distribution are thought to correspond to peaks and troughs in activity. Though the method is not without its controversies, it can be helpful for assessing the span of an archaeological period.

Data comes from the sites of Abri Pataud, Flageolet I, Grotte XVI, La Facteur, La Ferrassie, La Quina, La Rochette, Laugerie Haute, Le Piage, Peyrugues, Roc de Combe, Les Renardières, Le Raysse, Combe Saunière, Cro Magnon, Vignaud, Caminade, Castanet and Roc de Marcamps.

We see that the summed probability distribution for the region spans a period from around 44,000 to 22,000 BP, an exceptionally long period of time. The large tails on this distribution are likely to be the result of some erroneous dates, on material either incorrectly attributed to the Aurignacian, or to outlying sample materials. It is worth noting that this distribution was obtained through simple calibration of dates in Oxcal, without the use of Bayesian modelling techniques. Modelling of dates would change the distributions of outlying dates, which would reduce the range of the distribution.

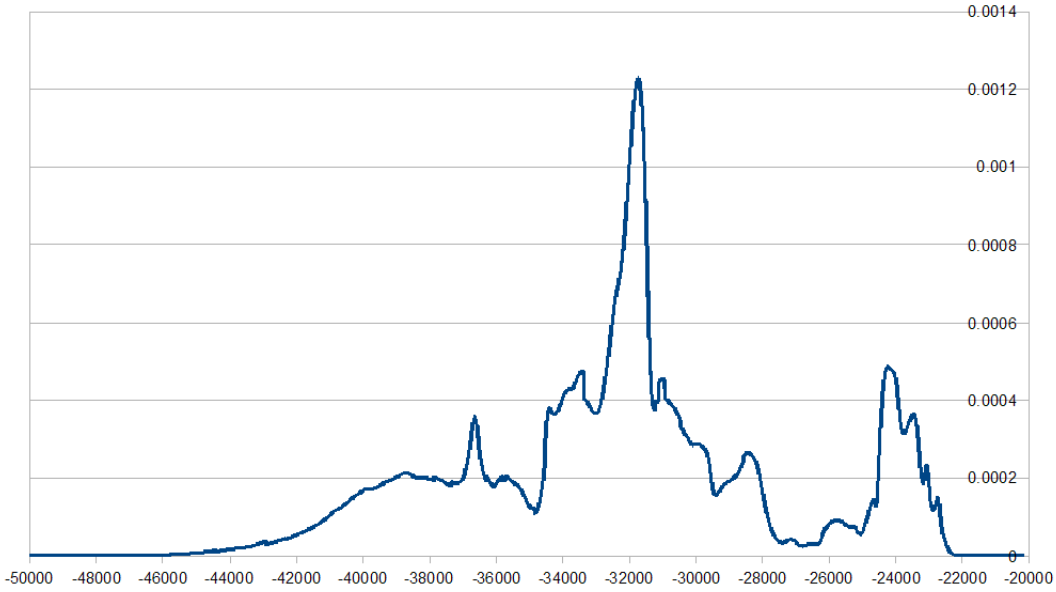

Figure 3.6: Summed Probability Distribution for the Aurignacian of Southwest France. Data comes from the sites of Abri Pataud, Flageolet I, Grotte XVI, La Facteur, La Ferrassie, La Quina, La Rochette, Laugerie Haute, Le Piage, Peyrugues, Roc de Combe, Les Renardières, Le Raysse, Combe Saunière, Cro Magnon, Vignaud, Caminade, Castanet and Roc de Marcamps. Radiocarbon dates, and their associated technocomplexes, are given in Appendix D

3.3.2 The Gravettian

What was once known as the Upper Périgordian (Périgordian IV-V) according to Peyony's scheme is now generally termed the Gravettian. However, the original term may occasionally appear in this study where excavators have used it. Type fossils of the Gravettian include *outillage à bord abattu*, tools with heavily reduced edges, (de Sonneville-Bordes, 1960) as well as Gravette points and, in some sub-phases, Noailles burins, Raysse burins and Font- Robert points. A key distinction from the preceding Aurignacian technocomplex is the elevated frequency of burins relative to scrapers (Demars and Laurent, 1992).

Typologists have now largely revised the old Peyrony scheme into that of Old, Middle and Recent Gravettian, with the Old Gravettian subdivided into two. The first subphase corresponds to the Périgordian IV, featuring a strong contingency of Gravette points and burins. The later stage of the Old Gravettian, corresponding to the Périgordian Va, prominently features the Font-Robert point, as well as shift away from burins towards scrapers.

The Middle Gravettian, has posed several problems in terms of chronological ordering and typology. Peyrony initially defined the Périgordian V sequence on the basis of the stratigraphy at La Ferrassie, Dordogne, where he observed a sequence of from top to bottom; Font-Robert points, truncated elements and Noailles burins (Peyrony, 1934) . The Fontirobertian (Périgordian Va), Périgordian with truncated elements (Périgordian Vb) and Noaillian (Périgordian Vc) were thus defined, predominantly on the basis of these type fossils. This sequence has been confirmed at other sites, such as Laraux, yet a level containing Font-Robert points, Noailles burins and truncated elements is also known from the site of Vachons, confusing the issue of chronology somewhat (Laville and Rigaud, 1973). The possibility exists that the Noaillian represents a separate culture which we should not subsume into the Gravettian, but instead coexisted with the Gravettian proper (David and Bricker, 1987). However, given the

consistent, albeit reduced, presence of Gravette points in Noaillian levels, the industry will be regarded here as a part of the overall Gravettian sequence, following on from (Rigaud, 2008).

The Recent Gravettian features two subphases, the first featuring an increase in scrapers. This scraper/burin index reverses in the following subphase (Demars and Laurent, 1992).

Aside from tool forms, the Gravettian sees some interesting developments across Europe. The celebrated 'Venus' figurines date from this period and are widespread across Europe. While we may never know the precise meaning of these figurines, that they have such a widespread distribution does inform us about the level of interaction between different groups in Europe. Elaborate burials, accompanied by grave goods also appear in the Gravettian of Europe, though interestingly, not in France (Pettitt, 2011). Sites such as Sungir in Russia, featured three interred bodies, which had been covered in ochre and were accompanied by thousands of beads and other offerings (Jochim, 2002). Again, the similarity of such elaborate burials across Europe, particularly in the East, suggests a degree of cultural affinity and contact between these regions. That these burials are missing from Southwest France is incredibly interesting, given how rich this region is in cultural artefacts from other periods. Whether the Gravettian is of special significance in terms of cultural innovation in the region will be explored in due course.

Dating the Gravettian

The summed probability distribution below was obtained from radiocarbon data from the following sites; Abri Pataud, Combe Saunière, Flageolet I, La Facteur, Laugerie Haute, Peyrugues, Roc de Combe, Renardières, Les Garennes, Le Raysse, Moulin de Laguenay, Cro le Biscop, Vignaud, La Ferrassie, Lespaux, Bergerie 2, Pègourie and Castellas.

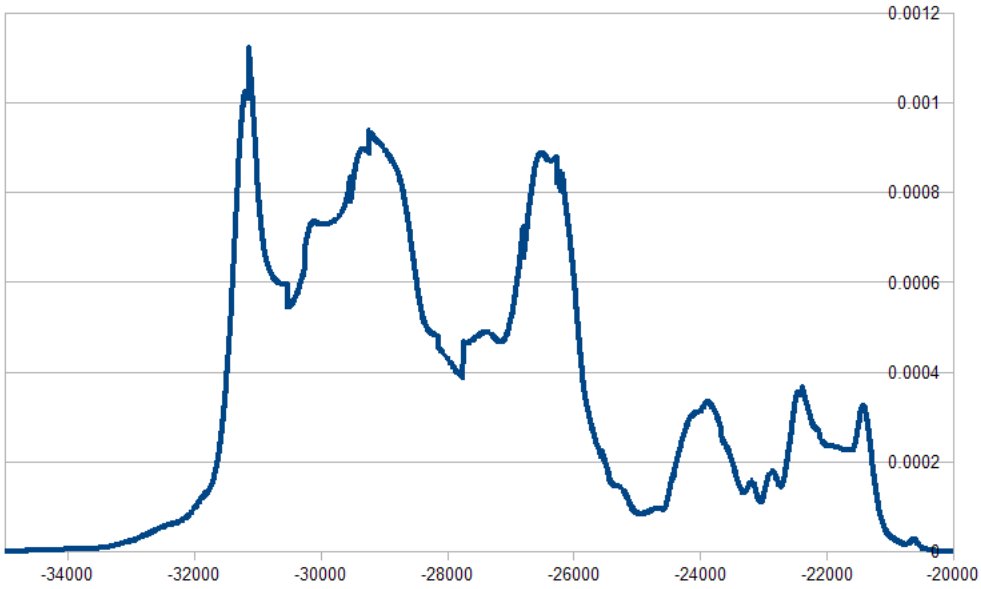

Figure 3.7: Summed Probability Distribution for the Gravettian of Southwest France. Data from the sites of: Abri Pataud, Combe Saunière, Flageolet I, La Facteur, Laugerie Haute, Peyrugues, Roc de Combe, Renardières, Les Garennes, Le Raysse, Moulin de Laguenay, Cro le Biscop, Vignaud, La Ferrassie, Lespaux, Bergerie 2, Pègourie and Castellas. Radiocarbon dates, and their associated technocomplexes, are given in Appendix D

The calibrated range for the Gravettian appears to be from around 34,000 to 20,000 BP.

3.3.3 The Solutrean

The Solutrean period coincides with the onset of the Last Glacial Maximum (LGM) and Heinrich Event 2 - a discharge of ice-meltwater into the North Atlantic, with cooling effects on European temperature (Renard, 2011). The coincidence of the Solutrean with these cold climatic events have largely defined the era and it has been regarded by some as a technocomplex adapted to the rigorous climatic conditions of the Cantabrian-Spain refuge zones (Straus, 1991a). Whilst this technocomplex accompanying the LGM is largely unique to the Southwest France region, the majority of complexes are homogenous across France as a whole, suggestive of the importance of the Solutrean as a cultural phase. The type fossils of the Solutrean are the laurel, and later, willow leaf points, which are instantly recognizable and often very beautiful. The industry has been regarded by some as intrusive to SW Europe, being introduced either by an invading culture, or through influence alone (Smith, 1966) and if indeed invasive, one is redrawn to the concept of refugees of the climatic downturn arriving with intrusive implements.

According to the classic typology of Smith (1966) the Solutrean is divisible into the Protosolutrean, Lower Solutrean, Middle Solutrean, Upper Solutrean and Final Solutrean. The Lower Solutrean features unifacial points, while the Middle Solutrean see laurel leaf points. The Upper Solutrean sees shouldered points and willow leaf points, some potentially too fine to have been used for practical purposes. The Protosolutrean in known from very few sites in Southwest France, just Laugerie Haute, Abri Casserole, and recently the site of Marseillon has been added to the list (Renard, 2011) albeit sharing more characteristics of the Protosolutrean as it is known in Iberia than with the French Solutrean. The lithic technology of Marseillon has been used to support evolution of the the Solutrean from the Gravettian, in riposte to the traditional view

of the Solutrean representing a full break from the preceding phase (Renard, 2011). According to this hypothesis of evolution between the industries, the transition occurs across the entire Solutrean region, with a great deal of interaction between France and Iberia, with a great deal of long-distance exchange occurring.

As well as its unique weaponry, the Solutrean is also characterized by the introduction of the eyed needle, which brings to mind the importance of clothing to LGM peoples. Solutrean hunting strategies are often epitomized by specialization on individual species; at the type-site of Solutré in central France the focus was clearly on the hunting of horses, while at Laugerie-Haute in the Dordogne up to 97 % of faunal remains are identified as Rangifer (Straus, 1991b).

Dating the Solutrean

The following summed probability distribution was obtained from radiocarbon data provenanced from Solutrean assemblages. Data was obtained from the sites of; Combe Saunière, Jamblancs, Laugerie Haute, Le Piage, Le Placard, Peyrugues, Roc de Sers and Cuzoul de Vers.

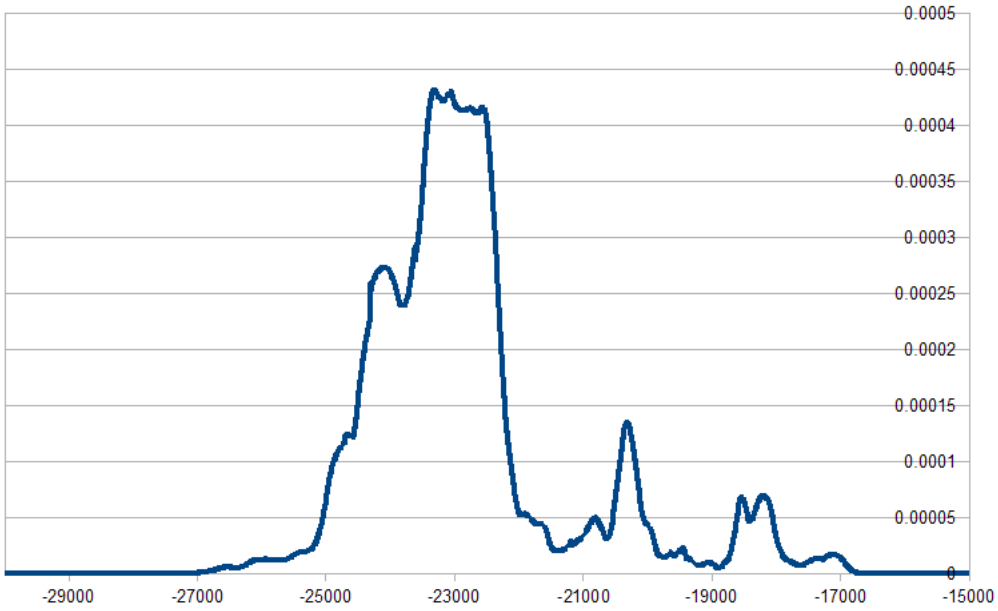

Figure 3.8: Summed Probability Distribution for the Solutrean of Southwest France. Data from the sites of; Combe Saunière, Jamblancs, Laugerie Haute, Le Piage, Le Placard, Peyrugues, Roc de Sers and Cuzoul de Vers. Radiocarbon dates, and their associated technocomplexes, are given in Appendix D

The summed probability distribution for the Solutrean ranges from around 27,000 BP to 17,000 BP.

3.3.4 The Badegoulian

Some researchers dispute the existence of the Badegoulian and it is occasionally treated as the earliest Magdalenian, the Magdalenian 0 and I. The industry is reminiscent of the Magdalenian but with a weak lamellar index and with less burins than scrapers, contrasting with the Magdalenian proper. There is also an abundance of raclettes in this phase and discoidal flake cores are also a common form amongst Badegoulian assemblages. The Badegoulian can be subdivided into the Early Badegoulian and Recent Badegoulian, synonymous with the Magdalenian 0 and I respectively. The Recent Badegoulian itself appears to be formed of three contemporaneous 'types', Chatenet, Croix-de-Fer and Initial Magdalenian, although the Initial Magdalenian is largely regarded as a distinct fascies (Fourloubey, 1998). The evolution from the Early Badegoulian to the Magdalenian proper appears to be characterized by a shift away from flakes (Fourloubey, 1998). Temporally, based on current radiocarbon consensus, the Badegoulian appears to occupy the period from 22-20,000 calibrated BP (Banks, 2011) and corresponds to the warm phase of the Lascaux Interstadial.

For the purposes of my study, the Badegoulian will be recognized as a separate industry. The interesting settlement pattern observed in this phase, with large numbers of open air settlements (White, 1985) also implies that it may be worth treating the Badegoulian as a separate phase to the Magdalenian, particularly in the course of a demographic study such as this.

Dating the Badegoulian

A further summed probability distribution was produced for the Badegoulian of Southwest France. Radiocarbon dates were taken from the sites of; Le Placard, Les Renardières, Jamblancs, Combe Saunière, Saint Germain, Les Peyrugues, Le Cuzoul de Vers, Pégourié and Abri Gandil.

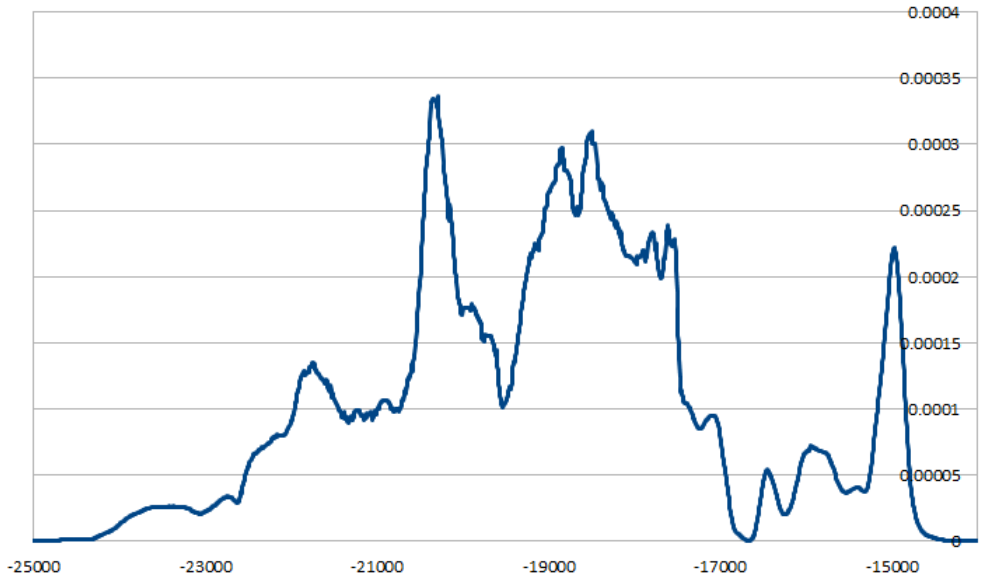

Figure 3.9: Summed Probability Distribution for the Badegoulian of Southwest France. Le Placard, Les Renardières, Jamblancs, Combe Saunière, Saint Germain, Les Peyrugues, Le Cuzoul de Vers, Pégourié and Abri Gandil. Radiocarbon dates, and their associated technocomplexes, are given in Appendix D

3.3.5 The Magdalenian

According to the classification scheme of Breuil, there are six phases of the Magdalenian, partitioned based on bone artefacts, particularly 'harpoons', with assemblages lacking harpoons, rightly or wrongly, apportioned to the Magdalenian II or III. Typologists have challenged and revised Breuils scheme on multiple occasions. (Demars and Laurent, 1992) propose using simply a system of Old, Middle and Recent instead of the Magdalenian I-VI sequence and the Magdalenian 0 and 1 are now largely separated from the Badegoulian, which had once been regarded as the Initial Magdalenian. Typical Magdalenian lithic tools include blades, bladelets and burins (Jochim, 2002), though, of course, bone tools are also incredibly important during this phase.

The notion of chronological progression from the Magdalenian I - VI has been challenged

occasionally. Peyrony argued for contemporaneity of the Early (Magdalenian I-III) and Late (Magdalenian IV-VI) stages of this period, and it has indeed been noted that the Magdalenian III and IV have never been seen 'in the same room together', so to speak and, indeed, nowhere has the entire progression of Magdalenian assemblages been observed in the same stratigraphic sequence (White, 1987). There is also evidence for overlapping of phases, and the reliance on dating many Magdalenian assemblages based on presence or absence of harpoons may have led to inaccurate dating of some assemblages.

The early Magdalenian occurs while climatic conditions are still adverse, following the LGM. However, conditions subsequently improve into the Later Magdalenian and this is reflected in changing settlement patterns, as people are able to leave the Southwest France region. The post-glacial reoccupation of northern latitudes in discussed fully in sections below.

As mentioned previously, the majority of Upper Palaeolithic art is currently provenanced to the Magdalenian period. Likewise, the majority of burials in Europe date from this period. While the Gravettian of Southwest France lacks the elaborate burials which we see in Eastern Europe, this is not the case for the Magdalenian, and burials at Saint Germain la Rivière are accompanied by a number of grave goods (Pettitt, 2011). The abundance of artworks and human burials from this period are indicative of an increasingly complex society in the region.

A summed probability distribution was produced from Magdalenian radiocarbon dates from the region, depicted below. Dates came from the following sites; Montgaudier, Chaire à Calvin, La Doue, Jamblancs, La Truffière, Gare de Couze, Le Pont d'Ambon, Combe Saunière, Flageolet I, Flageolet II, Grotte XVI, Combarelles, Commarque, Laugerie Basse, Laugerie Haute, Les Marseilles, La Faurélie II, Lascaux, Moulin du Roc, Roc de Marcamps, Faustin, Vidon, Le Morin, Fontgaban, Saint Germain, Jaurias, Moulin Neuf, Conduche, Les Peyrugues, Sainte Eulalie, Sanglier, Combe Cullier, Le Martinet, La Magdeleine la Plain, Le Courbet, Abri Gandil, La Plantade, La Faye,

Montrastuc, Fontalès and Les Eyzies.

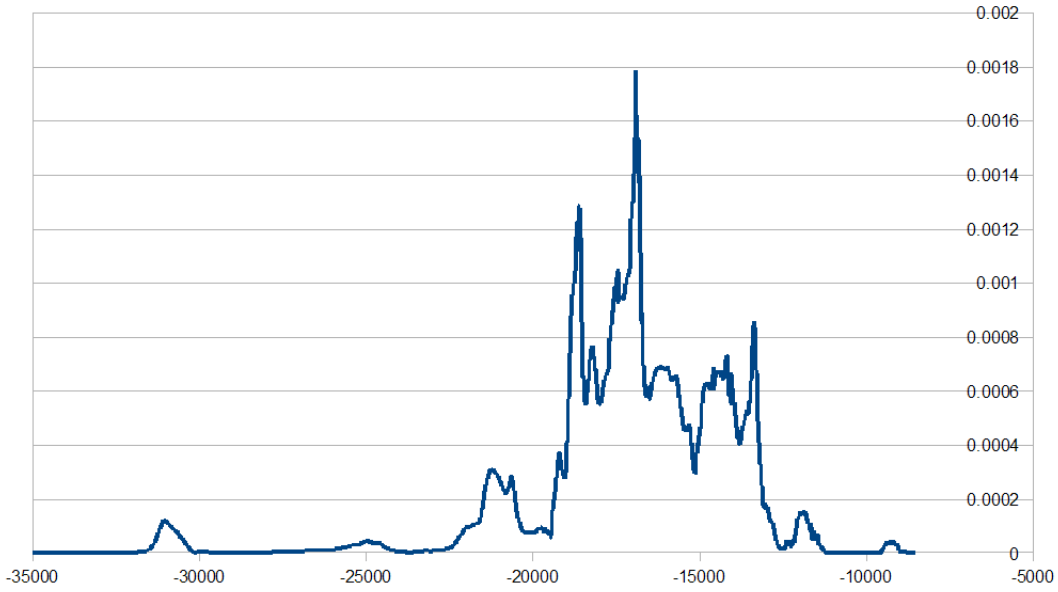

Figure 3.10: Summed Probability Distribution for the Magdalenian of Southwest France. Data from: Montgaudier, Chaire à Calvin, La Doue, Jamblancs, La Truffière, Gare de Couze, Le Pont d'Ambon, Combe Saunière, Flageolet I, Flageolet II, Grotte XVI, Combarelles, Commarque, Laugerie Basse, Laugerie Haute, Les Marseilles, La Faurélie II, Lascaux, Moulin du Roc, Roc de Marcamps, Faustin, Vidon, Le Morin, Fontgaban, Saint Germain, Jaurias, Moulin Neuf, Conduche, Les Peyrugues, Sainte Eulalie, Sanglier, Combe Cullier, Le Martinet, La Magdeleine la Plain, Le Courbet, Abri Gandil, La Plantade, La Faye, Montrastuc, Fontalès and Les Eyzies. Radiocarbon dates, and their associated technocomplexes, are given in Appendix D

3.3.6 The Azilian

Finally, the Azilian represents the post-glacial industry of the region and is arguably a lithic industry of considerably reduced complexity. This technocomplex mainly features an abundance of scrapers and points, with a limited bone industry and even less art, although decorated pebbles are known from this period. The Azilian point and Malaurie point are defining features (Demars and Laurent, 1992).

While undeniably different technologically, the extent of the disconnect between the terminal Pleistocene and premier Holocene phases may be somewhat exaggerated. The Magdalenian-Azilian transition at the advent of the Holocene is traditionally regarded as representing a 'crash' in terms of lifestyles, subsistence sophistication and populations (Mellars, 1985). With warming climatic conditions at the Palaeolithic-Mesolithic transition, some researchers have argued for a shift away from the specialized hunting of a limited range of animals in valley bottoms, towards the consumption of a broader range of food, rather than focussing on game available in valley bottoms. (Jones, 2007) has tested this hypothesis in terms of shifting land-use patterns, observing that, contrary to expectations, site elevation does not significantly increase into the Azilian period as would be expected if a shift away from specialized hunting in valley bottoms occurred. However, a general trend towards increasing variance across the Pleistocene-Holocene boundary *was* observed, potentially indicative of increasing dietary breadth. However, given the lack of evidence for a shift towards settlement at higher elevations in the Azilian and the apparent continuity in population size, outlined in Table 3.6, prior to embarking on our analyses it appears that the notion of a 'break' between the Magdalenian and Azilian phases may be exaggerated. In such a way, the situation at the end of the Pleistocene in France may reflect that of the Iberian Peninsula, where the relative subtlety of the transition there has previously been noted. While a shift from specialization to diversification has been noted in Cantabrian Spain (Aura et al., 1998), the less abrupt nature of this shift has also been observed, with Spain generally regarded as facing the end of the ice age in a less dramatic manner: *When the Ice Age world ended - dramatically in France and more subtely in Iberia...* (Aura et al., 1998). I will be examining the nature of the Magdalenian-Azilian transition in France in later chapters, as data produced for this thesis produced some interesting results on the topic.

Dating the Azilian

A summed probability distribution was obtained, to assess the range occupied by the Azilian. Dates for the Azilian were obtained from the sites of; Borie del Rey, Pech de Cavenie, Chez Jugie, Le Chien, Pont d'Ambon, Quéroy, Renardières, Pégourié and Sanglier.

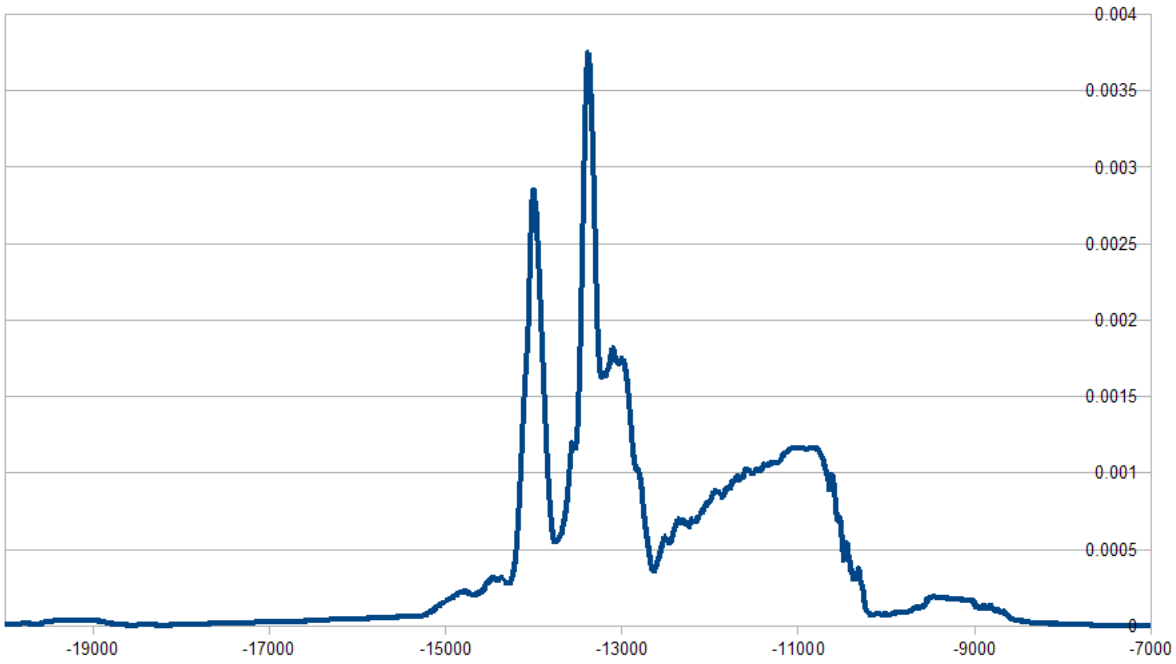

Figure 3.11: Summed Probability Distribution for the Azilian of Southwest France. Data from the sites of: Borie del Rey, Pech de Cavenie, Chez Jugie, Le Chien, Pont d'Ambon, Quéroy, Renardières, Pégourié and Sanglier. Radiocarbon dates, and their associated technocomplexes, are given in Appendix D.

§ 3.4 Summary of Technocomplexes

In summary, the technocomplexes that are relevant to this thesis are; the Aurignacian, Gravettian, Solutrean, Badegoulian, Magdalenian and Azilian. These are outlined in Table 3.4, which illustrates the key dates, tools and sites for these phases.

Table 3.4: Summary of Technocomplexes

Technocomplex	Dates (uncal BP)	Key Tools	Key Sites
Aurignacian	40,000 - 28,000	Carinate scrapers, split-base bone points. Scrapers dominate over burins.	La Ferrassie, Castanet, Abri Pataud
Gravettian	28,000 - 21,000	Gravette points, Noailles and Font-Robert points. Burins dominate over scrapers.	La Ferrassie, Laugerie Haute, Abri Pataud
Solutrean	21,000 - 18,000	Willow and laurel leaf points, Shouldered points. Scrapers dominate over burins.	Jamblancs (Jean Blancs), Combe Saunière.
Badegoulian	18,000 - 16,000	Raclettes. Scrapers dominate over burins	Badegoule, Les Peyrugues, Le Placard
Magdalenian	18,000 - 11,000	Bone harpoons. Burins dominate over scrapers	La Madeleine, Laugerie Haute.
Azilian	12,000 - 10,000	Azilian points. Scrapers dominate over burins	Pont d'Ambon, Pégourié.

§ 3.5 Settlement

3.5.1 Settlement in France

While this study will focus on the Southwest France region, it is worth taking some time to consider this small corner of Europe in its wider context. In terms of settlement, much of northern Europe sees occupation during the Early Upper Palaeolithic and populations only abandon it towards the Last Glacial Maximum. France overall is generally dominated by Southwest France throughout much of the Upper Palaeolithic, with this domination only coming to an end in the Late Glacial with the Magdalenian.

For this reason, for ease of description, we may regard the Southwest region as the 'core' region within France, with other areas serving as a 'periphery'. It can be seen from settlement maps that activity in the peripheral regions prior to and after the LGM are substantially higher than during this bracing phase of the Upper Palaeolithic. The images below, taken from (Demars, 1996) illustrate the occupation of France during several major technocomplexes. The Magdalenian explosion in activity across France is obvious, however there is also an apparent decline in activity from the Gravettian to the Solutrean in the peripheral zones, with many northern outposts disappearing.

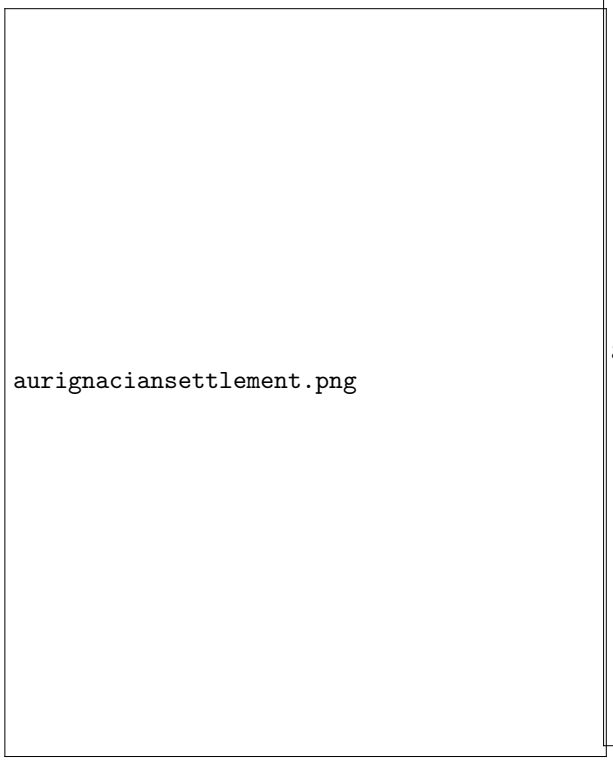

Figure 3.12: Aurignacian settlement in France. Image from (Demars, 1996)

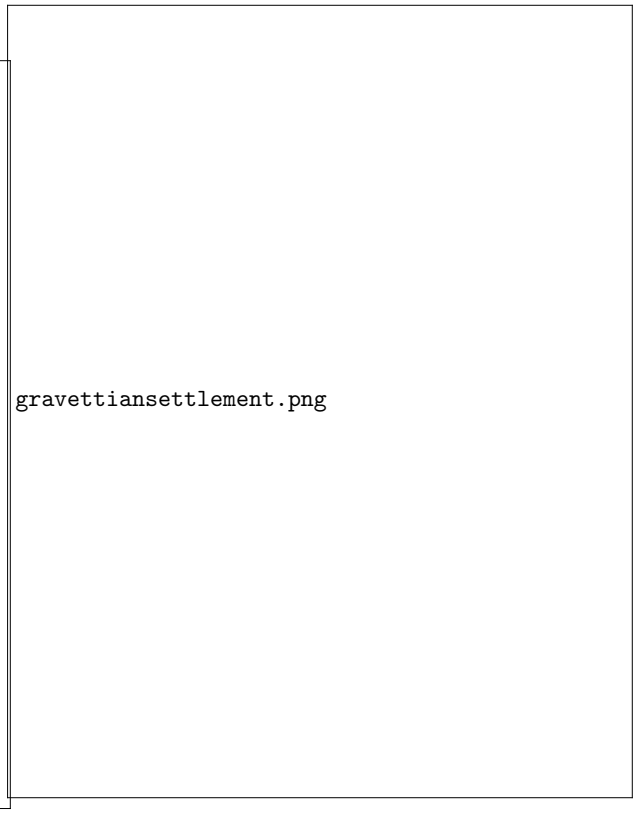

Figure 3.13: Gravettian settlement in France. Image from (Demars, 1996)

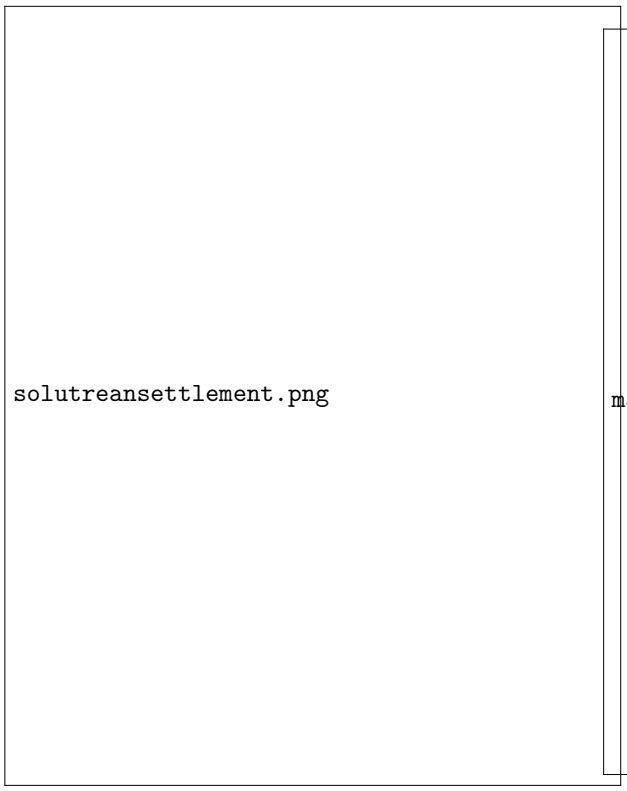

Figure 3.14: Solutrean settlement in France. Image from (Demars, 1996)

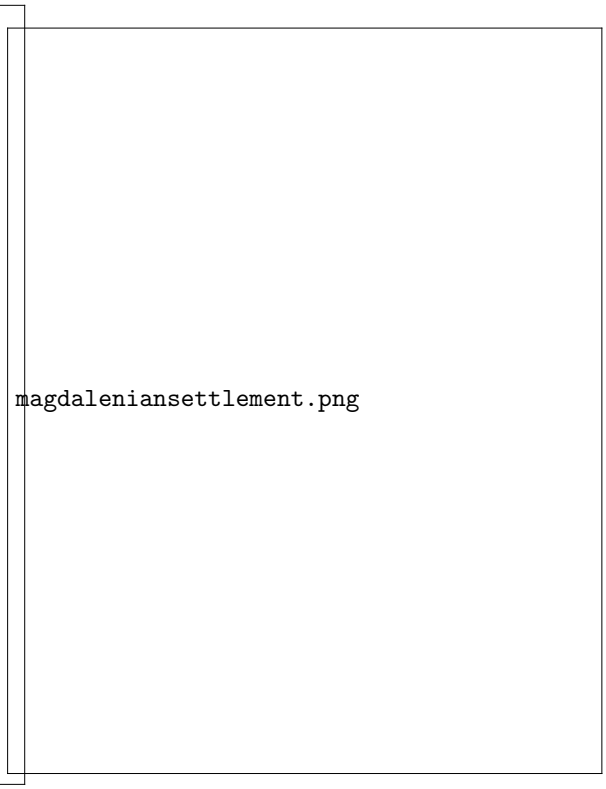

Figure 3.15: Magdalenian settlement in France. Image from (Demars, 1996)

3.5.2 Regional Settlement

Site counts and distributions here are taken from data from Pierre-Yves Demars' extensive archaeological database for Central and Western Europe. The database includes all published and many unpublished Upper Palaeolithic sites in the region, which Demars believes accounts for approximately 95 % of known locales. The approximate site/time density is also shown and I calculated this based on the estimated duration of each technocomplex. I also applied the taphonomic correction model of (Surovell et al., 2009) to the site frequencies. I have outlined this taphonomic correction approach in the methods chapter, as it is used in many sections of this thesis. However, I also felt it necessary to apply the curve at this early stage in proceedings, so will quickly outline it here. To briefly summarize, the correction method corrects for the gradual taphonomic erosion of older archaeological material. These taphonomic processes frequently create

the appearance of population increase over time, when actually the only visible signal is that of gradual destruction of material over time. You can see the taphonomically corrected site frequencies and site/time densities in Table 3.4. Taphonomic correction here makes some difference to site frequencies but very little difference to the demographic picture. We can see that when time is included as a factor, the Solutrean and Badegoulian have by far the greatest density of sites, interesting given their relative paucity in terms of absolute numbers. Likewise, while researchers frequently regard the Azilian as representing a 'crash', in both populations and lifestyles in southwest France, you will see from the site-time densities that this may not necessarily be the case. From site counts alone, prior to beginning my demographic investigation, it appears that the Solutrean and Badegoulian see the highest population density, followed by the Aurignacian and Gravettian. The Magdalenian, traditionally regarded as a time of 'population explosion' in prehistory has a relatively low density of sites when corrected for taphonomy and length of phase. While the Azilian does have the lowest density of sites in the whole Upper Palaeolithic period it is of the same order of magnitude and cannot be regarded as a population crash in the region on the basis of site counts alone. While Neanderthal demography is outside the scope of this thesis, it should be noted that Châtelperronian site-time densities may not be a particularly strong indicator of Neanderthal demography due to the virtually simultaneous use of other technocomplexes by this species. See Mellars and French (2011) for an analysis of Neanderthal demography on the basis of material culture evidence from several technocomplexes.

Table 3.5: Dates for Technocomplexes - uncalibrated radiocarbon years

Technocomplex	Age
Châtelperronian	40 - 35,000 BP
Aurignacian	40,000 - 28,000 BP
Gravettian	28,000 - 21,000 BP
Solutrean	21,000 - 18,000 BP
Badegoulian	18,000 - 16,000 BP
Magdalenian	18,000 - 11,000 BP
Azilian	12,000 - 10,000 BP

Table 3.6: Distribution of sites by Technocomplex. Corrected using method of Surovell et al. (2009)

Technocomplex	No. Sites	Sites/time	Corr. no. sites	Corr. sites/time
Châtelperronian	185	0.037	81.82	0.016
Aurignacian	392	0.033	152.46	0.013
Gravettian	399	0.057	101.53	0.015
Solutrean	403	0.134	76.81	0.026
Badegoulian	290	0.145	46.60	0.023
Magdalenian	524	0.074	69.32	0.010
Azilian	157	0.0785	148.34	0.074

Why is the Azilian regarded as a period of 'decline', given the apparent and immediate evidence to the contrary? Site/time densities, following taphonomic correction, are identical for these two industries. Traditional biases towards the Mesolithic (Price, 1987), and the role of the Azilian as a transitional industry towards this phase may play a part in the traditional view of demographic decline in the Azilian. However, while the two phases are starkly different in terms of lifestyle, settlement and subsistence (Mellars, 1985); but there is no *a priori* evidence for a *demographic* decline as such.

As well as the shifts in site numbers that occur temporally, shifts in settlement pattern also occur over time. The 'classic' region of the low Vézère Valley, whilst continuously occupied throughout the Upper Palaeolithic, does decline in dominance in certain periods. The region appears to experience its heydays in the most climatically rigorous phases , losing this dominance in more temperate phases (Demars, 1998). The Badegoulian (18000 - 16000 BP uncal), illustrates this point well, as not only does the Vézère lose its power with this technocomplex, but the Dordogne as a département sees a decline in settlement, with Gironde ascending to be the power-house of the Southwest. The Badegoulian also sees shifts in site-selection, with the majority of sites located in open-air locations. The Badegoulian, coinciding with the Lascaux Interstadial, represents such a temperate phase and contrasts dramatically with rigorous phases, such as the LGM , which coincides with the Solutrean technocomplex (21000-18000 BP uncal). The Dordogne and, in particular, the Vézère Valley, is the centre of Solutrean

occupation; with 30 % of sites found here (Demars, 1998). With the climatic upturn following the LGM, settlement again changes dramatically, and the Vézère once more loses its status, into the Magdalenian, river valleys to the North of the Vézére become populated, and open air sites flourish again.

White's (White, 1985) extensive study of Upper Palaeolithic settlement in the Périgord region also reveals some interesting patterns in site locations. As well as illustrating the close association between sites and rivers, White also demonstrated that the Solutrean rarely occurs as part of a continuous sequence. The Solutrean usually represents either the first or last occupation phase at a site and rarely occurs as part of a continuous sequence. Likewise the Magdalenian, while often associated with the Solutrean, also frequently occurs in pioneer settlements, with 75 % of Magdalenian occurrences found in new locations. These findings are in concurrence with Sonneville-Bordes' earlier conclusions. Additionally, White observed shifts in occupation over time; initial focus on the Vézère is replaced over time with populations moving north to the Isle Valley, and then the Dronne Valley. The settlement pattern proposed by White conforms to the general settlement model proposed by Zubrow (Zubrow, 1971), in which high population density in a region leads to gradual movement to less favourable areas. This is a logical model that is frequently used to explain hunter-gatherer movements and seems consistent with the data presented by White. This model will be revisited later on in this thesis, following further analysis of settlement patterns.

Figure 3.16 displays the locations of all Upper Palaeolithic sites contained in Demars (1996) extensive database of European archaeology, colour-coded according to techno-complex.

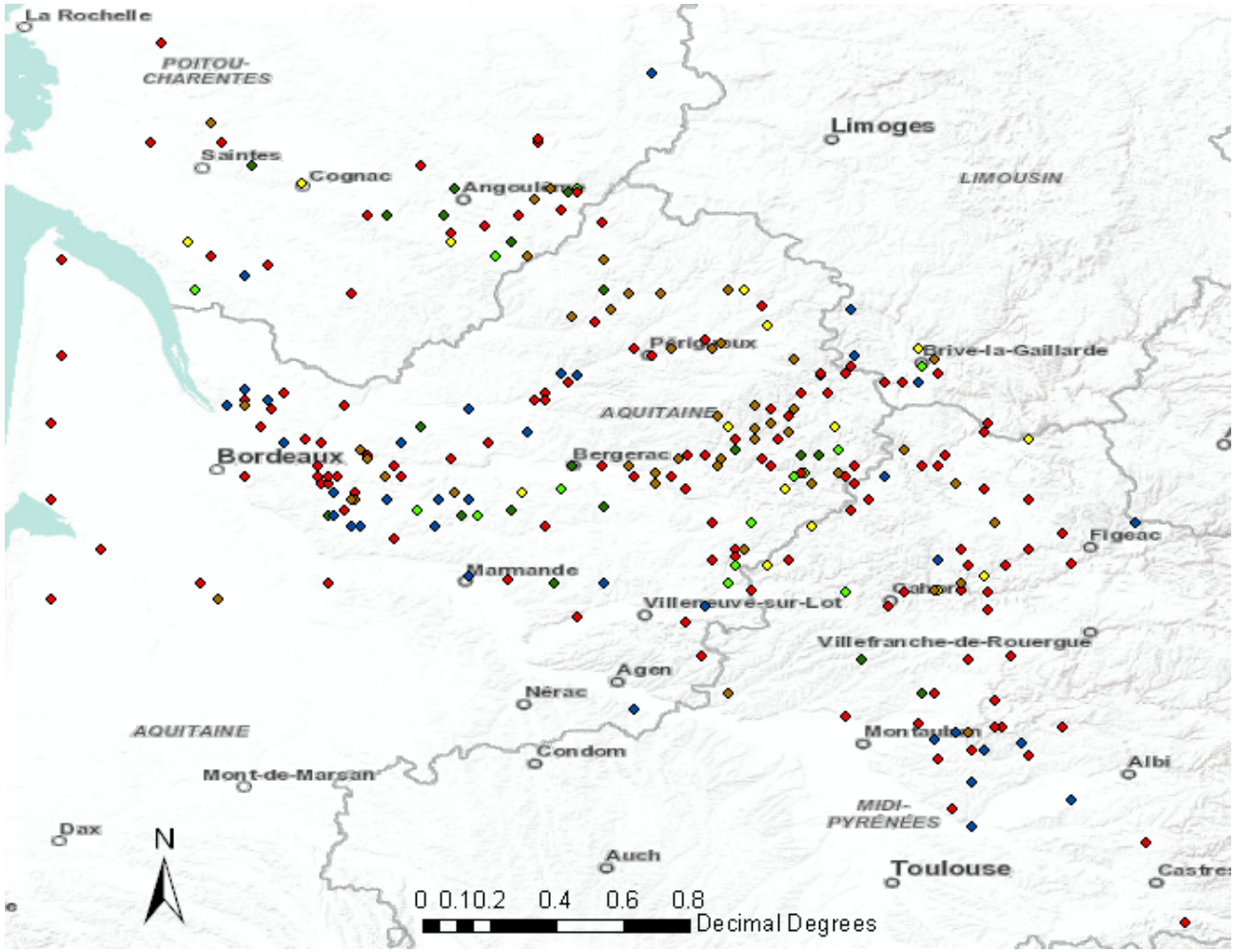

Figure 3.16: Distribution of Upper Palaeolithic sites in Southwest France by technocomplex. Dark green = Aurignacian. Bright green = Gravettian. Yellow = Solutrean. Blue = Badegoulian. Red = Magdalenian. Olive = Azilian. Data from P-Y Demars' archaeological database (Demars, 1996)

§ 3.6 Site Area

As well as considering the *frequencies* of site occurrences in order to estimate demographic parameters, previous researchers have given some consideration to the size of settlement locations. The following table, taken from (Mellars, 1973) depicts areal estimates for a number of Upper Palaeolithic locales. The data appears to suggest that there is a steady increase in site size throughout the Upper Palaeolithic trajectory. However, I would urge caution as it can be tricky to estimate the size of open air sites, such as Solvieux, in comparison to cave and shelter sites with more defined boundaries. In contrast to Mellars, White (White, 1985) suggested that both large and small sites are found in all Upper Palaeolithic subphases, arguing that both sorts of occurrences would be used for different parts of the seasonal round. If average site size did increase with time then not only would this suggest a steady increase in population density, but some change in social organization would also be necessary, given that hunter-gatherer group size tends to oscillate around a small mean. Population increase amongst modern hunter-gatherer groups tends to lead to 'budding off', rather than an increase in group size and therefore any increase in group size, as suggested by Mellars' interpretation, would necessitate drastic social reorganization and upheaval, though such huge social change in the Upper Palaeolithic is by no means precluded *a priori*.

I experimented with the use of site sizes as an indicator of population size in my masters thesis (Collins, 2008), using Naroll (1962)'s ethnographically derived estimates of numbers of individuals per m^2 of floor area. I decided against using the approach here, due to a number of problems with the method. It is difficult to estimate the extent of open air sites, for instance, which is a problem for working in phases where open air sites are common. However, it is still worth noting the overall trend towards larger sites in the Late Upper Palaeolithic, when compared to the Early and Middle Upper Palaeolithic.

Table 3.7: Site areal estimates, from (Mellars, 1973)

Period	Site	Size
Aurignacian	La Quina	$520m^2$
Aurignacian	Laussel	$600m^2$
Aurignacian	Abri Pataud	$500m^2$
Gravettian	Laussel	$720m^2$
Gravettian	Abri Pataud	$500m^2$
Gravettian	Les Vachons	$250m^2$
Gravettian	Laugerie Haute	$6300m^2$
Solutrean	Laugerie Haute	$6300m^2$
Solutrean	Badegoule	$1125m^2$
Magdalenian	Laugerie Haute	$6300m^2$
Magdalenian	La Madeleine	$5000m^2$
Magdalenian	Solvieux	$12,000m^2$

§ 3.7 Human Remains

Any demographic study must consider the bioarchaeological evidence for human remains in the region of study. Palaeodemography primarily takes its data from skeletal remains (Chamberlain, 2006) and for this reason may be distinguished from Archaeological Demography, which attempts to reconstruct past human demography from a variety of sources. Of course Palaeolithic human remains are woefully lacking, but there are some. And whilst we cannot hope to ascertain population densities and dynamics from the actual human remains available, study of the remains can furnish models through providing evidence for health and disease within the populations.

Upper Palaeolithic human remains are rare in Europe in general, but generally increase from the Aurignacian to the Gravettian with the advent of a complex pan-European system of burial, something which is not seen in the Gravettian of France (Pettitt, 2011). In total the Minimum Number of Individuals (MNI) for the entire Upper Palaeolithic period in France stands at just 300 and only eighteen of these are inhumations. The MNI for southwest France based on the material in the National Museum at Les Eyzies stands at just 17. Many of the surviving specimens from Palaeolithic France

are pathological, potentially indicating differential treatment of injured and disabled individuals. There is also some evidence for nutritional stress, in the form of enamel hypoplasia and harris lines on specimens, the evidence for such stress increases from the Early to the Late Upper Palaeolithic (Brennan, 1991), potentially reflecting climatic deterioration and resource stress.

§ 3.8 Changes in Resource Use across the Upper Palaeolithic

As outlined in Chapter Two, evidence for broad-spectrum food consumption, along with evidence for dietary shifts in prehistory can imply high local population densities. Stable isotope analysis conducted on Palaeolithic human remains from Europe suggests that marine resources were important in both the Early Upper Palaeolithic and the mid-Upper Palaeolithic, when compared to Middle Palaeolithic Neanderthal diets (Richards and Trinkaus, 2009) (Richards et al., 2001). This is certainly an interesting result and suggests that European mid-Upper Palaeolithic diets were boader-based than European Neanderthals. In accordance with the Broad-spectrum hypothesis the implication is that mid-Upper Palaeolithic populations were at greater densities than Middle Palaeolithic Neanderthal groups. A further stable isotope study conducted on Late Upper Palaeolithic individuals suggest that marine resources became especially important in this phase (Richards et al., 2005). However, it is worth noting that this research was conducted on skeletal material from the United Kingdom and it would be a bold leap to suggest that groups in France were also intensively exploiting marine resources based on this study.

The Upper Palaeolithic of Southwest France is largely characterized as *l'Age du Renne* due to the abundance of reindeer remains in assemblages. To this end, it is easy to view Palaeolithic hunters as highly specialized, with a static diet that did not change for thousands of years. While the dominance of reindeer and other herbivores in assemblages is absolutely apparent throughout most of the Upper Palaeolithic, there is also

some evidence for the inclusion of other species into the diet. In particular, it has been argued that salmon fishing was central to the economy of the region and allowed high population densities to be supported (Jochim, 1987), though this is contested somewhat with Pike-Tay et al. (1999) claiming that there is little evidence for intensive salmon exploitation in the Upper Palaeolithic of France, and that evidence for demographic change could instead reflect changes in landuse patterns. Fish remains in the Azilian of Pont d'Ambon are abundant and fish are known from the Noaillian of Abri Pataud. The centrality of bone harpoons to Magdalenian technology may make it appear that fishing was important in the Late Upper Palaeolithic, although the use of the term 'harpoon' may be misleading; as with most Upper Palaeolithic tools, we are not actually certain of their precise functional use. A study by Julien (1982) though, suggested that they were used as fishing spears, something which would suggest that aquatic resources *were* central to Late Upper Palaeolithic subsistence. Harpoons appear to have been used to disable prey whichwould otherwise readily escape, meaning that they would be ideal for catching fish (Román and Villaverde, 2012). In Cantabria there is a strong archaeological association between harpooon heads and fish remains and it does therefore seem likely that harpoons are related to the consumption of aquatic resources. There are also known depictions of fish in Upper Palaeolithic art, although, as previously discussed, the depiction of an animal in artwork is not necessarily indicative of its consumption. Isotopic analysis of twelve Magdalenian skeletons from the Les Eyzies region also demonstrated that three individuals had a maritime signal in their bone chemistry (Hayden et al., 1987); while this is obviously a low proportion of the skeletons sampled, it still suggests that some marine resources were being consumed. At present no stable isotope studies have been conducted on Early Upper Palaeolithic skeletons from Southwest France, therefore at present there are no results from bone chemistry for comparison with Hayden et al. (1987)'s results from the Late Upper Palaeolithic. Likewise, given the taphonomic and recovery problems which hinder the discovery of prehistoric fish bones, it is difficult to state whether an increase in consumption of

aquatic resources from the Early to Late Upper Palaeolithic is genuine. On the basis of current archaeological and isotopic evidence this would seem to be the case, but this may not be a genuine phenomenon. If the apparent shift to a broader-based diet *is* a genuine trend, the suggestion is that higher population densities were being supported in the Late Upper Palaeolithic. As well as the link between broad-based diets and high population densities, we are also aware that modern nomadic peoples who practice high levels of fishing are known to have amongst the highest population densities of any hunter-fisher-gatherer groups.

§ 3.9 Research Bias: A quick note

It is fair to say that the archaeology of Southwest France has received a great deal of attention in the past. There is a fair amount of clamouring from various corners to the effect that the archaeological record is skewed in favour of this region, eg (Rigaud and Simek, 1987). However, given that this thesis is solely concerned with the Southwest France region, we may treat any such bias, if it does exist, as a constant that will not affect our results. Equally, in Palaeolithic archaeology there is a tendency towards favouring 'older' sites in many instances; researchers are keen to find the 'first' evidence of virtually any human endeavour or occupation. It is possible that this is a problem in Palaeolithic archaeology, for instance with the selection of samples for radiocarbon dating and we should be aware of this. A final source of potential bias is taphonomic, and I have taken steps to address this natural bias throughout the analyses presented here. Ultimately, bias, both natural and human-introduced is a real phenomenon and we should be wary of it. I hope that I have taken sufficient steps to address potential bias in this work.

§ 3.10 Summary of Background Chapters

There are a variety of methods available for the study of prehistoric demography; site counts, 'dates as data', genetic evidence and the use of ethnography. However, what is the current state of knowledge regarding population processes in Southwest France during the Upper Palaeolithic in particular? Based on current evidence it does appear that the region served as a refuge zone into which populations contracted during inhospitable phases. The distribution of sites across France, alongside the apparent concentration of sites in the Southwest France region during the Solutrean phase, even after the taphonomic correction of these distributions all support the refugium concept. Likewise, the unique archaeology of this phase suggests that interesting social forces are at work. Given the theoretical link between population pressure and technological innovation, it does appear, prior to further analysis, that there is strong evidence for the refugium concept. This prior data also demonstrates that population is high in the Magdalenian, with both large numbers of sites and a seeming increase in the average size of sites. Again, given that the proliferation of artistic endeavours in largely restricted to this late Palaeolithic phase, the link between population and technology is, anecdotally at least, supported.

Given the available archaeological evidence prior to embarking on original research for this thesis, I believe that population in Southwest France is high during the Later Upper Palaeolithic; in the Solutrean and Magdalenian phases. However, in the light of the apparent causal link between climatic variables, as seen through ethnographic data, how can we assume populations would have responded to climatic stimulus in the Upper Palaeolithic? One would predict high populations in the Badegoulian, Late Magdalenian and Azilian, phases with generally warmer climates. The Solutrean, by contrast would be expected, based on climatic information alone, to have a comparatively reduced population. Prior to embarking on demographic research in the region, based on existing evidence alone, there appears to be a conflict between the archaeological and

climatic data. It seems, therefore, that the general, positive linear, relationship between climate and demography is interrupted in this instance. Equally, prior pan-European studies into demic contraction and expansion in the Upper Palaeolithic all point to the abandonment of northern latitudes during the LGM and the clustering of remaining human populations into southern refugia. Clearly, something very interesting is taking place and the normal 'rules' governing hunter-gatherer populations are not applying. It is now up to us to further test both the evidence for population dynamics in the Upper Palaeolithic and the theoretical link between population and innovation before any further speculation can take place regarding the apparent unique circumstances experienced by the study region in the extreme climatic conditions of the Pleistocene.

Chapter 4

Materials and Methods

This chapter introduces the methods and materials employed in this thesis. I provide a brief overview of the development of each method and a summary of their past applications to prehistoric demography, along with justifications for their inclusion in this study. In some instances, I try to further develop the methods, leading to a degree of 'feedback' between the methods and results chapters, which is unavoidable. I take some time to reflect on the methods developed here, in the light of the results that they produce, in the discussion chapter.

§ 4.1 Radiocarbon Methods

Archaeologists predominantly use radiocarbon dates for temporally placing horizons and establishing stratigraphic relationships. However, there has been a growing trend towards the use of radiocarbon dates to identify demographic signals in the past. The general premise is that cultural carbon is a by-product of human activity, which will therefore increase in the archaeological record as a function of increasing population size.

Radiocarbon dates provide valuable sources of evidence regarding human presence in the past and are abundant for the study region. The incorporation of both spatial

and temporal information into a single data point makes them useful for demographic studies, as we are able to observe expansions and contractions through space and time. In this section, I provide a general background to the radiocarbon method, as well as to some of the methods available for calibration of these dates, which are mainly Bayesian in form. I then develop and discuss a method for selecting prior probabilities for incorporation into Bayesian models, based on prior information regarding reliability.

W.F. Libby developed the technique of radiocarbon dating in the mid-20th century, publishing his identification of radiocarbon in living organisms in 1946 (Libby, 1946), followed by a stream of early dates (Arnold and Libby, 1949) (Arnold and Libby, 1951) and a Nobel Prize in 1960. The technique has dramatically altered the discipline of archaeology and it is one of the most significant developments in archaeological science, allowing the absolute dating of events in human history within the permitted range of the method. A study of human settlement and expansion in the Upper Palaeolithic would simply not be possible without the aid of radiocarbon dating.

For a more complete discussion of the scientific principles behind radiocarbon dating, the reader is directed to Taylor (1987). However, the radiocarbon dating method is essentially based on the principle that all living things contain the radioactive isotope ^{14}C, which is present in considerably smaller quantities than the stable isotopes ^{12}C and ^{13}C. Decay of ^{14}C occurs at a relatively constant rate and thus the date of the death of an organism can be dated. However, here the simplicity of the method ends, as a great deal of biological and physical processes will affect the initial ^{14}C content of a material. Notably, material which is of marine derivation will obtain carbon from the ocean, 'old carbon' depleted in ^{14}C through natural decay. Thus, marine derived materials will appear 'older' than terrestrial samples of a similar age. This is just a single, simple example of the effect of material choice on radiometric dating, and there are a great many processes which may alter the initial ^{14}C content of a sample.

The development of the radiocarbon method was a watershed moment in archaeology. However, a second, equally significant event was the development of the accelerator

mass spectrometer method (AMS). Prior to this, it had been necessary to count the decaying particles with the use of a Geiger counter. At present there are three main methods of measuring radiocarbon content in a sample; gas-proportional counting, liquid scintillation, and AMS. The former two are generally referred to under the umbrella-phrase of 'conventional dating'. Archaeologists and prehistorians generally regard AMS dating as superior to the alternative methods; there is a perception that a lesser degree of contamination will occur during AMS dating, as it requires a much smaller minimum sample size. However, as we shall see later on in this chapter, the picture is slightly more complicated than this and AMS dates are not always more reliable, though this issue needs further investigation.

Pretreatment methods have also developed over time. The introduction of ultrafiltration in recent years significantly affected radiocarbon results. This pretreatment method has been routinely applied at the Oxford AMS facility since 2000 and has been seen to improve the removal of contaminants prior to analysis (Higham et al., 2006).

Many issues affect the reporting of radiocarbon dates. Format may vary between journals and even the half-life of ^{14}C, essential for calculation of the radiocarbon age, has been subject to change. Libby initially calculated an average half-life of 5568 ± 30. Later on a new half-life of 5730 ± 40 was adopted by some in the radiocarbon community, although journals such as *Radiocarbon* continued to use the Libby half-life (Olsson, 2009). Debate over the choice of half-life was one of the first, but hardly the last, controversial topics in the reporting of radiocarbon measurements. A further historical issue in the reporting of radiocarbon determinations comes from *Radiocarbon*'s decision to convert dates to AD and BC years, a practice which continued until 1977 and can possibly causing confusion when dealing with datelists. Additionally, Antiquity introduced the use of BP versus bp notation to indicate calibrated and uncalibrated dates respectively, though the adoption of this notation varies.

Further complications in reporting also arise from the correction of dates to account for reservoir, or other, effects. (Craig, 1954) demonstrated that, conveniently, fractionation

undergone by ^{14}C is twice that of ^{13}C. This discovery has allowed ^{14}C determinations to be corrected for any fractionation occurring during preparation and measurement, through the measurement of stable isotopes in the sample. Determinations are usually normalized to a $\delta^{13}C$ value of $-25‰$, the mean value for C_3 plants. However, taking stable isotope measurements alongside ^{14}C determinations is far from the norm and datelists should be checked to see if ^{13}C normalization has taken place. Even at major radiocarbon laboratories, the consistent measurement of $^{13}C/^{12}C$ ratios is only a recent development, beginning around the year 2000 at the Oxford Radiocarbon Unit (Higham, 2010). Correction of dates for the Suess effect, the anthropogenic addition of carbon to the atmosphere through the burning of radiogenically 'dead' fossil fuels (Keeling, 1979), may also confuse datelists.

4.1.1 Calibration

Since the early days of radiocarbon dating it was apparent that ^{14}C determinations were not directly representative of calendar years. Since the early tree-ring data-set calibration curves, an enormous number of dating techniques have been employed to relate determinations to calendar years.

In order to translate a radiocarbon determination into an actual calendar date calibration is necessary. This is because the proportion of ^{14}C in the atmosphere has fluctuated over time, so a direct radiocarbon date will not correspond to a calendar date. In order to calibrate a radiocarbon date, the laboratory measurement error is first modelled with a Gaussian distribution. This Gaussian distribution is then utilized to obtain the 'wiggly' distribution that is characteristic of a calibrated radiocarbon date. Figures 4.1 and 4.2 are images of calibrated radiocarbon; graphical depictions of the calibration process are contained in these images. The Gaussian distribution shown on the left-hand side of the image is the uncalibrated date. The calibration curve (IntCal09) runs diagonally across the image (Reimer et al., 2009). The calibrated date is 'read off' of the curve from the normal distribution, and the calibrated date is produced.

The resolution of the calibrated date will depend both on the standard deviation of the uncalibrated date and the area of the calibration curve involved. Yet the shape of the calibration curve still has a large impact upon the shape of the calibrated probability distribution. Several areas of the curve contain large plateaus, where a range of calendar dates have indistinguishable ^{14}C signatures. Steeper areas of the curve will have the opposite effect on calibrated date ranges. As such, the shape of a calibrated date is largely determined by the area of the calibration curve involved. This is one criticism levelled at the 'dates as data' approach, which I will deal with in Chapter Five.

Figures 4.1 and 4.2 depict the effect of the curve and standard deviations on the calibration of some dates, produced in Oxcal. The effect of very large standard deviations on the distribution is evident.

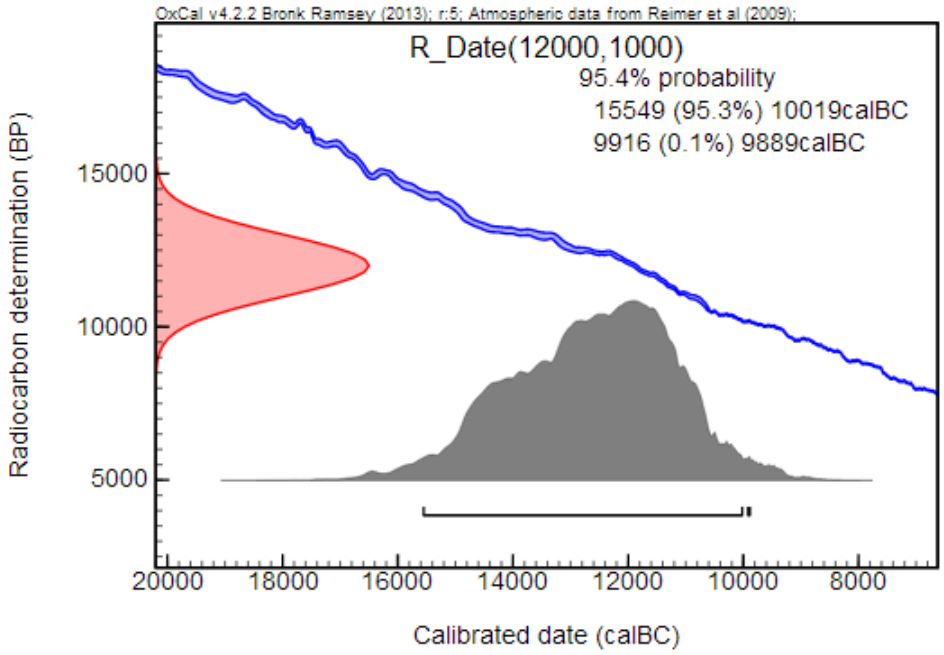

Figure 4.1: Simulated calibrated date with very large standard deviation

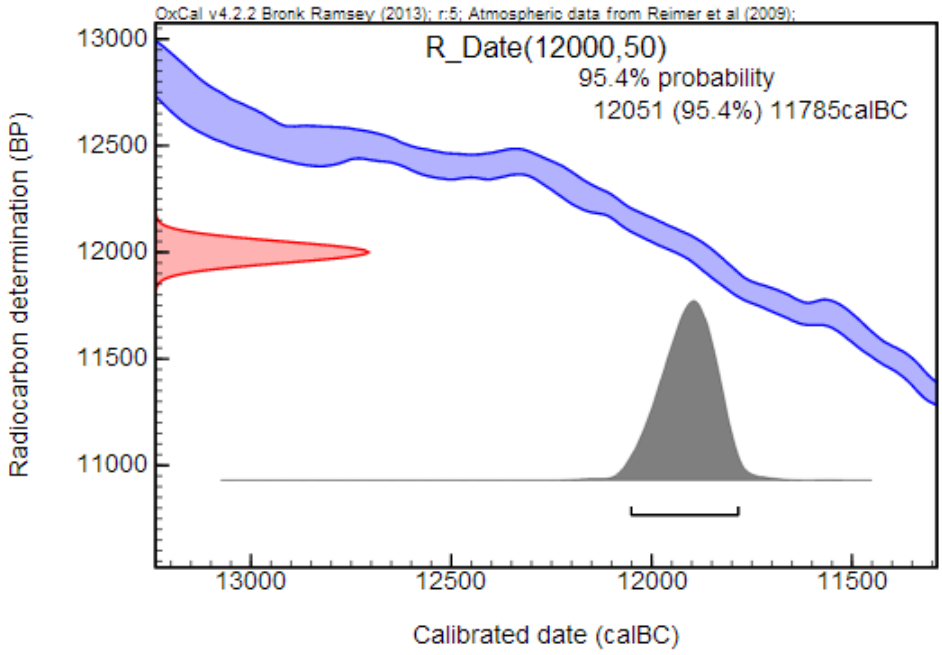

Figure 4.2: Simulated calibrated date with smaller standard deviation

The gradient of the calibration curve has a large impact on the shape of the calibrated distribution. Figures 4.3 and 4.4 indicate two radiocarbon dates with identical standard deviations. While the total ranges of the two calibrated dates are of a similar order of magnitude, note the wide peak for the second date.

The latest calibration curve available now extends the range of time that may be linked to a calendar age back to 50,000 BP for both terrestrial and marine samples (Reimer et al., 2009), meaning that all radiocarbon dates used in this study can be calibrated. This particular curve was created from a range of data sources, including tree-ring data up until 12.5 k BP and a variety of marine sources beyond this date. Formerly, whilst some calibration curves did extend back to this age, such as the Fairbanks *et al* curve based on uranium-series dating of corals (Fairbanks et al., 2005), they were not widely accepted or incorporated into calibration software. When calibrating, it is essential to use the correct curve for the samples reservoir origin, whether marine or terrestrial. With the introduction of Bayesian statistics to calibration, the posterior

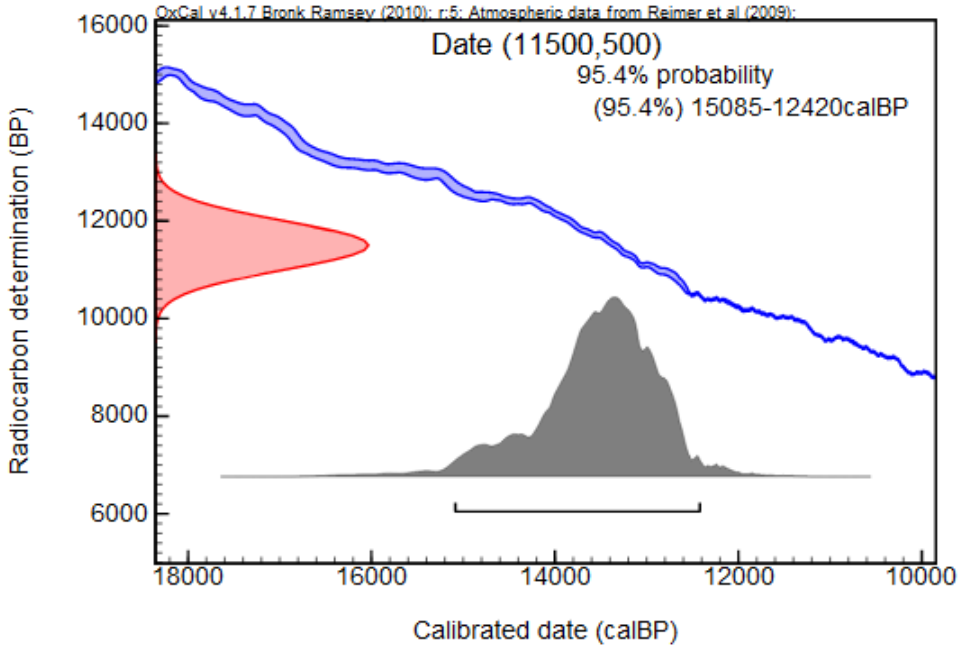

Figure 4.3: Calibrated date 11500 ± 250

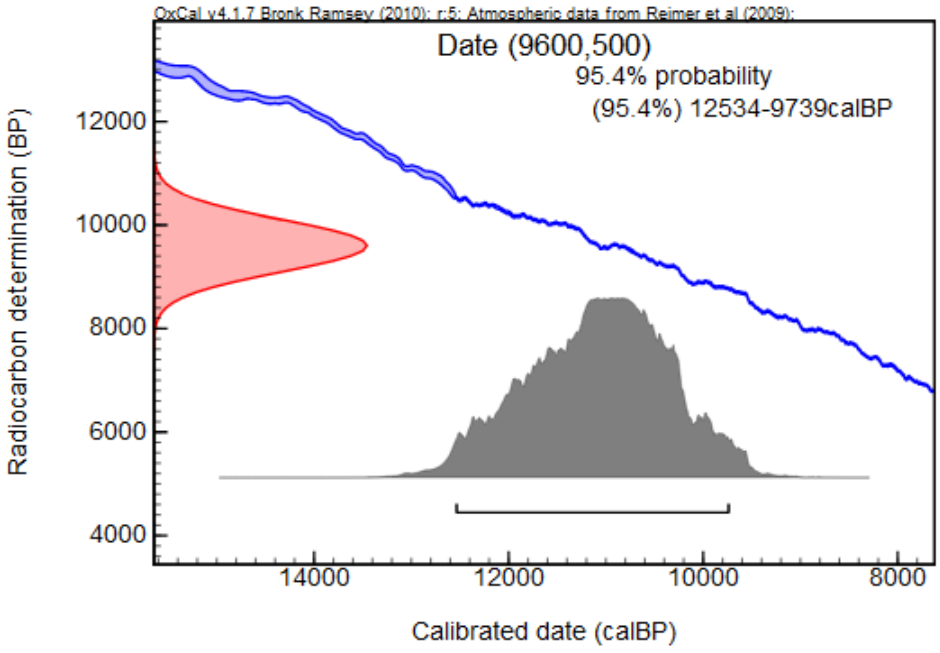

Figure 4.4: Calibrated date 10700 ± 250

probability distribution of the calendar age can be greatly reduced in range, increasing the resolution with which we observe the past. The imminent publication of a new calibration curve, IntCal13, is likely to further change the existing radiocarbon picture. We should be aware of this potential instability and that the introduction of a new curve can dramatically alter one's results.

The application of Bayesian statistics to the field of radiocarbon calibration has dramatically changed approaches to dating (Bayliss, 2009). Bayes' Theorem provides a method for formally using all available information to calculate the probability of an event. Bayesian statisticians accept that the probability of an event is dependent on the current state of knowledge regarding the event. In this sense, Bayesian probability is a form of conditional probability. Bayesian inference is suitable to archaeological applications, such as in dealing with dates, due to the wealth of information, which may accompany a sample. A sample may be excavated from a stratigraphic context and accompanied by informative artefacts; information gleaned from such additional data can be built into the Bayesian model, in the form of *priors*; 'prior probabilities' given the available information. The product of a Bayesian analysis is a *posterior probability*. Priors can be repeatedly updated, with former posterior probabilities becoming prior probabilities.

Bayes Theorem states that:

$$P(E1|E2) = \frac{P(E2|E1)}{P(E2)}P(E1) \tag{4.1}$$

where $P(E_1)$ is the prior probability of an event occurring and $P(E_1|E_2)$ is the posterior probability, the ultimate output of Bayesian Inference. The *likelihood* is given by$P(E_2)|P(E_1)$ (Buck et al., 1996).

The formula allows one to arrive at a posterior probability distribution, which is the conditional probability of an event, given all the available information. This additional information can be built into the probability calculation in a formal manner. Bayesian

statistics have impacted on radiocarbon dating for two reasons. First, Bayesian statistics have been instrumental in devising the calibration curves. Secondly, a Bayesian framework can be used to calibrate radiocarbon dates on the basis of additional information, such as stratigraphy; in archaeological situations, a great deal of prior information is obtained from stratigraphic sequences and contexts. I use this latter approach heavily in this thesis and outline it in later sections. Further prior information about the reliability of the date can be obtained from information regarding the dating of the sample. The approach that I use in this thesis involves assessing the reliability of a radiocarbon determination, based on information from the original archaeological and analytical publications. I develop criteria for scoring the reliability of a date, I then transform this score into a prior probability for use in the outlier models already available in statistical software, such as Oxcal (Ramsey, 2009b)(Ramsey, 2009a). I am able to furnish these models with further information, regarding the stratigraphy of the sites. Thus, as complete a picture as possible is built out of available information, regarding both the radiocarbon date and the site that it is from. I outline this scoring system in a later section and evaluate its use.

4.1.2 Radiocarbon Dates as Proxies for Human Activity

Two general approaches to 'dates as data' are used in prehistoric archaeology and they have both shared and distinct limitations. The first approach introduced by Rick (1987) involves plotting radiocarbon dates according to 'time-bins' and interpreting any peaks and troughs in the resulting curve as representative of changing activity levels in the past. As radiocarbon calibration is a probabilistic process, the conversion of a calibrated probability distribution into a single point value can be an enormous over-simplification. However, the alternative approach, which involves the summing together of probability distributions from calibrated dates, has been heavily criticized from a theoretical stand-point and is the subject of much debate (Blackwell and Buck, 2003). I am able to demonstrate in the results section that it is, however, a valid approach to

prehistoric demography. Both 'dates as data' approaches have to cope with research bias and taphonomic bias in the radiocarbon record and such biases can heavily obscure any demographic signal. Some methods have been developed to mitigate the effects of these biases and I have already utilized an approach to taphonomic correction in Chapter Three. This method is outlined in greater detail in section 4.1.3. Despite some limitations, it seems that we are unable to ignore radiocarbon dates as a source of demographic information. The many existing studies that make use of radiocarbon dates as a source of demographic information exemplify the usefulness of the 'dates as data' approach.

4.1.3 Taphonomic Correction

One criticism that can be levelled at attempts to access prehistoric demography through archaeological remains is that, due to the impact of destructive processes, more recent material is more likely to survive than older material. This means that if material remains are used as proxies for prehistoric populations then it will appear that population is constantly increasing over time, when actually this upwards trend in material remains is caused by taphonomic processes, rather than demographic ones. This taphonomic effect was noted by (Surovell and Brantingham, 2007) and a correction curve was proposed by (Surovell et al., 2009). The correction curve was produced through comparison of two datasets; a database of radiocarbon dated volcanic sediments and the GISP2 record of volcanism. These two records are independent and comparison of the two allows the rate of taphonomic destruction of sediments to be known. Using this method, the following correction curve was produced by (Surovell et al., 2009):

$$n_t = 5.726442 * 10^6 (t + 2176.4)^{-1.3925309} \tag{4.2}$$

$t = time$ and n_t =number of dates at t.

The Summed Probability Method

This method is one of the approaches to using 'dates as data' and by far the most controversial. Posterior probability distributions of calibrated dates are summed together, and the peaks and troughs are then interpreted as proxies for demographic events. The approach has been used by several researchers at the landscape-level (Shennan and Edinborough, 2007) (Tallavaara et al., 2010) (Gamble et al., 2005). Particularly pertinent is this last study, which not only utilized the summed probability method, but did so with regards to the Late Glacial population history of Europe. However as discussed above, many researchers are critical of the method (Blackwell and Buck, 2003).

In Oxcal the summed probability method is implemented through the use of the 'sum' function. The implementation of this function is described in the Oxcal online manual as such; 'the effect of this form of combination is to average the distributions and not to decrease the error margins as with other forms of combination' (Ramsey, 2005a). This is demonstrated in the following image; we see that the two dates are combined through the production of the average distribution of the two dates.

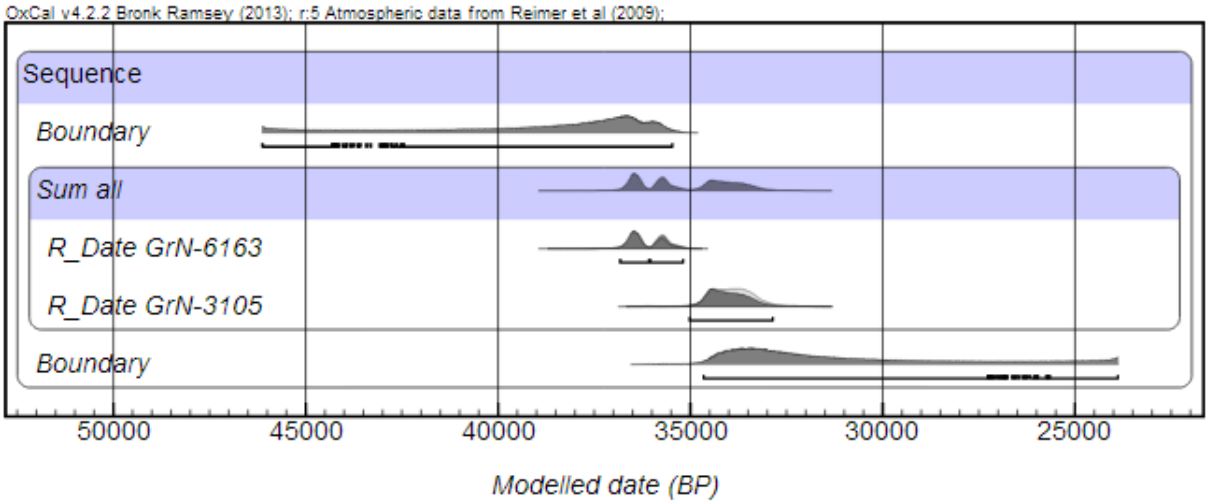

Figure 4.5: The effect of summing two radiocarbon dates in Oxcal

Chiverrell et al. (2011) heavily critiqued the summed probability method, on the basis that summed probability plots fail to distinguish between continuous occupation and

repeated short-lived occupations. However, Bayesian modelling of such dates, through the inclusion of stratigraphic information could allow the researcher to separate short-lived events from continuous occupation. The use of Bayesian models prior to the summing of distributions might help to overcome this problem, but it does not solve the issue of the heavy influence of the calibration curve on the shape of any summed probability distribution produced. A helpful assessment of the limitations and uses of the summed probability approach is provided by Williams (2012), who argues that, providing certain conditions are met, demographic signals *can* be obtained from the 'dates as data' approach. These conditions are as follows; a minimum of 500 radiocarbon dates should be used, sample size and average standard deviations must be reported and a moving average trendline should be used to offset the effects of the calibration curve. I have tried to follow these directions in the summed probability distributions that are produced in chapter five, over 500 dates are included in the overall distribution and the distribution is smoothed using a moving average. I have assessed the 'dates as data' method further, in the results chapter. It appears that, as with any technique in archaeology, any limitations should not necessarily preclude the use of a method. Instead, we must be aware of these limitations and work with them in mind. Methods may not be perfect, but very few are and in the field of prehistoric demography in particular, as many methods as possible should be used in the hope that where they converge a true demographic signal will be detected.

4.1.4 Calibration

All published radiocarbon dates used here were calibrated using Oxcal 4.0 (Ramsey, 2009b) and the Intcal09 terrestrial calibration curve (Reimer et al., 2009). For sites for which multiple radiocarbon dates were available, chronological models were constructed. Stratigraphic models can be constructed in Oxcal using the functions 'boundary' and 'phase', with dates obtained from the same phase of a site grouped together, separated by boundaries. Boundaries are calculated on the assumption that dates are

uniformly distributed throughout the sequence. Ramsey (2005b) provides good guidance as to the use of boundaries and phases in constructing Oxcal models.

Chronometric Hygiene

We can place all of the main causes of erroneous determinations into one of two camps. Either the sample material is unrelated to the archaeological event or horizon of interest, or it contains extraneous carbon, which may have arrived there through diagenesis or modern contamination. To avoid the latter problem, Libby and other early researchers recommended the use of materials with large, covalently bonded molecules, such as wood cellulose or charcoal, or other organic materials. Due to the largely inorganic nature of bone, this was not recommended as a sample material. However charcoal, whilst very unlikely to have been subject to diagenesis, is a material often found in small enough quantities to be stratigraphically mobile and therefore subject to dating errors of the former kind. With the introduction of AMS dating, sample sizes decreased and the risk of stratigraphically mobile samples being dated increased. Thus, when choosing sample materials, we must strike a balance between the suitability of the material in terms of resisting carbon exchange, against the likelihood that the material actually pertains to the correct context. In general, many materials that researchers previously rejected as unreliable sample matter are now regarded as usable; providing appropriate pretreatment is undertaken. Bone, in particular, whilst once regarded as a completely unreliable ^{14}C sample material, is now routinely used, following isolation of the organic fraction of the bone. Many contaminants can be eliminated through appropriate pretreatment processes, with acid and base treatments used to remove inorganic and organic contaminants respectively.

It is plainly apparent that not all radiocarbon dates will be as accurate as each other. When dealing with a database of dates and attempting to use them as data, it can be helpful to eliminate the 'deadwood'; the anomalous and misleading dates. However, I decided that rather than elimination, the systematic downgrading and downweighting

of suspect dates could allow for 'unreliable' dates to be dealt with in a formal manner. Many researchers have created similar systems and Spriggs (1989) and Spriggs and Anderson (1993) coined the phrase 'chronometric hygiene' to describe the process. Prior to this Waterbolk (1971) had discussed discrimination between dates and more recently Pettitt et al. (2003) lay out criteria for the assessment of radiocarbon dates.

Outlier Analysis and Prior Selection

The frequency of outliers in radiocarbon dating is commonly treated as 5 %, corresponding to the theoretical 1 in 20 probability of an error occurring by chance. This 0.05 prior was used by Higham et al. (2010) in their Bayesian analysis of the Grotte du Renne in Northern France and Bronk Ramsey, in his guide to using outlier analysis in Oxcal states that, '[the prior] defines the prior probability that the sample is an outlier; a typical value for this would be 0.05 for a 1 in 20 chance that the measurement needs to be shifted in some way' (Ramsey, 2009a). To explore the frequency of outliers in radiocarbon dating in general, I collated the results from radiocarbon intercomparison exercises and examined the frequencies of outliers amongst these results. The studies that I used for this were: the International Atomic Energy Agency Intercomparison Exercise 1990 (Rozanski et al., 1992), The Third International Radiocarbon Intercomparison Exercise (TIRI) (Scott, 2003a), the Fourth International Radiocarbon Intercomparison Exercise (FIRI) (Scott, 2003b), the Chauvet Cave Intercomparison Exercise (Cuzange et al., 2007) and the AMS and gas counter intercomparison exercise (Burleigh et al., 1986). Figure 4.6 depicts the distribution of outliers according to the frequencies of outliers in each sample *reported by the authors*.

The modal value is 10 %, which is clearly higher than the 5 % value that is widely given as the frequency of outliers in radiocarbon dating. The majority of studies used to create Figure 4.6 utilized the 1.5 x Inter-quartile range (IQR) method of outlier detection, with the exception of (Burleigh et al., 1986), which did not state the outlier detection method used. I therefore manually calculated outliers for results in (Burleigh

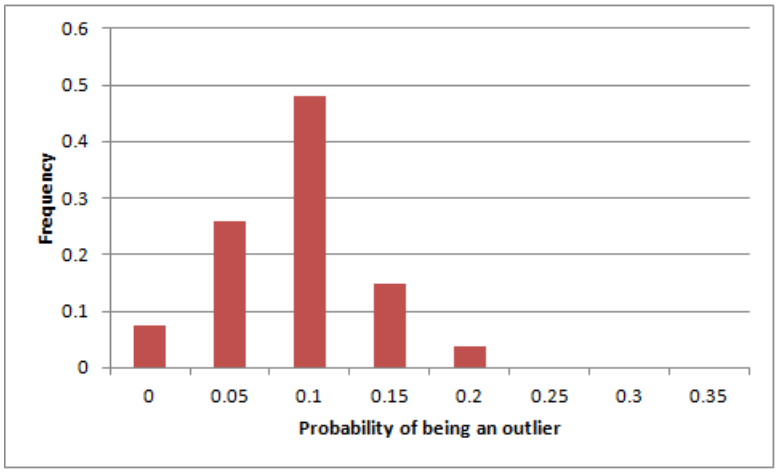

Figure 4.6: Distribution of radiocarbon outliers in data from (Rozanski et al., 1992), (Scott, 2003a) (Scott, 2003b), (Cuzange et al., 2007) and (Burleigh et al., 1986)

et al., 1986), using the 1.5 x IQR method from the raw data presented, but this made no difference to the distribution of outliers seen. Thus, it seems that a more realistic value for the frequency of outliers could be 10 %, rather than the 5 % value widely used as the prior probability of being an outlier, eg (Higham et al., 2011b). This is an interesting preliminary result that could be further explored in future.

I implemented outlier analysis in all stratigraphic models. The majority of published studies that use outlier analysis make use of uniform priors. However, I trialled the use of informative priors. The reasoning behind this was that all radiocarbon dates cannot realistically be assumed to be of equal reliability and that less reliable dates should not hold equal weight in chronological models. The premise that inequality exists amongst radiocarbon dates has previously been expressed by several authors, most notably Waterbolk (1971) and Pettitt et al. (2003), who attempted to construct check-lists by which radiocarbon dates could be assessed and graded for reliability, and then excluded if they failed to meet the expected criteria. These check-lists were mostly composed of factors such as the type of material dated (eg bone, burnt bone, shell), the method of dating and the archaeological fidelity of the stratigraphy. However, following an initial assessment of the radiocarbon dates from the region under study here I was able to observe empirically that many of the factors regarded as important by these

earlier researchers do not actually affect the reliability of a radiocarbon date. The key factor in the identification of outliers appears to be whether the sample was dated conventionally or through AMS.

I collected data regarding a variety of factors that are thought to influence the reliability of a radiocarbon date; method of dating, laboratory, decade dated and material dated. 276 dates from the study region, for which detailed chronological models could be built, were then modelled in Oxcal using outlier analysis. A uniform prior of 0.1 was used for every date. This meant that each date was modelled with a 10 % chance of being an outlier. I selected this uniform prior following observation of the frequencies of outliers in radiocarbon samples in general, as described above. I labelled dates as outliers if they were identified as > 95 % likely to be outliers by outlier analysis in Oxcal. Outliers were then assessed according to various variables, to observe which groups produced the greatest number of outliers and therefore can be regarded as least reliable.

While the frequency of outliers appeared to vary according to factors such as 'laboratory', the only factor to reveal a statistically significant difference as a result of a robust chi-square test in which 80 % of cells had an expected count of at least 5, was that of 'type of laboratory'. The proportions of outliers in various sample types are shown below, along with the results of chi-square tests in PASW statistics.

Table 4.1: Outliers by Laboratory Type

Laboratory type	No. samples	Percent outliers
AMS	100	11
Gas	117	3.5
Liquid	59	3.4

The only factor that was revealed to be significant following a robust chi-square test was that of 'Laboratory Type'. However, this does not necessarily indicate that this is the only factor affecting the probability of a sample being an outlier; it is likely that there are simply insufficient sample numbers available for the other criteria due to the

Table 4.2: Outliers by Laboratory Type: Chi-Square Test

	Value	df	Asymp. Sig (2-sided)
Pearson Chi-Square	6.357	2	.042
Likelihood Ratio	6.054	2	.048
N of Valid Cases	276		
1 cell (16.7 %) has expected count less than 5.			

Table 4.3: Outliers by Laboratory

Laboratory	No. samples	Percent outliers
AA	7	17
BM	8	34
Gif	47	9
GifA	11	10
GrN	70	10
Ly	51	0
OxA	82	12

Table 4.4: Outliers by Laboratory: Chi-Square Test

	Value	df	Asymp. Sig. (2-sided)
Pearson Chi-Square	17.559	6	.007
Likelihood Ratio	22.149	6	0.01
6 cells (42.9 %) have expected count less than 5.			

Table 4.5: Outliers by decade dated

Decade dated	No. samples	Percent outliers
1960	64	1.6
1970	31	0
1980	132	9
1990	32	18.5
2000	17	0

Table 4.6: Outliers by decade dated: Chi-Square Test

	Value	df	Asymp. Sig (2-sided)
Pearson Chi-Square	17.559	6	.007
Likelihood Ratio	22.149	6	.001
N of Valid Cases	276		
4 cells (40 %) have expected count less than 5.			

Table 4.7: Outliers by sample material

Decade dated	No. samples	Percent outliers
Amino acid	1	0
Bone	187	7.8
Burnt Bone	21	0
Charcoal	24	0
Collagen hydrolysate	7	14
Extract	8	0
Humic	2	0
Residue	8	0

Table 4.8: Outliers by Sample Material: Chi-Square Test

	Value	df	Asymp. Sig (2-sided)
Pearson Chi-Square	6.174	8	.628
Likelihood Ratio	9.949	8	.269
N of Valid Cases	276		
11 cells (61.1 %) have expected count less than 5.			

larger numbers of categories. I would therefore like to work on this topic further in future with a larger dataset. Unfortunately, it was not possible to increase the sample size for this study as I was limited to work with sites for which multiple radiocarbon dates are available. It would also be interesting to continue this research with reference to dates outside of Southwest France and across a larger swathe of time, in order to make stronger statements about the nature of radiocarbon dating in general. The distribution of outliers according to various factors are shown in Tables 4.1 to 4.8, along with their statistical analysis.

Curiously, the analysis suggests that conventional radiocarbon dates are *more* reliable than AMS dates. While this conflicts with the majority of received wisdom on the subject, there are plausible reasons why conventional radiocarbon dates may truly be more accurate than AMS dates. The accelerator method allows considerably smaller sample sizes to be submitted than those required by conventional dating methods. While this can reduce the potential for contamination, it does mean that samples may be submitted from small, potentially stratigraphically mobile artefacts and ecofacts. This is a plausible explanation for the results seen here. An alternative explanation involves pretreatment issues. Early AMS dating struggled with accurately dating bone samples, however the introduction of improved pretreatment methods, such as through the use of ultrafiltration, is thought to have rectified this problem. The vast majority of radiocarbon dates available from Southwest France are bone samples, so it is plausible that this could explain the disparity between the frequency of outliers in AMS and conventional dates in this thesis.

In order to further investigate *why* the AMS dates here produced more outliers, I subdivided the AMS samples into categories according to the decade that each sample was dated. Information on decade dated is readily available and is indicative of the pretreatment methods used; ultrafiltration was not widely applied until the year 2000. A chi-square test was performed in PASW statistics and the result was not significant. Thus we see that AMS dates do not improve over time, as would be expected if the high

frequency of outliers amongst the AMS samples was the result of improved pretreatment methods for bone samples. However, it is important to note that very few AMS dates in this study were produced after the year 2000, with most AMS dates from the 1980s and 1990s.

Decade * Outlier Crosstabulation

Count

		Outlier		Total
		No	Yes	
Decade	1980	57	6	63
	1990	18	5	23
	2000	14	0	14
Total		89	11	100

Table 4.9: Outliers in AMS dates by decade dated

Chi-Square Tests

	Value	df	Asymp. Sig. (2-sided)
Pearson Chi-Square	4.580[a]	2	.101
Likelihood Ratio	5.592	2	.061
N of Valid Cases	100		

a. 2 cells (33.3%) have expected count less than 5. The minimum expected count is 1.54.

Table 4.10: Chi-square test: Outliers in AMS dates by decade dated

On the basis of this, while I accept that the introduction of ultrafiltration probably did improve the reliability of AMS dating, for this study this does not seem to be relevant as most AMS dates included in the Bayesian models are older dates. There is no significant difference between AMS dates from the 1990s and the 2000s, even though 28% of 1990s AMS dates are outliers, and absolutely zero dates from the 2000s are outliers. The majority of AMS dates included in the study were dated prior to the year 2000. This means that if an AMS date and a conventional date are selected at random

from the region and the only information that we have about each date is the method of dating, on this basis we would regard the AMS date as less reliable. There are only a few AMS dates in the sample that are post-2000 and therefore more reliable than a typical AMS date. However, the disparity between AMS and conventional dates in this study can still be useful in this instance. Equally, other studies that chiefly utilize radiocarbon dates produced prior to 2000 could also assume that AMS dates will be less reliable than conventional dates. However, any study using a greater proportion of recent radiocarbon dates cannot make this assumption.

An analogy can be drawn between a person seeking to buy car insurance. A male will pay a higher premium than a female, as statistically males are more likely to suffer accidents than female drivers (this has actually changed recently, but the example still stands). This situation remains regardless of how careful an individual male may be when they are driving. If we include enough information about the individual (address, occupation, age, hours spent driving), we can get a better idea of how likely they are to crash. And if we were able to quantify some aspects of their personality and spatial awareness we would probably attain a near perfect understanding of their risk to the insurer. However, a male would rarely be charged a lower rate than a female as the group of male drivers, taken together, are a much greater risk. In my opinion, AMS dates are male drivers. AMS dates produced after the year 2000 are careful male drivers. It would be interesting for further work to be done on this topic to further resolve the issue of AMS reliability.

Prior Selection based on Outliers

Following the analysis of outlier frequencies according to sample type, I selected priors for use in outlier analysis based on available information regarding each sample, such as the laboratory involved and whether the sample was dated conventionally or through AMS. Priors ranged from 0.05 to 0.15, with AMS dates generally treated as less reliable than conventional dates, following the results of the analysis outlined above. Outlier

analysis in Oxcal downweights the impact of dates regarded as least reliable, meaning that anomalous dates do not need to be excluded. A full treatment of outlier analysis in Oxcal is provided in Ramsey (2009a).

Is the informative prior informative to the model?

To observe the impact of the prior selected on the model, the posterior distributions of dates modelled with uniform and informative priors were compared and the L2 norm was calculated. The image below depicts the 'before' and 'after' distributions for a radiocarbon date, OxA-583, with one distribution obtained from a model using informative priors, and another from a model using uniform priors. Generally the distributions differed by around 10 % and the ranges of the calibrated dates did not differ at all, though in the image below there is even less difference between the two distributions. Usually there was little difference to the modal value either. To this extent, we can see that the selection of an informative prior makes little difference to the mode or range of the calibrated date. However, approaches which make use of the *shape* of the calibrated distribution, such as the summed probability method, will be affected.

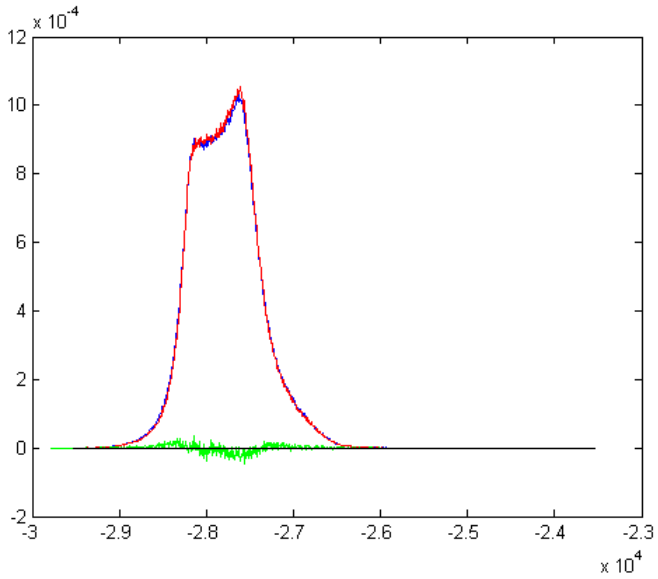

Figure 4.7: Difference between the calibrated distribution of a radiocarbon date, OxA583, run in a model using informative and uniform priors. The green line is the difference between the two distributions.

4.1.5 Model construction in Oxcal

As demonstrated above, the use of an informative prior made little difference to the overall chronological models for sites. It was therefore decided that a uniform prior of 0.05 should be used, as is generally done in the literature. Models were therefore constructed in Oxcal, using outlier analysis and a uniform prior of 0.05. Some example code is provided in the Appendix, to illustrate the way in which a typical model was constructed.

Where insufficient numbers of dates were available for individual sites to justify the construction of a model, I calibrated dates individually, unmodelled.

Following calibration, raw probability distribution data from all dates both modelled and unmodelled were collected from Oxcal and modal values and ranges of each distribution were obtained. Results are shown in Chapter Five.

§ 4.2 Kernel Density Estimation

Kernel Density Estimation (KDE), at its simplest produces smoothed, visually pleasing, histograms for univariate data (Baxter et al., 1997). However, bivariate KDEs can be used to represent archaeological data spatially, and to predict the density of artefacts or sites at locations that have not been sampled. In such instances, a Gaussian kernel is usually applied, which assumes that the data is normally distributed across space. The distribution will be centred over the point at which the sample was taken, with the tails of this distribution spreading away from the central point.

KDE can be useful for any spatial archaeology, where the aim is to display the intensity of occupation in a region on the basis of sampled data. The approach also allows you to prediction the density of archaeological finds in areas which have not been sampled, through interpolating from available data. Recent methodological development has expanded KDE so that it may also combine univariate and bivariate data, specifically with the intention of utilizing the probabilistic data contained in calibrated radiocarbon dates and depicting this information spatially (Grove, 2011). Collard et al. (2010) applied KDE in a similar manner to explore population dynamics in Britain during the Neolithic transition, through summing radiocarbon densities in 100 year time-bins for every point (x,y), in this way the spatial density of radiocarbon dates was taken as a proxy for human activity. However, this approach treated time as a discrete entity, through summing densities in 100-year bins. By contrast, the Grove approach treats time in a more continuous manner, as each year is analyzed individually. This approach has thus far only been applied to one dataset, that of radiocarbon dates from Mesolithic Cantabria, where Grove (2011) was able to observe changes in settlement and population density through the application of KDE to the radiocarbon data.

I applied Grove (2011)'s method here, as the spatial and temporal nature of the available data lent itself to this approach. Likewise, as this pioneering study utilized 60 radiocarbon dates in total, the expansion of the method to include the 500+ dates

available for the Upper Palaeolithic of Southwest France is an interesting methodological development.

To implement Grove (2011)'s method, I first calibrated radiocarbon dates, according to the method previously outlined. I then collated the raw data outputted from Oxcal and then averaged this data between individual sites, in order to first eliminate any potential research bias through the inclusion of multiple dates from single sites. I then arranged these averaged distributions from sites into data files, loaded into Matlab 7.2 and the following formula, from Grove (2011) was applied to the data:

$$\hat{f}_s(x,y) = \frac{1}{2\pi h^2}\Sigma v_i exp(-\frac{(x-X_i)^2+(y-Y_i)^2}{2h^2}) \tag{4.3}$$

where (x,y) are the coordinates of the point of interest and X_i, Y_i are the coordinates of a particular site. V is the sum of all integrals in the time slice of interest and h is the smoothing parameter, or bandwidth. In this manner the kernel density estimate for every point (x,y) was calculated for the time period (year BP) of interest. I have included the Matlab code used to create the KDEs in the appendix. Densities were then standardized and plotted on a surface chart in Matlab I repeated this process for every time-slice from 40,000 BP to 10,000 BP in order to visualise the intensity and organization of land-use in the study region. Through collating stills, it was possible to produce a video depicting land-use change throughout the period of interest. I was able to add this video into ArcGlobe 10 as a video layer, and the georeferenced movie that resulted is included with this thesis.

§ 4.3 Intra-site Lithic Density Method

As well as considering the density of sites or radiocarbon dates within a landscape, the actual density of artefacts within a site impacts on our perception of the intensity of landscape occupation. Intra-site artefact densities have been used by a number of authors as a means of accessing the relative intensity of site occupation. For example, Gamble (2002) looked at the density of lithics per surface area excavated at a number of Palaeolithic sites in Europe. I also trialled this approach for a few sites in the study region of Southwest France in my masters thesis (Collins, 2008). Lithics are certainly a good material to use in such studies, as they are incredibly durable and will not degrade with time, unlike anthropogenic carbon samples. It is worth noting, however, that we will still be dependent upon radiocarbon dates, on vulnerable organic artefacts, for dating lithic assemblages. Yet, in terms of obtaining demographic information from archaeological remains, durable artefacts will clearly be a useful material to use. However, a shortcoming of the surface area method is that is does not take into account the thickness of sediment in a level or the length of time represented by the level. An assemblage may have a very high density of lithic artefacts per metre squared, but actually represent a very long period of low-intensity at the site in question. Fortunately enough, the boundaries estimated as part of the Oxcal models produced can be used to 'frame' the archaeological data and subsequently allow the calculation of densities of lithic artefacts per square metre per annum. Modal values of calculated boundary distributions were used as the beginning and end points for each level, within which timeframe all the artefacts from that level were assumed to have accumulated. The need to estimate the duration of a level in order to calculate the *density* of lithic artefacts per m^3 necessitated the use of boundaries in Oxcal. If we had only required a point value to date each archaeological assemblage, then it would have been sufficient to average dates from the assemblage to obtain this date. However, the need to understand the length of time represented by levels at sites necessitated the boundary approach used

here.

To check the validity of using the boundary estimations as a measure of time, I examined the relationship between the estimated duration of levels and the thickness of sediment in that level. I expected that if the approach were valid, I would see a positive correlation between duration of level and thickness of sediment. Figure 4.8 illustrates the relationship between these two variables, for level durations up to 2000 years. Level duration is estimated from the Oxcal models produced for each site, as shown in the appendix, and level thickness was taken from the literature. Data is for La Ferrassie, levels J and E; Abri Pataud, levels 2,3,7,8,11,12 and 14; Laugerie Haute Est, levels 1, 23 and 31; Laugerie Haute Ouest, Lower, Middle and Upper Solutrean levels; Grotte XVI, level 0; Roc de Combe, levels 1,2,3,4,5,6 and 10; Flageolet I, levels II, IV, V, VI and IX; Le Facteur, levels 10, 11 and 21; La Rochette, levels 4 and 5; Cuzoul de Vers, levels 22,23,24,25 and 26; Le Piage, levels CE, F, G, J and K. This data is included as a table in the appendix.

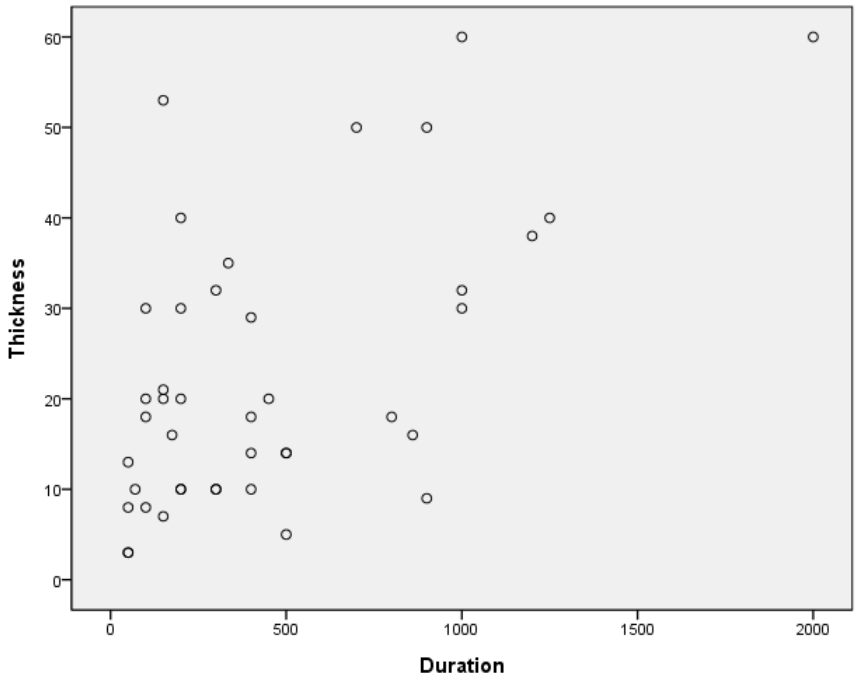

Figure 4.8: Level Duration and Thickness. Data on level thickness from the sites of La Ferrassie (Delporte, 1984), Abri Pataud (Farrand, 1995), Laugerie Haute Est (Bordes, 1958), Laugerie Haute Ouest (Peyrony and Peyrony, 1938), Grotte XVI (Hays, 1998), Roc de Combe (Labrot and Bordes, 1964), Flageolet I (Rigaud, 1969), Le Facteur (Delporte, 1968), La Rochette (Delporte, 1962), Cuzoul de Vers (Clottes and Giraud, 1996) and Le Piage (Champagne and Espitalié, 1981) Level duration calculated through production of site models, given in the appendix

A Pearson product moment correlation coefficient was calculated in PASW statistics for the dataset and it was confirmed that there is a strong positive correlation between the two variables, significant at the 0.01 level. This confirms the relationship between depth and time and suggests that the Oxcal boundary estimates are indeed valid for quantifying the duration of levels.

Table 4.11: Duration of level and thickness: correlation

		Duration	Thickness
Duration	Pearson Correlation	1	.577**
	Sig (2-tailed)		.000
	N	67	42
Thickness	Pearson Correlation	.577**	1
	Sig. (2-tailed)	.000	
	N	42	.48

After I ascertained that the Oxcal boundary calculations were satisfactory, I gathered data regarding the number of retouched tools from levels within the study region. Every level which has produced sufficient numbers of radiocarbon dates to anchor the level temporally was studied; where large sequences of dates are available estimates of the duration of the level could be produced in Oxcal. The total number of retouched tools was chosen over the use of simple numbers of worked stone in order to prevent the data being affected by the use of different recovery methods at excavations. Excavators of the 1960s, for example, often tended to overlook debitage.

§ 4.4 Diversity of lithic artefacts

Population pressure has been cited as a causal factor in human innovation, responsible for a great number of human 'firsts' and revolutions, as outlined in Chapter Two. Population pressure has been invoked as providing the impetus for humans to switch from hunting and gathering to farming during the Mesolithic (Cohen, 1979), as well as fuelling the development of the unique technocomplex that is the Solutrean (Smith, 1972).

To quickly recap; two potential mechanisms linking population pressure and innovation have been proposed and outlined in Chapter Two. In the first, population pressure is regarded as driving competition, in turn leading to increasing innovation as individuals solve problems critical to survival. This type of mechanism may equate to the Boserupian view of human innovation in the face of adversity. Alternatively, we can consider the likelihood of an innovation occurring as a density-dependent probability in human society, proportional to the number of individuals and their frequency of interaction. In this situation, a small group of sparsely populated individuals will have a diminished frequency of innovation compared to a densely populated group. The transmission of new ideas will also be more difficult in a sparsely populated area but will occur with relative ease in densely populated groups. The accumulation of cumulative knowledge within a society will be aided by population density, resulting in groups with an overall greater level of knowledge, both new and old. Overall, measures of cultural diversity can be regarded as suitable indicators of innovation levels and have been utilized as such in previous studies (Bocquet-Appel and Demars, 2000).

The key measures of variation in cultural diversity used in archaeology are all borrowed from ecology and measure either richness, evenness or heterogeneity (Bobrowsky and Ball, 1989). Richness is a simple enough concept, being the number of active categories in a dataset. Likewise, evenness is expressed most simply as the rank order of frequencies, from most represented to least represented. Heterogeneity, as a quantification of

both richness and evenness is more complex, but most usually expressed through the Shannon-Weaver index, given by

$$H = -\Sigma p_i \ln p_i \tag{4.4}$$

Where p_i is the proportion of the assemblage represented by the ith category.

Diversity measures, such as heterogeneity and richness, are commonly used by zooarchaeologists to indicate species diversity in faunal assemblages, eg (Nagaoka, 2001). However, one major problem with the use of such diversity measures is that they are heavily affected by sample size, which is clearly extremely problematic and can preclude any useful comparison between assemblages of different sizes. This is not such an issue for zooarchaeologists, who are likely to have relatively few categories represented in samples. However, when dealing with large numbers of categories, such as with Upper Palaeolithic stone tools, the sample size effect can be very problematic. The sample size effect is illustrated in Figure 4.9 for richness, based on the data collected from sites in Southwest France. Data came from 178 assemblages and citations are provided for these data sources in the appendix.

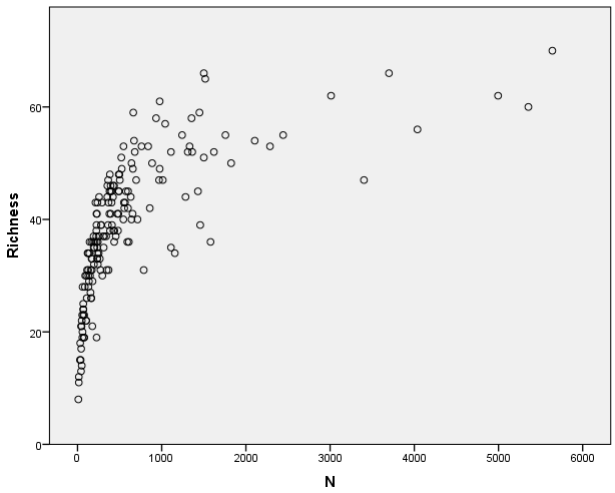

Figure 4.9: Relationship between sample size and richness

Heterogeneity is dependent upon the number of active categories, as the maximum

value of the index is $\ln(k)$, where k is the number of categories. The relationship between heterogeneity and richness (number of active categories) is shown below. Data sources given in appendix.

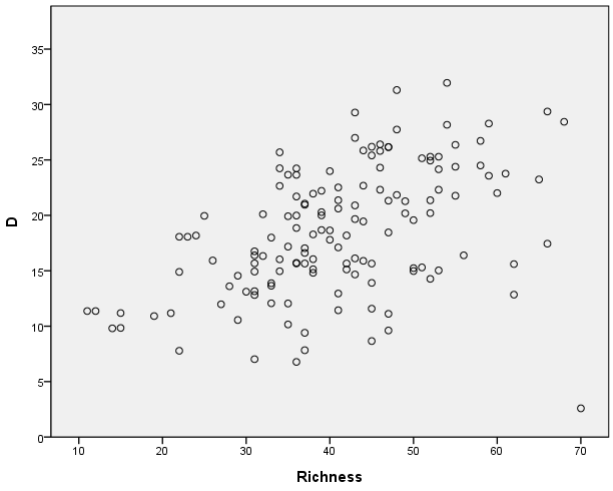

Figure 4.10: Relationship between richness and heterogeneity

To overcome the strong sample size effect evident in diversity measures, Kintigh (1989) devised a method for simulating diversity measures for samples of various sizes. In this manner, real-life assemblages can be compared to simulated assemblages of the same size and from the same time period. The frequency distribution of the relevant artefacts are first obtained, then assemblages are simulated conforming to this distribution and diversity measures are calculated. I adopted this approach here, in order to overcome the sample-size effect, which invariably affects diversity measures. In order to do so, I first collected lithic data from a selection of sites in the study region, using the typological system of de Sonneville-Bordes (1960). This system was chosen over others available as it is long-established and is applied by many researchers. Sonneville-Bordes herself was also such a prolific archaeologist that assemblages analysed by her alone would have been sufficient to obtain distributions of tool types for this thesis. The overwhelming majority of assemblages used in the analyses presented here were recorded using this precise system, with some exceptions. Some levels of Le Piage, recorded by Champagne, as well as assemblages pertaining to Delporte's excavations at La Ferrassie,

also featured an additional category of *lamelle appointée*, this category was subsumed into that of *divers*. Likewise, levels recorded from the site of Pégourié also featured additional categories, all of which were subsumed into that of *divers*. The only site that presented any real problems due to the typological system used was that of Roc de Marcamps. At this site the 105-type system was used, which differs so much from the 92-type system that this site had to be eventually excluded from the analyses. The 105-type system, which has not been officially published, does occasionally pop up in Upper Palaeolithic archaeology but unfortunately is not compatible with the 92-type system at all. Sonneville-Bordes' typology for Upper Palaeolithic stone tools is shown in the appendix.

Once I was able to establish the frequency distribution of tool types for each sub-phase of the Upper Palaeolithic, I was able to perform simulations, using Matlab 7.6 in the following manner. If a real-life Upper Solutrean assemblage featured 265 tools, a corresponding assemblage of 265 tools would be simulated based on the frequency distribution of tools from the Upper Solutrean. The simulation would then be repeated for a total of 1000 iterations and summary statistics on diversity measures collected from these iterations. I then calculated Observed minus Expected ratios for each assemblage; observed values being those recorded from the 'real life' assemblage and expected values being their simulated counterparts. The Matlab code used to create these simulations is included in the appendix.

The usefulness of diversity measures for measuring innovation can be defended on the grounds that human creativity is a statistical and social phenomenon. As discussed in Chapter Two, while individual creativity will contribute to innovation rates in societies, these rates are largely determined by the ability of the society at large to sustain the innovation. Therefore, the analysis of overall diversity within the society is a good proxy measure for innovation.

§ 4.5 Summary of Methods

To summarize, I use the following methods in this thesis:

- 'Dates as Data' in the form of summed probability distributions and histograms of modal values of individual dates as a proxy measure for population
- Intra-site lithic densities as a proxy measure for population
- Kernel Density Estimation as a means of visualizing population processes spatially and as a means of including the probabilistic nature of radiocarbon calibration into the visual interpretation of 'dates as data'
- Lithic diversity data as a proxy measure for human innovation

Chapter 5

Results

§ 5.1 Radiocarbon Results

Following data-collection and calibration, the raw data produced in Oxcal was collated and analysed. This data was in the form of probability distributions, with the probability mass function for each five year interval encompassed by the range of the calibrated date outputted. Using this data, I was able to transform the probability distribution into a point value through calculating the mode for each probability distribution. These results are depicted in Figure 5.1, plotted according to 1000 year interval time-bins.

As discussed previously, demographic signals may be obscured through taphonomic processes (Surovell and Brantingham, 2007) and this may be the case with the data under observation here. Some 'upswing' is visible in the chart in Figure 5.1, with the fewest dates observed from the earliest years of the Upper Palaeolithic, 41,000 BP to 32,000 BP. It is possible that any demographic signal may be obscured through the loss of older material to taphonomic processes. It was therefore necessary to apply the correction curve proposed by Surovell et al. (2009) in order to control this taphonomic signal. Equation 5.1, taken from Surovell et al. (2009) was applied to the data. The corrected results are shown in Figure 5.2.

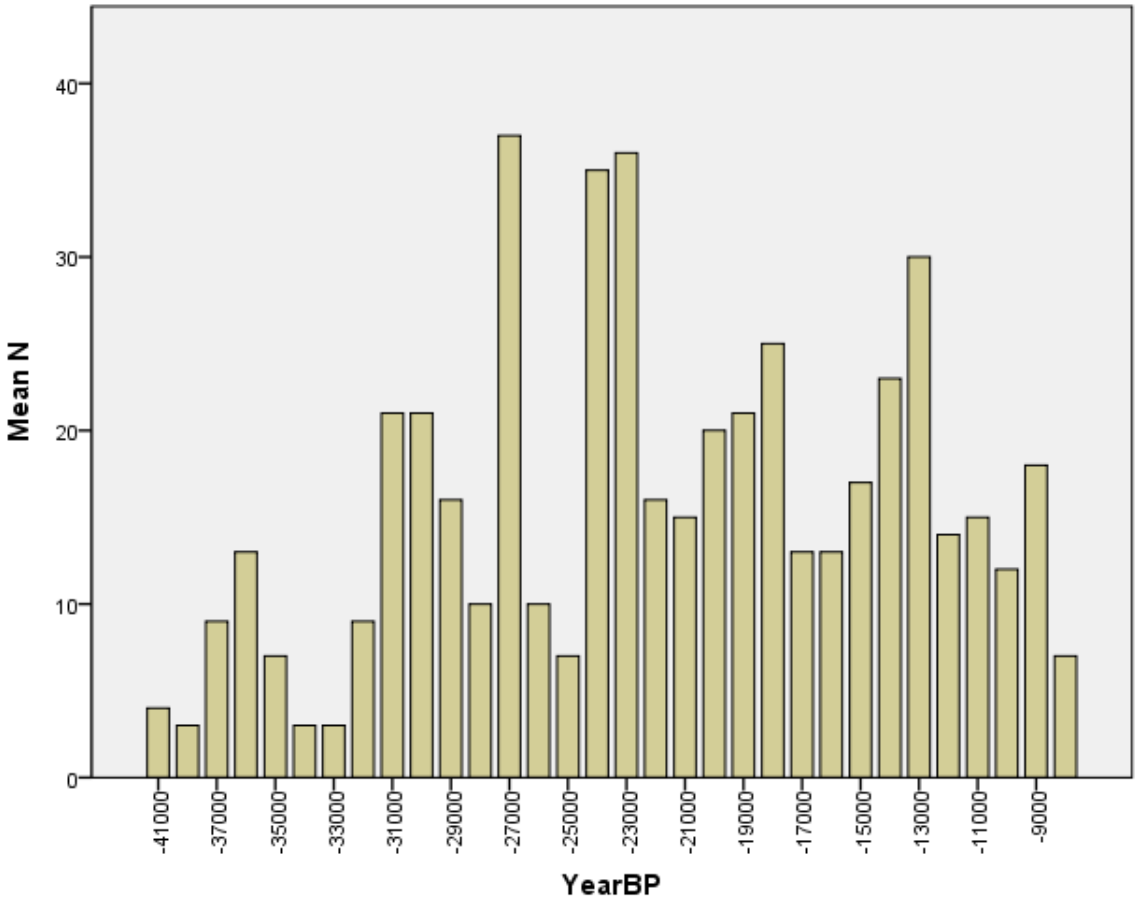

Figure 5.1: Frequency of radiocarbon dates by 1000-year time-bin. Modal values of calibrated radiocarbon date distributions were collated and assigned to time-bins.

$$n_t = 5.726442 * 10^6 (t + 2176.4)^{-1.3925309} \tag{5.1}$$

$t = time$ and n_t =number of dates at t.

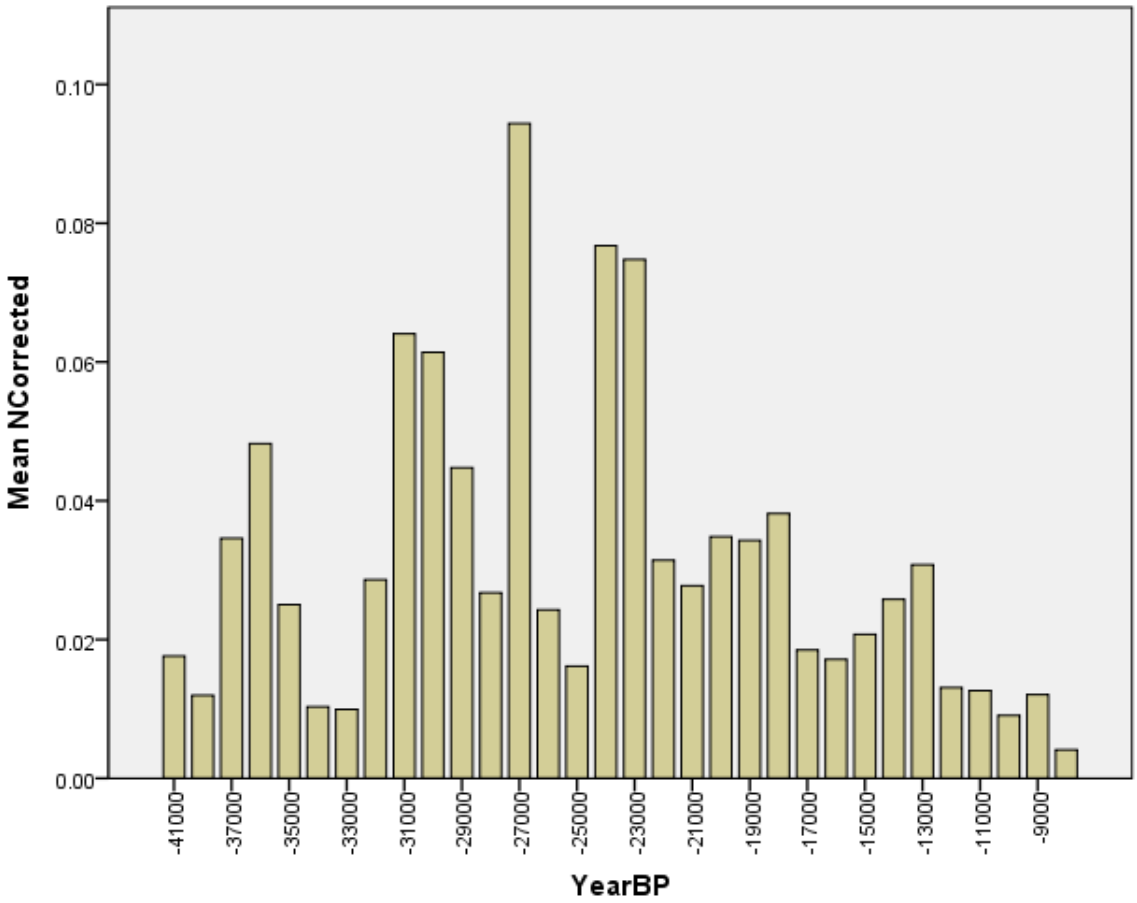

Figure 5.2: Frequency of radiocarbon dates by 1000-year interval time-bin, corrected using Surovell et al. (2009). Modal values of calibrated radiocarbon date distributions were collated, as for Figure 5.1, and then the correction curve was applied to this distribution.

Following taphonomic correction, a picture of changing human activity in the region is produced. Notable peaks in radiocarbon date frequency are seen at 31,000 to 30,000 BP, 27,000 BP and 22,000 to 23,000 BP. Notable troughs appear at 32,000 to 33,000 BP and at 25,000 BP. The Later Upper Palaeolithic in general seems to display a relative

lack of activity.

Summed probability plots were then produced for calibrated dates. Despite the many problems and controversies surrounding the use of these plots, discussed in Chapter Two, it was felt that they should be produced as part of the analyses in order to test the validity of the approach. The probability density function was first averaged between sites, in order to eliminate research bias, and then averaged across the whole region. The results of this process are shown below, first for modelled dates alone and then for all calibrated dates, both modelled and unmodelled. Any disparity between the two distributions is likely to tell us more about research agendas in prehistory than about demography. This is because the chief reason why dates cannot be modelled is that only one or two radiocarbon dates have been produced from the site where the samples originated. Multiple radiocarbon dates, preferably in stratigraphic sequence, are required in order for a Bayesian model to be produced. The summed probability distribution in Figure 5.3 is obtained from sites where multiple dates are available, and therefore well known sites such as Abri Pataud and La Ferrassie contribute significantly towards this distribution. By contrast, these well-researched sites hold less influence over the summed probability distribution in Figure 5.4. Instead, the picture produced in this image is largely dependent on sites for which only one or two dates have been produced, such as Limeuil and Gabillou, and for which research focus has been significantly less intense. The increased frequency of 'spikes' in the Later Upper Palaeolithic in the unmodelled distribution, suggests that the focus in radiocarbon dating the region has tended to be fixed upon older sites, to the detriment of many Magdalenian sites. Indeed there may be some bias in the selection of samples for dating in general, with more 'glory' ascribed to the identification of old material in Palaeolithic studies than for younger finds.

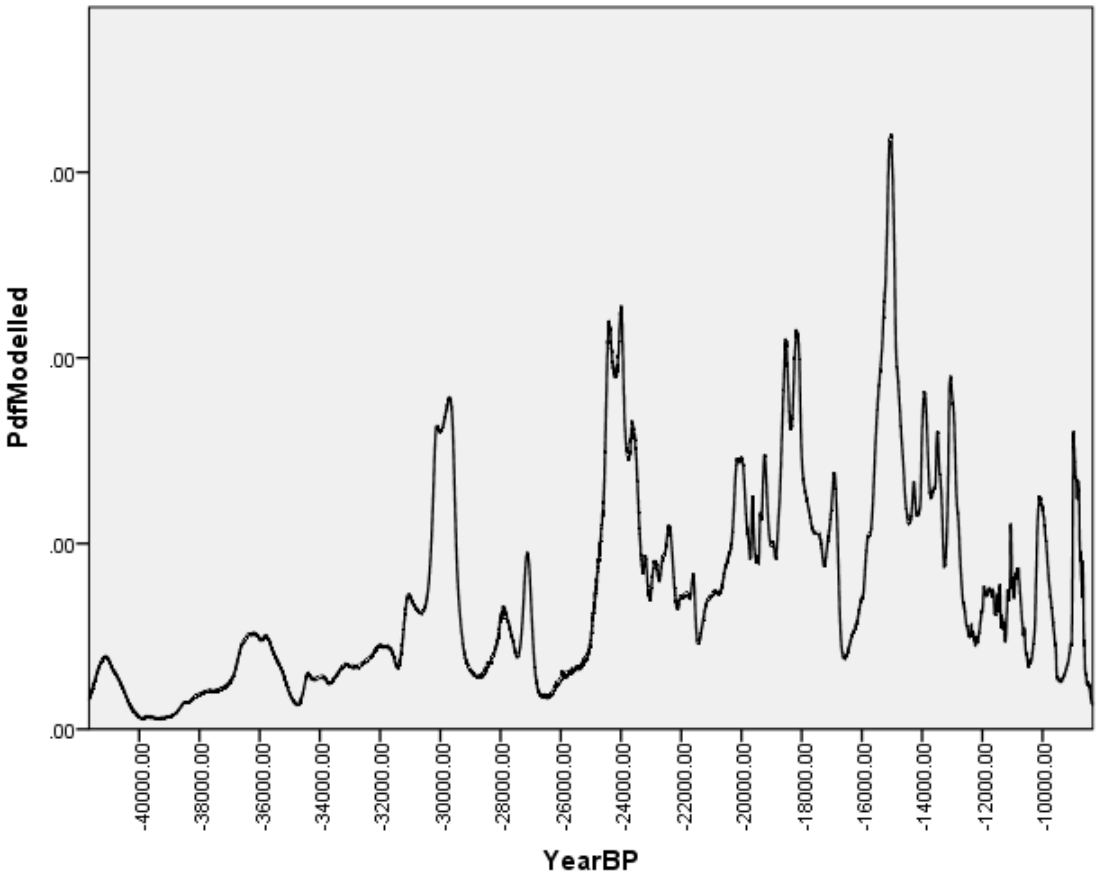

Figure 5.3: Summed probability distribution for all calibrated radiocarbon dates for which Bayesian models could be built. Data from 398 radiocarbon dates, from 169 levels at 34 sites. Full list of dates given in the appendix.

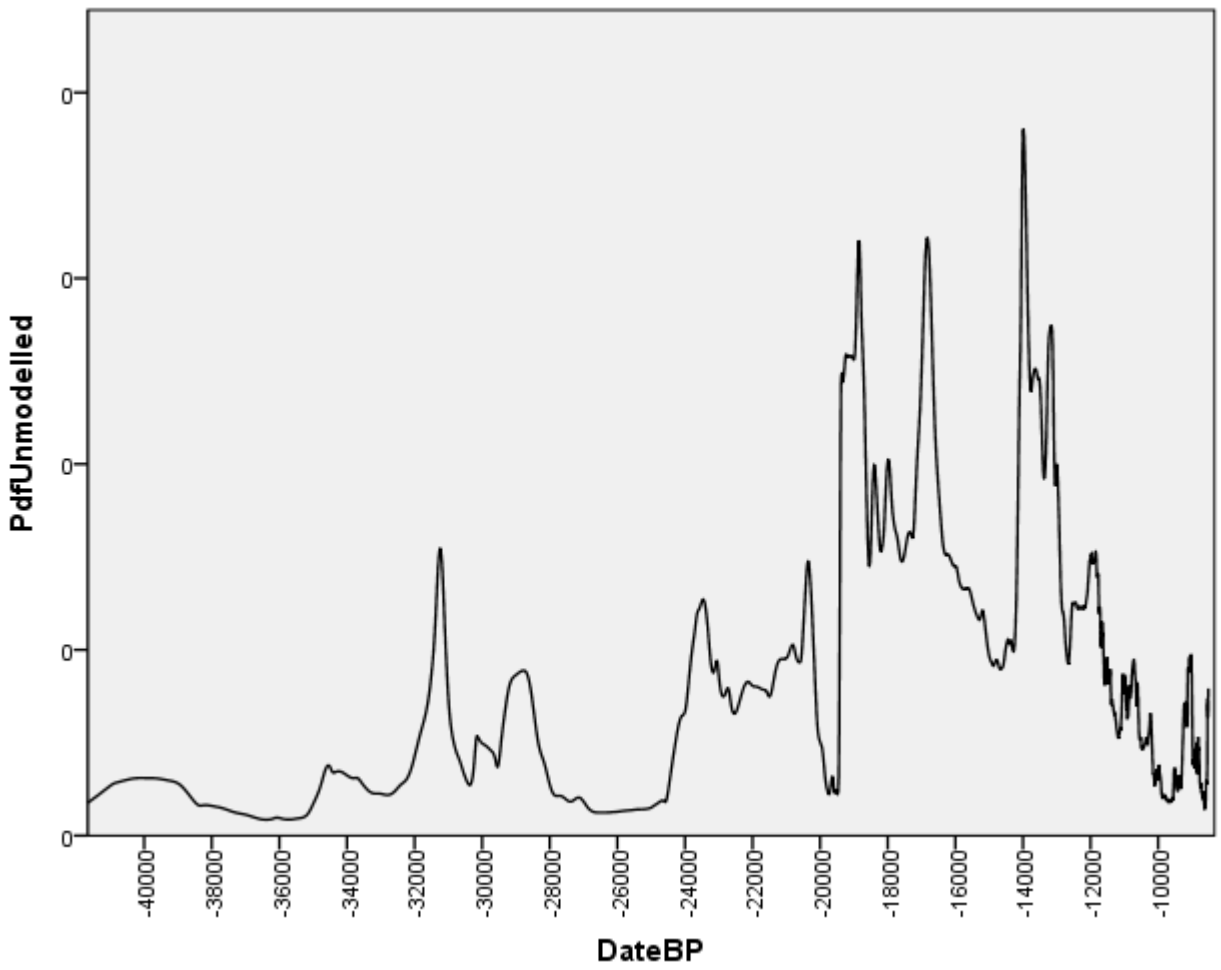

Figure 5.4: Summed probability distribution for all calibrated radiocarbon dates for which Bayesian models could not be built. Data from 132 radiocarbon dates, from 51 sites.

Finally, all radiocarbon dates, both modelled and unmodelled were combined to produce the summed probability distribution in Figure 5.5.

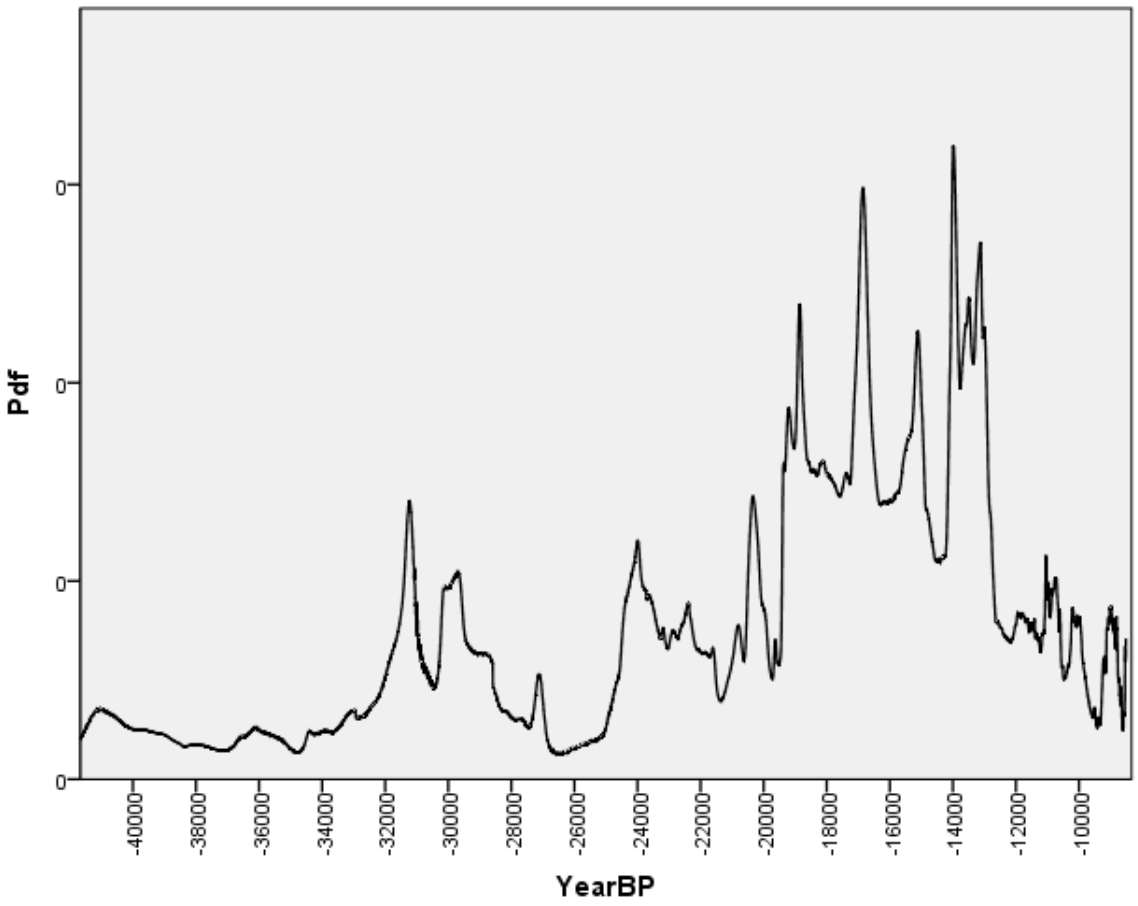

Figure 5.5: Summed probability distribution for all radiocarbon dates, both modelled and unmodelled. Data from 530 radiocarbon dates.

In terms of obtaining a demographic signal from a summed probability distribution, it is most appropriate for *all* available radiocarbon dates to be utilized. To exclude dates from sites which have not been extensively dated could introduce a degree of research bias into the analysis, given that only dates available from sites with sequences of reliable dates could be modelled. For this reason, the summed probability distribution obtained on all dates from the region, both modelled and unmodelled will be 'carried forwards' in this thesis as the most appropriate distribution to use for obtaining a demographic signal. It was therefore necessary to apply the taphonomic correction curve of (Surovell et al., 2009) to this distribution, and the corrected distribution is shown in Figure 5.6.

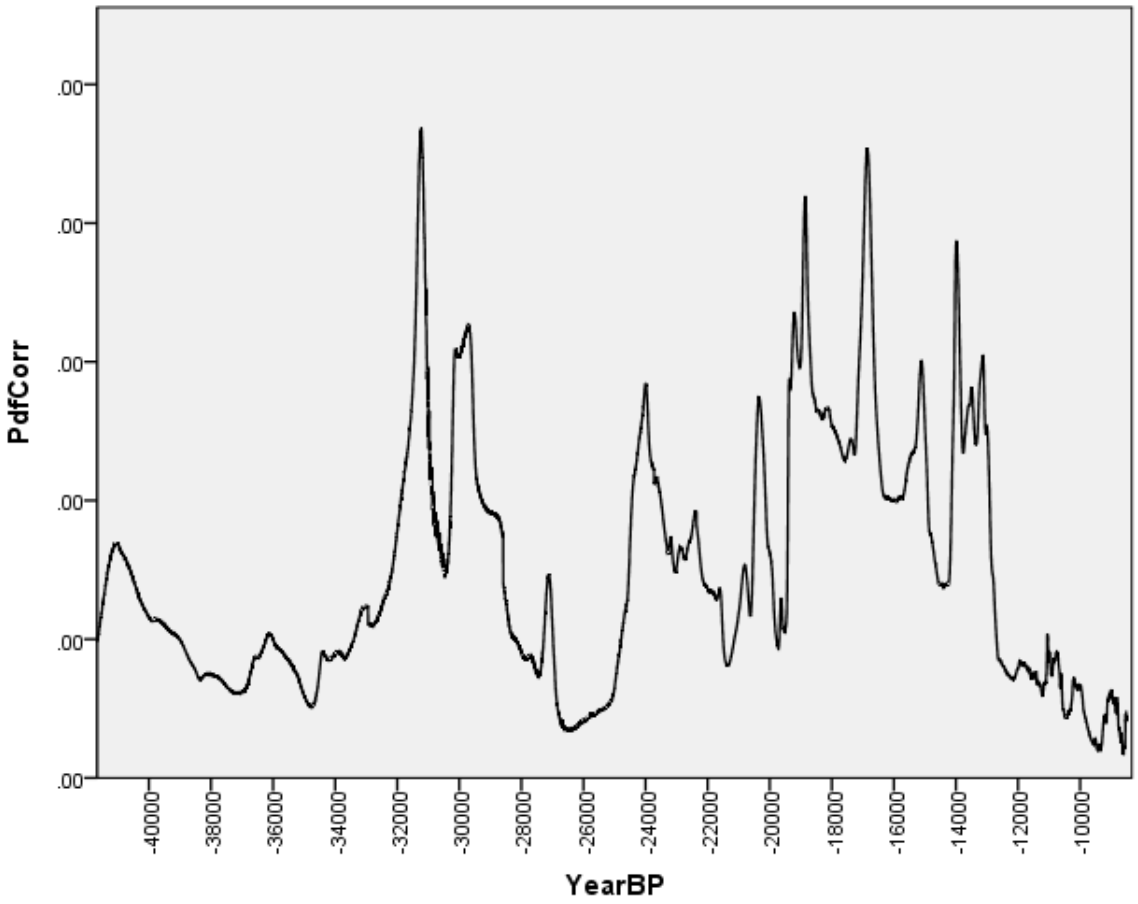

Figure 5.6: All Dates from the region, modelled and unmodelled. Calibrated and corrected for taphonomy using method of Surovell et al. (2009)

5.1.1 Impact of Bayesian Dating

To assess the importance of the Bayesian calibration method, a summed probability distribution was also produced for all dates which had been modelled previously using the Bayesian methods outlined in Chapter Four. The summed probability distribution obtained from these, simply calibrated dates, is shown in Figure 5.7 alongside the distribution obtained from the corresponding dates, which had been modelled using Bayesian methods. In this figure the blue line represents the prior, unmodelled distribution, while the green line is the posterior, modelled distribution. The shape of the distributions are remarkably similar, indicating that the Bayesian analyses had very little impact on the shape of the summed probability distributions. Indeed, the overwhelming majority of peaks and troughs in the distributions are observed at the same temporal loci. However, a notable exception is seen at approximately 27,000 BP, with the appearance of a small 'spike' in activity not seen in the prior distribution.

The similarity of the prior and posterior distributions would suggest that the production of Bayesian models for sites is of little importance for a landscape-wide study such as this, particularly given the large amount of additional information, and subsequently time, required to produce such models. I would therefore advocate that, for the production of regional summed probability, simple calibration will suffice in most cases. However, given that the production of Bayesian, chronological models in Oxcal allows the calculation of boundaries between strata, something which was necessary for the calculation of stone-tool densities within levels, which has been outlined in section 5.3. Thus, while the Bayesian method may have been of little use in the 'dates as data' methods employed here, they should still have impacted on later methods used in this thesis.

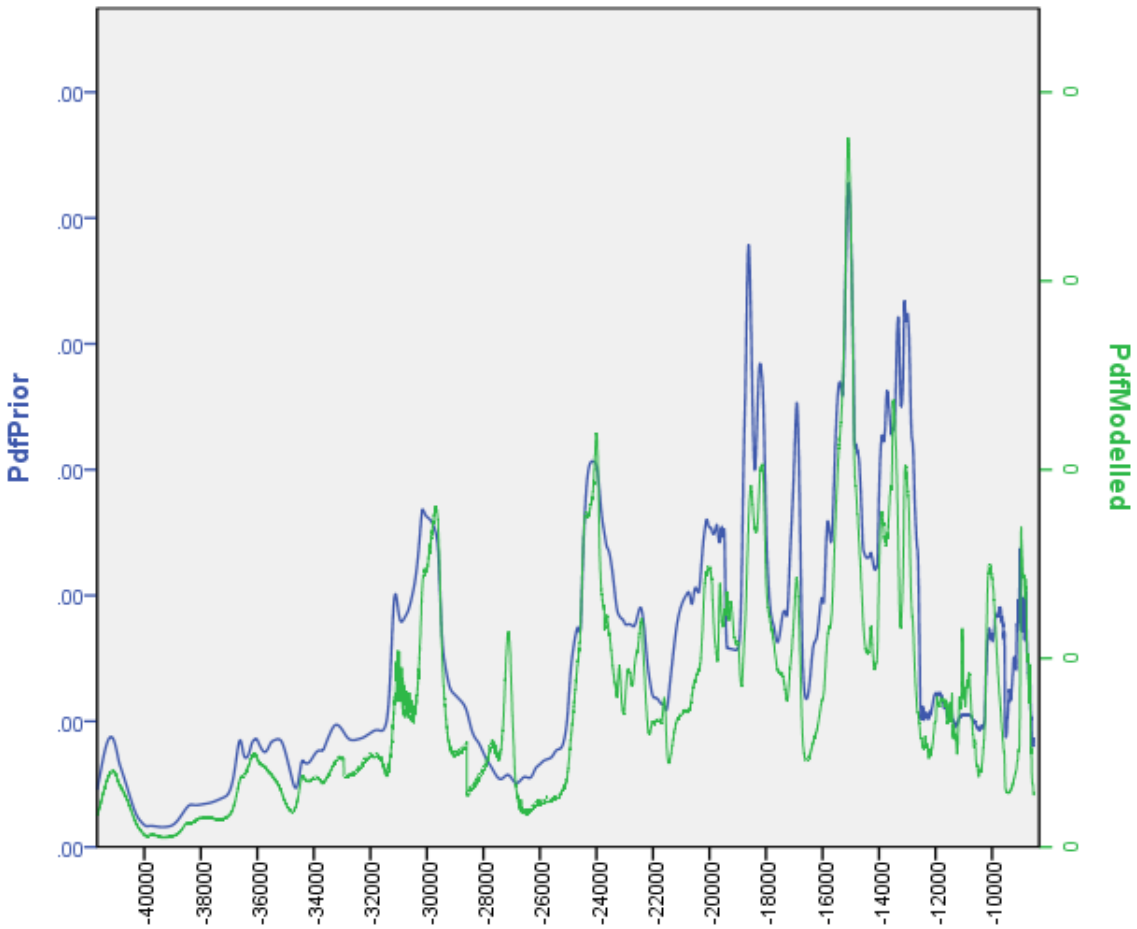

Figure 5.7: The blue line is the summed probability of calibrated radiocarbon dates that have not been modelled, but that could have been. The green line is the summed probability distribution of these same dates, after they have been calibrated and modelled.

5.1.2 Testing the Summed Probability Method

Given the controversial nature of the summed probability method, as outlined in Chapter Two, it was felt necessary to test whether a true demographic signature is present in the data. In order to do so, a simulated dataset was produced using the Rsimulate function in Oxcal 4.1, whereby all dates were evenly distributed through time. The simulated dataset spanned the entire Upper Palaeolithic period and featured a sequence of dates at 50 year intervals. The simulated and 'real' dataset were of exactly the same magnitude (n=530). Such a uniform distribution of radiocarbon dates would be expected if the population of the region had remained static over time and taphonomic factors did not affect the frequency of radiocarbon dates sampled. Figure 5.8 displays the summed probability distribution of the simulated dataset against the summed probability distribution obtained on the real-life radiocarbon dataset for the region, after taphonomic correction. It is clear that there is a difference between the two distributions, which demonstrates that a demographic signal *can* be obtained from summed probability distributions.

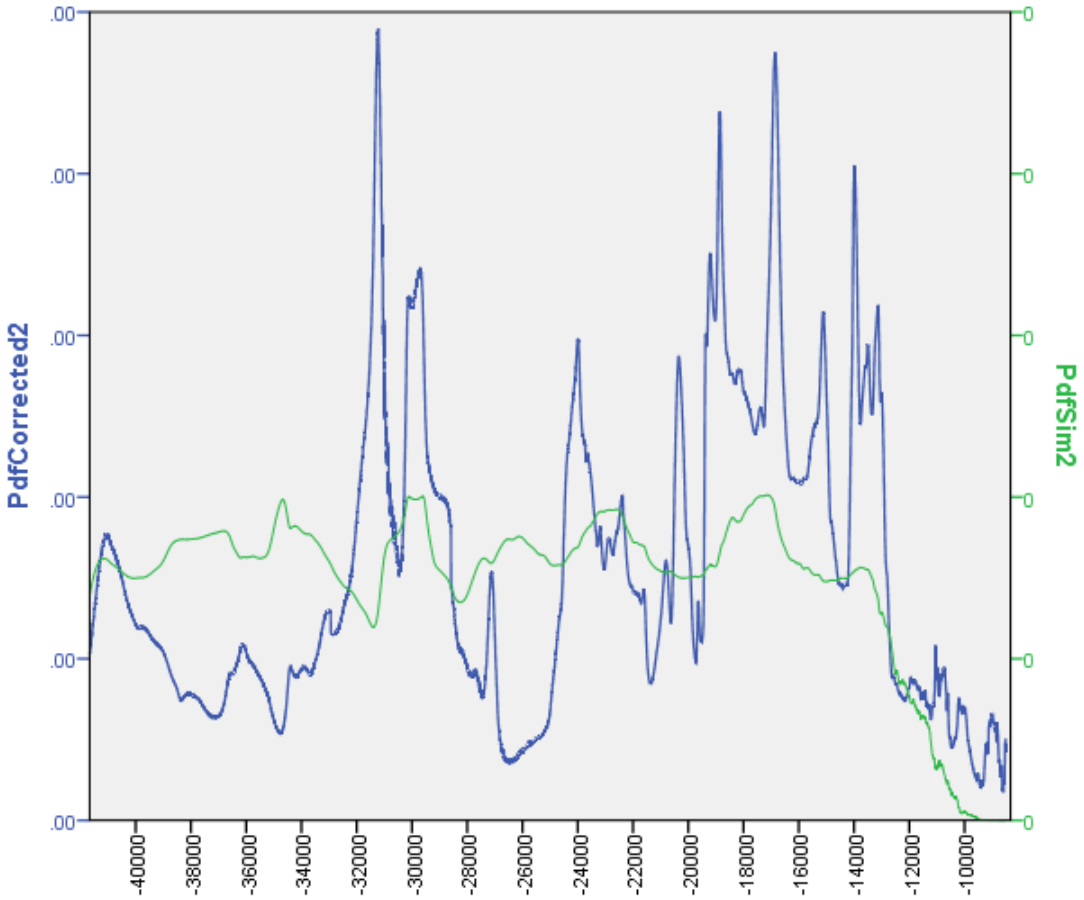

Figure 5.8: Comparison of summed probability distribution for all dates from the region (blue) and the simulated dataset (green). The blue line has been corrected using the method of Surovell et al. (2009)

For ease of visual analysis, the residuals of these graphs were calculated and these are plotted in Figure 5.9. Essentially, the simulated dataset has been subtracted from the 'real' dataset, and the peaks and troughs remaining in the distribution once the uniform distribution has been removed are evident.

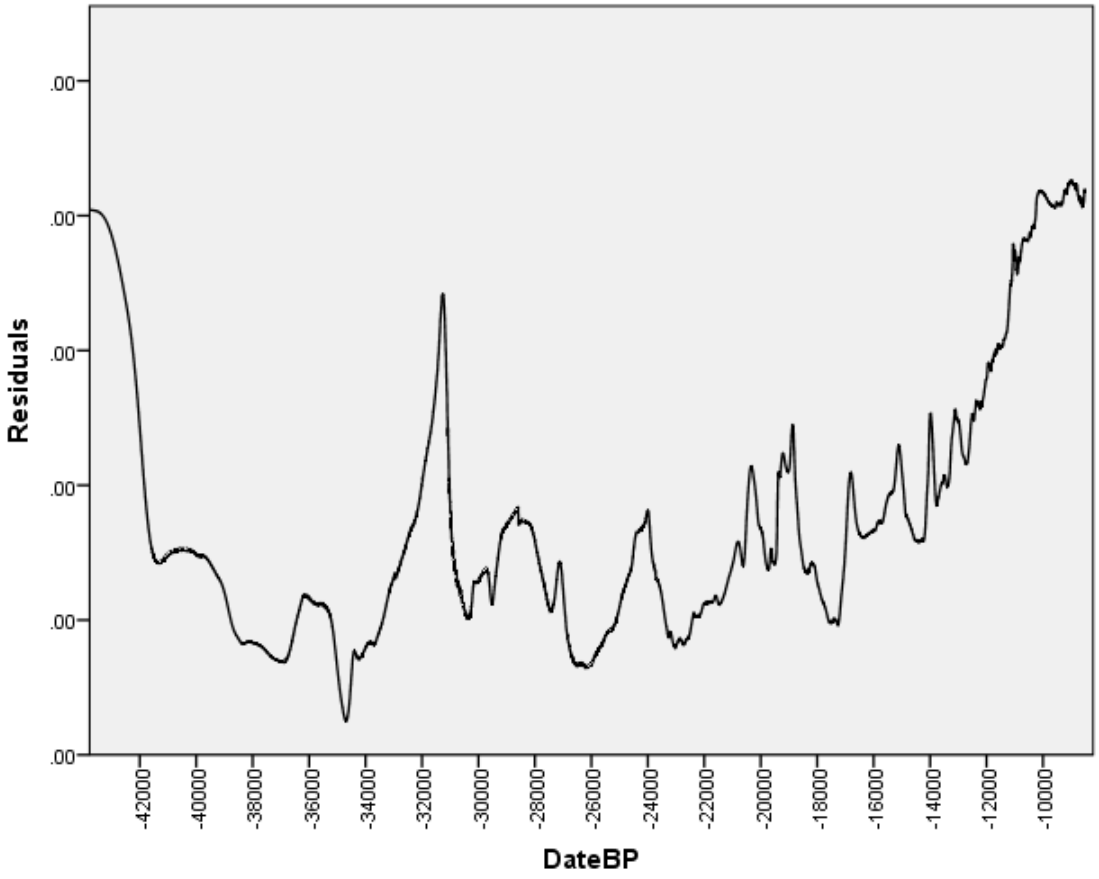

Figure 5.9: Residuals: the 'real' dataset corrected using the method of Surovell et al. (2009), minus the simulated dataset. The simulated dataset has not been corrected, as dates from this dataset are evenly distributed so have not been subject to any 'taphonomic destruction'.

A Kolmogorov-Smirnov test was performed on the pdf pertaining to the radiocarbon data from Southwest France, to test whether the distribution conforms to a uniform distribution; confirming that, indeed, a non-uniform distribution is observed. We can

conclude that a demographic signal is obtained from the summed probability distribution.

One-Sample Kolmogorov-Smirnov Test

		PdfCorrected
N		7273
Uniform Parameters[a,b]	Minimum	.00
	Maximum	.00
Most Extreme Differences	Absolute	.344
	Positive	.344
	Negative	.000
Kolmogorov-Smirnov Z		29.368
Asymp. Sig. (2-tailed)		.000

a. Test distribution is Uniform.

b. Calculated from data.

Table 5.1: Kolmogorov-Smirnov test to check that the summed probability distribution for the region conforms to a uniform distribution

The summed probability distributions presented above conform to the recommendations in Williams (2012) for the inclusion of a minimum of 500 radiocarbon dates, when both modelled and unmodelled dates are treated together. However, it was thought necessary to implement another of Williams' suggestions; the smoothing of the summed distribution through a 500-800 year moving average to eliminate any residual effects from the calibration curve. The resulting graph is depicted in Figure 5.10.

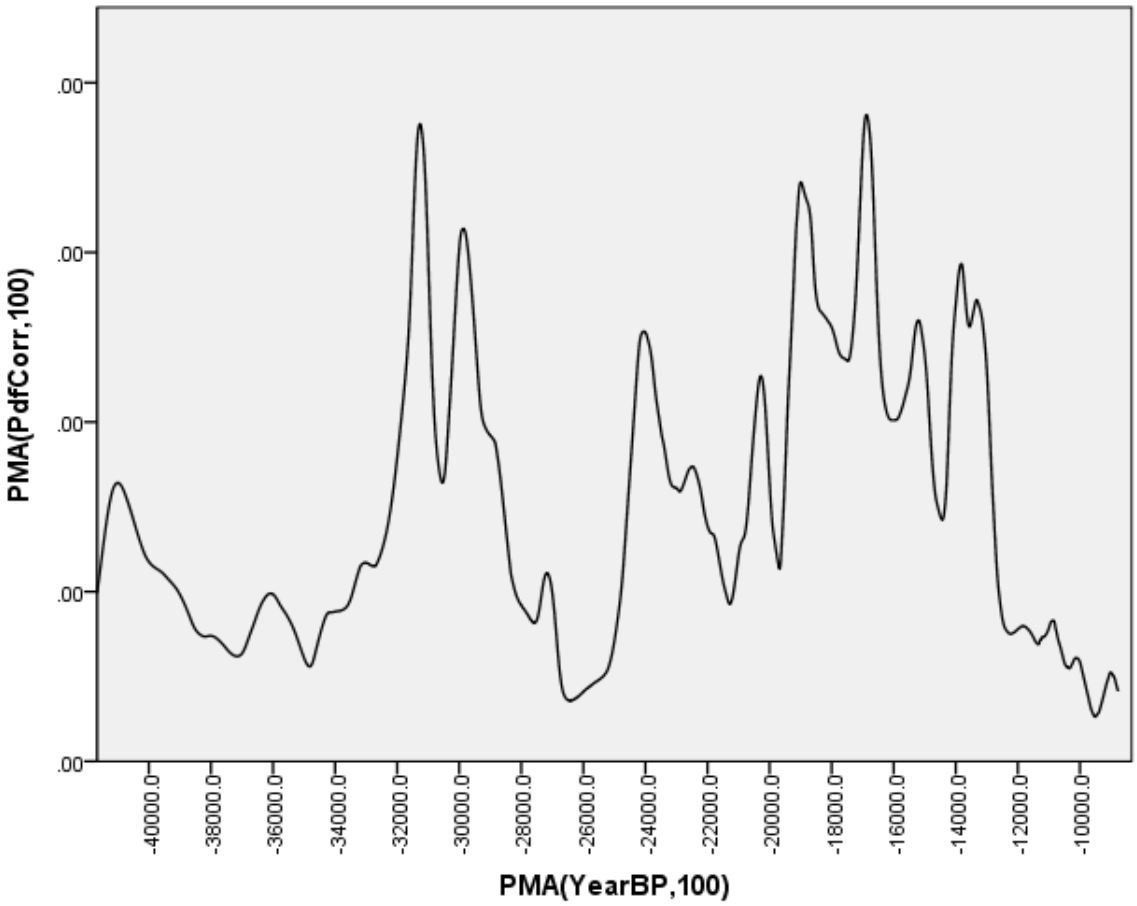

Figure 5.10: Summed probability distribution for all radiocarbon dates from the region (n=530), following calibration and taphonomic correction using the method of Surovell et al. (2009). The distribution has also been smoothed using a 500-year prior moving average

As well as helping to further eliminate any effects the calibration curve has in obscuring demographic signals, the smoothed graph also has the advantage of being much easier to view, with general trends, peaks and troughs much more visible. This final summed

probability distribution has now been rigorously corrected and tested to ensure that a true demographic signal is visible. It has been corrected for taphonomic bias, corrected for calibration effects using a moving average, and has been tested against a simulated dataset to ensure that population processes are visible. While detractors of the method are likely to remain, I hope that I have done everything in my power to assuage their concerns.

On the basis then of this final summed probability distribution, the following observations can be made with regards to population dynamics in the region. First, activity at the start of the Upper Palaeolithic appears to be reasonably high, certainly much higher than is suggested by the frequency of modal values of radiocarbon dates alone. A steep increase in human activity takes place at approximately 32,000 BP, with another peak in activity following shortly afterwards at around 30,000 BP. Activity then declines sharply, reaching a low-point at 26,000 BP. This is followed by an increase in activity at 24,000 BP and then another decline. Further increases occur at 20,000 BP and18,000 BP. A decline in activity is observed with the transition to the Azilian at around 12,000 BP. However, as I will discuss in the next chapter, I am unconvinced by this Azilian demographic decline and believe that the dip in radiocarbon activity in the Azilian is actually an artefact of data collection and analysis.

It was then considered pertinent to investigate any possible link between population processes as evidenced by radiocarbon dates and climate, given the theoretical importance of the LGM to developments in the Palaeolithic of Southwest France. The following image displays the summed probability distribution from all radiocarbon dates, corrected for taphonomic loss and smoothed using a 500-year prior moving average, to data from the NGRIP ice-core. In essence, the blue line rises and falls with global temperature and the green line rises and falls with human activity levels. Many peaks in global temperature coincide with phases of decreased human activity in the region, for instance at 34,000 BP and 28,000 BP. Most notably the decline in human activity from 12,000 BP onwards appears to be concurrent with the rise in global temperature

at the onset of the Holocene. Though, as introduced above, I am suspicious of this Late Glacial population decline.

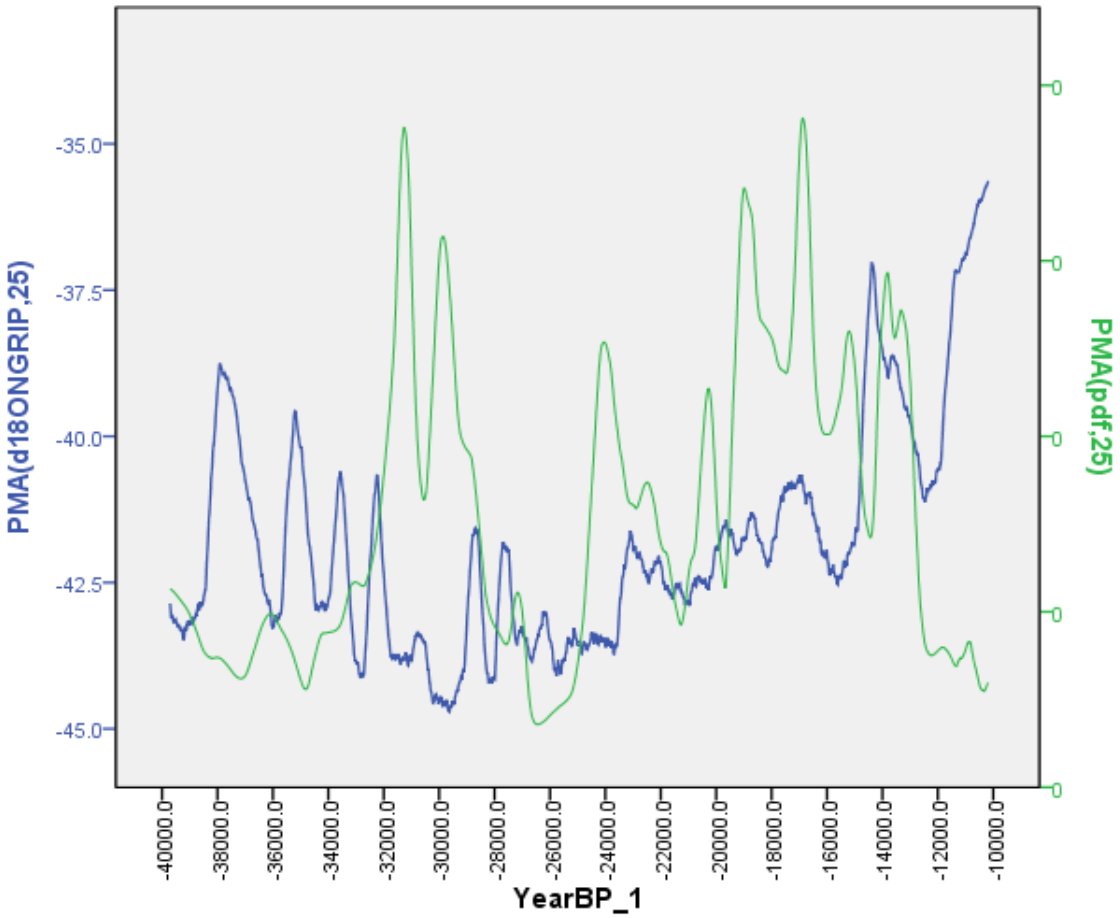

Figure 5.11: Summed probability distribution for all dates from the region, following taphonomic correction and smoothed using a 500-year prior moving average (green line) and $\delta^{18}O$ values from the NGRIP ice core (blue line)

A cross-correlation was performed in PASW statistics, which demonstrated that a weak negative correlation, which is significant at the 0.01 level, exists between the two time series and is evident at every lag tested (Figure 5.12 and Table 5.2). This confirms that a negative relationship between the distribution of radiocarbon dates and global temperatures exists, implying that as global temperatures decrease, a corresponding increase in human activity is seen in Southwest France. This would be consistent with the refugium hypothesis in general, although it is interesting to note that the LGM

itself is by no means the period where this relationship is most dramatically evident. Instead, the relationship is observed throughout the entire Upper Palaeolithic period.

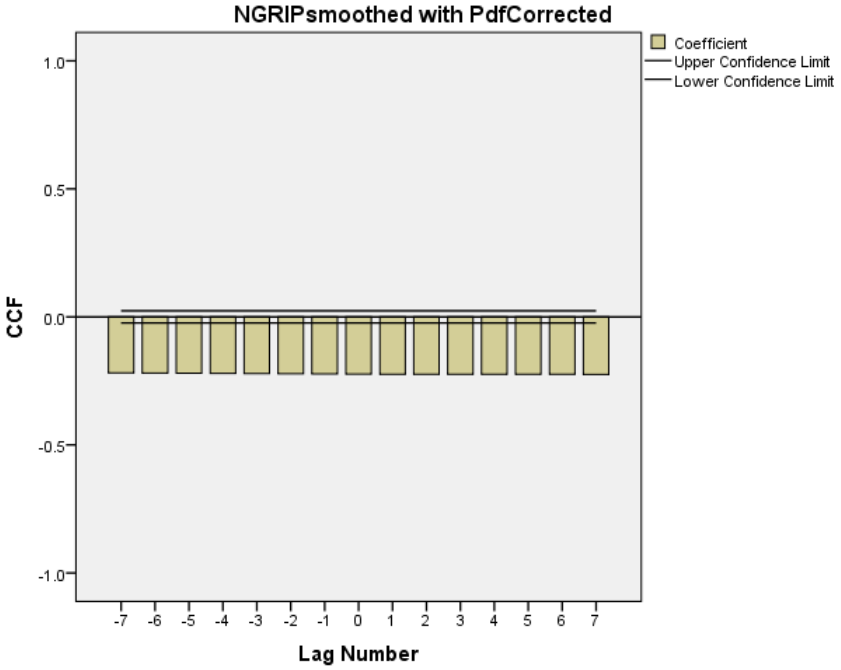

Figure 5.12: Cross Correlation of NGRIP and summed probability distribution

NGRIPsmoothed with PdfCorrected

Cross Correlations

Series Pair: NGRIPsmoothed with PdfCorrected

Lag	Cross Correlation	Std. Error[a]
-7	-.219	.012
-6	-.219	.012
-5	-.220	.012
-4	-.221	.012
-3	-.222	.012
-2	-.222	.012
-1	-.223	.012
0	-.224	.012
1	-.224	.012
2	-.224	.012
3	-.224	.012
4	-.224	.012
5	-.224	.012
6	-.224	.012
7	-.224	.012

a. Based on the assumption that the series are not cross correlated and that one of the series is white noise.

Table 5.2: Cross Correlation of NGRIP and summed probability distribution

§ 5.2 Kernel Density Estimation Results

The Kernel Density Estimation method of Grove (2011) was applied to the dataset in the manner described in Chapter Three. A video depicting the changing KDEs throughout the period of interest is contained on the disc supplied with this thesis and stills from this video are shown below for periods of particular interest. In the images, the KDE has not been scaled to 1 in each image; rather, the images are scaled to 1 for the *duration* of the Upper Palaeolithic. In this manner, images can be compared to see relative changes in activity through time.

As the KDE method essentially smears the summed probability distribution across the region, it may be useful to refer to the summed probability distributions produced in the previous section when referring to the distributions below. To begin with we shall examine the periods which appear to have seen greatest human activity in the

region, with the following images all from periods where 'peaks' occur on the summed probability distribution. All KDE dates are given in calibrated radiocarbon years.

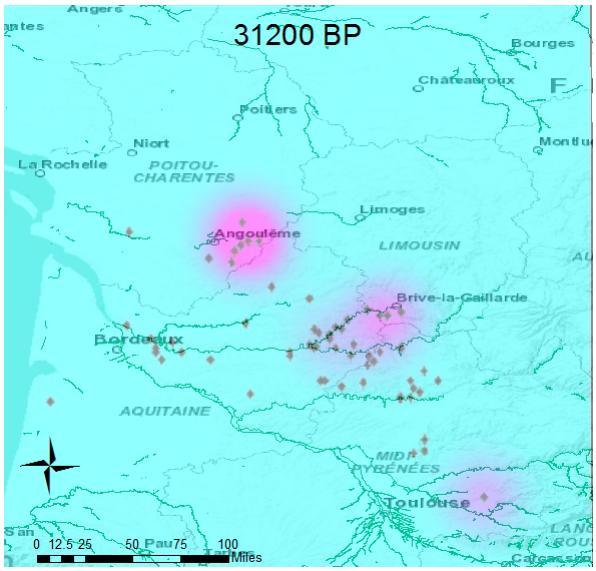

Figure 5.13*a*: KDE 31200 BP

It is interesting to see that the spikes in activity do not all share the same settlement patterns. Some such periods are very centralized, such as at 20450 BP, whereas other densely occupied phases feature multiple centres of activity, such as at 16950 BP and at 19200 BP. The phase 13950 BP is particularly interesting, given that it appears to consist of one incredibly large centre of activity; a continuous area of high population density. That this period is followed in quick succession by a decline in activity makes it especially noteworthy.

Changing settlement patterns are symptomatic of population change in general. It stands to reason that a growing population will need to spread out and occupy more land in order to support itself. This process is commonly noted in social anthropology as 'budding off'. Equally, expansion and contraction of hunter-gatherer ranges is known to occur with both decreases in resource availability and increases in population, which would have the same effect. It is also why population growth and movement are frequently modelled with the reaction-diffusion equation; the reaction part corresponds to demographic increase and the diffusion part corresponds to population dispersal follow-

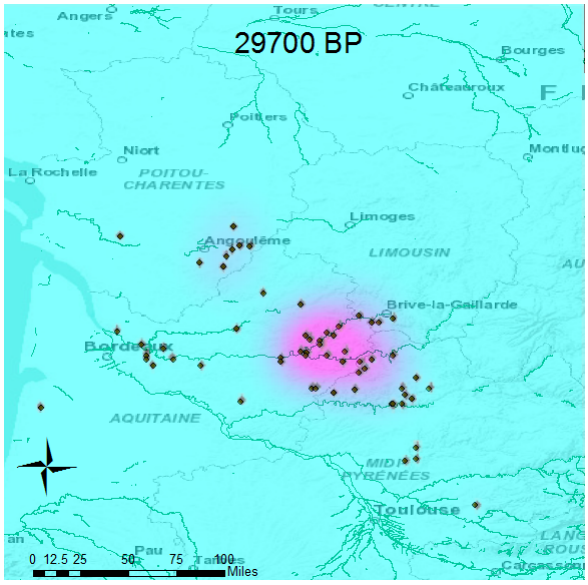

Figure 5.13*b*: KDE 29700 BP

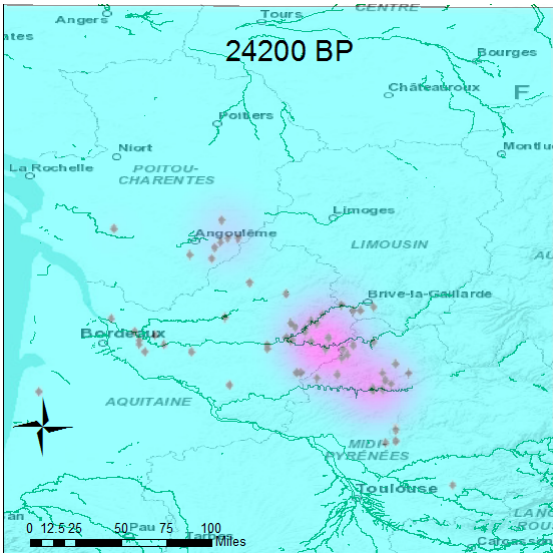

Figure 5.13*c*: KDE 24200 BP

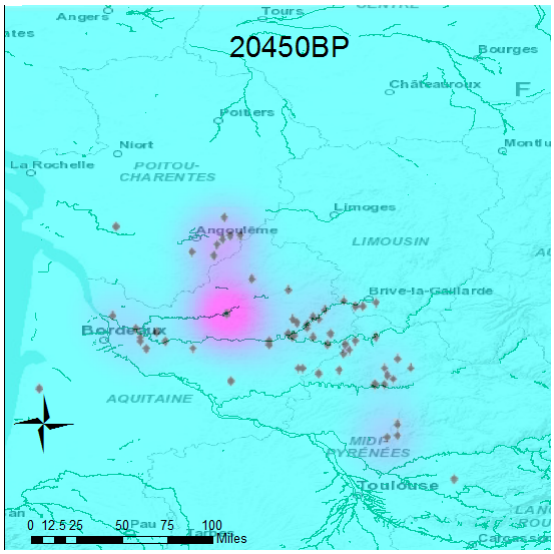

Figure 5.13*d*: KDE 20450 BP

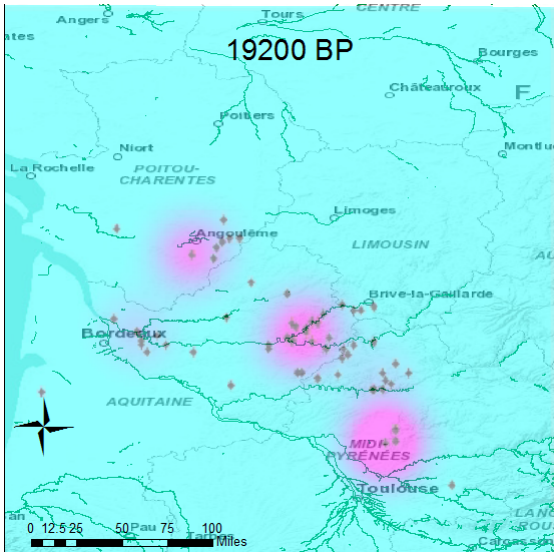

Figure 5.13*e*: KDE 19200 BP

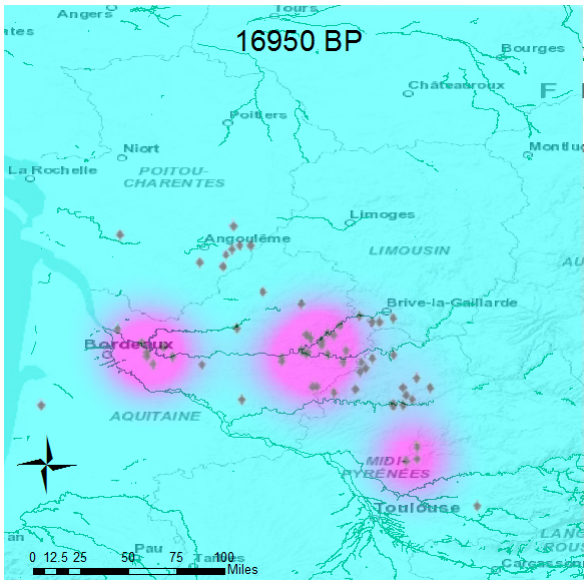

Figure 5.13*f*: KDE 16950 BP

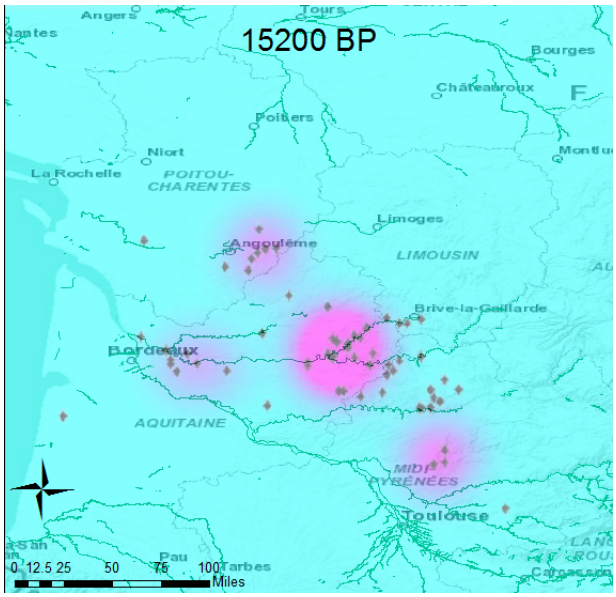

Figure 5.13*g*: KDE 15200 BP

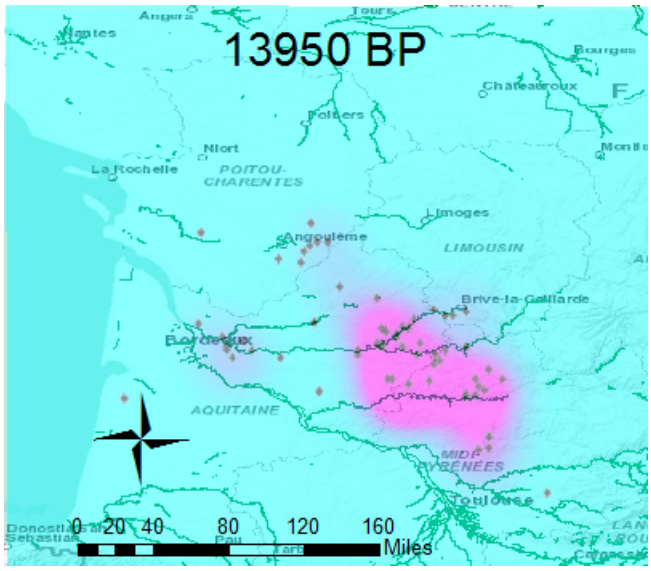

Figure 5.13*h*: KDE 13950 BP

ing this reaction. Zubrow (1971) modelled this process as a series of movements from optimal, to less optimal, resource zones. When population levels are low, groups will occupy the areas where resources are most abundant and conditions are most amiable. This is fairly logical; people will only settle in peripheral regions when the optimal resource zone is so crowded that resource-availability in this zone decreases. Is this process evident in the study region and period? It would be surprising if it were not. Certainly, the three distinct areas of dense settlement seen at 19,200 BP suggests that this process has occurred. Later on, in the Late Upper Palaeolithic, we see large blobs of continuous activity, rather than the distinct, separate areas of occupation that occur elsewhere. It seems that budding-off from most optimal region has occurred in both phases, though perhaps through slightly different processes. It is also possible that the optimal resource zones have change over time, accounting for the different settlement patterns in different, densely occupied phases.

§ 5.3 Intra-site Lithic Density Results

Intra-site lithic densities were calculated in the manner described in Chapter Four. The results were first analysed according to technocomplex and Figure 5.14 displays the densities of tools by surface area excavated (per m^2). Figure 5.15 displays the densities of tools by surface area and level duration (per m^3). The estimated duration of levels for Figure 5.15 were obtained from the Oxcal models developed for each site, as shown in the appendix. Estimated durations could not be produced for all assemblages, only those 'sandwiched' in well dated sequences. A full list of assemblages used for this analysis is included in the appendix.

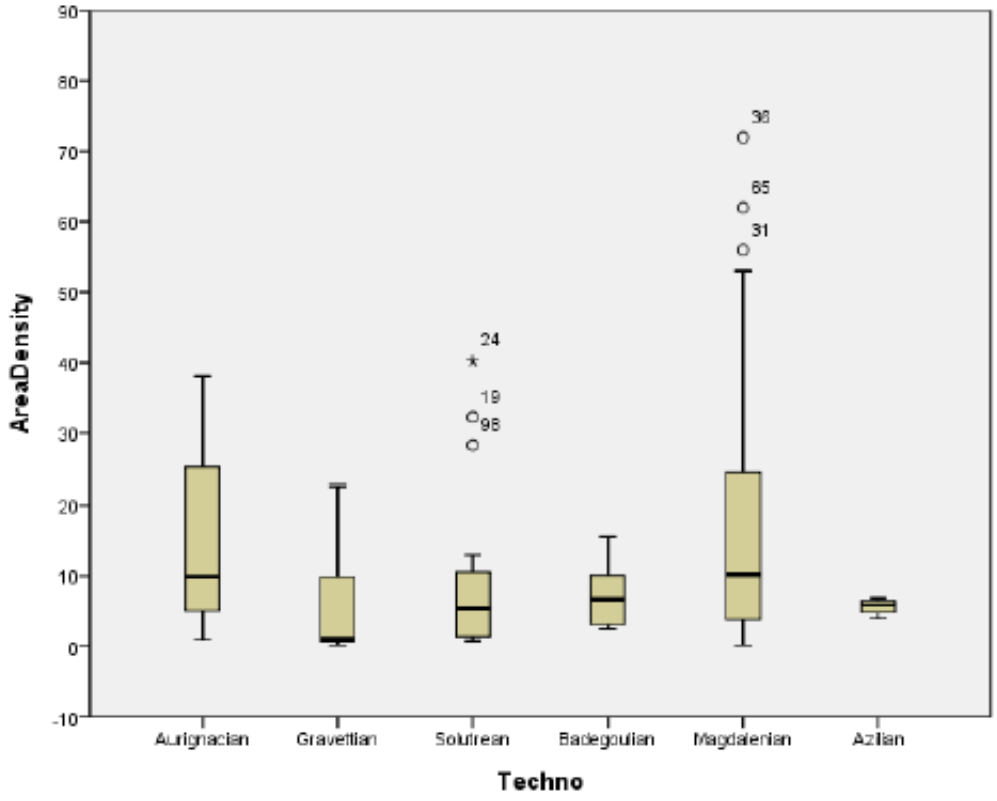

Figure 5.14: Density of stone tools per m^2 excavated, organized by technocomplex

I performed statistical tests on the site density data, to examine if the various technocomplexes were significantly different. I expected that the densities of tools by surface area excavated, without any consideration of the duration of time represented by a

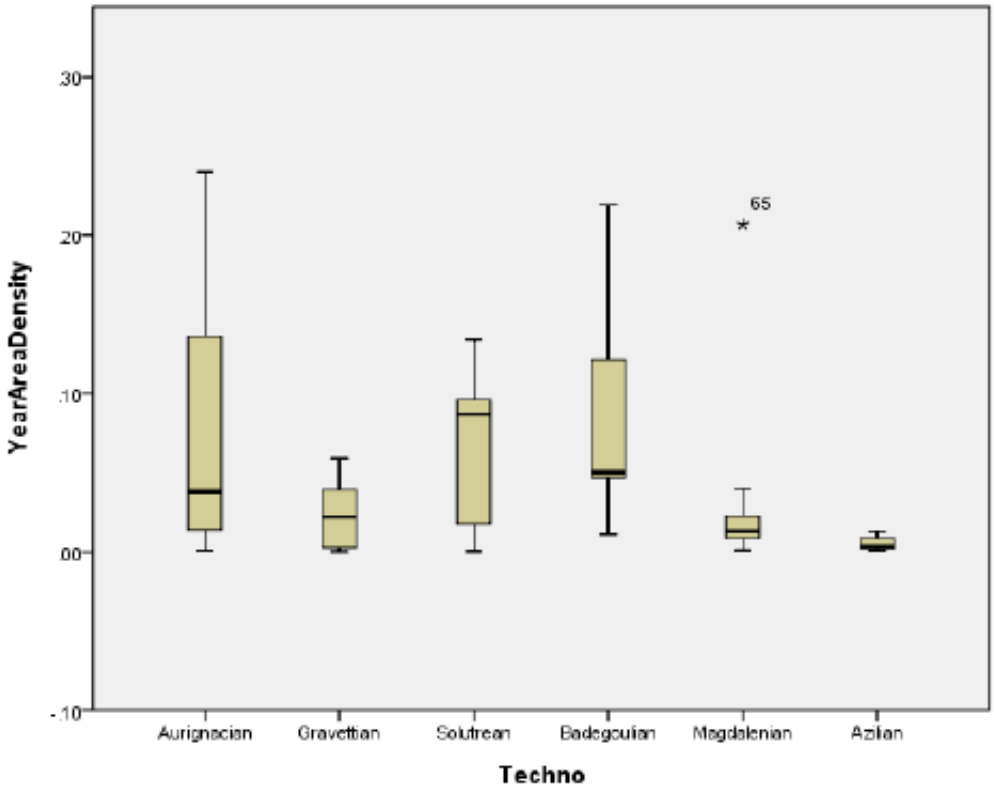

Figure 5.15: Density of stone tools per m^3, per year, organized by technocomplex

level, would be very uninformative. However, I performed tests on both datasets as a matter of formality, with interesting results. The results of the Kruskal-Wallis tests on both datasets, performed in PASW statistics are shown in Figures 5.16 and 5.17. Surprisingly, statistically significant differences were observed between technocomplexes in each dataset, contrary to expectation. I had thought that the importance of time as a factor would be so strong as to obscure any differences between technocomplexes when analysed simply according to the density of tools per m^2 excavated. However, this was not the case. A possible explanation for this surprising statistically significant result may be that as the samples are all from the same region and broad time period, sedimentation rates may have been uniform enough to overcome the lack of consideration given to time as a factor in the analysis. Of course, it is worth noting that when time is included as a factor in the analysis a higher level of significance is attained, so it is worth considering the length of time that a deposit took to form.

Hypothesis Test Summary

	Null Hypothesis	Test	Sig.	Decision
1	The distribution of AreaDensity is the same across categories of Techno.	Independent-Samples Kruskal-Wallis Test	.047	Reject the null hypothesis.

Asymptotic significances are displayed. The significance level is .05.

Figure 5.16: Results of the Kruskal-Wallis test on densities of stone tools per m^2 excavated, ordered by major technocomplex

Hypothesis Test Summary

	Null Hypothesis	Test	Sig.	Decision
1	The distribution of YearAreaDensity is the same across categories of Techno.	Independent-Samples Kruskal-Wallis Test	.010	Reject the null hypothesis.

Asymptotic significances are displayed. The significance level is .05.

Figure 5.17: Results of the Kruskal-Wallis test on densities of stone tools per m^2 excavated, ordered by major technocomplex

Having established that there *is* a statistically significant difference between the densities of tools by m^2 and m^3 when grouped by technocomplex, it was then considered

necessary to further examine *how* the technocomplexes differed. Mann-Whitney U-tests were first performed on pairs of technocomplexes for the variable 'density of tools per m^3', using PASW statistics. This variable is considered here as likely to be more meaningful than 'density of tools per m^2', due to the importance of level duration for interpreting demography based on archaeological remains.

	Aurignacian	Gravettian	Solutrean	Badegoulian	Magdalenian	Azilian
Aurignacian	N/A	NS	NS	NS	S *	S *
Gravettian	NS	N/A	NS	S *	NS	NS
Solutrean	NS	NS	N/A	NS	NS	NS
Badegoulian	NS	S*	NS	N/A	S**	S*
Magdalenian	S*	NS	NS	S**	N/A	NS
Azilian	S*	NS	NS	S*	NS	N/A

Table 5.3: Mann-Whitney U Tests on Tool Densities per m^3: NS = not significant, S = Significant, N/A = not applicable. * = significant at 0.05 level, ** = significant at 0.01 level, *** = significant at 0.001 level

	Aurignacian	Gravettian	Solutrean	Badegoulian	Magdalenian	Azilian
Aurignacian	N/A	.049	.820	.442	.029	.026
Gravettian	0.49	N/A	.218	.024	.744	.282
Solutrean	.820	.218	N/A	.685	.200	.142
Badegoulian	.442	.024	.685	N/A	.005	.014
Magdalenian	.029	.744	.200	.005	N/A	.051
Azilian	.026	.282	.142	.014	.051	N/A

Table 5.4: Mann-Whitney U Tests on Tool Densities per m^3

The Aurignacian is significantly different from the Magdalenian and Azilian. The Gravettian differs only from the Badegoulian. The Solutrean does not significantly differ from any technocomplex. The Badegoulian appears to display a break with the more recent phases, differing significantly from both the Magdalenian and Azilian. While the Magdalenian is at odds with both the Aurignacian and Badegoulian. These results have been tabulated below, along with p-values for significance, for ease of comprehension. Full statistical details for each test pair are included in the appendix.

While the Solutrean appears to have the highest average density of tools when time is considered as a factor, it is not statistically significantly different from any other technocomplex. According to the hypothesis that the Solutrean served as a refuge zone, subsequently with a greater population density, we would expect to see significantly higher densities of tools in this phase. It may be that sample size was not sufficient (n=5), and that a larger sample size would demonstrate a significant relationship. It was not possible to increase the sample size for this study, as we were limited to studying sites with well-dated sequences. The length of time that a level took to form could not be estimated unless multiple radiocarbon dates, in sequence, were available for the sites of interest. Without instigating a dating programme for more Solutrean sites I was unable to increase the sample size for the Solutrean. As discussed previously, the lack of well-dated, Late Upper Palaeolithic sequences is likely to be the result of bias towards the Early Upper Palaeolithic.

However, as a larger sample size was available for densities of tools per m^2, I was able to compare the technocomplexes according to this variable. There are obvious limitations with analysing tools per m^2 instead of per m^3, as the length of time that a level has taken to form has an obvious effect on our perception of prehistoric populations through the remains that they left behind. However, we have already seen through the use of a Kruskal-Wallis test in Figure 5.16 that there is a statistically significant difference between the density of tools per m^2 when grouped by technocomplex. We would not expect such a statistically significant result if site-formation processes completely obscured any original differences in tool numbers between technocomplexes.

The results of Mann-Whitney U-tests for tool densities per m^2 are shown in Tables 5.5 and 5.6. Full statistical tables are provided in the appendix.

A key 'break' occurs between the density-data for the Early and Late Upper Palaeolithic; the last two chronological phases differ significantly from both the earliest phase and the Badegoulian. Likewise, the Magdalenian and Azilian, contrary to expectations, are very similar to each other in terms of lithic densities at sites. We introduced ear-

	Aurignacian	Gravettian	Solutrean	Badegoulian	Magdalenian	Azilian
Aurignacian	N/A	S*	NS	NS	NS	NS
Gravettian	S*	N/A	NS	NS	NS	NS
Solutrean	NS	NS	N/A	NS	NS	NS
Badegoulian	NS	NS	NS	N/A	NS	NS
Magdalenian	NS	NS	NS	NS	N/A	S*
Azilian	NS	NS	NS	NS	S*	N/A

Table 5.5: Mann-Whitney U Tests on Tool Densities per m^2

	Aurignacian	Gravettian	Solutrean	Badegoulian	Magdalenian	Azilian
Aurignacian	N/A	.034	.338	.157	.552	.239
Gravettian	.034	N/A	.405	.218	.082	.428
Solutrean	.338	.405	N/A	.817	.374	.705
Badegoulian	.157	.218	.817	N/A	.085	.734
Magdalenian	.552	.082	.817	.085	N/A	.043
Azilian	.239	.428	.705	.734	.043	N/A

Table 5.6: Mann-Whitney U Tests on Tool Densities per m^2

lier the notion of a disconnect in lifestyles between these two Late Upper Palaeolithic phases. However, this is certainly not supported on the basis of lithic density data. Likewise, notice the restricted ranges for lithic densities in these two technocomplexes, which suggests a lack of site variability in these phases, as well as a slight decline in average lithic density. This decline in range of lithic density is potentially indicative of changing land use patterns from the Early to Late Upper Palaeolithic. A lack of site variability would suggest homogeneity in site function, possibly suggesting a shift to a more sedentary pattern of living. The notion of sedentism amongst pre-agricultural peoples has been expressed for sometime, (Henry, 1985) (Brown, 1985), as has the concept of semi-sedentism in the Upper Palaeolithic of the Dordogne (Mellars, 1985), but the statistical analyses here may provide further evidence for it.

Figures 5.18 and 5.19 display the lithic densities for all assemblages studied, against the year in which the assemblage is thought to date from. The year is based on the mid-point of the level, as assessed from the modal dates of the modelled boundaries of the phase. An assemblage with a modal value of 15,154 BP for the modelled end point and 15,624 BP for the projected start point would be assigned a date of 15,389 BP. Figure 5.18 depicts simply the density of tools per m^2 of surface area excavated, whereas Figure 5.19 includes time as a factor.

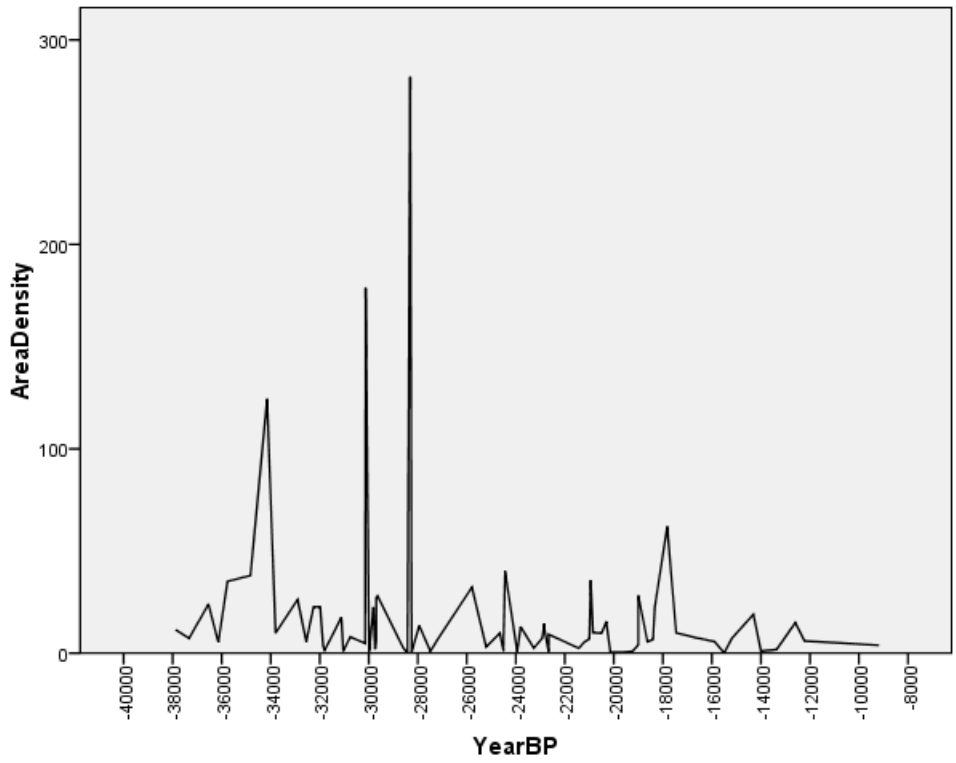

Figure 5.18: Lithic densities per m^2, plotted over time

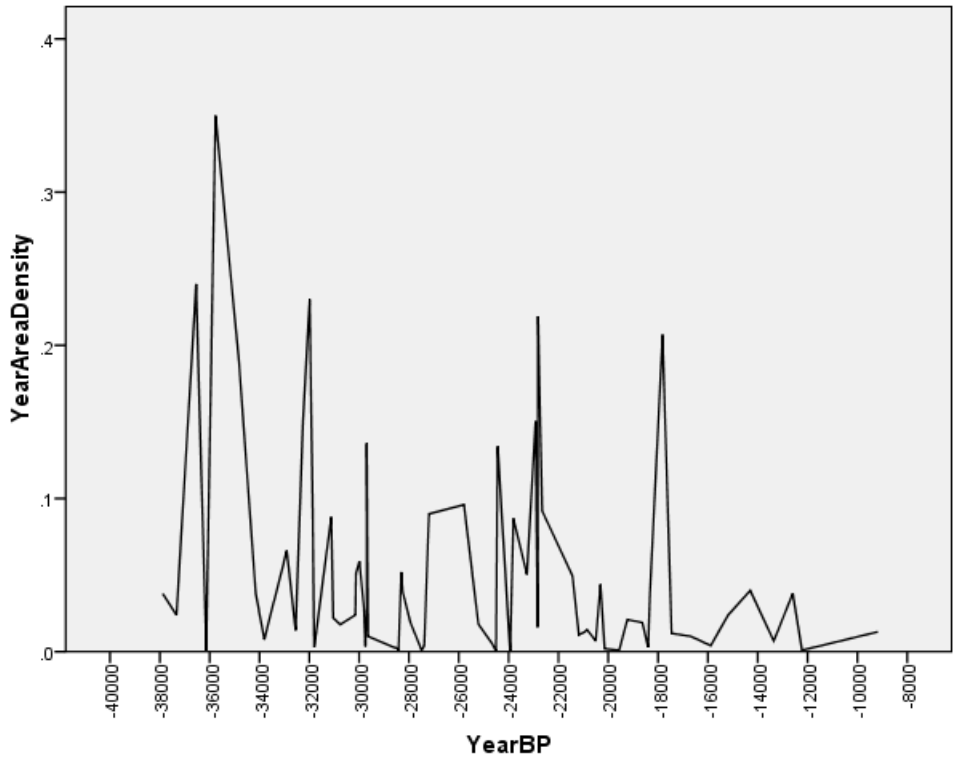

Figure 5.19: Lithic densities per m^3 , plotted over time

There are several peaks and troughs in the plots, most notably at 37000 BP, 35000 BP, 32000 BP, 23000 BP and 18000 BP.

§ 5.4 Diversity results

5.4.1 Distribution of tools

Data was collected on the distribution of lithics at each site for which data was available, in the manner outlined in the methods section. The distributions of tools at each site were compiled to produce overall distributions for each technocomplex, which in turn were used to inform the simulations. The overall distributions of tools, by technocomplex, are shown in the tables in Appendix C.

This distribution of Aurignacian tools is displayed graphically in Figure 5.20; the dominance of a few tool types, particularly the *grattoir simple en bout de lame* is striking. See the Appendix for a full breakdown of the Sonneville-Bordes tool typology.

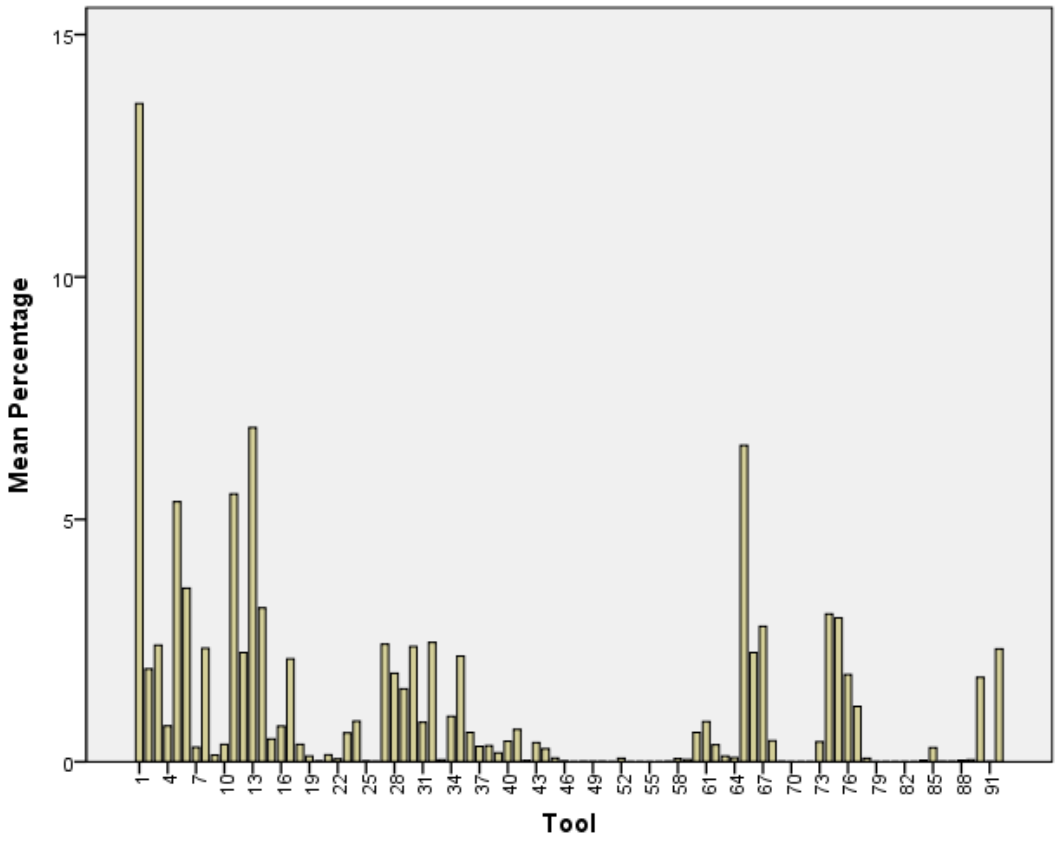

Figure 5.20: Distribution of tools from Aurignacian assemblages sampled. Data from 35,637 tools from 79 assemblages. Assemblages included in the data; Abri Blanchard (de Sonneville-Bordes, 1960) , Abri Caminade Aurignacian I F, I G, II, II D2, II D2 Upper (de Sonneville-Bordes, 1960) , Abri Castanet (de Sonneville-Bordes, 1960), Abri Cellier Aurig I and II (de Sonneville-Bordes, 1960), Lartet Aurig I (de Sonneville-Bordes, 1960), Metairie Aurig (de Sonneville-Bordes, 1960), Patary Aurig (de Sonneville-Bordes, 1960), Abri Pataud L6, L7, L8, eboulis 8-11, L11, L12, L13, L14 (Movius, 1975), Poisson (de Sonneville-Bordes, 1960), Renne (de Sonneville-Bordes, 1960), Faurelie (de Sonneville-Bordes, 1960), Chanlat couche 1, couche II (de Sonneville-Bordes, 1960), Cottes (de Sonneville-Bordes, 1960), Fonteniuoux (de Sonneville-Bordes, 1960), Dufour (de Sonneville-Bordes, 1960), Facteur 21, Facteur 19 (Delporte, 1968), La Ferrassie K7, K6, K5, K4, K3c, K3b, K3a, K3, K2, J, I2, I1, H, Gf, GsNo, GsN1, GsS, F, E1s, E1, E1b, E1d, E (Delporte, 1984) , La Ferrassie Peyrony Aurignacian I, II, III, IV (de Sonneville-Bordes, 1960), La Rochette Aurignacian 5d, 4, 3 (Delporte, 1964), Laugerie Haute Ouest Couche D, Le Moustier , Le Piage K, J, G-I, F (Champagne and Espitalié, 1981), Roc de Combe L5, L6, 7a, 7b, 7c (de Sonneville-Bordes, 2002).

The distribution of Gravettian tools is depicted in Figure 5.21.

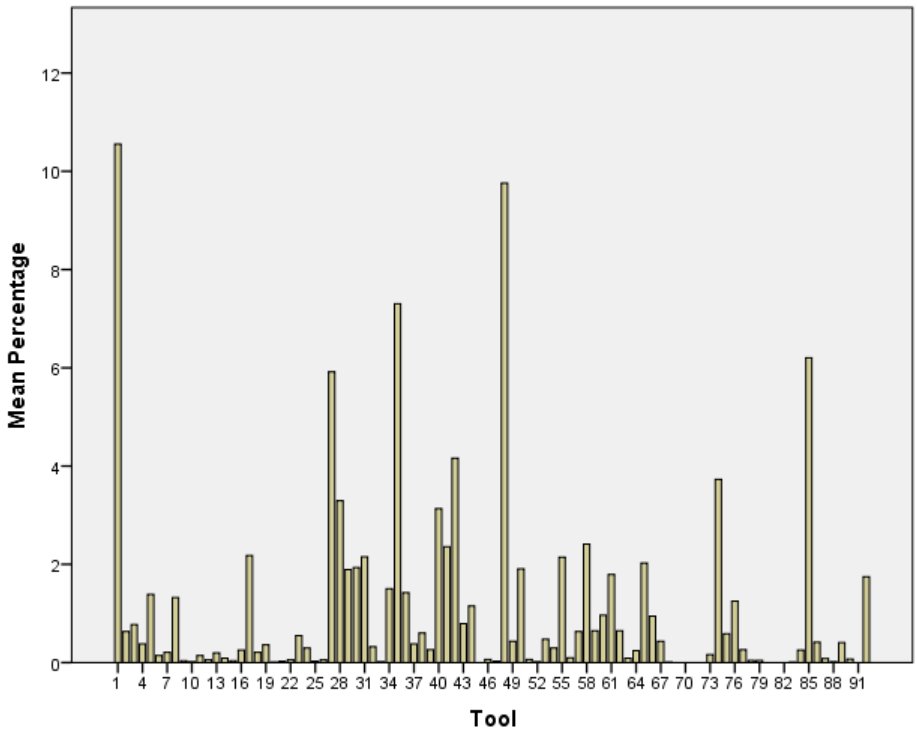

Figure 5.21: Distribution of tools from Gravettian assemblages sampled. Data from 26,584 tools from 29 assemblages. Assemblages included in the data; Abri Labattut (de Sonneville-Bordes, 1960), Abri Pataud L2, L3, L4, L4 middle, L4 upper, L4a, Eboulis 3-4, L5 (Movius, 1975), Fourneau du Diable (de Sonneville-Bordes, 1960) , Facteur 10-11 (Delporte, 1968), Ferrassie Peyrony J, K, L (de Sonneville-Bordes, 1960), Laraux L5, Noaillian (de Sonneville-Bordes, 1960), Laugerie Haute Est IIIi, III2 , Pegourie L10 (Séronie-Vivien, 1995) , Roc de Combe L1, L2, L3, L4 (de Sonneville-Bordes, 2002), Roc de Gavaudun (de Sonneville-Bordes, 1960), Roque Saint Christophe, Saint Christophe Fitte (de Sonneville-Bordes, 1960), Font Robert (de Sonneville-Bordes, 1960).

The distribution of tools in the Solutrean is shown in Figure 5.22.

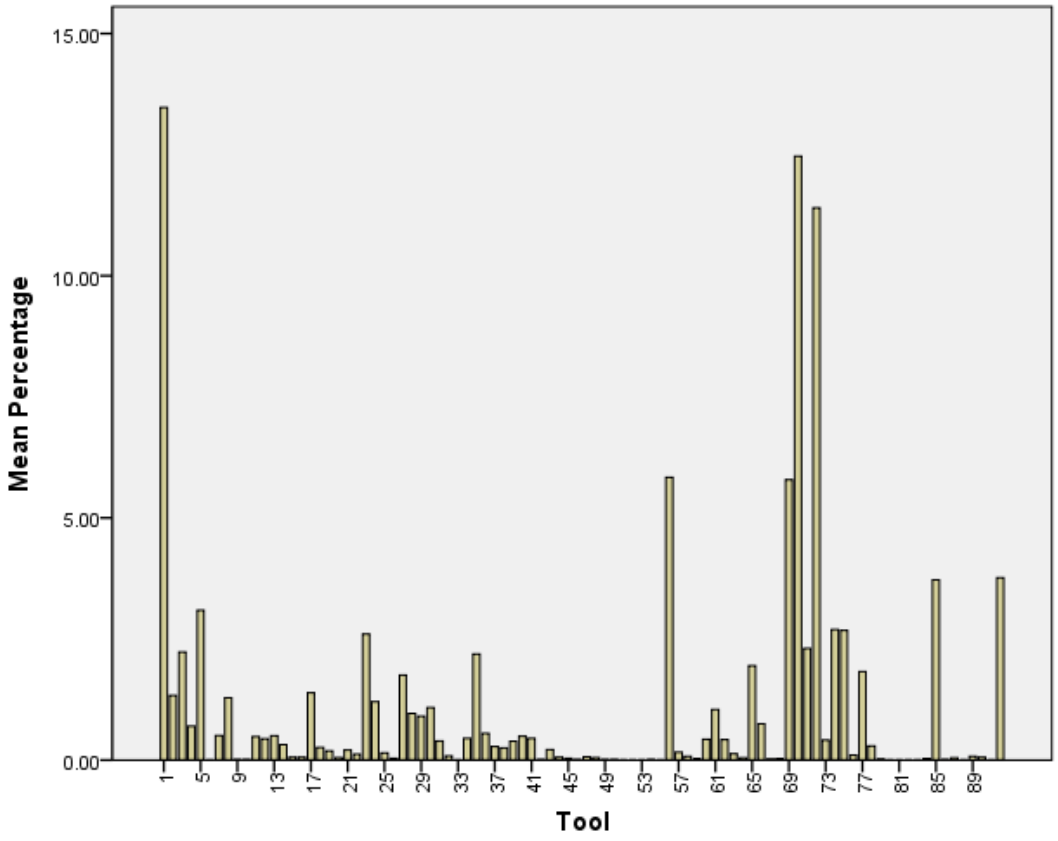

Figure 5.22: Distribution of tools from Solutrean assemblages sampled. Data from 11,613 tools from 18 assemblages. Data from the following assemblages; Badegoule Peyrony excavations (de Sonneville-Bordes, 1960), Badegoule Peyrille excavations (de Sonneville-Bordes, 1960), Fourneau Lower Terrace, Solutrean I Upper Terrace, Solutrean II Upper Terrace, Solutrean III (de Sonneville-Bordes, 1960), Jean Blanc Est and Ouest , Laugerie Haute Est H', H"-H"', Laugerie Haute Ouest G, H', H", H"' (de Sonneville-Bordes, 1960), Pech de Boissiere Upper Sol I, Upper Sol II (de Sonneville-Bordes, 1960), Eulalie Couche IV, Couche D (Lorblanchet et al., 1973)

As expected, the type fossils of the Solutrean are dominant; laurel leaf, willow leaf and shouldered points.

The Badegoulian tool distribution is depicted in Figure 5.23. Raclettes (tool no. 78) are absolutely dominant in this phase, as expected. The phase was formally known as the Magdalenian 0 or the Magdalenian with raclettes, and it is not difficult to see why.

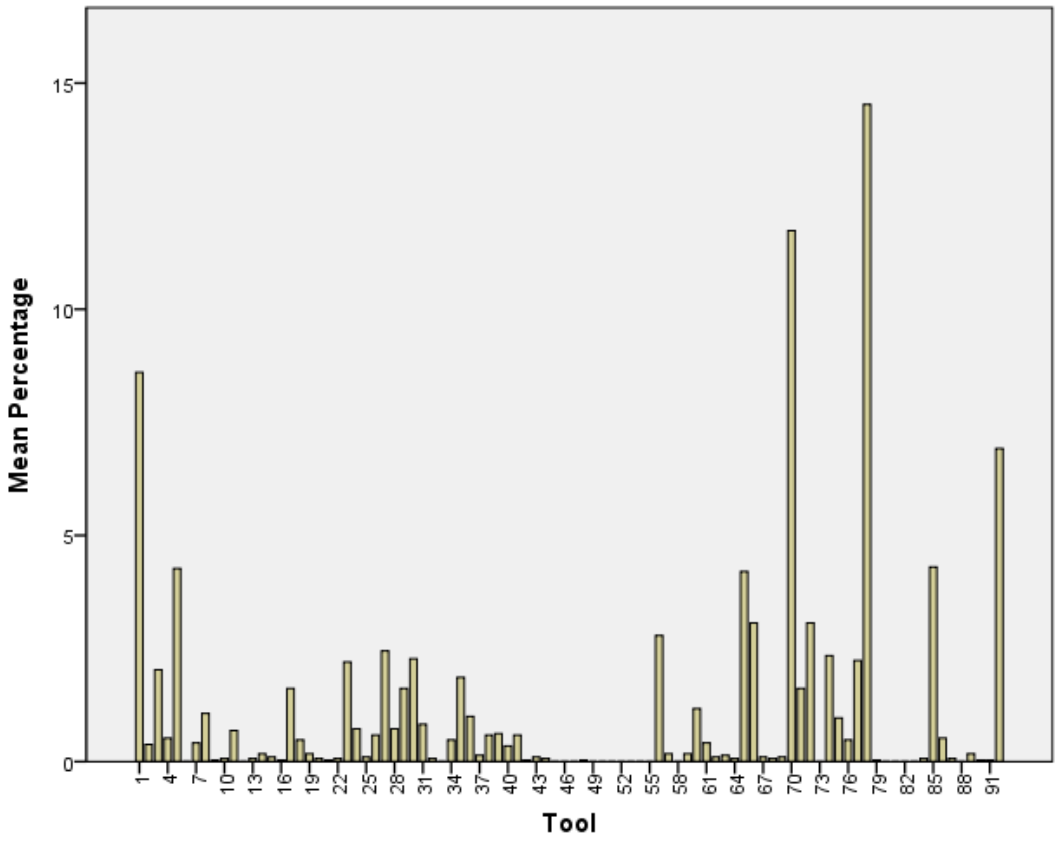

Figure 5.23: Distribution of tools from Badegoulian assemblages sampled. Data from 2,905 tools from 9 assemblages; Badegoule Peyrony excavations (de Sonneville-Bordes, 1960), Badegoule Peyrille excavations (de Sonneville-Bordes, 1960), Jamblancs (Jean Blancs) Est and Ouest (de Sonneville-Bordes, 1960), Pégourié couche 8A, 8B, 8C, 9A and 9B (Séronie-Vivien, 1995)

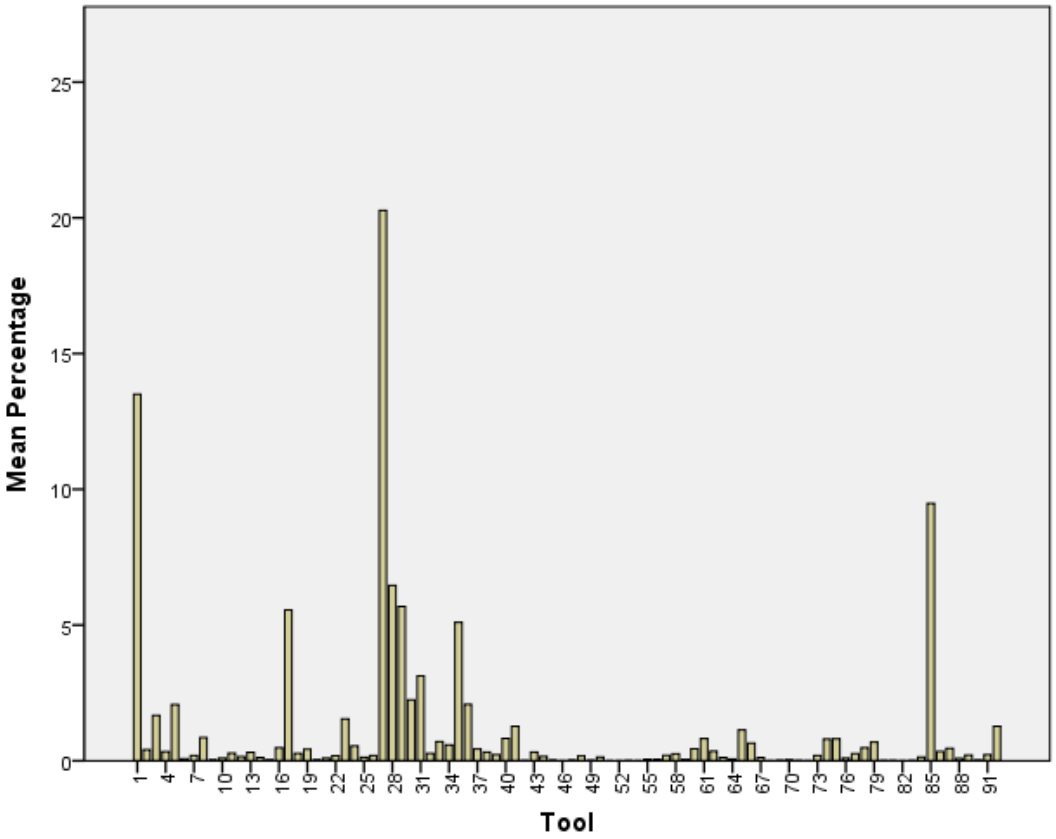

Figure 5.24: Distribution of tools from Magdalenian assemblages sampled. Data from 35,524 tools from 46 assemblages. Data from the following sites; Villepin (de Sonneville-Bordes, 1960), Mege (de Sonneville-Bordes, 1960), Cap Blanc (de Sonneville-Bordes, 1960), Les Eyzies (de Sonneville-Bordes, 1960), Chez Galou (de Sonneville-Bordes, 1960), Crabillat (de Sonneville-Bordes, 1960), Flageolet II (Rigaud, 1970), Font Brunel (de Sonneville-Bordes, 1960) , Fourneau du Diable (de Sonneville-Bordes, 1960), Gare de Couze (de Sonneville-Bordes, 1960) (Fitte and Sonneville-Bordes, 1962), Puy de Lacan (de Sonneville-Bordes, 1960), Jolivet (de Sonneville-Bordes, 1960), La Doue (Mazière, 1984), La Forge (de Sonneville-Bordes, 1960), La Madeleine (de Sonneville-Bordes, 1960), Laugerie Haute Est (de Sonneville-Bordes, 1960), Limeuil (de Sonneville-Bordes, 1960), Liveyre (de Sonneville-Bordes, 1960), Longueroche (de Sonneville-Bordes, 1960), Mairie (de Sonneville-Bordes, 1960), Metairie (de Sonneville-Bordes, 1960), Recourbie (de Sonneville-Bordes, 1960), Reverdit (de Sonneville-Bordes, 1960), Saint Cirq (de Sonneville-Bordes, 1960), Saint Germain (de Sonneville-Bordes, 1960), Saint Eulalie (Lorblanchet et al., 1973), Solvieux (de Sonneville-Bordes, 1960), Soucy (de Sonneville-Bordes, 1960), Valojoux (de Sonneville-Bordes, 1960)

The distribution of tools in Azilian assemblages is shown in Figure 5.25. It is no surprise to learn that the dominant tool type here is the Azilian point (tool no. 91).

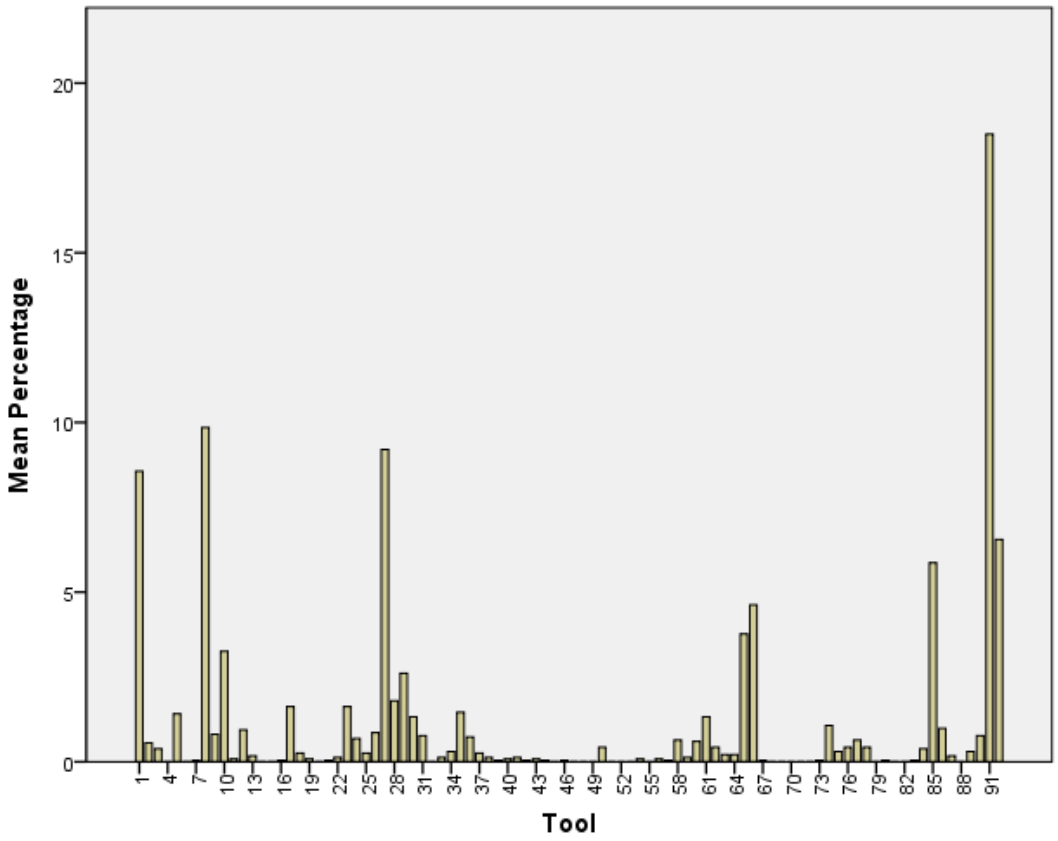

Figure 5.25: Distribution of Azilian tools. Data from 2,336 tools from 9 assemblages. Data from Villepin (de Sonneville-Bordes, 1960), Cap Blanc (de Sonneville-Bordes, 1960), Eyzies (de Sonneville-Bordes, 1960), La Madeleine (de Sonneville-Bordes, 1960), Longueroche (de Sonneville-Bordes, 1960), Pégourié (Séronie-Vivien, 1995)

5.4.2 Diversity measures by technocomplex

After the distribution of tools for each technocomplex was established, simulations were run to obtain the diversity indicators in the manner outlined in Chapter Four. The results of the analyses are shown below and the following plots depict the Observed-Expected richness and Observed-Expected D by technocomplex, respectively. To recap from Chapter Four, Observed-Expected richness and D are variables obtained through comparison of real and simulated assemblages. The 'real' assemblage is the observed value, while the 'expected' assemblage is the simulated value. Most values for observed-expected are negative. This is an inherent quality of the method. Every 'real life' assemblage used in the dataset is compared to a simulated dataset corresponding to the same technocomplex and sample size. This simulated dataset is drawn from the underlying distribution of tools for that technocomplex. There are more active categories for each technocomplex than there are within any assemblage belonging to that technocomplex. Therefore, 'observed' will always be less than 'expected', resulting in negative values for 'observed' - 'expected'.

The Gravettian is the most 'depleted' in technology, when compared to the other technocomplexes, although this may be a function of the diversity of the minor technocomplexes subsumed into this phase. Surprisingly there is no great break between the Magdalenian and the Azilian, as one would expect given the archaeological evidence for a cultural shift and, indeed, possible 'decline' with the onset of the Azilian.

A Kruskal-Wallis test was performed in PASW statistics (Figure 5.27) , confirming that the variable 'Observed-Expected richness' is significantly different across the technocomplexes.

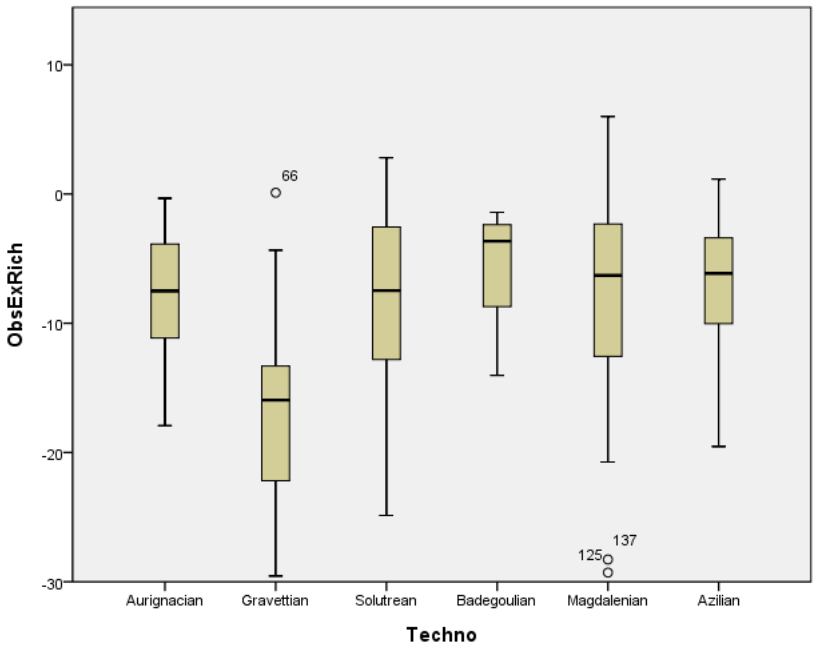

Figure 5.26: Observed-Expected richness ordered by technocomplex

Hypothesis Test Summary

	Null Hypothesis	Test	Sig.	Decision
1	The distribution of ObsExRich is the same across categories of Techno.	Independent-Samples Kruskal-Wallis Test	.000	Reject the null hypothesis.

Asymptotic significances are displayed. The significance level is .05.

Figure 5.27: Results of a Kruskal-Wallis test on lithic diversity by technocomplex

Technocomplexes were then coded and a Mann-Whitney test was performed (Tables 5.7 and 5.8) to further test which groups differed from each other, demonstrating that the Gravettian is significantly different to all other technocomplexes, but that no other groups displayed any significant differences. This confirms the Gravettian's status as a diversity-deficient phase. We will discuss potential causes of this deficiency in due course.

Figure 5.28 displays Observed-Expected D, the heterogeneity variable, by technocomplex.

	Aurignacian	Gravettian	Solutrean	Badegoulian	Magdalenian	Azilian
Aurignacian	N/A	S*	NS	NS	NS	NS
Gravettian	S***	N/A	S**	S***	S***	S*
Solutrean	NS	S**	N/A	NS	NS	NS
Badegoulian	NS	S***	NS	N/A	NS	NS
Magdalenian	NS	S*	NS	NS	N/A	NS
Azilian	NS	S*	NS	NS	S*	N/A

Table 5.7: Mann-Whitney U Tests on Tool Diversity (richness) by Technocomplex

	Aurignacian	Gravettian	Solutrean	Badegoulian	Magdalenian	Azilian
Aurignacian	N/A	.000	.860	.271	.886	.820
Gravettian	.000	N/A	.001	.000	.000	.002
Solutrean	.860	.001	N/A	.382	.758	.758
Badegoulian	.271	.000	.382	N/A	.433	.627
Magdalenian	.886	.002	.758	.627	N/A	.957
Azilian	.820	.002	.758	.627	.957	N/A

Table 5.8: Mann-Whitney U Tests on Tool Diversity (richness) by Technocomplex

Again, it is the Gravettian which displays the least diversity, when measured in terms of 'evenness'. Another Kruskal-Wallis test confirmed that there is a statistically significant difference between the technocomplexes with regards to this variable. A Mann-Whitney test also demonstrated that, again, the Gravettian differs from all other technocomplexes in terms of heterogeneity. However, in addition, statistically significant differences were observed between the Aurignacian and Magdalenian and between the Solutrean and Magdalenian. Tables 5.9 and 5.10 display the results of these tests.

	Aurignacian	Gravettian	Solutrean	Badegoulian	Magdalenian	Azilian
Aurignacian	N/A	S***	NS	NS	S***	NS
Gravettian	S***	N/A	S**	S**	S***	S***
Solutrean	NS	S**	N/A	NS	S*	NS
Badegoulian	NS	S**	NS	N/A	NS	NS
Magdalenian	S***	S***	S*	NS	N/A	NS
Azilian	NS	S***	NS	NS	NS	N/A

Table 5.9: Mann-Whitney U Tests on Tool Diversity (heterogeneity) by Technocomplex

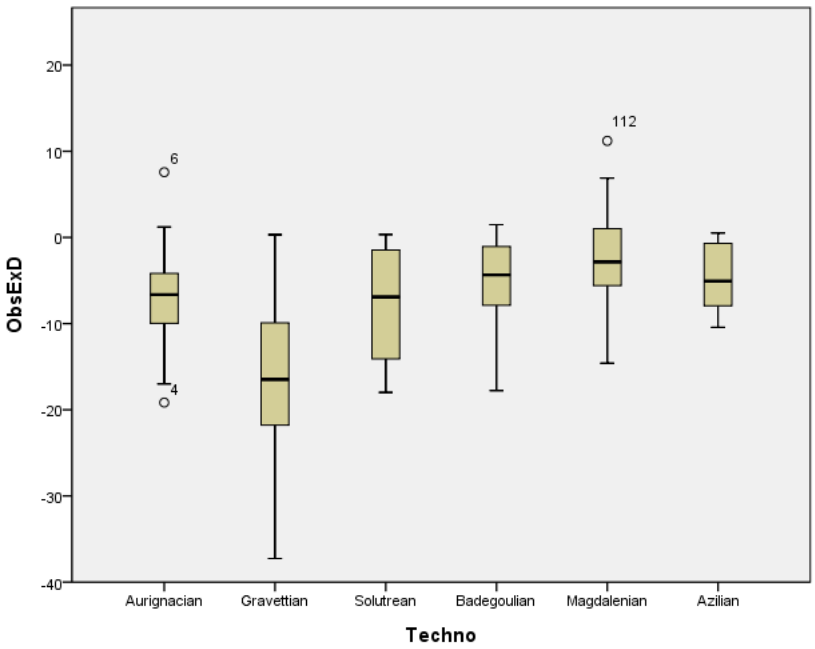

Figure 5.28: Observed-Expected D by technocomplex

Hypothesis Test Summary

	Null Hypothesis	Test	Sig.	Decision
1	The distribution of ObsExD is the same across categories of Techno.	Independent-Samples Kruskal-Wallis Test	.000	Reject the null hypothesis.

Asymptotic significances are displayed. The significance level is .05.

Figure 5.29: Kruskal-Wallis test on Observed-Expected D by technocomplex

	Aurignacian	Gravettian	Solutrean	Badegoulian	Magdalenian	Azilian
Aurignacian	N/A	.000	.705	.393	.000	.352
Gravettian	.000	N/A	.001	.001	.000	.000
Solutrean	.705	.001	N/A	.433	.003	.298
Badegoulian	.393	.001	.433	N/A	.181	.965
Magdalenian	.000	.000	.003	.181	N/A	.125
Azilian	.352	.000	.298	.965	.125	N/A

Table 5.10: Mann-Whitney U Tests on Tool Diversity (heterogeneity) by Technocomplex

5.4.3 Diversity over time in the Upper Palaeolithic

Figure 5.30 displays the variables of richness and D, plotted over time. The two measures of Richness and D are not independent, as demonstrated in Figure 4.10. Thus any apparent trends linking the two variables are to be expected. The diversity measures fluctuate wildly over time, with notable 'spikes' at 35,000 BP, 21,000 BP and 17,000 BP. Troughs occur at 30,000 BP, 28,000 BP, 24,000 BP and 13,000 BP.

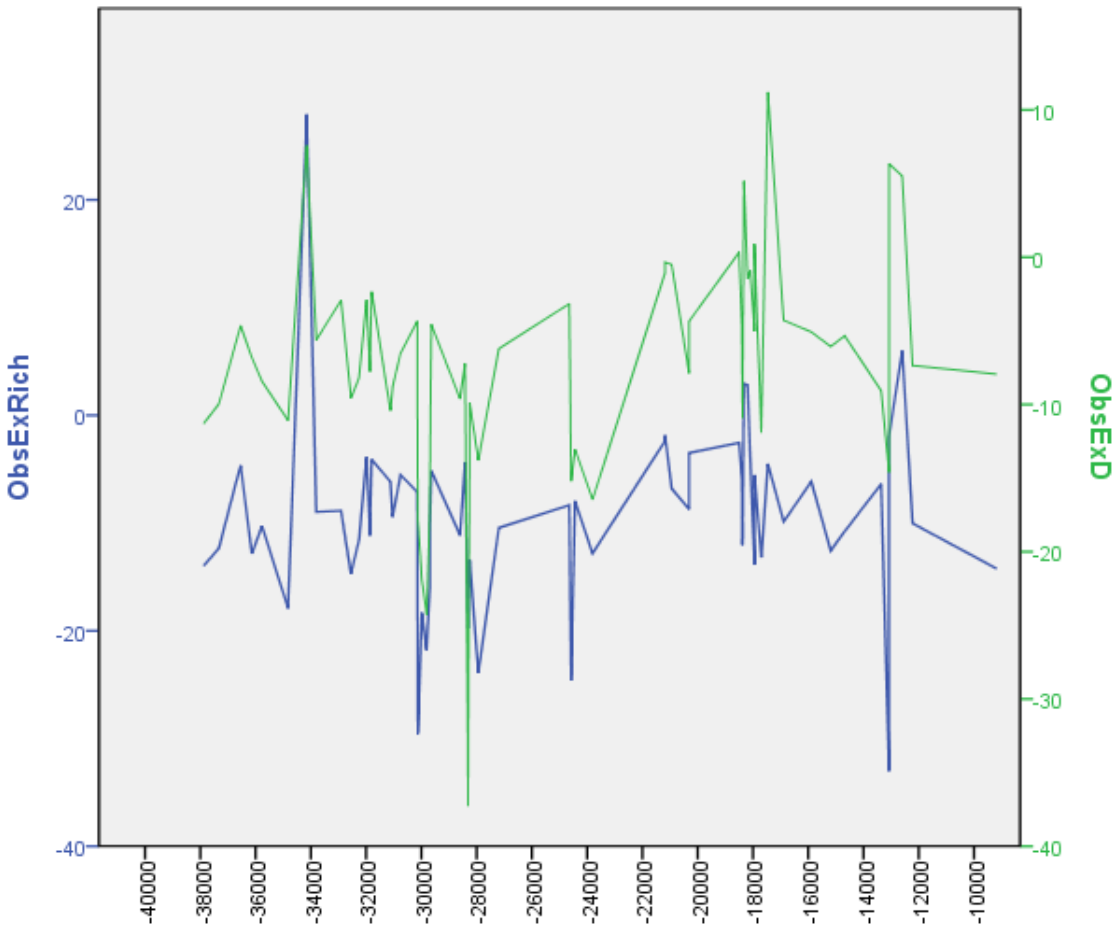

Figure 5.30: The diversity measures Observed-Expected Richness and D over time

§ 5.5 Climate as a Variable

5.5.1 Temperature and Diversity

The following analyses show diversity values over time. It is useful for us to look at diversity values over time, as well as grouped by technocomplex for two reasons. First, changes over time within technocomplexes can be seen. Secondly, we can mitigate against assemblages which have been incorrectly assigned to technocomplexes. I have also included temperature as a variable in the next analyses, to observe the interactions of innovation and climate. Smoothed $\delta^{18}O$ values from the NGRIP ice core are used here as a proxy for temperature. The lowest values for this variable correspond to low global temperature, and vice versa. Figure 5.31 depicts NGRIP values against Observed-Expected richness, with the blue line corresponding to NGRIP values and the green line corresponding to Observed-Expected richness.

There appears to the eye to be a negative correlation between the two variables. A cross-correlation analysis in PASW statistics (Figures 5.32 and 5.33) revealed a positive correlation at a lag of 3, this suggests that there is a delay between climatic change influencing human cultural behaviour.

However, as there *appeared* to be something more interesting taking place in the data, I decided to explore the relationship between the rate of change of the variables of temperature (NGRIP) and richness.

While time-series data cannot be treated as independent, the derivatives of a time series can be treated as essentially independent data, as the rate of change between two points in a time-series will not be dependent on the rate of change between the previous two points. As such a Pearson correlation analysis was performed (Table 5.11) on the derivatives of NGRIP and richness, revealing a negative correlation which was statistically significant at the 0.05 level. It thus appears that the *rate of change* of temperature and the *rate of change* in assemblage richness are negatively related, with

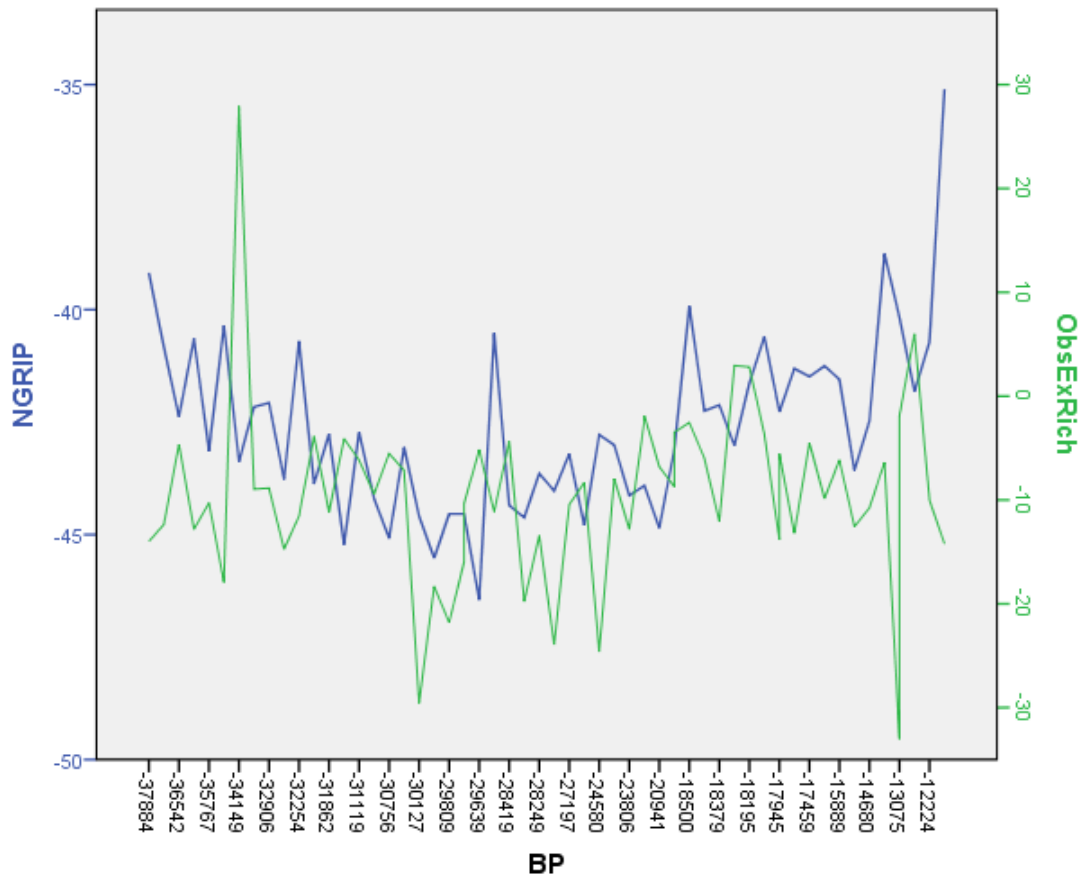

Figure 5.31: Richness (observed-expected richness) over time, against NGRIP values

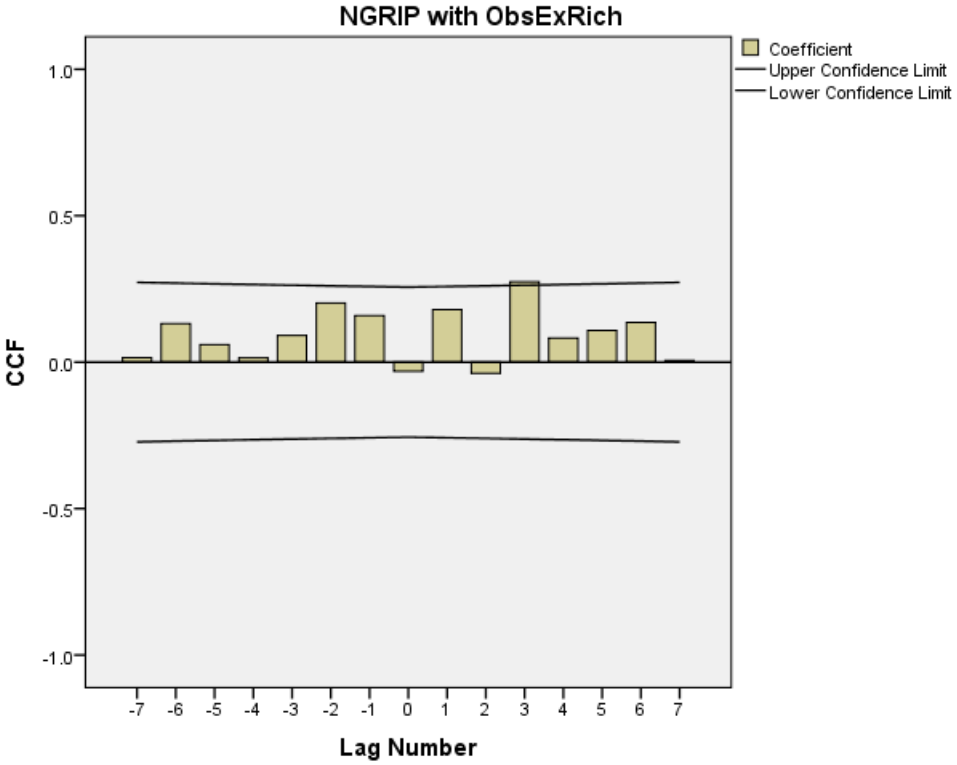

Figure 5.32: Derivatives of NGRIP against derivatives of richness

NGRIP with ObsExRich

Cross Correlations

Series Pair: NGRIP with ObsExRich

Lag	Cross Correlation	Std. Error[a]
-7	.015	.136
-6	.132	.135
-5	.060	.134
-4	.014	.132
-3	.091	.131
-2	.202	.130
-1	.159	.129
0	-.031	.128
1	.179	.129
2	-.038	.130
3	.275	.131
4	.082	.132
5	.108	.134
6	.135	.135
7	.006	.136

a. Based on the assumption that the series are not cross correlated and that one of the series is white noise.

Figure 5.33: Cross Correlation richness and NGRIP

a *positive* change in temperature eliciting a *negative* change in artefact diversity.

Correlations

		NGRIPchange	ChangeRich
NGRIPchange	Pearson Correlation	1	-.257*
	Sig. (2-tailed)		.047
	N	60	60
ChangeRich	Pearson Correlation	-.257*	1
	Sig. (2-tailed)	.047	
	N	60	60

*. Correlation is significant at the 0.05 level (2-tailed).

Table 5.11: Cross Correlation richness and NGRIP

However, despite the apparent negative relationship between temperature and richness, this trend flipped several times over the course of the Upper Palaeolithic. Figure 5.35 displays the ratio of derivatives (derivatives of NGRIP/derivatives of richness) over time throughout the Upper Palaeolithic. Points below the zero line pertain to phases where this negative relationship holds true; above the line and a positive relationship is active instead. We see that this relationship has fluctuated between a positive and negative relationship throughout the Upper Palaeolithic.

The relationship between heterogeneity and temperature was then explored in a similar manner. The two variables are shown below, over time.

A cross-correlation analysis revealed that the two variables correlate at lags -2, -1, 1 and 3, again suggesting that behavioural changes lag behind climatic ones somewhat.

When the derivatives of temperature and heterogeneity were plotted there did not appear to be any relationship between the two variables and this was confirmed by a Pearson correlation analysis, which did not return a statistically significant result.

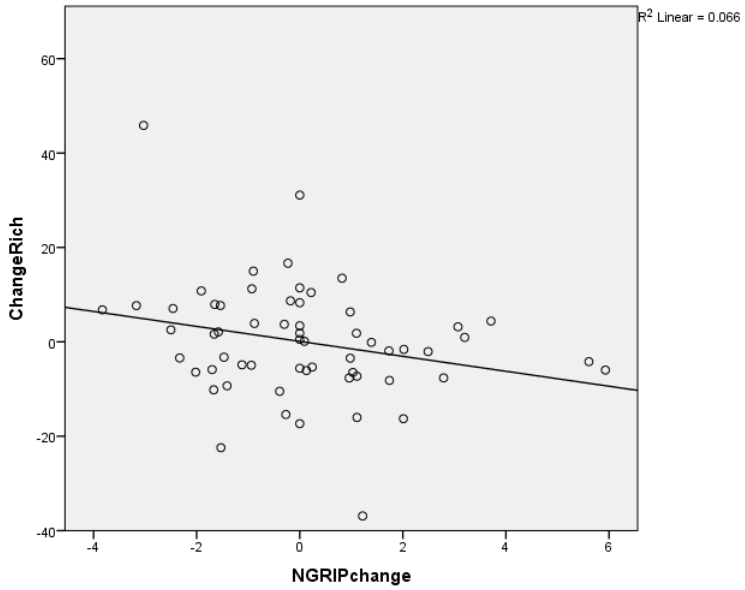

Figure 5.34: Ratio of NGRIP against derivatives of richness (Observed-Expected richness)

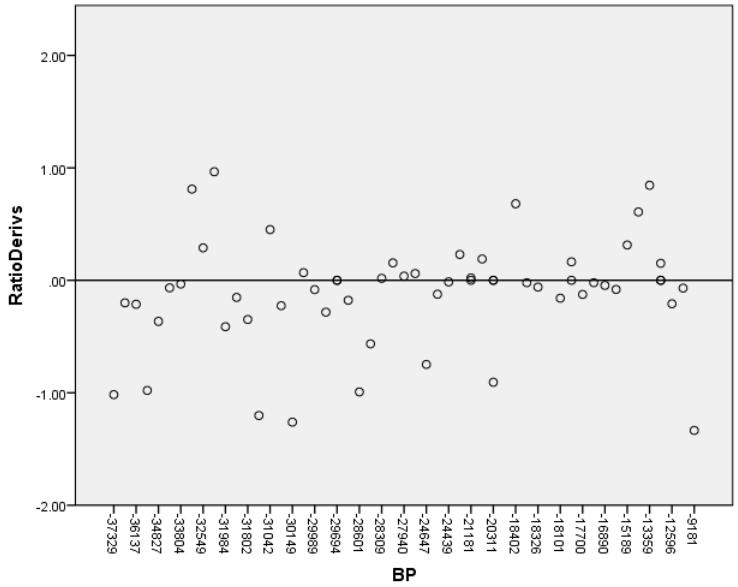

Figure 5.35: Ratio of derivatives over time - derivatives of NGRIP/derivatives of richness) plotted by date

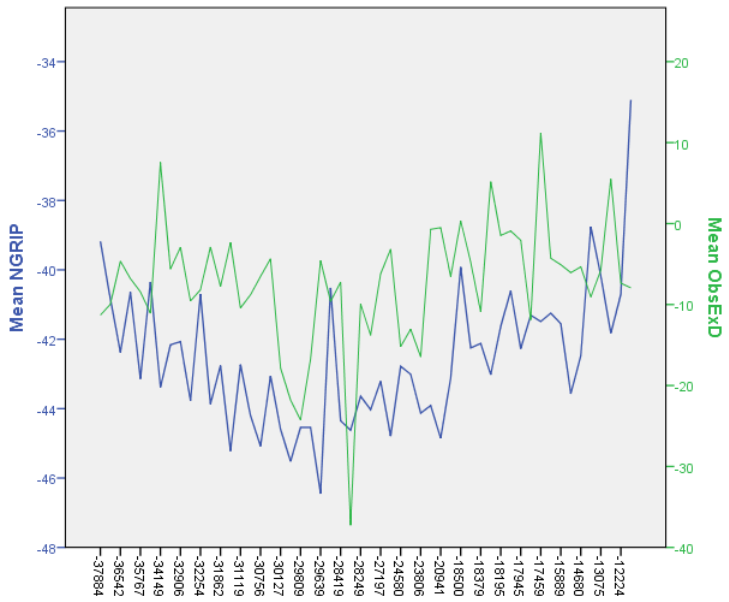

Figure 5.36: Heterogeneity over time, against NGRIP values

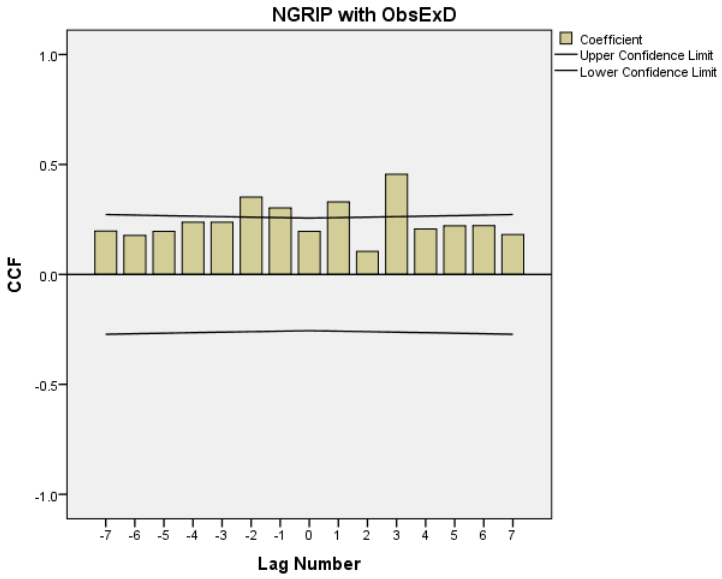

Figure 5.37: CCF heterogeneity and NGRIP

NGRIP with ObsExD

Cross Correlations

Series Pair: NGRIP with ObsExD

Lag	Cross Correlation	Std. Error[a]
-7	.197	.136
-6	.177	.135
-5	.196	.134
-4	.238	.132
-3	.237	.131
-2	.351	.130
-1	.303	.129
0	.196	.128
1	.330	.129
2	.105	.130
3	.456	.131
4	.207	.132
5	.221	.134
6	.222	.135
7	.181	.136

a. Based on the assumption that the series are not cross correlated and that one of the series is white noise.

Table 5.12: CCF heterogeneity and NGRIP

Chapter 6

Discussion and Conclusions

In order to simplify my main arguments, I have divided my key results into four main groups, concerned with; methodology, demography, innovation and implications for human behaviour. In addition, I have included a further, minor category, containing unexpected results that came to light during this study.

Key methodological findings

- The summed probability approach produces a demographic signal and is a useful approach in prehistoric demography.
- Taphonomic and research bias can be overcome.
- The use of an informative prior in Bayesian modelling is not worthwhile.
- Bayesian modelling is not justified for landscape-wide, dates as data studies.
- Innovation levels can be measured using lithic diversity data.
- Demographic data can be obtained from intra-site lithic-densities.

Key demographic results

- The radiocarbon data shows peaks in activity at: 32,000 BP, 30,000 BP, 24,000 BP, 20,000 BP, 18,000 BP, 16,000 BP and 14,000 BP.
- The peak at 24,000 coincides with the LGM and the peak at 20,000 with the end of the LGM.
- Lithic-density data peaks at: 37,000 BP, 35,000 BP, 32,000 BP, 23,000 BP and 18,000 BP.
- Radiocarbon and lithic data do not corroborate on the peak in activity in the LGM. The lithic data shows only peak towards the start of the LGM at 23,000 BP.
- Radiocarbon and lithic data corroborate on peaks in activity at 32,000 and 18,000 BP.
- Radiocarbon and prior studies (archaeological, genetic) corroborate the LGM refugium concept.
- There are peaks in radiocarbon activity in other phases that are even more dramatic than during the LGM. The region is serving as a refuge zone in the Upper Palaeolithic. However, this is not temporally confined to the LGM.
- Where radiocarbon and lithic-density data disagree, I believe that the radiocarbon result is more reliable and should be preferred.
- There is a demographic and technological break between the Gravettian and Solutrean.
- KDE results show changing settlement patterns over time.

Key innovation results

- The Gravettian is depleted in assemblage diversity, in comparison to all other technocomplexes. It is also one of the mildest phases climatically.
- The Badegoulian sees the greatest assemblage diversity. It is also an especially mild phase.
- When diversity data is plotted over time, rather than by technocomplex, we see an overall negative relationship between temperature and innovation. This relationship does flip a few times across the period of interest but is mostly negative.
- The conflicting innovation data from the Gravettian and Badegoulian do not negate this relationship. A different mechanism relating demography to innovation is at work in each technocomplex; the mother of invention and the numbers game mechanisms, respectively.
- Settlement patterns will impact on innovation transmission rates.

Implications for human behaviour

- In the modern world there is a positive relationship between ET and population density.
- This relationship is reversed in Palaeolithic Southwest France, so that population increases in colder periods.
- The unique refugium circumstances of the LGM reverse the normal 'rules' relating climate and population.
- In the modern world, latitude and innovation are positively correlated. A negative relationship between ET and innovation is therefore implied, so that there is a negative relationship between ET and innovation in modern world hunter-gatherers.

- The same relationship between climate and innovation exists in the study region and period.

- Why is the relationship between ET and population reversed? When the other relationships are unchanged from prehistory to the present day? The answer lies in the *mechanisms* that link demography and innovation. In the modern world , and at some points in the study period, the *mother of invention* process is at work. Throughout the majority of the study period, the *numbers game* process is in action.

Further interesting results

- The Magdalenian/Azilian transition does not involve demographic decline. This is at odds with current dogma.

- Magdalenian hunter-gatherers are relatively sedentary.

§ 6.1 Methodological Findings

The summed probability approach does produce a true demographic signal and is a useful approach to prehistoric demography

The dates as data approach is highly controversial (Blackwell and Buck, 2003) (Chiverrell et al., 2011). However, it has delivered results here and I have demonstrated that it is a robust method. Initially, I thought that the approach would not be useful, given the controversies surrounding it. I set about producing summed probability distributions chiefly for the purpose of further discrediting the approach. In analysis I was proved wrong and the approach became a cornerstone of my work. The comparison of the summed probability distribution for the study region with a simulated dataset, drawn from a uniform distribution, demonstrated conclusively that the sample of radiocarbon dates do not conform to a uniform distribution. If population size was static across the

Upper Palaeolithic, our probability distribution would have resembled the flat, even distribution from the simulated dataset.

Taphonomic and research bias can be overcome

Taphonomic bias has the potential to severely obscure demographic signals (Surovell and Brantingham, 2007). The correction curve provided by (Surovell et al., 2009) was incredibly helpful. It transformed our dataset from an otherwise meaningless, geologically created dataset, into an archaeologically useful dataset, containing demographic meaning.

As I corrected the radiocarbon dataset for taphonomic bias, tested it against a uniform distribution and smoothed it with a moving average, following Williams (2012), I am confident in the dates as data results presented here.

As well as potential taphonomic bias, research bias is a grave problem in archaeology. It has been noted that the Southwest France region is intensively studied (Rigaud and Simek, 1987) and it is currently unfashionable to study the region, for this reason. However, I don't believe that research bias towards Aquitaine is a problem for this study. This entire thesis has focussed on Southwest France, so we can treat any research bias as a *constant*. Research bias would be a problem if we were comparing two regions. But this is not an issue in this study.

Another source of research bias is that of favouring older sites, or particular periods. I feel that this is a more serious issue for this study. In the Palaeolithic a lot of glory is ascribed to locating old sites; finding the first instances of particular behaviour or artefacts. I feel that this partially explains the steep decline in radiocarbon data during the Azilian phase; researchers are less interested in the Late Upper Palaeolithic. Equally, compare the summed probability distributions obtained from modelled and unmodelled dates (Figures 5.3 and 5.4). Modelled dates are from sites which have produced multiple radiocarbon dates. Unmodelled dates are from sites where only one or two radiocarbon dates have been produced. You can see from these figures

that dating programmes are biased against Late Upper Palaeolithic sites; many of the Magdalenian peaks seen in Figure 5.3 are absent from Figure 5.4. This is a problem and we should be aware of it.

Some research bias will also be introduced due to the nature of the particular study. For example, for this project I was interested in looking at evidence for population change in the Upper Palaeolithic of France, so I collected data on the Upper Palaeolithic of France. I didn't collect data on the Middle Palaeolithic or Azilian, as this was beyond the time constraints of the project. However, not collecting Mesolithic data has harmed the Azilian data. The Magdalenian portion of the summed probability plot has benefitted from receiving the tails from the calibrated Azilian radiocarbon dates. The Azilian has lost out by not receiving the tails from the Mesolithic radiocarbon dates. In such a way, the very nature of my research has led to research bias. However, any archaeological study will be limited to some temporal phase though, and this problem will be encountered by anyone producing summed probability distributions, unless they collect data from phases bracketing the time period of interest.

The outlook for overcoming research bias is bleak at present. However, taphonomic bias can be overcome.

The use of an informative prior in Bayesian modelling is not worthwhile

I devoted part of this thesis to elaborating a system for 'chronometric hygiene' (following Waterbolk (1971) and Spriggs (1989)). I was able to observe disparities in frequencies of outliers amongst samples from different laboratories, samples dated using different dating methods, dated in different decades and different sample materials. However, only one robust, statistically significant result was obtained, from 'dating method.' AMS dates produced *more* outliers than conventional dating methods. This could be due to either small, stratigraphically mobile samples being dated through AMS techniques, or could be the result of the difficulties of pretreating bone samples in the early days of radiocarbon dating. Given the high frequency of bone samples included

in this study, and the apparent decline in radiocarbon outliers through time in the study region and period, the latter explanation seems to be supported. However, in future I would like to examine a larger sample of radiocarbon dates, to see if other factors influence the quality of a radiocarbon date, and to investigate if informative priors can be reliably applied to outlier models. Many statistical analyses here failed on the basis of sample size, rather than producing statistically insignificant results and I believe that expanding the sample size to include other regions and periods would reveal statistically significant results in other factors. Unfortunately I was unable to increase the sample size for this study, due to the necessity for using only dates obtained from well-dated stratigraphic sequences. I could not produce Bayesian models for sites for which only one or two dates were available. Thus my sample size was limited by circumstances beyond my control.

I used the discrepancies in dating quality between various types of samples to elicit prior probabilities for outlier analysis in Oxcal. As you can see from Figure 4.6, this made virtually no difference to posterior distributions and was clearly more trouble than it was worth. After observing the limited effects of using informative priors, and given the tendency for most researchers to use uniform priors, I used uniform priors for the Bayesian models shown for each site in the appendix, and 'carried forwards' for to the results chapter. I advise sticking to a uniform prior in most cases.

Bayesian modelling is not justified for landscape-wide, dates as data studies

I also spent considerable time developing Bayesian models in Oxcal that incorporated stratigraphic information about sites. Example code is provided in the Appendix, to demonstrate how a typical model was produced and the models themselves are included in Chapter Four. You can see from Figure 5.7 that Bayesian analysis made little difference to the overall summed probability distribution for the region. The two distributions share almost all peaks and troughs and paint virtually identical demographic pictures. Only one solitary peak, at 27,000 BP appears in just the modelled distribution. On this basis I would advise against the use of Bayesian models for

anybody embarking on a landscape-wide population study using summed probability distribution. However, this does not mean that Bayesian models are useless. For refining chronology at individual sites they are very useful eg (Higham et al., 2011a). They were also useful in this study for providing boundary estimates for levels. I used these boundaries to estimate level duration, which made the intra-site lithic-density method possible.

Demographic data can be obtained from intra-site lithic-densities but it is less preferable to radiocarbon data

The intra-site lithic-density approach is less controversial than the summed probability approach. It has been utilized by prehistorians in general (Gamble, 2002) and for the study region specifically (Mellars and French, 2011) (Collins, 2008). The durability of lithic remains means that they are not subject to taphonomic bias. However, as we are reliant on radiocarbon dates to add a temporal dimension to the density data, we will always be exposed to the dangers of dating cultural carbon. Lithics are more durable than samples for radiocarbon dating, but we are reliant on radiocarbon dates for dating lithics. Changing settlement systems can impact on intra-site lithic densities, meaning that they will not always be indicative of relative population size. I outlined some different hunter-gatherer landuse systems in Chapter Three and these systems will leave different archaeological traces. Different site types will produce differential densities of lithics. They are unlikely to produce different numbers of hearths. For this reason, where radiocarbon and lithic data disagree, I am inclined to favour results produced through the dates as data method.

Innovation levels can be measured using lithic diversity data

The modified method of Kintigh (1989) was successful at providing innovation data. The universal application of the Sonneville-Bordes typology to Upper Palaeolithic excavations made it very simple to apply. The social nature of human innovation, outlined in Chapter Two, means that diversity of archaeological is an ideal proxy for human

innovation. Individual creativity is important for ideogenesis but innovations will only be visible archaeologically if they have been transmitted and are able to survive in the population for long enough to leave archaeological traces.

§ 6.2 Key demographic results

The radiocarbon data shows us peaks in activity at: 32,000 BP, 30,000 BP, 24,000 BP, 20,000 BP, 18,000 BP, 16,000 BP and 14,000 BP

The taphonomically-corrected summed probability distributions have peaks at these points. There is also a rapid crash in activity in the Late Upper Palaeolithic. Though this late crash could be caused by truncating data-collection at the end of the Upper Palaeolithic, as discussed previously.

The peak at 24,000 BP coincides with the LGM and the peak at 20,000 BP with the end of the LGM

Do the peaks in activity support the LGM refugium hypothesis? The peak at 24,000 is towards the start of the LGM and the peak at 20,000 is just at the end of the LGM. Many of the other peaks are more dramatic. If the region was serving as a refuge zone, I would argue, on the basis of the radiocarbon data alone, that it was a refugium at several points during the Upper Palaeolithic, not just in the LGM.

Lithic-density data peaks at: 35,000 BP, 32,000 BP and 23,000 BP. A smaller, local maximum occurs at 18,000 BP. When grouped by techno-complex, Solutrean assemblages have the greatest density of tools

The peaks at 24,000 and 20,000 BP correspond to the start and end of the LGM. No peaks occur during the LGM. The lithic-density data, analyzed over time, does not support the LGM refugium hypothesis.

When I grouped lithic-density data by technocomplex the Solutrean saw the highest average density of tools. This was not a statistically significant result, though this is

likely to be the result of sample-size. I conjecture that with a bigger sample size we would see a statistically significant result and this is something to be explored in future. From Figure 5.15 we can see that the average density of tools is much higher in the Solutrean than in other technocomplexes. Unfortunately, external limits were placed on my data collection. As well as needing lithic data from excavated sites, they had to be sites where sequences of radiocarbon dates were available, so that I could estimate the length of time represented by the level. The only way for me to increase the sample size would be to initiate a dating programme at a few Solutrean sites. This could be a future direction for work, but unfortunately I was not able to complete it for this study.

Radiocarbon and lithic data do not corroborate each other with regards to the peak in activity in the LGM. They do corroborate over other peak periods

In the field of prehistoric demography, we must use as many methods as possible and hope that where they agree a demographic signal is obtained. As the radiocarbon and lithic data overlap at 32,000 BP, 24/23,000 BP and 18,000 BP, I accept that these periods were truly times of demographic expansion.

What of the points where they disagree? Are the summits observed in the Late Upper Palaeolithic in the radiocarbon data false signals? I am inclined to accept the radiocarbon data over the lithic data, where the two datasets disagree, for several reasons. First, the Magdalenian loses out in any demographic study based on lithics due to the abundance of bone artefacts dating to this technocomplex. It was not possible to include bone artefacts in the present study, due to time constraints. Secondly, the impact of land-use systems on lithics could have warped the results. If lifestyles changed dramatically into the Magdalenian then the densities of lithics at sites would have been similarly affected. Unfortunately, this is a pitfall of hunter-gatherer archaeology.

Intersection of radiocarbon and prior studies (archaeological, genetic) cor-

roborate regarding the LGM refugium concept. However, prior studies imply a more dramatic increase in activity than we have evidence for here

Prior studies using genetic and archaeological data largely corroborate the notion of high population density in the region during the Solutrean. Bocquet-Appel et al. (2005)'s study, introduced in Chapters Two and Three estimated a European metapopulation size of 5885 during the LGM, compared to a European metapopulation size of 4776. Estimates of metapopulation size were produced through 'back-projecting' hunter-gatherer population densities onto the modelled size of the geographic range of hunter-gatherers in several phases of the Upper Palaeolithic. As well as estimating a slight increase in European population size from the Gravettian to the Solutrean, the authors also support the notion of a Southern European refuge zone. It follows that if an overall increase in European population occurred from the Gravettian to the Solutrean, alongside a decrease in the geographic range of hunter-gatherers in the LGM, that a *drastic* increase in activity in Southwest France would occur. The data in this thesis does not present the extreme increase in activity that we would expect under the circumstances outlined in Bocquet-Appel et al. (2005).

As demonstrated in Chapter Three, the Solutrean does have the highest density of sites for any technocomplex, when time is considered as a factor. This strongly supports the notion of an intense increase in activity with the LGM. When we consider the radiocarbon data in this thesis, we see a local peak in activity, but no more dramatic than in other phases. I believe that the lithic data, when grouped by technocomplex, would demonstrate that the Solutrean has the greatest average density of tools, if the sample size were increased. When analyzed over time, the lithic data shows a peak at 23,000 BP, corresponding to the Solutrean.

Prior genetic studies confirm that a population bottleneck occurred at the time of the LGM, which was followed by population expansion out of Southern Europe (Achilli et al., 2005). However, it is Iberia, not France, that is favoured as a refugium. The prolonged presence of humans in Southwest France and Iberia cannot be doubted. This

is evident from Demars' settlement maps, (Demars, 1996), presented in Chapter Three. However, I am unable to clarify whether France or Spain was the main refugium. This would require further study. It is entirely possible that the Aquitaine region was the northern limit of a southern European refuge zone, rather than the main refugium itself. Whether France or Spain was the main refuge zone is an interesting question to be answered in future work.

In summary, prior studies and the site count data presented in Chapter Three all point to high activity levels in the Solutrean. Intra-site lithic density data, grouped by technocomplex also supports this. Radiocarbon data also points to relatively high activity in the LGM, though this is eclipsed by other phases. On balance, I accept the LGM refugium hypothesis but also argue that Southwest France was a refugium throughout the Upper Palaeolithic, whenever conditions took a turn for the worse.

There are peaks in activity in other phases, which are even more dramatic than in the LGM. The region is serving as a refuge zone in the Upper Palaeolithic. However, this is not temporally confined to the LGM

The refugium concept is supported on the basis of radiocarbon data presented here. It is not supported on the basis of lithic data but, as outlined above, the radiocarbon data is more reliable than the lithic data. Outside of the peaks, during, just before and just after the LGM, the summed probability plot is punctuated by many other spikes in activity. On the radiocarbon data alone, we can see that high levels of activity occur in the LGM and also in other phases, such as at 30,000 BP and also at many points in the Late Upper Palaeolithic.

There is a technological and demographic break between the Gravettian and Solutrean

Traditionally, the Solutrean is viewed as an intrusive industry (Smith, 1966). This view sits well with the refugium concept and we can imagine climate refugees arriving into the region, bringing new technology with them. In recent years, some authors

have proffered evidence for continuity between these phases, seeing the Solutrean as an evolution of late Gravettian industries (Renard, 2011). Our diversity data (Figure 5.26) demonstrates a clear break between the Gravettian and Solutrean in terms of assemblage richness. However, the Gravettian also differs from every other Upper Palaeolithic technocomplex in this respect. It is the Gravettian that appears intrusive, on the basis of assemblage diversity, not the Solutrean.

Superficially, Gravettian and Solutrean technology are very different. The Solutrean presents a range of type fossils which, with the exception of the Badegoulian, do not appear in other phases and certainly not in the Gravettian. The Solutrean type fossils, particularly the willow leaf points, are not particularly practical. The scraper/burin ratio is relatively stable across the Solutrean, at 80 per cent scrapers and 20 per cent burins. This ratio fluctuates wildly in the Gravettian, though burins always dominate over scrapers (Demars and Laurent, 1992). The severe differences between the Solutrean and Gravettian, on such a fundamental and practical level as scraper/burin ratios, proves that they are very distinct technocomplexes. Renard argued for technological evolution from the Gravettian to the Solutrean within the wider Franco-Cantabrian refuge zone (Renard, 2011). However, the fundamental differences in technology and assemblage diversity clearly demonstrate that they are distinct industries. This fits with the notion of climate refugees arriving South, initiating new technology in the region.

This technological break is the result of the demographic break that occurs from the Gravettian to the Solutrean. Site counts, (Chapter Three) demonstrate a dramatic increase in population from the Gravettian to the Solutrean. Our radiocarbon data shows Gravettian populations to fluctuate, with a very low trough at 26,000 BP before peaking at 24,000 BP, around the time of the transition from Gravettian to Solutrean. There is then a decline in activity, before the 20,000 BP peak. As discussed previously, the Solutrean also has the highest average density of lithic tools per m^2 per year. This was not a statistically significant result, though I believe it would be statistically sig-

nificant if I were able to overcome external limits on sample size. I do therefore believe that there is a genuine demographic break between the Gravettian and Solutrean.

§ 6.3 Key Innovation Results

The Gravettian is depleted in assemblage diversity, in comparison to all other technocomplexes. It is also one of the mildest phases climatically

When I analyzed diversity data by technocomplex, a key significant result was that the Gravettian is depleted in diversity measures when compared to all other technocomplexes. With the mild conditions of the Gravettian, this supports the theory that climate and innovation are negatively correlated. The Denekamp Interstadial partially overlaps with the Gravettian and no particularly bracing climatic phases are found in the Gravettian. It must be noted that the variety of sub-phases that constitute the Gravettian could be expected to affect the diversity results for the overall phase. However, the range covered by the Gravettian results (Figure 5.26) is not particularly large and the core of the results are well below those of all other technocomplexes. I accept that the Gravettian is significantly depleted in innovation levels in comparison to all other phases. The hospitable climatic conditions in Europe during this phase are likely culprits for this creative depletion.

It is worth noting that elsewhere in Europe, the Gravettian sees the development of rich traditions in art and culture. Elaborate burials, richly ornamented with a variety of grave goods are found in this phase, from Britain to Russia (Pettitt, 2011). These are strangely lacking from Southwest France. Venus figurines are widely exchanged across Gravettian Europe, indicative of vast social networks operating over great distances (Gamble, 1986). In Eastern Europe, sites pertaining to the Pavlovian culture, part of the wider Gravettian technocomplex, see a range of objects, including marionettes and engraved objects (Farbstein, 2011). The Gravettian of Southwest France is fairly unremarkable in terms of artistic endeavours. It certainly does not produce the magnificent

cave art of the Magdalenian. The phase is one of the least remarkable and diverse of the Upper Palaeolithic in Southwest France. This is likely to be a result of relatively low population density in the region during the Gravettian, when compared to other phases. Groups are able to occupy other parts of Europe and choose to do so. This low population density in Southwest France at this time means that the 'numbers game' hypothesis is completely removed. We are then into 'the mother of invention' territory, and favourable climate means that there is no pressure to innovate.

The Badegoulian sees the greatest assemblage diversity. It is also an especially mild phase.

In contrast to the Gravettian, the Badegoulian is one of the richest phases, yet it also occurs in a hospitable phase, during the Laugerie Interstadial. The phase is so hospitable that occupants of Southwest France shift their habitation sites and open-air settlements become common (White, 1985). We also have evidence here for a peak in activity coinciding with the Badegoulian, evidenced by radiocarbon data. I conjecture that the high population density at this time initiates the 'numbers game' mechanism. The differences in assemblage diversity in the Badegoulian and Gravettian are thus explained; a separate mechanism is at work in each phase. In the Gravettian, there is no pressure to innovate from the environment and population densities are too low for innovation rates to increase through cultural transmission. In the Badegoulian, the climate is also too hospitable for it to create any pressure to innovate. However, population is high enough that cultural transmission increases in the manner described in Chapter Two and we see high levels of assemblage diversity.

When diversity data is plotted over time, rather than by technocomplex, we can see an overall negative relationship between temperature and innovation. This relationship flips a few times across the period of interest.

Settlement patterns will impact on innovation transmission rates.

We saw earlier how KDE images show changing settlement patterns in the region over

time. Settlement patterns will impact on innovation rates. High population density within a small area will increase the number of social networks. This in turn will increase the probability that an innovation will be transmitted, as outlined in Chapter Two. One of the highest points in terms of assemblage diversity, occurs in our data at 12,500 BP. Temporally, this is very close to the period 12,950 BP; a time of sprawling, continuous occupation over a very large area. The centralization of high population density, into the large, 'urban' area will have aided transmission of innovation and kept diversity levels high.

§ 6.4 Implications for human behaviour

In the modern world there is a positive relationship between ET and population density. This relationship is reversed in the study region and period.

I demonstrated in Chapter Two that there is a positive relationship between ET and population density amongst modern hunter-gatherers. Environmental determinism is an unpopular approach in the modern world (Judkins et al., 2008) but it is difficult to deny the effect that climatic variables have upon human groups, particularly ones living so close to nature. This positive relationship is fairly intuitive; the warmer the environment inhabited by a hunter-gatherer group, the greater the abundance of biomass. The level of biomass available will determine the carrying capacity of the environment. However, I demonstrated in Chapter Four that this relationship between temperature and human activity is reversed in the study region and period. The cross-correlation of the radiocarbon summed probability distribution and smoothed values for NGRIP demonstrates this relationship. This negative relationship between temperature and population holds true for the majority of the Upper Palaeolithic, with the exception of the period 15,000 to 11,000 BP, when the relationship briefly becomes positive.

The unique refugium circumstances of the LGM reverse the normal 'rules' relating climate and population.

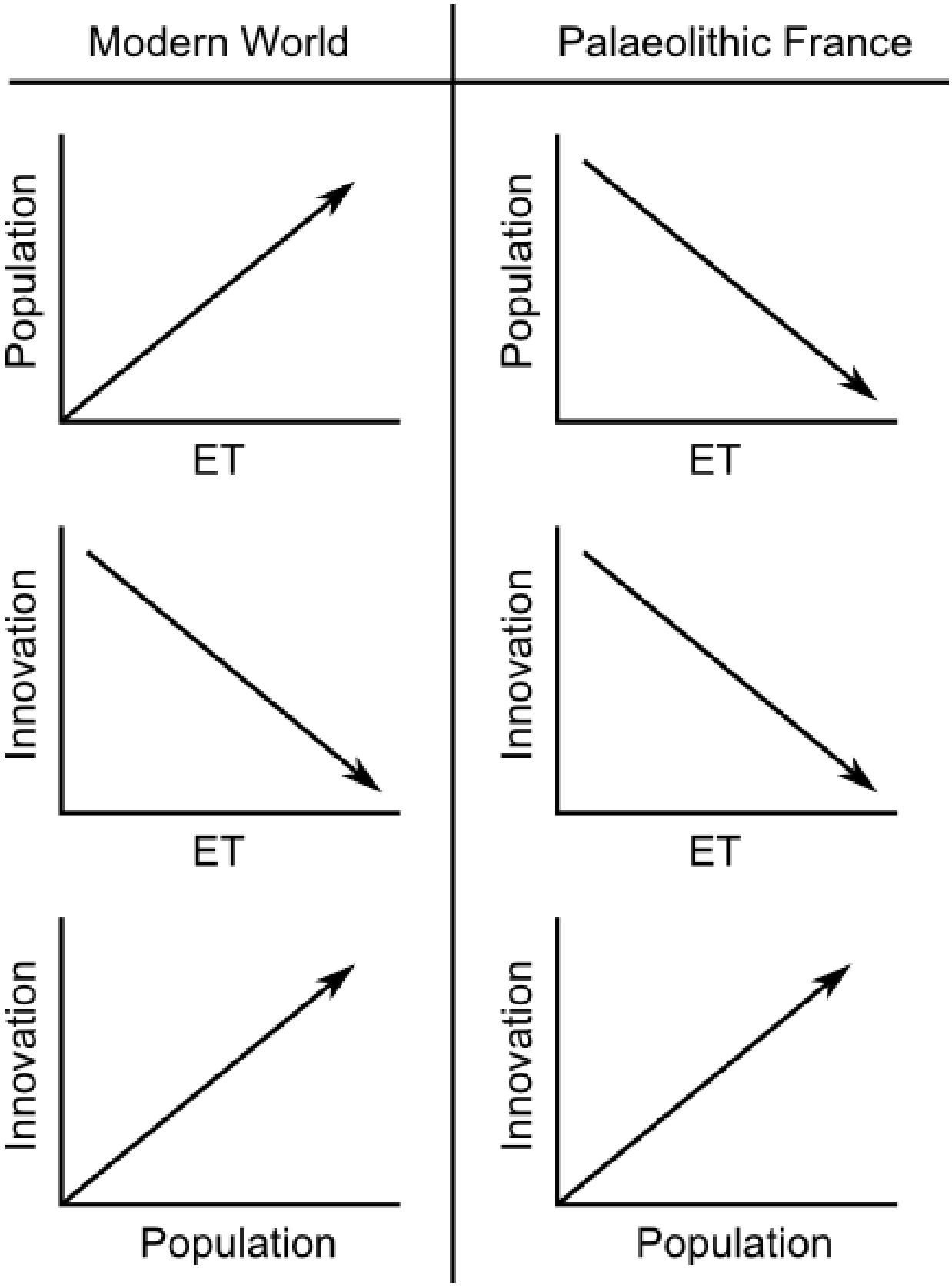

Figure 6.1: Relationship between key variables. These are shown as broad trends. ET is effective temperature. Relationships between these variables in the modern world are derived from broad trends amongst modern hunter-gatherers. Relationships for Palaeolithic France are based on observations from data in this thesis.

Why is the relationship reversed from prehistoric to modern times? Given the arguments against using ethnography as a data source for prehistoric archaeology (Wobst, 1974), it is possible that modern hunters do not accurate reflect their Palaeolithic forebears. However as the positive relationship between ET and population is so intuitive and logical, I accept that the modern relationship does reflect the 'normal' relationship between humans and the environment. I argue instead that the negative relationship between temperature and population in the Upper Palaeolithic is the result of unique, refugium circumstances that flip normal rules governing human behaviour. Activity amongst modern hunter-gatherers is determined by biomass availability, and additional constraints placed upon them by neighbouring farming peoples. The availability of biomass in Palaeolithic Southwest France is well documented (Mellars, 1985). We can assume that biomass availability was not the determining factor in population size in the region. Instead, the extent of the ice sheets and the local temperature outside of the refuge zone determined population in Southwest France. Cold temperatures in more northerly latitudes would have led to migration into Southwest France. This explains the reversed relationship between temperature and demography from prehistoric France to the present day.

The disparity between modern and ancient hunter-gatherers is a warning against blind use of environmentally-deterministic approaches. Back-projecting data from hunter-gatherers into the past, in this project, would not have been appropriate. The unique refugium conditions mean that the relationship between the environment and humans seen in the modern world was not in action in the past. However, we must accept that humans are influenced by their habitats and invoke environmental variables where appropriate.

In the modern world, latitude and innovation are positively correlated. A negative relationship between ET and innovation is therefore implied. The same relationship between climate and innovation exists in the study region and period.

A significant correlation was observed between $\delta^{18}O$ values and diversity proxies at several lags. The implication is that there is a slight delay between climate change and human technological responses. In the modern world, a positive correlation links latitude and assemblage diversity in hunter-gatherer society (Torrence, 1983). As latitude and temperature are directly related, this means that a negative relationship between temperature and artefact diversity exists today. We have already discussed the negative correlation between these two variables that is evident in Palaeolithic France. The relationship is the same from prehistoric to modern times.

Why is this relationship unchanged from prehistory to now? When the relationship between demography and population is reversed?

We could claim that a universal law, linking environment and innovation, is evident. I think that the situation is more complex than this. Innovation amongst hunter-gatherers in the modern world correlates with both temperature and population. Keeley (1988) demonstrated that a strong positive relationship links hunter-gatherer complexity and population density. In prehistoric France, we observe a positive relationship between population and innovation and a negative relationship between temperature and innovation. This suggests that there is not a universal law linking innovation and demography, evident in both the modern and ancient world.

The answer may lie in the *mechanisms* that link demography and innovation. In the modern world , and at some points in the study period, the *mother of invention* process is at work. Throughout the majority of the study period, the *numbers game* process is at work.

We saw in Chapter Two that there are two possible mechanisms that link population and innovation. First, there is the notion of necessity as the mother of invention; adverse conditions created by inhospitable climatic conditions drive humans to adapt and create inventive solutions to problems. Secondly, there is the simple numbers game mechanism; high population densities increase the probability of an innovation

occurring, whilst simultaneously increasing the number of social connections between individuals, aiding transmission of the innovation. The relationship between population and innovation is positive in both modern and ancient times. Yet the correlation between temperature and population has reversed from Palaeolithic France to contemporary hunter-gatherers. I argue that this is because separate mechanisms are in action.

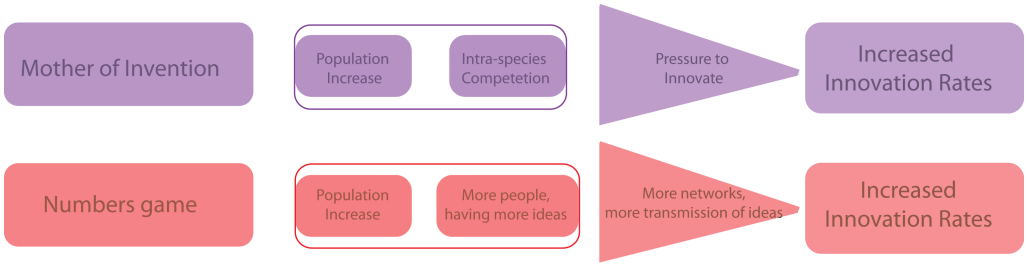

Figure 6.2: Two mechanisms linking population and innovation

Temperature within the refuge zone, even during the LGM, would not have been extreme. Barron *et al* estimated a mean August temperature of $11^0C - 14^0C$ in the refuge zone (Barron et al., 2003) . The numbers game process will have been operating, as conditions will not have been taxing enough to create pressure to innovate. Archaeologists have argued for an abundance of game animals in the refugium and the climate was not too taxing. Given the evidence for favourable conditions in LGM Southwest France, I cannot believe that the environment in the refuge zone created any pressure to innovate. NGRIP climate data tells us about temperatures in Greenland, not local temperature. Wherever NGRIP data points to a dip in temperature, this is a proxy for *global* temperature, not *local* temperature within the refuge zone. Thus, any point where NGRIP dips and a positive response in human innovation is elicited, corresponds to a period where *global* temperature declines and humans contract upon Southwest France. I think that the evidence shows that it is generally the numbers games mechanism that links population and innovation within the refuge zone, not

pressure to innovate imposed by climate. The exception is the Gravettian, as outlined above, where the mother of invention process is in action. This is not because the conditions in the Gravettian are so bracing as to cause pressure to innovate, but precisely because they are not and deinnovation occurs.

We also saw in Chapter Five that a significant negative relationship links the derivatives of temperature and richness. Why would the rate of change be significant? Sudden drops in temperature would elicit rapid movement of climate refugees in Southwest France. This in turn would lead to the sort of density-dependent increase in human innovation outlined above, as predicted by the numbers game model. Slow change in European climate would elicit similarly slow responses. It is unfortunate that we are unable to examine the relationship between the derivatives of diversity data for modern hunter-gatherers, as they live in the static present. Unless sudden, devastating climate change occurs, we shall have to make do with data from prehistoric hunter-gatherers.

KDE results show changing settlement patterns over time.

For much of the Upper Palaeolithic, the Vézère Valley dominates settlement. The Les Eyzies region, at the confluence of the Dordogne and the Vézère, is a focal point for activity at many points. From our KDE images we can see that at several points in prehistory it is the only area represented by radiocarbon dates, for example at around 31,000 BP and 29,000 BP. Conversely, there are several phases in prehistory where population is dispersed, notably at 19,000 BP and 16,000 BP. There are also some periods where occupation is a continuous blob of activity, such as at 14,000 BP, where the Vézère Valley and surrounding region are engulfed by the same activity zone.

Demars (1998) has already demonstrated that the Vézère Valley fluctuates in dominance. Although he argued that it is at its most dominant during cold phases and loses centrality during hospitable phases. This is partially supported by our KDE analysis. The period 31,000 BP, when the Vézère is the only centre of occupation, is also represented by a trough in NGRIP and is one of the coldest phases in Europe. The same

can be said of 29,000 BP, another phase where the Vézère Valley dominates the KDE maps. However, the LGM displays more dispersed settlement and we can see that there are three centres of occupation at 19,000 BP.

At around 20,000 BP we see high levels of human activity and occupation of several areas. This coincides with the Lascaux Interstadial and the Badegoulian. This technocomplex is noted for the preponderance of open-air sites (White, 1985), presumably because of the improved climatic conditions of this phase. It is likely that settlement locales were influenced by the climate at this phase and as well as seeing large numbers of open air sites in this phase, our KDEs show dispersed settlement patterns.

I believe that dispersed settlement patterns are symptomatic of high population density. We saw in Chapter Three that hunter-gatherer groups disperse in response to population growth. This is why the reaction-diffusion equation is frequently used to model population growth and dispersal. Anthropologists have documented groups 'budding off' in hunter-gatherer societies, in response to population pressure. It stand to reason that once population outpaces resources, individuals will need to migrate from the core region in order to support themselves. Zubrow modelled this process as a shift away from settlement just in a core, optimal resource zone, to more dispersed occupation (Zubrow, 1971). I believe that this is what we are seeing at points of high population density. This is why we see three distinct areas of settlement at 19,000 BP, and continuous 'blobs' of settlement in the Magdalenian. High population in these phases means inhabitants have to expand their occupation out of the optimal resource zone. I identify the Vézère Valley as the optimal resource zone, due to the exceptionally high density of sites in this region.

§ 6.5 Further interesting results

The Magdalenian/Azilian transition does not involve demographic decline. This is at odds with current dogma.

Received wisdom on the nature of the Magdalenian/Azilian transition states that demographic decline occurs at this boundary. It is equally thought that an enormous disconnect in lifestyles occurs (Mellars, 1985). The summed probability distribution that I produced dips dramatically at approximately 12,000 BP. This could be simply interpreted as indicative of a sudden decline in population. That this dip corresponds beautifully with postglacial climatic amelioration could further support this argument, given the links between temperature and innovation that I have just outlined. However, I do not accept this post-glacial decline, for several reasons. I have already outlined above the potential bias introduced through not collecting data into the Mesolithic. This will have unfairly impacted on the Azilian, through removing the Mesolithic tails from the summed probability distribution. The same dip exists in the simulated dataset (Figure 5.8), confirming this view.

In Chapter Three, section 3.4.2 I outlined site/time densities for all major technocomplexes. A slight decrease in site/time density does exist, but it is very small. There is therefore no evidence for a demographic decline from the Magdalenian to the Azilian on the basis of site count data or radiocarbon data. The two periods are distinct in terms of technology and subsistence. The Azilian sees a shift towards resource diversification in both France and Iberia and the lithic technology is very different. However, I reject the idea of a demographic crash at the onset of the Holocene. I believe that this idea is a fallacy, designed to fit with our belief that LGM hunters were so well adapted to their environments that they could not cope with environmental change at the end of the Pleistocene

Magdalenian hunter-gatherers are relatively sedentary.

The intra-site tool-densities for the Magdalenian are very low. They also show an exceptionally restricted range. This is at odds with the radiocarbon data, which shows a number of peaks in Magdalenian. I have already stated that where the radiocarbon and lithic data disagree, I am inclined to accept the radiocarbon data's version of events. However, I think that the lithic data should not be dismissed as meaningless

in this instance. It can tell us about settlement patterns. I argue that the restricted range of tool densities in the Magdalenian is the result of a shift towards sedentism in this phase. A nomadic group, exploiting a range of sites, as described in Binford (1980) would leave assemblages with a variety of tool densities. A dwelling site would be larger, and more densely occupied with tools, than an ephemeral hunting location. The evidence presented here shows that the Magdalenians were using homogenous sites. I think that the only explanation is that the Magdalenians were more sedentary than their forebears. The idea of sedentism in the Upper Palaeolithic is not a new idea, Mellars (1985) argued for semisedentism in the region and we are aware of sedentism amongst Mesolithic hunter-gatherers (Rowly-Conwy, 1983). I see no reason why Palaeolithic hunter-gatherers could not be partially sedentary, if resources allowed and the data presented here supports this idea.

A population that alters its settlement pattern will experience demographic change. Nomadic populations face additional limits to fertility, compared to sedentary populations When the need to be able to carry small children is removed, hunter-gatherers will lift artificial constraints on fertility, reducing infanticide and abortion. Sedentism can therefore change the parameters constraining intrinsic population growth. Therefore sedentary populations will tend to be larger, given the same resources, then nomadic populations.

We saw in Chapters Two that changes in subsistence activity can provide evidence for demographic stress. Following Flannery (1969), Cohen (1979) and later Stiner and Munro (2002), shifts in subsistence choice to species of lower nutritional value can indicate resource stress. There is some evidence for increasing dietary breadth in the Late Upper Palaeolithic, as fish consumption becomes important into the Magdalenian. The adoption of fish consumption in the Late Upper Palaeolithic is likely to have increased the carrying capacity of the environment enormously, allowing massive population growth. Modern hunter-gatherer-fisher societies, where fish consumption is very high, are known to practise sedentism. I conjecture that the Late Upper Palae-

olithic societies of Southwest France were very similar in organization to these modern, fishing societies and that is why we see evidence for sedentism in the Magdalenian of Southwest France.

§ 6.6 Summary

In summary, Southwest France served as a refugium during the LGM. This is evidenced through site counts, lithic-density data, radiocarbon data and the extraordinary break which we see between the Gravettian and the Solutrean technocomplexes. However, the region also served as a refugium at other points during the Upper Palaeolithic, notably at 32,000 BP, 30,000 BP and at several points during the Magdalenian.

I have also demonstrated that population, climate and innovation all interact with each other. In the modern world population and innovation are positively correlated, as are climate and population. Climate and innovation are negatively correlated. In prehistoric France, population and innovation are positively correlated, climate and population are negatively correlated. I explain these switched relationships as a result of the two possible mechanisms that link population and innovation.

§ 6.7 Future Directions

I have highlighted some areas for future work throughout this thesis. I would like to increase the sample of Solutrean sites in the lithic-density data. This could only be done by initiating a radiocarbon dating programme at several Solutrean sites in the region. I would also like to continue radiocarbon data-collection into the Mesolithic, to further explore the idea of demographic decline from the Magdalenian to the Azilian, which at present I am unconvinced by. I would also like to embark on a study of osteodontokeratic artefact variability in the Upper Palaeolithic, this may change the current picture of assemblage diversity.

I have left some questions unanswered about the relationship between France and Iberia. Is Iberia the main refugium? I would like to look at population processes in Iberia in future, to see whether they synchronize with events in France and whether Aquitaine is just the northern tip of a Spanish refugium. As with any study, in answering our research questions we have raised new, tantalizing questions for future study. However, having established a methodology here for dealing with archaeological demography, answering these new questions should be a more straightforward activity.

Chapter 7

Appendix A

§ 7.1 Chapter Two data tables

Table 7.1 contains data relevant for the graphs in Figures 2.2, 2.3 and 2.4.

Table 7.1: Hunter-Gatherer population density and Effective Temperature. Data from Binford (2001)

Group	Density	ET
Pun an	11.8	25.27
Batek	43	25.19
Kubu	9.2	24.39
Shompen	39.54	24.33
Onge	40.1	24.27
Jarwa	44.65	23.69
Ayta Pinatubo	91.89	23.37
North Island	33.38	23.29
Semang	17.57	23.26
Veddah	18.5	22.89

Continued on next page

Table 7.1 – continued from previous page

Group	Density	ET
Hill Pandaran	70.37	22.22
Agta Casiguran	87	21.61
Agta Isabela	42	21.4
Agta North Luzon	37.94	21.28
Chenchu	123.3	20.45
Mrabri	23.16	19.77
Paliyans	9.63	18.62
Birhor	22	17.38
Kadar	50	14.35
Cholanaickan	70.5	14.34
Nayaka	70	14.33
Ainu Hokkaido	34.8	12.31
Orogens	4.3	11.37
Ket	1.64	11.19
Gilyak	19.31	4.6
Yukaghir	0.61	10.29
Nganasan	0.46	9.71
Siberian Eskimo	4.7	9.23
Paraujano	35	25.51
Shiriana	15.6	24.8
Akuriyo	7.04	24.75
Yaruro Pume	19.95	24.53
Guahibo	17.63	24.16
Nukak	9.34	21.74
Bororo	51.36	21.3

Continued on next page

Table 7.1 – continued from previous page

Group	Density	ET
Guato	6.74	20.53
Siriono	6	20.4
Yuqui	1.66	20.35
Nambikwara	7.78	19.85
Calusa	38.73	17.83
Guayaki Ache	3.48	17.46
Botocudo	9.8	17.34
Heta	9.6	16.56
Aweikomo	4.1	16.39
Tehuelche	1.89	13.19
Chono	13.64	12.12
Alacaluf	14.98	11.13
Ona	7.27	9.76
Yahgan	28.42	9.6
Aka	9.06	23.5
Bayaka	17.47	23.5
Bambote	25	22.45
Baka	13.63	22.4
Efe	15.96	21.55
Mbuti	44	20.49
Mikea	4.36	19.22
Hukwe	2.9	17.54
Hai Om	3.84	17.23
Hadza	24	17.06
Dorobo Okiek	40.81	16.69

Continued on next page

Table 7.1 – continued from previous page

Group	Density	ET
Sekele	1.52	16.64
!Kung	6.6	16.52
Nharo	0.5	16.06
GWi	2.93	15.82
Kua	6.36	15.76
!Ko	1.03	15.44
Auni-khomani	0.64	15.21
Xegwi	3.57	14.89
Xam	2.43	14.8
Kaurareg	35	22.81
Larikia	40	22.34
Gunwinggu	17.84	22.3
Mirrngadja	38.5	21.89
Anbara	43.7	21.63
Gidjingali	72.7	21.37
Murngin Yolngu	11.76	21.19
Jeidji Forestriver	17	21.11
Wikmunkan	19.31	21.04
Kakadu	8.8	20.97
Nunggubuyu	23	20.59
Yintjingga	31	20.59
Yir-yoront	8	20.55
Tiwi	37.5	20.24
Kuku Yalanji	50	20.23
Groote Eylandt	22.9	20.06

Continued on next page

Table 7.1 – continued from previous page

Group	Density	ET
Walmbaria	58	19.93
Mulluk	45	19.66
Worora	11	19.41
Lungga	4.5	19.3
Lardil	30	19.19
Kaiadilt	66	19.19
Karadjeri	3.75	19.01
Mamu	45	18.6
Kariera	9.5	18.26
Warunggu	16.28	18.24
Djaru	3.98	17.82
Walbiri	1.16	17.77
Ngatjan	59.8	17.74
Mardudjara	0.75	17.18
Ildawongga	0.45	17.11
Pintubi	1.5	16.89
Undanbi	21.74	16.68
Jinibarra	16	16.68
Karuwali	2	16.58
Alyawara	1.21	16.48
Ngatatjara	0.4	16.42
Badjalang	13.4	16.39
Pitjandjara	0.6	16.33
Dieri	1.93	16.33
Arenda southern	1.1	16.29

Continued on next page

Table 7.1 – continued from previous page

Group	Density	ET
Jankundjara	1	16.09
Arenda northern	2.66	15.98
Ualaria	9	15.98
Nakako	0.87	15.88
Ooldea	0.47	15.47
Barkindji	15.43	15.42
Karuna	18	15.34
Wongaibon	5.12	15.29
Jaralde	40	14.95
Mineng	7	14.83
Tjapwurong	35	14.46
Bunurong	25.04	14.12
Kurnai	17.7	13.51
Tasmanians eastern	8.17	12.74
Tasmanians western	13.35	12.51
Seri	25.48	17.55
Cahuilla	43.75	16.41
Cupeno	48.8	16.14
Kiliwa	12.25	15.96
Diegueno	18.1	15.37
LakeYokuts	38.1	15.33
Serrano	17.58	15.24
Luiseno	67.9	15.24
Wukchumi	24.21	15.17
Tubatulabal	17.2	15.09

Continued on next page

Table 7.1 – continued from previous page

Group	Density	ET
Nomlaki	35	14.85
North Foothill Yokuts	38.29	14.77
Patwin	82	14.77
Gabrielino	64.9	14.61
Monache	28.7	14.59
Eastern Porno	127	14.52
Clear Lake Pomo	308.7	14.49
Wintu	58.82	14.49
Chumash	118.2	14.39
Chimariko	50	14.37
Nisenan	39.75	14.37
Salinan	37.4	14.29
Pomo southern	110.8	14.21
Sinkyone	136.44	14.21
Lessik	97.2	14.09
Miwok Coast	53.57	13.82
Mattole	116.4	13.79
Miwok Lake	65	13.77
Yuki Proper	131.6	13.76
Wappo	120.6	13.73
Pomo northern	108.4	13.71
Yana	31.3	13.6
Miwok	24.54	13.55
Tekelma	12.85	13.55
Yuki Coast	66.96	13.53

Continued on next page

Table 7.1 – continued from previous page

Group	Density	ET
Tolowa	122	13.35
Shasta	25	13.32
Hupa	80	13.1
Tututni	67.07	13.06
Karok	46.9	12.86
Atsugewi	17.93	12.84
Wiyot	107.93	12.72
Maidu Mountain	23.5	12.57
Yurok	131	12.55
Achumawi	17.25	12.5
Modoc	22.89	12.38
Klamath	13.36	11.93
Guaicura	6	16.69
Chichimec	9	16.63
Death Valley	1.29	16.52
Karankawa	21	16.5
Coahuilenos	1.68	16.36
Panamint Shoshoni	2.12	15.34
Yavapai	1.48	15.2
Koso Mountain Shoshoni	8.57	14.95
Walapai	3.86	14.84
Kawaiisu Shoshoni	11.9	14.62
Saline Valley Shoshoni	2.32	14.15
Antarianunts Southern Paiute	3.45	13.86
Owens Valley Paiute	38.04	13.79

Continued on next page

Table 7.1 – continued from previous page

Group	Density	ET
Kawich Mountain Shoshoni	1.99	13.72
Kaibab Southern Paiute	3.71	13.59
Mono Lake Paiute	5.9	13.52
Deep Spring Paiute	3.54	13.48
Salmon-eater Shoshoni	6.9	13.44
Pyramid Lake Paiute	18.53	13.39
Ute Timanogas	3.47	13.34
Cattail Paiute	22	13.34
Fish Lake Paiute	3.89	13.2
Honey Lake Paiute	10.6	13.15
Hukunduka Shoshoni	2.96	13.11
Gosiute Shoshoni	1.67	13.11
Spring Valley Shoshoni	6.09	12.97
White Knife Shoshoni	11.71	12.95
Rainroad Valley Shoshoni	4.28	12.89
Reese River Shoshoni	16.7	12.86
North Fork Paiute	16.04	12.86
Grouse Creek Shoshoni	1.64	12.83
Ute Wimonantci	2.6	12.82
Bear Creek Paiute	1.1	12.81
Antelope Valley Shoshoni	1.13	12.77
Washo	14.9	12.69
Suprise Valley Paiute	13.59	12.68
Wind River Shoshoni	1.87	12.66
Ruby Valley Shoshoni	13.79	12.58

Continued on next page

Table 7.1 – continued from previous page

Group	Density	ET
Bohogue North Shoshoni	1.04	12.56
Uintah Ute	7.48	12.36
Harney Valley Paiute	1.24	12.33
Sheep-eater Shoshoni	6.24	12.22
Little Smoky Shoshoni	1.82	12.15
Uncompahgre Ute	4.29	11.48
Lipan Apache	0.51	15.83
Comanche	2.33	14.95
Chiricahua Apache	1.16	14.81
Kiowa	1.4	14.41
Kiowa Apache	4.14	14.02
Cheyenne	4.82	13.29
Arapahoe	7.5	13.2
Crow ’	5.81	12.67
Teton Lakota	8.77	12.67
Kutenai	2.01	12.46
Bannock	2.31	12.35
Gros-Ventre	3.37	12.21
Plains Ojibwa	2.79	11.96
Piegan	2.54	11.94
Blackfoot	3.46	11.64
Assiniboine	3.21	11.6
Plains Cree	2.73	11.53
Blood	4.44	11.48
Sarsi	1.75	11.36

Continued on next page

Table 7.1 – continued from previous page

Group	Density	ET
Squamish	56.5	12.8
Alsea	96.8	12.77
Puyallup	36.75	12.76
Twana	32.4	12.75
Chehalis	21.97	12.64
Nootka	153.9	12.63
Chinook	33.8	12.6
Coos	104.2	12.58
Lillooet	23.5	12.56
Lummi	104.63	12.39
Quinault	58.7	12.34
Stalo	66	12.32
Cowichan	34.75	12.28
Tillamook	41.32	12.26
Comox	55	12.15
Bella-bella	20.51	12.08
Quileute	104.3	12.03
Clallam	70	11.94
Makah	123	11.84
Haisla	19.1	11.77
Kwakiutl	68.7	11.74
Tsimshim	41.9	11.73
Haida	97.09	11.71
Bella-coola	13	11.55
Tlingit	11.42	11.25

Continued on next page

Table 7.1 – continued from previous page

Group	Density	ET
Gitksan	23.58	11.11
Konaig	30.6	11.05
Eyak	5.86	10.7
Kuskowagmut	17.3	10.62
Chugash	12.1	10.47
Aleut	54.65	10.28
Nunavak	19.22	9.98
Tenino	19	13.49
Umatiela	10.5	13.37
Wenatchi	50.17	13.01
Yakima	27	12.96
Wishram	231.7	12.95
Coeur d'Alene	1.5	12.58
Sinkaietk	14.51	12.53
Okanogan	13.27	12.44
Sanpoil	11.2	12.41
Nez-perce	8.88	12.36
Thompson	33.2	12.36
Kalispel	1.5	12.25
Objibwa-Kitchibuan	5	12.14
Kitkitegon	3.09	11.95
Micmac	4.32	11.95
Flathead	1.5	11.85
Rainy River Ojibwa	1.21	11.74
North Saulteaux	1.2	11.73

Continued on next page

Table 7.1 – continued from previous page

Group	Density	ET
Shuswap	12.4	11.64
Pekangekum Ojibwa	3.08	11.53
Round Lake Ojibwa	1.75	11.3
Alcatcho	7.5	11.26
Nipigon Ojibwa	0.87	11.25
Mistassini Cree	0.58	11.22
Ojibwa Northern Albany	1.43	11.17
Waswanip Cree	0.41	11.14
Weagamon Ojibwa	0.51	11.09
Montagnais	0.41	11.09
Sekani	0.82	11.07
Beaver	0.51	11.07
Slave	1	11.01
Kaska	0.9	11
Tahltan	1.16	10.96
Chilcotin	11.52	10.91
Carrier	7.59	10.89
Mountain	0.78	10.88
Han	1.8	10.88
Hare	0.33	10.85
Attawapiskat Cree	1.43	10.84
Koyukon	1.09	10.84
Chippewyan	0.46	10.83
Kutchin	1.7	10.75
Ingalik	2.71	10.75

Continued on next page

Table 7.1 – continued from previous page

Group	Density	ET
Satudene	0.55	10.73
Nabesna	0.77	10.73
Rupert House Cree	0.9	10.72
Dogrib	0.88	10.72
Tanaina	4.86	10.71
Tutchone	0.92	10.68
Holikachuk	1.52	10.63
Naskapi	0.42	10.32
Norton Sound Inuit	7.61	10.67
Kobuk Inuit	2.67	10.35
Kotzebue Sound Inuit	6.63	10.35
Labrador Inuit	2.78	10.28
Great Whale Inuit	1.86	10.11
Caribou Inuit	0.3	10.11
Noatak Inuit	2.2	10.05
Nunamiut Inuit	0.96	9.87
Mackenzie Inuit	3.84	9.84
Sivokamiut Inuit	15	9.81
Point Hope Inuit	4.2	9.8
Copper Inuit	0.43	9.78
Utkuhikhaling-miut	0.38	9.62
Aivilingmiut Inuit	0.32	9.58
Ingulik Inuit	0.54	9.52
West Greenland	4.73	9.31
Baffin Island Inuit	1.26	9.29

Continued on next page

Table 7.1 – continued from previous page

Group	Density	ET
Netsilik Inuit	0.25	9.08
Angmakaslik	7.72	9.02
Tareumiut Inuit	3.86	8.85
Polar Inuit	0.41	8.64

Chapter 8

Appendix B

§ 8.1 Chapter Four Appendices

The data tables in Appendix B contain data relevant to Chapter Four - the methods chapter. The first table contains data on archaeological site formation, specifically the link between level duration and thickness of the level's sediment. This relationship was central to the premise that the length of time represented by an archaeological level can be estimated from the sediment. The second table contains data that demonstrates the relationship between sample size and assemblage diversity, where N is the sample size, richness is the number of active categories, and D is the heterogeneity (evenness) variable. The relationship between sample size and diversity was of central importance in the development of the measurement of diversity in this thesis.

Table 8.1: Level Thickness and Duration Data. 'Level' thickness obtained from excavator's drawings and descriptions, as referenced in the 'Bibliography' column. 'Level duration' obtained from Bayesian models for the sites, which are included in Appendix D.

Level	**Duration (years)**	**Thickness (cm)**	**Bibliography**
La Ferrassie J Aurignacian	150	20	(Delporte, 1984)
La Ferrassie E Aurignacian	70	10	(Delporte, 1984)
Abri Pataud 2 Protomagdalenian	2000	60	(Farrand, 1995)
Abri Pataud 3 Gravettian	700	50	(Farrand, 1995)
Abri Pataud 6 Aurignacian	200	10	(Farrand, 1995)
Abri Pataud 7 Aurignacian	100	20	(Farrand, 1995)
Abri Pataud 8 Aurignacian	100	30	(Farrand, 1995)
Abri Pataud 11 Aurignacian	200	30	(Farrand, 1995)
Abri Pataud 12 Aurignacian	300	10	(Farrand, 1995)
Abri Pataud 14 Aurignacian	300	10	(Farrand, 1995)
Laugerie Haute Est Level 31 Solutrean	335	35	(Bordes, 1958)
Laugerie Haute Est Level 23 Solutrean	175	16	(Bordes, 1958)
Laugerie Haute Est Level 1 Magdalenian	860	16	(Bordes, 1958)
Laugerie Haute Ouest Lower Solutrean	300	32	(Peyrony and Peyrony, 1938)

Continued on next page

Table 8.1 – continued from previous page

Level	Duration	Thickness	Bibliography
Laugerie Haute Ouest Middle Solutrean	150	53	(Peyrony and Peyrony, 1938)
Laugerie Haute Ouest Upper Solutrean	100	18	(Peyrony and Peyrony, 1938)
Roc de Combe 1 Gravettian	200	40	(Labrot and Bordes, 1964)
Roc de Combe 2 Gravettian	150	21	(Labrot and Bordes, 1964)
Roc de Combe 3 Gravettian	150	7	(Labrot and Bordes, 1964)
Roc de Combe 4 Gravettian	500	14	(Labrot and Bordes, 1964)
Roc de Combe 5 Aurignacian	400	29	(Labrot and Bordes, 1964)
Roc de Combe 6 Aurignacian	400	18	(Labrot and Bordes, 1964)
Roc de Combe 10 Chatelperronian	1000	32	(Labrot and Bordes, 1964)
Flageolet I IV Gravettian	900	9	(Rigaud, 1969)
Flageolet I V Gravettian	400	14	(Rigaud, 1969)
Flageolet I VI Gravettian	500	14	(Rigaud, 1969)
Flageolet II II Magdalenian	1200	38	(Rigaud, 1969)
Flageolet II IX Magdalenian	1000	30	(Rigaud, 1969)
Le Facteur 21 Aurignacian	500	5	(Delporte, 1968)

Continued on next page

Table 8.1 – continued from previous page

Level	Duration	Thickness	Bibliography
Le Facteur 10,11 Gravettian	800	18	(Delporte, 1968)
La Rochette 5 Aurignacian	1250	40	(Delporte, 1962)
La Rochette 4 Aurignacian	400	10	(Delporte, 1962)
Cuzoul de Vers 22 Badegoulian	100	8	(Clottes and Giraud, 1996)
Cuzoul de Vers 23 Badegoulian	50	13	(Clottes and Giraud, 1996)
Cuzoul de Vers 24 Badegoulian	50	8	(Clottes and Giraud, 1996)
Cuzoul de Vers 25 Badegoulian	50	3	(Clottes and Giraud, 1996)
Cuzoul de Vers 26 Badegoulian	50	3	(Clottes and Giraud, 1996)
Le Piage K Aurignacian	450	20	(Champagne and Espitalié, 1981)
Le Piage J Aurignacian	200	20	(Champagne and Espitalié, 1981)
Le Piage G Aurignacian	200	10	(Champagne and Espitalié, 1981)
Le Piage F Aurignacian	1000	60	(Champagne and Espitalié, 1981)
Le Piage CE Magdalenian/Solutrean	900	50	(Champagne and Espitalié, 1981)

Table 8.2: Diversity and Sample Size

Assemblage	N	Richness	D	Bibliography
La Ferrassie Aurignacian I Couche F	2442	55	21.77	(de Sonneville-Bordes, 1960)
La Ferrassie Aurignacian II Couche H	4037	56	16.40	(de Sonneville-Bordes, 1960)
La Ferrasssie Aurignacian III Couche H	362	39	18.68	(de Sonneville-Bordes, 1960)
La Ferrassie Aurignacian IV	473	41	11.44	(de Sonneville-Bordes, 1960)
Le Ferrassie Aurignacian Couche L	15	11	11.37	(Delporte, 1984)
La Ferrassie Aurignacian Couche K	2105	54	28.17	(Delporte, 1984)
La Ferrassie Aurignacian Couche J	385	38	21.95	(Delporte, 1984)
La Ferrassie Aurignacian Couche I	497	48	27.74	(Delporte, 1984)
La Ferrassie Aurignacian Couche H	120	34	25.69	(Delporte, 1984)
La Ferrassie Aurignacian Couche G	502	47	26.16	(Delporte, 1984)
La Ferrassie Aurignacian Couche F	86	28	19.62	(Delporte, 1984)
La Ferrassie Aurignacian Couche E	236	34	22.66	(Delporte, 1984)
Faurelie Aurignacian II	525	49	20.18	(de Sonneville-Bordes, 1960)
Abri Lartet Aurignacian I	713	40	18.65	(de Sonneville-Bordes, 1960)
Abri de Poisson Aurignacian I	422	46	22.31	(de Sonneville-Bordes, 1960)

Continued on next page

Table 8.2 – continued from previous page

Assemblage	N	Richness	D	Assemblage Citation
Abri Cellier Aurignacian I	354	44	25.85	(de Sonneville-Bordes, 1960)
Abri Cellier Aurignacian II	520	51	25.15	(de Sonneville-Bordes, 1960)
Le Moustier Aurignacian	231	41	20.61	(de Sonneville-Bordes, 1960)
Abri du Renne Aurignacian	575	45	26.19	(de Sonneville-Bordes, 1960)
Abri de la Mtairie	392	45	25.41	(de Sonneville-Bordes, 1960)
Abri Blachard Aurignacian I	481	38	14.81	(de Sonneville-Bordes, 1960)
Abri Castanet Aurignacian I	1824	50	15.24	(de Sonneville-Bordes, 1960)
Abri Castanet Aurignacian II	1283	44	15.90	(de Sonneville-Bordes, 1960)
Abri Caminade Ouest, Aurignacian I	237	43	26.99	(de Sonneville-Bordes, 1960)
Abri Caminade Ouest, Aurignacian II	384	48	31.31	(de Sonneville-Bordes, 1960)
Abri Caminade Est Aurignacian I Couche G	143	36	24.24	(de Sonneville-Bordes, 1960)
Abri Caminade Aurignacian I Couch F	234	35	23.66	(de Sonneville-Bordes, 1960)
Abri Caminade Est Aurignacian II Couche D 2i	291	43	29.28	(de Sonneville-Bordes, 1960)
Abri Caminade Est, Aurignacian II D2s	166	36	23.65	(de Sonneville-Bordes, 1960)
Abri de Patary Aurignacian I	241	32	20.10	(de Sonneville-Bordes, 1960)

Continued on next page

Table 8.2 – continued from previous page

Assemblage	N	Richness	D	Assemblage Citation
Grotte de Chanlat Aurignacian Couche I	1757	55	24.38	(de Sonneville-Bordes, 1960)
Grotte de Chanlat Couche II, Aurignacian	1362	52	25.29	(de Sonneville-Bordes, 1960)
Grotte des Font-Yves, Aurignacian	1354	58	26.72	(de Sonneville-Bordes, 1960)
Grotte Dufour Aurignacian	1242	55	26.36	(de Sonneville-Bordes, 1960)
Abri Pataud Couche 6	368	43	19.66	(Movius, 1975)
Abri Pataud Couche 7 Aurignacian	632	44	22.68	(Movius, 1975)
Abri Pataud Couche 8 Aurignacian	434	46	25.81	(Movius, 1975)
Abri Pataud Couche 11 Aurignacian	609	36	19.98	(Movius, 1975)
Abri Pataud Couche 12 Aurignacian	102	22	14.90	(Movius, 1975)
Abri Pataud Couche 13 Aurignacian	37	15	11.18	(Movius, 1975)
Abri Pataud Couche 14 Aurignacian	161	26	15.93	(Movius, 1975)
Roc de Combe Level 5 Aurignacian	409	39	22.50	(de Sonneville-Bordes, 2002)
Roc de Combe Level 6 Aurignacian	435	36	20.84	(de Sonneville-Bordes, 2002)
Roc de Combe Level 7 Aurignacian	544	40	23.99	(de Sonneville-Bordes, 2002)
Facteur Level 21 Aurignacian	68	25	19.95	(Delporte, 1968)

Continued on next page

Table 8.2 – continued from previous page

Assemblage	N	Richness	D	Assemblage Citation
Facteur Level 19 Aurignacian	126	34	24.24	(Delporte, 1968)
La Rochette Aurignacian 5d	256	44	24.76	(Delporte, 1964)
La Rochette Aurignacian 5c	148	30	21.25	(Delporte, 1964)
La Rochette Aurignacian 4	394	41	27.32	(Delporte, 1964)
La Rochette Aurignacian 3	42	21	15.34	(Delporte, 1964)
Le Piage Aurignacian Couche K	657	49	24.63	(Champagne and Espitalié, 1981)
Le Piage Aurignacian Couche J	405	43	25.86	(Champagne and Espitalié, 1981)
Le Piage Aurignacian Couche G-I	2286	53	15.97	(Champagne and Espitalié, 1981)
Le Piage Aurignacian Couche F	235	33	18.96	(Champagne and Espitalié, 1981)
Laugerie-Haute Ouest Aurignacian V couche D	1620	52	21.36	(de Sonneville-Bordes, 1960)
Abri Pataud eboulis 8-11	78	23	13.80	(Movius, 1975)
Laugerie Haute Est couche B, Perigordian III	858	42	15.11	(de Sonneville-Bordes, 1960)
Laugerie-Haute Est Couche BPerigordian III2	369	31	16.76	(de Sonneville-Bordes, 1960)
Abri de la Roque Saint-Christophe Upper Perigordian	968	47	21.32	(de Sonneville-Bordes, 1960)
Abri de la Roque Saint Christophe Upper Perigordian	195	32	16.33	(de Sonneville-Bordes, 1960)

Continued on next page

Table 8.2 – continued from previous page

Assemblage	N	Richness	D	Assemblage Citation
Grotte de Font-Robert, Upper Perigordian	1500	66	29.37	(de Sonneville-Bordes, 1960)
La Ferrassie Grande Abri, Couche J	886	50	14.98	(de Sonneville-Bordes, 1960)
La Ferrassie, Perigordian, Couche K	192	35	17.18	(de Sonneville-Bordes, 1960)
La Ferrassie, Upper Perigordian, Couche L	15	12	11.37	(de Sonneville-Bordes, 1960)
Abri de Laraux, Upper Perigordian, couche 5	191	37	21.06	(de Sonneville-Bordes, 1960)
Abri de Laraux, Upper Perigordian, Couche 3	490	48	21.83	(de Sonneville-Bordes, 1960)
The Roc de Gavaudun, Upper Perigordian	393	46	26.41	(de Sonneville-Bordes, 1960)
Abri Labattut, Lower Couche	354	46	24.30	(de Sonneville-Bordes, 1960)
Abri Labattut Couche Superior	403	45	13.91	(de Sonneville-Bordes, 1960)
Fourneau-du-Diable, Perigordian IV	555	42	15.66	(de Sonneville-Bordes, 1960)
Abri Pataud Gravettian Couche 3	1309	52	24.94	(Movius, 1975)
Abri Pataud Gravettian Couche 4	5355	60	22.01	(Movius, 1975)
Abri Pataud Gravettian Couche 5	5640	70	2.59	(Movius, 1975)
Roc de Combe Level 1 Gravettian	1041	57	21.23	(de Sonneville-Bordes, 2002)
Roc de Combe Level 2 Gravettian	179	29	10.56	(de Sonneville-Bordes, 2002)

Continued on next page

Table 8.2 – continued from previous page

Assemblage	N	Richness	D	Assemblage Citation
Roc de Combe Level 3 Gravettian	109	26	19.16	(de Sonneville-Bordes, 2002)
Roc de Combe Level 4 Gravettian	140	34	22.12	(de Sonneville-Bordes, 2002)
Facteur levels 10,11 Gravettian	1110	52	14.27	(Delporte, 1968)
Pegourie Couche 10 Gravettian	29	15	9.84	(Séronie-Vivien, 1995)
Abri Pataud eboulis 3-4 Noaillian	379	45	26.51	(Movius, 1975)
Abri Pataud Protomagdalenian	1156	34	16.03	(Movius, 1975)
Laugerie-Haute Ouest, Couche G, Protosolutrean	1331	53	22.31	(de Sonneville-Bordes, 1960)
Laugerie-Haute Ouest, H Unifacial points	600	45	11.58	(de Sonneville-Bordes, 1960)
Laugerie-Haute Est, H	933	58	24.50	(de Sonneville-Bordes, 1960)
Laugerie-Haute Ouest, H, Middle Solutrean	454	37	7.84	(de Sonneville-Bordes, 1960)
Badegoule, Upper Solutrean, Peyrony	838	53	24.16	(de Sonneville-Bordes, 1960)
Badegoule Upper Solutrean, Peyrille Excavations	654	41	12.95	(de Sonneville-Bordes, 1960)
Pech de la Boissiere, Upper Solutrean I	760	53	25.30	
Pech de la Boissiere, Upper Solutrean, II	976	61	23.77	
Jean-Blanc, Solutrean, Est	154	27	11.98	

Continued on next page

Table 8.2 – continued from previous page

Assemblage	N	Richness	D	Assemblage Citation
Jean-Blanc Ouest, Solutrean	127	31	16.39	
Fourneau-du-Diable Lower Terrace	1012	47	11.12	(de Sonneville-Bordes, 1960)
Fourneau-du-Diable, Upper Terrace, Solutrean I	1110	35	10.16	(de Sonneville-Bordes, 1960)
Fourneau-du-Diable, Upper Terrace, Solutrean II	786	31	7.02	(de Sonneville-Bordes, 1960)
Fourneau-du-Diable, Upper Terrace, Solutrean III	1430	45	8.66	(de Sonneville-Bordes, 1960)
Laugerie-Haute Ouest Middle Solutrean H”’	169	31	15.67	
Sainte Eulalie Solutrean Couche IV	10	8	7.58	(Lorblanchet et al., 1973)
Sainte Eulalie Solutrean Couche D	42	13	9.36	(Lorblanchet et al., 1973)
Laugerie-Haute Est H”-H”’	227	36	15.14	
Pegourie Couche 8A Badegoulian	341	37	16.61	(Séronie-Vivien, 1995)
Pegourie Couche 8B Badegoulian	156	31	14.93	(Séronie-Vivien, 1995)
Pegourie Couche 8C Badegoulian	203	36	18.86	(Séronie-Vivien, 1995)
Pegoruie Couche 9A Badegoulian	187	36	21.70	(Séronie-Vivien, 1995)
Pegourie Couche 9B Badegoulian	67	24	18.18	(Séronie-Vivien, 1995)
Jean Blanc Est Magdalenian with raclettes	295	30	6.36	

Continued on next page

Table 8.2 – continued from previous page

Assemblage	N	Richness	D	Assemblage Citation
Jean Blanc Ouest Magdalenian with raclettes	164	26	9.69	
Badegoule Magdalenian with raclettes, Peyrony	222	37	20.31	(de Sonneville-Bordes, 1960)
Badegoule Magdalenian with raclettes, Peyrille	105	30	22.24	(de Sonneville-Bordes, 1960)
Laugerie-Haute Est, Protomagdalenian	641	50	19.57	
Laugerie-Haute Est, Lower Magdalenian, Couche I	671	54	31.95	(de Sonneville-Bordes, 1960)
Laugerie-Haute Est Lower Magdalenian Couche II	680	52	20.20	(de Sonneville-Bordes, 1960)
Laugerie-Haute Est, Lower Magdalenian, Couche 3	1448	59	28.28	(de Sonneville-Bordes, 1960)
Saint-Germaine-la-Riviere, Lower Terrace, Magdalenian III	437	38	15.13	(de Sonneville-Bordes, 1960)
Saint-Germaine-la-Riviere, Upper Terrace, Magdalenian III	280	39	20.29	(de Sonneville-Bordes, 1960)
Roq Saint Cirq, Magdalenian with triangles, Couche brun	489	45	15.65	
Roq Saint Cirq, Couche brune inferior, Magdalenian with triangles	421	44	19.45	
Roq Saint Cirq, Couche brune superieur, Magdalenian with triangles	425	38	16.05	
Roq Saint Cirq, Couche Rouge, Magdalenian with Triangles	280	39	22.21	
Abri de Crabillat, Magdalenian with triangles	546	53	15.03	
Jolivet, triangles	225	41	21.37	(de Sonneville-Bordes, 1960)

Continued on next page

Table 8.2 – continued from previous page

Assemblage	N	Richness	D	Assemblage Citation
Puy de Lacan (triangles), A Lower Couche	599	42	18.18	
Puy de Lacan (triangles), Middle Couche B	591	36	15.66	
Puy de Lacan (triangles) Upper Couche C	1457	39	8.55	
La Madeleine, Lower Couche, Magdalenian IV	3699	66	17.44	(de Sonneville-Bordes, 1960)
La Madeleine, Middle Couche, Magdalenian V	3011	62	15.60	(de Sonneville-Bordes, 1960)
La Madeleine, Upper Couche, Magdalenian VI	4995	62	12.85	(de Sonneville-Bordes, 1960)
Villepin, Lower Couche, Magdalenian VI1	167	33	17.99	(de Sonneville-Bordes, 1960)
Villepin, Middle Couche, Magdalenian VI2	662	59	23.57	(de Sonneville-Bordes, 1960)
Chateau des Eyzies, Magdalenian V-VI	200	35	19.92	(de Sonneville-Bordes, 1960)
Chateau des Eyzies, Middle Magdalenian	252	37	9.40	(de Sonneville-Bordes, 1960)
Chateau des Eyzies, Upper Magdalenian	50	22	18.07	(de Sonneville-Bordes, 1960)
Liveyre, Magdalenian	173	33	13.65	(de Sonneville-Bordes, 1960)
Longueroche, Upper Magdalenian, Lower couche	135	29	14.55	(de Sonneville-Bordes, 1960)
Longueroche, Upper Magdalenian, Middle Couche	305	37	17.04	(de Sonneville-Bordes, 1960)
Limeuil, Upper Magdalenian	3402	47	9.61	(de Sonneville-Bordes, 1960)

Continued on next page

Table 8.2 – continued from previous page

Assemblage	N	Richness	D	Assemblage Citation
Font-Brunel, IPH Series	56	23	18.07	(de Sonneville-Bordes, 1960)
Font-Brunel Final Magdalenian MP Series	50	14	9.81	(de Sonneville-Bordes, 1960)
Soucy Magdalenian VI	1580	36	6.78	(de Sonneville-Bordes, 1960)
Gare du Couze Magdalenian VI Peyrony series	364	47	26.16	
Fourneau-du-Diable Perigordian	223	38	18.28	(de Sonneville-Bordes, 1960)
Mege Magdalenian V	265	33	13.88	(de Sonneville-Bordes, 1960)
Mairie Lower Couche	234	33	12.07	(de Sonneville-Bordes, 1960)
Mairie Upper Couche	378	41	17.10	(de Sonneville-Bordes, 1960)
Abri du Cap-Blanc, Laianne Excavations, Lower Couche. General Magdalenian	346	31	13.16	
Abri du Cap-Blanc, Laianne Excavations, Upper Couche, General Magdalenian	641	40	17.79	
Abri du Cap-Blanc, Peyrony Excavations, General Magdalenian	310	35	12.05	
Abri de la Forge General Magdalenian	1500	51	15.31	(de Sonneville-Bordes, 1960)
Metairie, General Magdalenian	129	28	13.60	(de Sonneville-Bordes, 1960)
Abri Reverdit, General Magdalenian	1517	65	23.24	(de Sonneville-Bordes, 1960)
Solvieux	976	49	21.28	(de Sonneville-Bordes, 1960)

Continued on next page

Table 8.2 – continued from previous page

Assemblage	N	Richness	D	Assemblage Citation
Abri de Recourbie I, General Magdalenian	550	43	14.67	(de Sonneville-Bordes, 1960)
Abri de Recourbie II, General Magdalenian	564	43	16.12	(de Sonneville-Bordes, 1960)
Chez-Galou, General Magdalenian	241	36	15.72	(de Sonneville-Bordes, 1960)
Gare du Couze Magdalenian 0.1 to 0.2	225	39	19.10	(Fitte and Sonneville-Bordes, 1962)
Gare du Couze Magdalenian 0.2 to 0.3	213	43	20.90	(Fitte and Sonneville-Bordes, 1962)
Gare du Couze Magdalenian 0.3 to 0.45	103	22	7.78	(Fitte and Sonneville-Bordes, 1962)
Gare du Couze Magdalenian o.45 to 0.55	128	30	13.11	(Fitte and Sonneville-Bordes, 1962)
Gare du Couze 0.55 to 0.7	57	19	10.91	(Fitte and Sonneville-Bordes, 1962)
Flageolet II Level IX Magdalenian	696	47	9.86	(Rigaud, 1970)
La Doue Magdalenian	80	19	6.50	(Mazière, 1984)
Sainte Eulalie Magdalenian Couche 1	60	28	20.12	(Lorblanchet et al., 1973)
Sainte Eulalie Magdalenian Couche 2	31	18	15.46	(Lorblanchet et al., 1973)
Sainte Eulalie Magdalenian Couche B	43	17	10.89	(Lorblanchet et al., 1973)
Sainte Eulalie Magdalenian Couche 3	91	30	21.19	(Lorblanchet et al., 1973)
Sainte Eulalie Magdalenian Couche C	69	23	15.03	(Lorblanchet et al., 1973)

Continued on next page

Table 8.2 – continued from previous page

Assemblage	N	Richness	D	Assemblage Citation
Valojoulx yellow lower couche	59	20	11.83	
Valojoulx red middle couche	114	31	22.81	
Valojoulx black upper couche	74	19	9.70	
Pegourie Couche 4 Azilian	176	21	11.17	(Séronie-Vivien, 1995)
Pegourie Couche 5 Azilian	272	31	12.81	(Séronie-Vivien, 1995)
Pegourie Couche 6 Azilian	251	34	14.96	(Séronie-Vivien, 1995)
Pegourie Couche 7 Azilian	317	37	15.65	(Séronie-Vivien, 1995)
Abri de Villepin. Upper Couche C. Azilian	226	19	9.30	(de Sonneville-Bordes, 1960)
Cap Blanc.	70	24	16.58	(de Sonneville-Bordes, 1960)
Chateau des Eyzies Azilian	48	21	14.29	(de Sonneville-Bordes, 1960)
La Madeleine. Extra-upper couche.	485	41	10.81	(de Sonneville-Bordes, 1960)
Longueroche	491	45	20.40	(de Sonneville-Bordes, 1960)

§ 8.2 Useful Code

The following code is included to illustrate how methods were applied. It is also hoped that readers will be able to adapt and utilize some sections of code for their own research. Matlab code was written with help from James Hook.

8.2.1 Oxcal code

The following sample code illustrates how a typical Oxcal chronological model was produced. Copying into the 'code view' window of Oxcal will allow readers to see how a typical model in this thesis was produced.

```
Plot( )
{
Outlier_Model("SSimple",N(0,2),0,"s"); % outlier model selected.
Sequence("Flageolet I")
{
Boundary("Start V"); % First boundary, starting the sequence
Phase("V")
{
R_Date("Ly-2721", 22520, 500)
{
Outlier(0.07); % probability of determination being an outlier
};
R_Date("OxA-447", 25700, 700) % radiocarbon date, uncalibrated
{
Outlier(0.15);
};
};
```

```
Boundary("End V");
Boundary("Start IV");
Phase("IV")
{
R_Date("Ly-2128", 22950, 500)
{
Outlier(0.07);
};
R_Date("OxA-596", 23250, 500)
{
Outlier(0.15);
};
};
Boundary("End IV");
Boundary("Start I-III");
Phase("I-III")
{
R_Date("Ly-2185", 18610, 440)
{
Outlier(0.07);
};
R_Date("OxA-448", 24600, 700)
{
Outlier(0.15);
};
};
Boundary("End I-III");
};
```

```
};
```

8.2.2 Diversity methods Matlab code

The following code can be used to quickly apply the (Kintigh, 1989) simulation method to archaeological data, using Matlab. Users will need to create two sorts of files; an m-file containing the distribution of artefact types, divided into appropriate categories and another m-file which produces the simulations and collates the summary statistics for these simulations.

Code produced with assistance from James Hook.

```
function P=Aurignacion1

for i=1:1:92   % 92 categories here as using Sonneville-Bordes' typology.
    P(i)=0;
end

P=[ % Fill-in total number of tools in each category here, in sequence
];



% convert number to probability

t=0;
for i=1:1:92
    t=t+P(i); % count total number of objects
end
for i=1:1:92
    P(i)=P(i)/t; % normalize to get a probability distribution
```

```
end

end



function SimPlentyAss

% repeatedly simulates P

T=1000; % number of simulations

P=UPalTotal2012; % loads assemblage (use appropriate file name)
.

N=491; % number of samples

for k=1:1:T

    for i=1:1:93
        PS(i)=0; % calculates summed probabilities
        for j=1:1:i-1
         PS(i)=PS(i)+P(j);
        end
    end

    for i=1:1:92 % initialize sample array
        S(i)=0; % S(i)=number of object-i's found in simulation
    end
```

```
for n=1:1:N
    r=rand; % random number uniform in [0,1]
    for i=1:1:92
        if (r>PS(i))
            if (r<PS(i+1)) % so if r lies in the interval [PS(i),PS(i+1)]
                S(i)=S(i)+1; % record finding another object i
            end
        end
    end
end

% now S contains a sample of N things drawn from the probability measure P

Active=0; % number of active categories
for i=1:1:92
    if (S(i)>0)
        Active=Active+1;
    end
end

Shannon=0; % shannon index
for i=1:1:92
    if (S(i)>0)
        Shannon=Shannon-(S(i)/N)*log(S(i)/N);
    end
end
```

```
    D=exp(Shannon);

    % record statistics

    ActiveA(k)=Active;
    ShannonA(k)=Shannon;
    DA(k)=D;

end

% Active categories

for i=1:1:92
    ACC(i)=0; % initialize active category distribution
end
for k=1:1:T
    ACC(ActiveA(k))=ACC(ActiveA(k))+1/T;
end
MeanAcc=0;
for i=1:1:92
    MeanAcc=MeanAcc+ACC(i)*i;
end
VarAcc=0;
for i=1:1:92
    VarAcc=VarAcc+ACC(i)*(i-MeanAcc)^2;
end
SdAcc=VarAcc^0.5;
```

```
plot(ACC);
MeanAcc
SdAcc
pause;

% Shannon index

MeanShan=0;
for k=1:1:T
    MeanShan=MeanShan+ShannonA(k)/T;
end
VarShan=0;
for k=1:1:T
    VarShan=VarShan+(ShannonA(k)-MeanShan)^2;
end
SdShan=VarShan^0.5;
PlotShan=sort(ShannonA);
for k=1:1:T
    P(k)=k/T;
end
plot(PlotShan,P);
MeanShan
SdShan
pause;

% D

MeanD=0;
```

```
for k=1:1:T
    MeanD=MeanD+DA(k)/T;
end
VarD=0;
for k=1:1:T
    VarD=VarD+(DA(k)-MeanD)^2;
end
SdD=VarD^0.5;
PlotD=sort(DA);
for k=1:1:T
    P(k)=k/T;
end
plot(PlotD,P);
MeanD
SdD

end
```

8.2.3 KDE Matlab code

```
function KDEBP

h=0.2; % smoothing parameter;
```

```
Tb=-45719.5; % bottom end of time range
Tt=-6564.5; % top end
Tint=5; % interval used in pd's
N=1+(Tt-Tb)/Tint; % number of time steps

Nsites=83; % number of sites being used

% array of locations

    x(1)=1.03; % X,Y location of ith radiocarbon date.
    y(1)=44.93;

% array of pd

load('Data')

for i=1:1:N
    Psum(1,i)=Y1(i);
    Psum(2,i)=Y2(i);
    Psum(3,i)=Y3(i);% P(j,i) is the value of the summed pd for the jth site at the ith
    Psum(4,i)=Y4(i); % Up to value of the ith site location


end

xmin=-2; % xmin,ymin is bottom left corner of plot
xint=0.01; % xint,yint determine resolution.  Interval used in x coordinates
ymin=42.5;
```

```
yint=0.01; % interval used in y coordinates
Nx=500; % number of points to be plotted.  Number of pixels.
Ny=500; % so Ymax=ymin+Ny*yint
ymax=ymin+yint*Ny;

for iii=1:1:120 %timesteps

Year=-40000.5+250*iii;
tplot=floor((Year-Tb)/Tint); % plot time
%tplot=232; % this is putting in an exact data index (time step).
% Make image

maX=0;
miN=1000;

for xi=1:1:Nx+1
    for yi=1:1:Ny+1
        A(xi,yi)=0;
        for i=1:1:Nsites
            A(xi,yi)=A(xi,yi)+Psum(i,tplot)*exp((-(xmin+xi*xint-x(i))
            ^2-(ymin+yi*yint-y(i))^2)/(2*h^2))/(2*pi*h^2);% Grove (2011)'s formula
        end
        maX=max(maX,A(xi,yi));
        miN=min(miN,A(xi,yi));
        B(xi,yi)=0;
    end
end
```

```
for xi=1:1:Nx+1;
    for yi=1:1:Ny+1;
        A(xi,yi)= 256*A(xi,yi)*50; % Scaling.
B(xi,Ny+2-yi)=A(xi,yi);
    end
end

B=B';

image(B)
axis off
hold on
c=Year-1950;
text(xmin+Nx*xint,ymin+0.8*Ny*yint,[num2str(c),'BP'],'FontSize',20)
% the year label on the images
for i=1:1:Nsites
    plot((x(i)-xmin)/xint,(ymax-y(i))/yint,'.','color','black');
end
colormap(cool) % determines the colour scheme used in the images.
pause(0.01);


VIDEO(iii)=getframe; %this makes the video and outputs it as an avi
hold off
end
movie(VIDEO,1,4)
pause;
movie(VIDEO,1,4)
```

```
movie2avi(VIDEO,'FILE.avi','Compression','Cinepak','fps',4)
 % This outputs movie file to your computer
```

Chapter 9

Appendix C

§ 9.1 Chapter Five Appendices

§ 9.2 The Sonneville-Bordes tool typology and tool distributions by technocomplex: Tables

Table 9.1: Sonneville-Bordes' typology

No.	Tool (French name)
1	Grattoir simple sur bout de lame
2	Grattoir atypique
3	Grattoir double
4	Grattoir ogival
5	Grattoir sur lame retouchée
6	Grattoir sur lame aurignacienne
7	Grattoir en éventail
8	Grattoir sur éclat
9	Grattoir circulaire
10	Grattoir unguiforme
	Continued on next page

Table 9.1 – continued from previous page

No.	Tool (French name)
11	Grattoir caréneé
12	Grattoir caréneé atypique
13	Grattoir à museau
14	Grattoir à museau plat
15	Grattoir nucléiforme
16	Rabot
17	Grattoir-burin
18	Grattoir-lame tronquée
19	Burin-lame tronquée
20	Perçoir-lame tronquée
21	Perçoir-grattoir
22	Perçoir-burin
23	Perçoir
24	Bec
25	Perçoir multiple
26	Microperçoir
27	Burin dièdre droit
28	Burin dièdre déjeté
29	Burin diédre d'angle
30	Burine d'angle sur cassure
31	Burine diédre multiple
32	Burin busqué
33	Burin bec-de-perroquet
34	Burin sur troncature droite
35	Burin sur troncature oblique

Continued on next page

Table 9.1 – continued from previous page

No.	Tool (French name)
36	Burin sur troncature concave
37	Burin sur troncature convexe
38	Burin transversal sur troncature latérale
39	Burin transversale sur encoche
40	Burin multiple sur troncature
41	Burin multiple mixte
42	Burin de Noailles
43	Burin de Noailles
44	Burin plan
45	Couteau type Audi
46	Pointe de Châtelperron
47	Pointe de Châtelperron atypique
48	Pointe de la Gravette
49	Pointe de la Gravette atypique
50	Micrograveette
51	Pointe des Vachons
52	Pointe des Font-Yves
53	Pièce gibbeuse à bord abattu
54	Fléchette
55	Pointe à soie
56	Pointe à cran atypique
57	Pièce à cran
58	Lame à bord abattu total
59	Lame à bord abattu partiel
60	Lame à troncature retouchée droit

Continued on next page

Table 9.1 – continued from previous page

No.	Tool (French name)
61	Lame à troncature retouchée oblique
62	Lame à troncature retouchée concave
63	Lame à troncature retouchée convexe
64	Lame bitronquée
65	Lame à retouche continue sur un bord
66	Lame à retouche contniue sur deux bords
67	Lame aurignacienne
68	Lame étranglée
69	Pointe à face plane
70	Feuille de laurier
71	Feuille de saule
72	Pointe à cran typique (solutréenne)
73	Pic
74	Encoche
75	Denticulé
76	Pièce esquillée
77	Racloir
78	Raclette
79	Triangle
80	Rectangle
81	Trapeze
82	Rhombe
83	Segment de cercle
84	Lamelle tronquée
85	Lamelle à dos

Continued on next page

Table 9.1 – continued from previous page

No.	Tool (French name)
86	Lamelle à dos tronquée
87	Lamelle à dos denticulée
88	Lamelle denticulée
89	Lamelle à denticulée
90	Lamelle Dufour
91	Pointe azilienne
92	Divers

Table 9.2: Distribution of tools - Aurignacian assemblages

Tool no.	Tool	Total	Percentage
1	Grattoir simple sur bout de lame	4839	13.58
2	Grattoir atypique	683	1.92
3	Grattoir double	857	2.40
4	Grattoir ogival	264	0.74
5	Grattoir sur lame retouchée	1911	5.36
6	Grattoir sur lame aurignacienne	1276	3.6
7	Grattoir en éventail	107	0.30
8	Grattoir sur éclat	835	2.34
9	Grattoir circulaire	50	0.14
10	Grattoir unguiforme	128	0.36
11	Grattoir caréneé	1968	5.52
12	Grattoir caréneé atypique	803	2.25
13	Grattoir à museau	2456	6.89

Continued on next page

Table 9.2 – continued from previous page

No.	Tool	Total	Percentage
14	Grattoir à museau plat	1131	3.17
15	Grattoir nucléiforme	167	0.47
16	Rabot	261	0.73
17	Grattoir-burin	756	2.12
18	Grattoir-lame tronquée	127	0.36
19	Burin-lame tronquée	42	0.12
20	Perçoir-lame tronquée	5	0.02
21	Perçoir-grattoir	51	0.14
22	Perçoir-burin	21	0.06
23	Perçoir	212	0.59
24	Bec	299	0.84
25	Perçoir multiple	5	0.01
26	Microperçoir	2	0.01
27	Burin dièdre droit	865	2.4
28	Burin dièdre déjeté	651	1.83
29	Burin diédre d'angle	536	1.50
30	Burine d'angle sur cassure	847	2.38
31	Burine diédre multiple	291	0.82
32	Burin busqué	877	2.46
33	Burin bec-de-perroquet	14	0.04
34	Burin sur troncature droite	334	0.94
35	Burin sur troncature oblique	777	2.18
36	Burin sur troncature concave	216	0.61
37	Burin sur troncature convexe	113	0.32
38	Burin transversal sur troncature latérale	118	0.33

Continued on next page

Table 9.2 – continued from previous page

No.	Tool	Total	Percentage
39	Burin transversale sur encoche	65	0.18
40	Burin multiple sur troncature	151	0.42
41	Burin multiple mixte	238	0.67
42	Burin de Noailles	8	0.02
43	Burin de nucléiforme	140	0.39
44	Burin plan	96	0.27
45	Couteau type Audi	28	0.08
46	Pointe de Châtelperron	5	0.01
47	Pointe de Châtelperron atypique	0	0
48	Pointe de la Gravette	1	0.00
49	Pointe de la Gravette atypique	1	0.00
50	Micrograveette	2	0.00
51	Pointe des Vachons	0	0
52	Pointe des Font-Yves	25	0.07
53	Pièce gibbeuse à bord abattu	0	0
54	Fléchette	0	0
55	Pointe à soie	0	0
56	Pointe à cran atypique	0	0
57	Pièce à cran	1	0.00
58	Lame à bord abattu total	22	0.06
59	Lame à bord abattu partiel	16	0.04
60	Lame à troncature retouchée droit	215	0.60
61	Lame à troncature retouchée oblique	295	0.82
62	Lame à troncature retouchée concave	124	0.35
63	Lame à troncature retouchée convexe	41	0.12

Continued on next page

Table 9.2 – continued from previous page

No.	Tool	Total	Percentage
64	Lame bitronquée	30	0.08
65	Lame à retouche continue sur un bord	2326	6.53
66	Lame à retouche contniue sur deux bords	802	2.25
67	Lame aurignacienne	996	2.79
68	Lame étranglée	155	0.43
69	Pointe à face plane	1	0.00
70	Feuille de laurier	0	0
71	Feuille de saule	0	0
72	Pointe à cran typique (solutréenne)	0	0
73	Pic	147	0.41
74	Encoche	1087	3.05
75	Denticulé	1057	2.97
76	Pièce esquillée	641	1.80
77	Racloir	407	1.14
78	Raclette	25	0.07
79	Triangle	0	0
80	Rectangle	0	0
81	Trapeze	0	0
82	Rhombe	0	0
83	Segment de cercle	0	0
84	Lamelle tronquée	10	0.03
85	Lamelle à dos	104	0.29
86	Lamelle à dos tronquée	1	0.00
87	Lamelle à dos denticulée	2	0.01
88	Lamelle denticulée	10	0.03

Continued on next page

Table 9.2 – continued from previous page

No.	Tool	Total	Percentage
89	Lamelle à denticulée	15	0.04
90	Lamelle Dufour	621	1.74
91	Pointe azilienne	2	0.01
92	Divers	829	2.33

Table 9.3: Distribution of tools - Gravettian assemblages

Tool no.	Tool	Total	Percentage
1	Grattoir simple sur bout de lame	2059	7.75
2	Grattoir atypique	414	1.56
3	Grattoir double	174	0.65
4	Grattoir ogival	212	0.80
5	Grattoir sur lame retouchée	494	1.86
6	Grattoir sur lame aurignacienne	20	0.08
7	Grattoir en éventail	97	0.36
8	Grattoir sur éclat	249	0.94
9	Grattoir circulaire	14	0.05
10	Grattoir unguiforme	12	0.05
11	Grattoir caréneé	32	0.12
12	Grattoir caréneé atypique	45	0.17
13	Grattoir à museau	40	0.15
14	Grattoir à museau plat	23	0.09
15	Grattoir nucléiforme	70	0.26
16	Rabot	82	0.31

Continued on next page

Table 9.3 – continued from previous page

No.	Tool	Total	Percentage
17	Grattoir-burin	440	1.66
18	Grattoir-lame tronquée	57	0.21
19	Burin-lame tronquée	95	0.36
20	Perçoir-lame tronquée	16	0.06
21	Perçoir-grattoir	14	0.05
22	Perçoir-burin	31	0.12
23	Perçoir	189	0.71
24	Bec	185	0.70
25	Perçoir multiple	19	0.07
26	Microperçoir	31	0.12
27	Burin dièdre droit	1005	3.79
28	Burin dièdre déjeté	933	3.51
29	Burin diédre d'angle	351	1.32
30	Burine d'angle sur cassure	758	2.85
31	Burine diédre multiple	466	1.75
32	Burin busqué	59	0.22
33	Burin bec-de-perroquet	11	0.04
34	Burin sur troncature droite	288	1.08
35	Burin sur troncature oblique	1393	5.24
36	Burin sur troncature concave	686	2.58
37	Burin sur troncature convexe	172	0.65
38	Burin transversal sur troncature latérale	99	0.37
39	Burin transversale sur encoche	62	0.23
40	Burin multiple sur troncature	634	2.38
41	Burin multiple mixte	516	1.94

Continued on next page

Table 9.3 – continued from previous page

No.	Tool	Total	Percentage
42	Burin de Noailles	2051	7.71
43	Burin de nucléiforme	98	0.37
44	Burin plan	750	2.82
45	Couteau type Audi	9	0.03
46	Pointe de Châtelperron	22	0.08
47	Pointe de Châtelperron atypique	12	0.05
48	Pointe de la Gravette	1965	7.39
49	Pointe de la Gravette atypique	354	1.33
50	Micrograveette	399	1.50
51	Pointe des Vachons	799	3.01
52	Pointe des Font-Yves	12	0.05
53	Pièce gibbeuse à bord abattu	94	0.35
54	Fléchette	166	0.62
55	Pointe à soie	249	0.94
56	Pointe à cran atypique	22	0.08
57	Pièce à cran	278	1.05
58	Lame à bord abattu total	317	1.19
59	Lame à bord abattu partiel	122	0.46
60	Lame à troncature retouchée droit	223	0.84
61	Lame à troncature retouchée oblique	376	1.41
62	Lame à troncature retouchée concave	359	1.35
63	Lame à troncature retouchée convexe	66	0.25
64	Lame bitronquée	49	0.18
65	Lame à retouche continue sur un bord	1083	4.07
66	Lame à retouche contniue sur deux bords	449	1.69

Continued on next page

Table 9.3 – continued from previous page

No.	Tool	Total	Percentage
67	Lame aurignacienne	48	0.18
68	Lame étranglée	10	0.04
69	Pointe à face plane	9	0.03
70	Feuille de laurier	9	0.03
71	Feuille de saule	9	0.03
72	Pointe à cran typique (solutréenne)	9	0.03
73	Pic	33	0.12
74	Encoche	1524	5.73
75	Denticulé	264	0.99
76	Pièce esquillée	242	0.91
77	Racloir	106	0.40
78	Raclette	14	0.05
79	Triangle	16	0.06
80	Rectangle	14	0.05
81	Trapeze	9	0.03
82	Rhombe	9	0.03
83	Segment de cercle	9	0.03
84	Lamelle tronquée	56	0.21
85	Lamelle à dos	629	2.37
86	Lamelle à dos tronquée	94	0.35
87	Lamelle à dos denticulée	18	0.07
88	Lamelle denticulée	12	0.05
89	Lamelle à denticulée	87	0.33
90	Lamelle Dufour	40	0.15
91	Pointe azilienne	9	0.03

Continued on next page

Table 9.3 – continued from previous page

No.	Tool	Total	Percentage
92	Divers	434	1.63

Table 9.4: Distribution of tools - Solutrean

Tool no.	Tool	Total	Percentage
1	Grattoir simple sur bout de lame	1565	13.48
2	Grattoir atypique	155	1.33
3	Grattoir double	259	2.23
4	Grattoir ogival	81	0.70
5	Grattoir sur lame retouchée	359	3.09
6	Grattoir sur lame aurignacienne	0	0
7	Grattoir en éventail	59	0.51
8	Grattoir sur éclat	149	1.28
9	Grattoir circulaire	1	0.01
10	Grattoir unguiforme	1	0.01
11	Grattoir caréneé	56	0.48
12	Grattoir caréneé atypique	51	0.44
13	Grattoir à museau	58	0.50
14	Grattoir à museau plat	37	0.32
15	Grattoir nucléiforme	7	0.06
16	Rabot	7	0.06
17	Grattoir-burin	161	1.39
18	Grattoir-lame tronquée	30	0.26
19	Burin-lame tronquée	22	0.19

Continued on next page

Table 9.4 – continued from previous page

No.	Tool	Total	Percentage
20	Perçoir-lame tronquée	6	0.05
21	Perçoir-grattoir	24	0.21
22	Perçoir-burin	14	0.12
23	Perçoir	302	2.60
24	Bec	140	1.21
25	Perçoir multiple	17	0.15
26	Microperçoir	4	0.03
27	Burin dièdre droit	204	1.76
28	Burin dièdre déjeté	112	0.97
29	Burin diédre d'angle	105	0.90
30	Burine d'angle sur cassure	126	1.08
31	Burine diédre multiple	46	0.40
32	Burin busqué	10	0.09
33	Burin bec-de-perroquet	0	0
34	Burin sur troncature droite	52	0.45
35	Burin sur troncature oblique	254	2.19
36	Burin sur troncature concave	64	0.55
37	Burin sur troncature convexe	32	0.28
38	Burin transversal sur troncature latérale	29	0.25
39	Burin transversale sur encoche	45	0.39
40	Burin multiple sur troncature	57	0.50
41	Burin multiple mixte	52	0.45
42	Burin de Noailles	1	0.01
43	Burin de nucléiforme	25	0.22
44	Burin plan	7	0.06

Continued on next page

Table 9.4 – continued from previous page

No.	Tool	Total	Percentage
45	Couteau type Audi	4	0.03
46	Pointe de Châtelperron	1	0.01
47	Pointe de Châtelperron atypique	8	0.07
48	Pointe de la Gravette	6	0.05
49	Pointe de la Gravette atypique	1	0.01
50	Micrograveette	1	0.01
51	Pointe des Vachons	0	0
52	Pointe des Font-Yves	0	0
53	Pièce gibbeuse à bord abattu	0	0
54	Fléchette	1	0.01
55	Pointe à soie	0	0
56	Pointe à cran atypique	678	5.84
57	Pièce à cran	19	0.16
58	Lame à bord abattu total	9	0.08
59	Lame à bord abattu partiel	3	0.03
60	Lame à troncature retouchée droit	50	0.43
61	Lame à troncature retouchée oblique	121	1.04
62	Lame à troncature retouchée concave	49	0.42
63	Lame à troncature retouchée convexe	15	0.13
64	Lame bitronquée	5	0.04
65	Lame à retouche continue sur un bord	226	1.95
66	Lame à retouche contniue sur deux bords	87	0.75
67	Lame aurignacienne	2	0.02
68	Lame étranglée	3	0.03
69	Pointe à face plane	672	5.79

Continued on next page

Table 9.4 – continued from previous page

No.	Tool	Total	Percentage
70	Feuille de laurier	1448	12.47
71	Feuille de saule	268	2.31
72	Pointe à cran typique (solutréenne)	1324	11.40
73	Pic	48	0.41
74	Encoche	313	2.70
75	Denticulé	311	2.68
76	Pièce esquillée	12	0.10
77	Racloir	212	1.83
78	Raclette	34	0.30
79	Triangle	2	0.02
80	Rectangle	0	0
81	Trapeze	0	0
82	Rhombe	0	0
83	Segment de cercle	0	0
84	Lamelle tronquée	3	0.26
85	Lamelle à dos	432	3.72
86	Lamelle à dos tronquée	1	0.01
87	Lamelle à dos denticulée	5	0.04
88	Lamelle denticulée	0	0
89	Lamelle à denticulée	9	0.08
90	Lamelle Dufour	7	0.06
91	Pointe azilienne	0	0
92	Divers	437	3.76

Table 9.5: Distribution of tools - Badegoulian

Tool no.	Tool	Total	Percentage
1	Grattoir simple sur bout de lame	250	8.61
2	Grattoir atypique	11	0.38
3	Grattoir double	59	2.03
4	Grattoir ogival	15	0.52
5	Grattoir sur lame retouchée	124	4.27
6	Grattoir sur lame aurignacienne	0	0
7	Grattoir en éventail	12	0.41
8	Grattoir sur éclat	31	1.07
9	Grattoir circulaire	1	0.03
10	Grattoir unguiforme	2	0.07
11	Grattoir caréneé	20	0.69
12	Grattoir caréneé atypique	0	0
13	Grattoir à museau	2	0.07
14	Grattoir à museau plat	5	0.17
15	Grattoir nucléiforme	3	0.10
16	Rabot	1	0.03
17	Grattoir-burin	47	1.62
18	Grattoir-lame tronquée	14	0.48
19	Burin-lame tronquée	5	0.17
20	Perçoir-lame tronquée	2	0.07
21	Perçoir-grattoir	1	0.03
22	Perçoir-burin	2	0.07
23	Perçoir	64	2.20
24	Bec	21	0.72
25	Perçoir multiple	3	0.10

Continued on next page

Table 9.5 – continued from previous page

No.	Tool	Total	Percentage
26	Microperçoir	17	0.59
27	Burin dièdre droit	71	2.44
28	Burin dièdre déjeté	21	0.72
29	Burin diédre d'angle	47	1.62
30	Burine d'angle sur cassure	66	2.27
31	Burine diédre multiple	24	0.83
32	Burin busqué	2	0.07
33	Burin bec-de-perroquet	0	0
34	Burin sur troncature droite	14	0.48
35	Burin sur troncature oblique	54	1.86
36	Burin sur troncature concave	29	1.00
37	Burin sur troncature convexe	4	0.0.14
38	Burin transversal sur troncature latérale	17	0.59
39	Burin transversale sur encoche	18	0.62
40	Burin multiple sur troncature	10	0.34
41	Burin multiple mixte	17	0.59
42	Burin de Noailles	1	0.03
43	Burin de nucléiforme	3	0.10
44	Burin plan	2	0.07
45	Couteau type Audi	0	0
46	Pointe de Châtelperron	0	0
47	Pointe de Châtelperron atypique	0	0
48	Pointe de la Gravette	1	0.03
49	Pointe de la Gravette atypique	0	0
50	Microgravette	0	0

Continued on next page

Table 9.5 – continued from previous page

No.	Tool	Total	Percentage
51	Pointe des Vachons	0	0
52	Pointe des Font-Yves	0	0
53	Pièce gibbeuse à bord abattu	0	0
54	Fléchette	0	0
55	Pointe à soie	0	0
56	Pointe à cran atypique	81	2.79
57	Pièce à cran	5	0.17
58	Lame à bord abattu total	0	0
59	Lame à bord abattu partiel	5	0.17
60	Lame à troncature retouchée droit	34	1.17
61	Lame à troncature retouchée oblique	12	0.41
62	Lame à troncature retouchée concave	3	0.10
63	Lame à troncature retouchée convexe	4	0.14
64	Lame bitronquée	2	0.07
65	Lame à retouche continue sur un bord	122	4.20
66	Lame à retouche contniue sur deux bords	89	3.06
67	Lame aurignacienne	3	0.10
68	Lame étranglée	2	0.07
69	Pointe à face plane	3	0.10
70	Feuille de laurier	341	11.74
71	Feuille de saule	47	1.62
72	Pointe à cran typique (solutréenne)	89	3.06
73	Pic	0	0
74	Encoche	68	2.34
75	Denticulé	28	0.96

Continued on next page

Table 9.5 – continued from previous page

No.	Tool	Total	Percentage
76	Pièce esquillée	14	0.48
77	Racloir	65	2.24
78	Raclette	422	14.53
79	Triangle	1	0.03
80	Rectangle	0	0
81	Trapeze	0	0
82	Rhombe	0	0
83	Segment de cercle	0	0
84	Lamelle tronquée	2	0.07
85	Lamelle à dos	125	4.30
86	Lamelle à dos tronquée	15	0.52
87	Lamelle à dos denticulée	2	0.07
88	Lamelle denticulée	0	0
89	Lamelle à denticulée	5	0.17
90	Lamelle Dufour	1	0.03
91	Pointe azilienne	1	0.03
92	Divers	201	6.92

Table 9.6: Distribution of tools - Azilian

Tool no.	Tool	Total	Percentage
1	Grattoir simple sur bout de lame	200	8.56
2	Grattoir atypique	13	0.56
3	Grattoir double	9	0.39

Continued on next page

Table 9.6 – continued from previous page

No.	Tool	Total	Percentage
4	Grattoir ogival	0	0
5	Grattoir sur lame retouchée	33	1.41
6	Grattoir sur lame aurignacienne	0	0
7	Grattoir en éventail	1	0.04
8	Grattoir sur éclat	230	9.85
9	Grattoir circulaire	19	0.81
10	Grattoir unguiforme	76	3.25
11	Grattoir caréneé	2	0.09
12	Grattoir caréneé atypique	22	0.94
13	Grattoir à museau	4	0.17
14	Grattoir à museau plat	0	0
15	Grattoir nucléiforme	0	0
16	Rabot	1	0.04
17	Grattoir-burin	38	1.63
18	Grattoir-lame tronquée	6	0.26
19	Burin-lame tronquée	2	0.09
20	Perçoir-lame tronquée	0	0
21	Perçoir-grattoir	1	0.04
22	Perçoir-burin	3	0.13
23	Perçoir	38	1.63
24	Bec	16	0.68
25	Perçoir multiple	6	0.26
26	Microperçoir	20	0.86
27	Burin dièdre droit	215	9.20
28	Burin dièdre déjeté	42	1.80

Continued on next page

Table 9.6 – continued from previous page

No.	Tool	Total	Percentage
29	Burin diédre d'angle	61	2.61
30	Burine d'angle sur cassure	31	1.33
31	Burine diédre multiple	18	0.77
32	Burin busqué	0	0
33	Burin bec-de-perroquet	3	0.13
34	Burin sur troncature droite	7	0.30
35	Burin sur troncature oblique	34	1.46
36	Burin sur troncature concave	17	0.73
37	Burin sur troncature convexe	6	0.26
38	Burin transversal sur troncature latérale	3	0.13
39	Burin transversale sur encoche	1	0.04
40	Burin multiple sur troncature	2	0.09
41	Burin multiple mixte	3	0.13
42	Burin de Noailles	1	0.04
43	Burin de nucléiforme	2	0.09
44	Burin plan	1	0.04
45	Couteau type Audi	0	0
46	Pointe de Châtelperron	1	0.04
47	Pointe de Châtelperron atypique	0	0
48	Pointe de la Gravette	0	0
49	Pointe de la Gravette atypique	0	0
50	Micrograveette	10	0.43
51	Pointe des Vachons	0	0
52	Pointe des Font-Yves	0	0
53	Pièce gibbeuse à bord abattu	0	0

Continued on next page

Table 9.6 – continued from previous page

No.	Tool	Total	Percentage
54	Fléchette	2	0.09
55	Pointe à soie	0	0
56	Pointe à cran atypique	2	0.09
57	Pièce à cran	1	0.04
58	Lame à bord abattu total	15	0.64
59	Lame à bord abattu partiel	3	0.13
60	Lame à troncature retouchée droit	14	0.60
61	Lame à troncature retouchée oblique	31	1.33
62	Lame à troncature retouchée concave	10	0.43
63	Lame à troncature retouchée convexe	5	0.21
64	Lame bitronquée	5	0.21
65	Lame à retouche continue sur un bord	88	3.8
66	Lame à retouche contniue sur deux bords	108	4.62
67	Lame aurignacienne	1	0.04
68	Lame étranglée	0	0
69	Pointe à face plane	0	0
70	Feuille de laurier	0	0
71	Feuille de saule	0	0
72	Pointe à cran typique (solutréenne)	0	0
73	Pic	1	0.04
74	Encoche	25	1.07
75	Denticulé	7	0.30
76	Pièce esquillée	10	0.43
77	Racloir	15	0.64
78	Raclette	10	0.43

Continued on next page

Table 9.6 – continued from previous page

No.	Tool	Total	Percentage
79	Triangle	0	0
80	Rectangle	1	0.04
81	Trapeze	0	0
82	Rhombe	0	0
83	Segment de cercle	1	0.04
84	Lamelle tronquée	9	0.39
85	Lamelle à dos	137	5.86
86	Lamelle à dos tronquée	23	0.98
87	Lamelle à dos denticulée	4	0.17
88	Lamelle denticulée	0	0
89	Lamelle à denticulée	7	0.30
90	Lamelle Dufour	18	0.77
91	Pointe azilienne	432	18.49
92	Divers	153	6.55

§ 9.3 Results: Lithic Densities

The following data tables display results from intra-site lithic densities. Level duration was estimated using the 'phase' and 'boundary' functions in Oxcal.

Level thickness is given in cm. Technocomplexes are abbreviated in the following manner:

- A = Aurignacian
- G = Gravettian

- S = Solutrean
- B = Badegoulian
- M = Magdalenian
- Az = Azilian

Table 9.7: Intra-site Lithic Density Data

Site	Level	Techno	N	Years	Thickness	Area	Tool/area	Tool/area/year
La Ferrassie	L	A	15		40	17 m2	0.88	
La Ferrassie	K	A	2116	3300	10	17 m2	124.47	0.038
La Ferrassie	J	A	385	150	20	17 m2	22.65	0.15
La Ferrassie	I	A	385	100		17 m2	22.65	0.23
La Ferrassie	H	A	120	-	20	17 m2	7.06	-
La Ferrassie	G	A	477	4270		17 m2	28.06	0.01
La Ferrassie	E	A	113	70	10	17 m2	6.65	0.09
Abri Pataud	2	A	1156	2000	60	117m	9.88	0.0049
Abri Pataud	6	A	368	200	10	21m	17.52	0.088
Abri Pataud	7	A	632	100	20	18m	35.11	0.35
Abri Pataud	8	A	434	100	30	18m	24.11	0.24
Abri Pataud	11	A	609	200	30	16m	38.06	0.19
Abri Pataud	12	A	102	300	10	14m	7.29	0.024
Abri Pataud	13	A	37	-	10	14m2	2.64	-
Abri Pataud	14	A	161	300	10	14m2	11.5	0.038

Continued on next page

Table 9.7 – continued from previous page

Site	Level	Techno	N	Years	Thickness	Area	Tool/area	Tool/area/year
Laugerie Haute Ouest	A	A	1620			48 m2	33.75	-
Roc de Combe	5	A	140	400	29	39 m2	3.59	0.089
Roc de Combe	6	A	178	400	18	32 m2	5.56	0.014
Roc de Combe	7	A	172	6000	36	32 m2	5.38	0.0009
Le Facteur	21	A	73	500	5	50 m2	1.46	0.00292
La Rochette	5d	A	256	-		15 m2	17.07	-
La Rochette	5c	A	148	1250		15 m2	9.87	0.008
La Rochette	5 total	A	404	1250	40	15 m2		
La Rochette	4	A	394	400	10	15 m2	26.27	0.066
La Rochette	3	A	42	-	15	15 m2	2.8	-
Le Piage	K	A	672	450	20	84 m2	8	0.0177777778
Le Piage	J	A	405	200	20	84 m2	4.8214285714	0.0241071429
Le Piage	G	A	2286	200	10	84 m2	27.2142857143	0.1360714286
Le Piage	F	A	235	1000	60	84 m2	2.7976190476	0.002797619
Abri Pataud	3	G	1309	700	50	97m	13.49	0.019

Continued on next page

Table 9.7 – continued from previous page

Site	Level	Techno	N	Years	Thickness	Area	Tool/area	Tool/area/year
Abri Pataud	4	G	5359	3500	40	30m	178.63	0.051
Abri Pataud	5	G	5640	5400	40	20m	282	0.052
Roc de Combe	1	G	242	200	40	39 m2	6.2	0.03
Roc de Combe	2	G	35	150	21	39 m2	0.9	0.059
Roc de Combe	3	G	23	150	7	39 m2	0.6	0.039
Roc de Combe	4	G	42	500	14	39 m2	1.07	0.022
Flageolet I	I III	G	88	4000	34	72 m2	1.2	0.00031
Flageolet I	IV	G	73	900	9	72m2	1	0.001
Flageolet I	V	G	72	400	14	72m2	1	0.0025
Flageolet I	VI	G	141	500	14	72m2	2	0.0035
Le Facteur	10 11	G	1130	800	18	50 m2	22.6	0.02825
Pégourié	10	G	29	900		45 m2	0.65	0.0007
Laugerie Haute Est	31	S	355	335	35	11 m2	32.27	0.096
Laugerie Haute Est	23	S	34	175	16	11 m2	3.09	0.018
Laugerie Haute Ouest	Lower S	S	1931	300	32	48 m2	40.23	0.134

Continued on next page

Table 9.7 – continued from previous page

Site	Level	Techno	N	Years	Thickness	Area	Tool/area	Tool/area/year
Laugerie Haute Ouest	Middle S	S	623	150	53	48 m2	12.98	0.087
Laugerie Haute Ouest	Upper S	S		100	18	48 m2	-	-
Laugerie Haute Ouest	Final S	S		100		48 m2	-	-
Jamblancs	B.	S	68			50 m2	1.36	
Jamblancs	D.	S	68			50 m2	1.36	
Jamblancs	F.	S	44			50 m2	0.88	
Cuzoul de Vers	28	S	51	-	10	40 m2	1.275	-
Sainte Eulalie	IV	S	10	-		4 m2	2.5	-
Peyrugues	12	S	20	1700		29 m2	0.69	0.0004
Pech de la Boissiere	Upper S I	S	760	.		93 m2	8.085106383	
Pech de la Boissiere	Upper S II	S	977	.		93 m2	10.5053763441	
Badegoule	A and C	S	848		45	30 m2	28.2666666667	
Fourneau-du-Diable	I	S	1010			188 m2	5.3723404255	
Fourneau-du-Diable	II	S	785			188 m2	4.1755319149	
Fourneau-du-Diable	III	S	1430			188 m2	7.6063829787	

Continued on next page

Table 9.7 – continued from previous page

Site	Level	Techno	N	Years	Thickness	Area	Tool/area	Tool/area/year
Combe Saunière I	Ivb	S	350			50 m2	7	
Pégourié	8	B	699	350		45 m2	15.53	0.044
Pégourié	9	B	258	500		45 m2	5.73	0.011
Cuzoul de Vers	22	B	368	100	8	40 m2	9.2	0.092
Cuzoul de Vers	23	B	438	50	13	40 m2	10.95	0.219
Cuzoul de Vers	24	B	301	50	8	40 m2	7.525	0.1505
Cuzoul de Vers	25	B	101	50	3	40 m2	2.525	0.0505
Cuzoul de Vers	26	B	99	50	3	40 m2	2.475	0.0495
Cuzoul de Vers	27	B	143	-	3	40 m2	3.575	-
Laugerie Haute Est	2	M	393	2700	13	11 m2	35.72	0.013
Laugerie Haute Est	1	M	110	860	16	11 m2	10	0.012
La Madeleine	Upper	M	3699	-		416 m2	8.89	-
La Madeleine	Middle	M	3011	300		416 m2	7.24	0.024
La Madeleine	Lower	M	4995	1100		416 m2	12.01	0.011
Gare de Couze	0.1-0.2	M	4m2	-		225	56	

Continued on next page

Table 9.7 – continued from previous page

Site	Level	Techno	N	Years	Thickness	Area	Tool/area	Tool/area/year
Gare de Couze	0.2 0.3	M	4m2	-		213	53	
Gare de Couze	0.3-0.45	M	4m2			103	26	
Gare de Couze	0.45-0.55	M	4m2			128	32	
Gare de Couze	0.55-0.7	M	4m2	2300	15	57	14	0.006
Gare de Couze	All dated levels	M	4m2	4000	60	288	72	0.018
Grotte XVI	0	M	570	500		30 m2	19	0.04
Flageolet II	II	M		1200	38	38 m 2		
Flageolet II	IX	M	433	1000	30	38 m2	11.4	0.012
Gandil	C20	M	137	50		132 m2	1.04	0.021
Gandil	C23	M	74	450		132 m2	0.56	0.001
Gandil	C25	M	72	350		132 m2	0.55	0.002
La Doue	M	M	80	250		44 m2	1.82	0.007
Roc de Marcamps	2	M	620	300		10 m2	62	0.207
Roc de Marcamps	3	M	57	300		10 m2	5.7	0.019
Roc de Marcamps	4	M	101	700		10 m2	10.1	0.0144

Continued on next page

Table 9.7 – continued from previous page

Site	Level	Techno	N	Years	Thickness	Area	Tool/area	Tool/area/year
Jamblancs	2.	M	98	1450		10 m2	9.8	0.007
Sainte Eulalie	I	M	60	400		4 m2	15	0.038
Sainte Eulalie	II	M	31	-		4 m2	10.25	-
Sainte Eulalie	III	M	91	600		4 m2	22.75	0.038
Peyrugues	3	M	613	800		80 m2	7.66	0.01
Peyrugues	18	M	86	700		29 m2	2.97	0.004
Solvieux	3-A	M	2184			2000 m2	1.092	
Solvieux	1-I	M	294			2000 m2	0.147	
Solvieux	1-II	M	258			2000 m2	0.129	
Le Piage	CE	M/S	1215	900	50	84 m2	14.4642857143	0.0160714286
Solvieux	2-III	P	896			2000 m2	0.448	
Solvieux	6-M	P	564			2000 m2	0.282	
Solvieux	4-B	P	223			2000 m2	0.1115	
Pégourié	4	Az	176	300		45 m2	3.91	0.013
Pégourié	5	Az	270	5600		45 m2	6	0.001

Continued on next page

Table 9.7 – continued from previous page

Site	Level	Techno	N	Years	Thickness	Area	Tool/area	Tool/area/year
Pégourié	6	Az	256	1500		45 m2	5.69	0.004
Pégourié	7	Az	304	2000		45 m2	6.76	0.003

§ 9.4 Results: Lithic Assemblage Diversity

The following table contains data on assemblage diversity.

Categories are abbreviated as follows:

- SimRich = simulated value for richness
- SimD = simulated value for D

Table 9.8: Assemblage diversity data

Techno	**Assemblage**	**N**	**Richness**	**D**	**SimRich**	**SimD**
A	La Ferrassie A I Couche F	2442	55	21.76967	63.814	32.409
A	La Ferrassie A II Couche H	4037	56	16.3959	66.626	32.5853
A	La Ferrasssie A III Couche H	362	39	18.68039	48.949	29.9866
A	La Ferrassie A IV	473	41	11.44047	51.493	30.6036
A	Le Ferrassie A Couche L	15	11	11.36787	11.336	10.4077
A	La Ferrassie A Couche K Delporte (level non-subdivided)	2105	54	28.1696319819	26.067	20.5941
A	La Ferrassie A Couche J Delporte	385	38	21.9533612459	49.547	30.127
A	La Ferrassie A Couche I Delporte	497	48	27.7418497377	51.868	30.6464
A	La Ferrassie A Couche H Delporte	120	34	25.6901511081	36.438	25.8364
A	La Ferrassie A Couche G Delporte	502	47	26.1588226598	52.158	30.7282
A	La Ferrassie A Couche F Delporte	86	28	19.6179637464	32.205	23.8555
A	La Ferrassie A Couche E Delporte	236	34	22.6552051323	44.443	28.8685
A	Faurélie A II	525	49	20.18224	52.688	30.8525
A	Abri Lartet A I	713	40	18.64671	55.346	31.3576
A	Abri de Poisson A I	422	46	22.30949	50.453	30.4139

Continued on next page

Table 9.8 – continued from previous page

Techno	Assemblage	N	Richness	D	SimRich	SimD
A	Abri Cellier A I	354	44	25.84993	48.716	30.0023
A	Abri Cellier A II	520	51	25.14925	52.388	30.7402
A	Le Moustier A	231	41	20.61107	44.204	28.6617
A	Abri du Renne A	575	45	26.18801	53.408	30.9992
A	Abri de la Mtairie	392	45	25.40612	49.808	30.2057
A	Abri Blachard A I	481	38	14.80967	51.728	30.6451
A	Abri Castanet A I	1824	50	15.24024	61.919	32.2366
A	Abri Castanet A II	1283	44	15.89531	59.656	31.9701
A	Abri Caminade Ouest	237	43	26.98889	44.554	28.8508
A	Abri Caminade Ouest	384	48	31.30648	49.556	30.1005
A	Abri Caminade Est	143	36	24.23634	38.578	26.7223
A	Abri Caminade A I Couch F	234	35	23.66311	44.268	28.7228
A	Abri Caminade Est A II Couche D 2i	291	43	29.27562	46.728	29.4406
A	Abri Caminade Est A II D2s	166	36	23.6529	40.542	27.409
A	Abri de Patary A I	241	32	20.10242	44.58	28.8389

Continued on next page

Table 9.8 – continued from previous page

Techno	Assemblage	N	Richness	D	SimRich	SimD
A	Grotte de Chanlat A Couche I	1757	55	24.38466	61.702	32.1327
A	Grotte de Chanlat Couche II	1362	52	25.29178	60.091	32.0132
A	Grotte des Font-Yves	1354	58	26.71865	59.917	31.9926
A	Grotte Dufour A	1242	55	26.36156	59.319	31.9687
A	Abri Pataud Couche 6	368	43	19.6647971804	49.166	30.0765
A	Abri Pataud Couche 7 A	632	44	22.677462352	54.275	31.1124
A	Abri Pataud Couche 8 A	434	46	25.8052394158	50.651	30.4496
A	Abri Pataud Couche 11 A	609	36	19.9838457295	53.92	31.0605
A	Abri Pataud Couche 12 A	102	22	14.8968699879	34.345	24.8637
A	Abri Pataud Couche 13 A	37	15	11.1821124462	21.144	17.62
A	Abri Pataud Couche 14 A	161	26	15.9260251818	39.978	27.2302
A	Roc de Combe Level 5 A	409	39	22.4958839	50.159	30.2689
A	Roc de Combe Level 6 A	435	36	20.8399695938	50.726	30.4024
A	Roc de Combe Level 7 A	544	40	23.9868861073	52.828	30.7918
A	Facteur Level 21 A	68	25	19.9543224293	29.094	22.2962

Continued on next page

Table 9.8 – continued from previous page

Techno	Assemblage	N	Richness	D	SimRich	SimD
A	Facteur Level 19 A	126	34	24.2438754122	37.105	26.0599
A	La Rochette A 5d	256	44	24.7591555164	45.178	28.9386
A	La Rochette A 5c	148	30	21.2495194232	38.96	26.8713
A	La Rochette A 4	394	41	27.3214673056	49.849	30.2456
A	La Rochette A 3	42	21	15.3425990685	22.656	18.5385
A	Le Piage A Couche K	657	49	24.6344929095	54.528	31.1695
A	Le Piage A Couche J	405	43	25.858465812	50.13	30.2073
A	Le Piage A Couche G-I	2286	53	15.9713090382	63.344	32.3458
A	Le Piage A Couche F	235	33	18.9551067059	44.136	28.573
A	Laugerie-Haute Ouest A	1620	52	21.3603074145	61.18	32.1826
A	Abri Pataud eboulis 8-11	78	23	13.7953679938	30.861	23.2305
G	Laugerie Haute Est couche B P III	858	42	15.11908	70.315	38.11
G	Laugerie-Haute Est Couche BP III2	369	31	16.758	58.355	35.7789
G	Abri de la Roque Saint-Christophe Upper P	968	47	21.32386	71.956	38.2729
G	Abri de la Roque Saint Christophe Upper P	195	32	16.33302	48.658	32.8107

Continued on next page

Table 9.8 – continued from previous page

Techno	Assemblage	N	Richness	D	SimRich	SimD
G	Grotte de Font-Robert Upper P	1500	66	29.3711	77.635	38.8966
G	La Ferrassie Grande Abri Couche J	886	50	14.97584	70.817	38.2195
G	La Ferrassie P Couche K	192	35	17.18086	48.416	32.7266
G	La Ferrassie Couche L	15	12	11.36787	11.896	11.0523
G	Abri de Laraux couche 5	191	37	21.06022	48.47	32.8506
G	Abri de Laraux	490	48	21.83862	62.669	36.8763
G	The Roc de Gavaudun Upper P	393	46	26.4103	59.315	35.9134
G	Abri Labattut Lower Couche	354	46	24.30235	57.858	35.663
G	Abri Labattut Couche Superior	403	45	13.90501	59.671	36.0991
G	Fourneau-du-Diable P IV	555	42	15.65882	64.185	37.0425
G	Abri Pataud G Couche 3	1309	52	24.9409407633	75.921	38.7363
G	Abri Pataud G Couche 4	5355	60	22.0088428659	89.557	39.8323
G	Abri Pataud G Couche 5	5640	70	2.5908633588	89.759	39.8573
G	Roc de Combe Level 1 G	1041	57	21.2256779397	72.944	38.4
G	Roc de Combe Level 2 G	179	29	10.5584165952	47.321	32.3528

Continued on next page

Table 9.8 – continued from previous page

Techno	Assemblage	N	Richness	D	SimRich	SimD
G	Roc de Combe Level 3 G	109	26	19.1635494236	39.433	29.0652
G	Roc de Combe Level 4 G	140	34	22.116657168	43.424	30.9073
G	Facteur levels 10 11 G	1110	52	14.266143806	73.787	38.5285
G	Pégourié Couche 10 G	29	15	9.8402532482	19.352	17.0627
G	Abri Pataud eboulis 3-4 Noaillian	379	45	26.5065898449	58.766	35.8934
G	Abri Pataud ProtoM	1156	34	16.0317788834	74.244	38.5802
S	Laugerie-Haute Ouest	1331	53	22.30943	61.331	25.4709
S	Laugerie-Haute Ouest	600	45	11.58151178	52.95	24.6233
S	Laugerie-Haute Est H	933	58	24.495	57.659	25.1758
S	Laugerie-Haute Ouest H	454	37	7.835287	49.811	24.2901
S	Badegoule	838	53	24.15767	56.669	25.0699
S	Badegoule	654	41	12.95103	54.185	24.8511
S	Pech de la Boissiere	760	53	25.28966	55.542	24.9427
S	Abri du Pech de la Boissiere	976	61	23.76551	58.186	25.23
S	Jean-Blanc S Est	154	27	11.97789	36.127	21.5553

Continued on next page

Table 9.8 – continued from previous page

Techno	Assemblage	N	Richness	D	SimRich	SimD
S	Jean-Blanc Ouest S	127	31	16.39153	33.553	20.8506
S	Fourneau-du-Diable	1012	47	11.11945	58.527	25.2184
S	Fourneau-du-Diable	1110	35	10.15627	59.613	25.3582
S	Fourneau-du-Diable	786	31	7.02324	55.872	25.0076
S	Fourneau-du-Diable	1430	45	8.658597	62.023	25.5262
S	Laugerie-Haute Ouest Middle S H”’	169	31	15.6723434024	37.265	21.8686
S	Sainte Eulalie S Couche IV	10	8	7.5785828326	7.787	7.2772
S	Sainte Eulalie S Couche D	42	13	9.3643689749	19.996	15.4532
S	Laugerie-Haute Est H”-H”’	227	36	15.1368291986	41.115	22.7659
B	Pégourié Couche 8A B	341	37	16.6056950369	45.709	24.4896
B	Pégourié Couche 8B B	156	31	14.9291929502	36.319	22.3113
B	Pégourié Couche 8C B	203	36	18.8582447997	39.484	23.205
B	Pegoruie Couche 9A B	187	36	21.6996594321	38.367	22.7618
B	Pégourié Couche 9B B	67	24	18.178851548	25.847	18.5209
B	Jean Blanc Est M with raclettes	295	30	6.3598422822	44.04	24.1409

Continued on next page

Table 9.8 – continued from previous page

Techno	Assemblage	N	Richness	D	SimRich	SimD
B	Jean Blanc Ouest M with raclettes	164	26	9.6869083845	36.848	22.4697
B	Badegoule M	222	37	20.3123326228	40.647	23.3636
B	Badegoule M	105	30	22.2413636512	31.412	20.7581
M	Laugerie-Haute Est	641	50	19.56629	57.866	20.7292
M	Laugerie-Haute Est Couche I	671	54	31.95271	58.499	20.7446
M	Laugerie-Haute Est Lower M Couche II	680	52	20.19992	58.8	20.7
M	Laugerie-Haute Est Lower M Couche 3	1448	59	28.28194	68.236	21.3996
M	Saint-Germaine-la-Rivière	437	38	15.13412	51.831	20.1567
M	Saint-Germaine-la-Rivière	280	39	20.29141	44.539	19.3894
M	Roq Saint Cirq	489	45	15.64807	53.667	20.3037
M	Roq Saint Cirq	421	44	19.45122	51.328	20.1205
M	Roq Saint Cirq	425	38	16.05086	51.478	20.1444
M	Roq Saint Cirq	280	39	22.2107	44.575	19.3262
M	Abri de Crabillat	546	53	15.03247	55.392	20.4969
M	Jolivet	225	41	21.36572	41.02	18.8656

Continued on next page

Table 9.8 – continued from previous page

Techno	Assemblage	N	Richness	D	SimRich	SimD
M	Puy de Lacan	599	42	18.1848	56.965	20.6168
M	Puy de Lacan	591	36	15.66128	56.743	20.5307
M	Puy de Lacan	1457	39	8.5451810146	68.291	21.4068
M	La Madeleine	3699	66	17.44161	75.852	21.7236
M	La Madeleine	3011	62	15.59978	74.567	21.6678
M	La Madeleine	4995	62	12.84607	77.684	21.8182
M	Villepin	167	33	17.9923	35.963	17.9847
M	Villepin	662	59	23.57381	58.34	20.6702
M	Chateau des Eyzies	200	35	19.9188	39.034	18.5606
M	Chateau des Eyzies	252	37	9.404648	42.696	19.0841
M	Chateau des Eyzies	50	22	18.06766	42.696	19.0841
M	Liveyre	173	33	13.64609	36.595	18.1048
M	Longueroche	135	29	14.55306	32.819	17.3614
M	Longueroche	305	37	17.03948	45.837	19.4178
M	Limeuil	3402	47	9.613472	75.282	21.7304

Continued on next page

Table 9.8 – continued from previous page

Techno	Assemblage	N	Richness	D	SimRich	SimD
M	Font-Brunel	56	23	18.06607	21.223	14.332
M	Font-Brunel	50	14	9.805972	19.914	13.7929
M	Soucy M VI	1580	36	6.775955	69.018	21.3838
M	Gare du Couze	364	47	26.16466	48.927	19.8175
M	Fourneau-du-Diable	223	38	18.27836	40.872	18.7932
M	Mege M V	265	33	13.88122	43.758	19.223
M	Mairie	234	33	12.06783	41.598	18.9831
M	Mairie	378	41	17.10424	49.549	19.93
M	Abri du Cap-Blanc	346	31	13.15733	48.114	19.8129
M	Abri du Cap-Blanc	641	40	17.79219	57.929	20.6555
M	Abri du Cap-Blan	310	35	12.04884	46.181	19.4972
M	Abri de la Forge	1500	51	15.30546	68.533	21.4007
M	Metairie	129	28	13.60269	32.237	17.2527
M	Abri Reverdit	1517	65	23.2372	68.767	21.4334
M	Solvieux	976	49	21.27912	63.621	21.0793

Continued on next page

Table 9.8 – continued from previous page

Techno	Assemblage	N	Richness	D	SimRich	SimD
M	Abri de Recourbie I	550	43	14.66557	55.56	20.4531
M	Abri de Recourbie II	564	43	16.11713	55.914	20.4721
M	Chez-Galou General M	241	36	15.71803	42.221	19.0674
M	Gare du Couze M 0.1 to 0.2	225	39	19.9967219692	40.924	18.8798
M	Gare du Couze M 0.2 to 0.3	213	43	20.8961059573	40.269	18.8568
M	Gare du Couze M 0.3 to 0.45	103	22	7.7818124288	28.789	16.5403
M	Gare du Couze M o.45 to 0.55	128	30	13.1118630265	32.136	17.3399
M	Gare du Couze 0.55 to 0.7	57	19	10.9097833867	21.238	14.2498
M	Flageolet II Level IX M	696	47	9.8591304585	59.038	20.7639
M	La Doue M	80	19	6.5011340922	25.369	15.5707
M	Sainte Eulalie M Couche 1	60	28	20.1663990124	22.006	14.6684
M	Sainte Eulalie M Couche 2	31	18	15.458668952	15.181	11.6672
M	Sainte Eulalie M Couche B	43	17	10.885116514	18.209	13.0518
M	Sainte Eulalie M Couche 3	91	30	21.1878411952	27.061	16.013
M	Sainte Eulalie M Couche C	69	23	15.0273540741	23.675	15.2013

Continued on next page

Table 9.8 – continued from previous page

Techno	Assemblage	N	Richness	D	SimRich	SimD
M	Valojoulx yellow lower couche	59	20	11.8256913263	21.774	14.537
M	Valojoulx red middle couche	114	31	22.812895425	30.336	16.9104
M	Valojoulx black upper couche	74	19	9.7039278562	24.461	15.4211
Az	Pégourié Couche 4 Az	176	21	11.174429691	35.228	19.1115
Az	Pégourié Couche 5 Az	272	31	12.8094303983	41.025	20.1684
Az	Pégourié Couche 6 Az	251	34	14.9596736606	40.146	20.0351
Az	Pégourié Couche 7 Az	317	37	15.6548673558	42.964	20.4018
Az	Abri de Villepin.	226	19	9.3049848197	38.54	19.7332
Az	Cap Blanc.	70	24	16.5757474282	23.869	16.0622
Az	Chateau des Eyzies.	48	21	14.2853199396	19.85	14.5077
Az	La Madeleine. Extra-upper couche.	485	41	10.8082703934	48.401	21.1281
Az	Longueroche	491	45	20.3975215202	48.389	21.0882

9.4.1 Mann Whitney U-tests on densities of tools

The following tables display statistical details of Mann Whitney U-tests performed in section 5.3. These tests were used to evaluate if there are statistically significant differences in tool densities between pairs of technocomplexes. This was evaluated in terms of tool densities per m^2 and m^3

Mann Whitney tests on tool densities per m^2

Ranks

	Technoc	N	Mean Rank	Sum of Ranks
AreaDensity	1	27	23.22	627.00
	2	13	14.85	193.00
	Total	40		

Table 9.9: Mann Whitney U-test, comparing densities of tools per m^2 between Aurignacian and Gravettian assemblages

Test Statistics[a]

	AreaDensity
Mann-Whitney U	102.000
Wilcoxon W	193.000
Z	-2.123
Asymp. Sig. (2-tailed)	.034
Exact Sig. [2*(1-tailed Sig.)]	.034[b]

a. Grouping Variable: Technoc

b. Not corrected for ties.

Table 9.10: Mann Whitney U-test, comparing densities of tools per m^2 between Aurignacian and Gravettian assemblages

Ranks

	Technoc	N	Mean Rank	Sum of Ranks
AreaDensity	1	27	18.33	495.00
	3	7	14.29	100.00
	Total	34		

Table 9.11: Mann Whitney U-test, comparing densities of tools per m^2 between Aurignacian and Solutrean assemblages

Test Statistics[a]

	AreaDensity
Mann-Whitney U	72.000
Wilcoxon W	100.000
Z	-.958
Asymp. Sig. (2-tailed)	.338
Exact Sig. [2*(1-tailed Sig.)]	.357[b]

a. Grouping Variable: Technoc

b. Not corrected for ties.

Table 9.12: Mann Whitney U-test, comparing densities of tools per m^2 between Aurignacian and Solutrean assemblages

Ranks

	Technoc	N	Mean Rank	Sum of Ranks
AreaDensity	1	27	19.33	522.00
	4	8	13.50	108.00
	Total	35		

Table 9.13: Mann Whitney U-test, comparing densities of tools per m^2 between Aurignacian and Badegoulian assemblages

Test Statistics[a]

	AreaDensity
Mann-Whitney U	72.000
Wilcoxon W	108.000
Z	-1.414
Asymp. Sig. (2-tailed)	.157
Exact Sig. [2*(1-tailed Sig.)]	.166[b]

a. Grouping Variable: Technoc

b. Not corrected for ties.

Table 9.14: Mann Whitney U-test, comparing densities of tools per m^2 between Aurignacian and Badegoulian assemblages

Ranks

	Technoc	N	Mean Rank	Sum of Ranks
AreaDensity	1	27	25.30	683.00
	5	25	27.80	695.00
	Total	52		

Table 9.15: Mann Whitney U-test, comparing densities of tools per m^2 between Aurignacian and Magdalenian assemblages

Test Statistics[a]

	AreaDensity
Mann-Whitney U	305.000
Wilcoxon W	683.000
Z	-.595
Asymp. Sig. (2-tailed)	.552

a. Grouping Variable: Technoc

Table 9.16: Mann Whitney U-test, comparing densities of tools per m^2 between Aurignacian and Magdalenian assemblages

Ranks

	Technoc	N	Mean Rank	Sum of Ranks
AreaDensity	1	27	16.74	452.00
	6	4	11.00	44.00
	Total	31		

Table 9.17: Mann Whitney U-test, comparing densities of tools per m^2 between Aurignacian and Azilian assemblages

Test Statistics[a]

	AreaDensity
Mann-Whitney U	34.000
Wilcoxon W	44.000
Z	-1.179
Asymp. Sig. (2-tailed)	.239
Exact Sig. [2*(1-tailed Sig.)]	.262[b]

a. Grouping Variable: Technoc

b. Not corrected for ties.

Table 9.18: Mann Whitney U-test, comparing densities of tools per m^2 between Aurignacian and Azilian assemblages

Ranks

	Technoc	N	Mean Rank	Sum of Ranks
AreaDensity	2	13	9.69	126.00
	3	7	12.00	84.00
	Total	20		

Table 9.19: Mann Whitney U-test, comparing densities of tools per m^2 between Gravettian and Solutrean assemblages

Test Statistics[a]

	AreaDensity
Mann-Whitney U	35.000
Wilcoxon W	126.000
Z	-.832
Asymp. Sig. (2-tailed)	.405
Exact Sig. [2*(1-tailed Sig.)]	.438[b]

a. Grouping Variable: Technoc

b. Not corrected for ties.

Table 9.20: Mann Whitney U-test, comparing densities of tools per m^2 between Gravettian and Solutrean assemblages

Ranks

	Technoc	N	Mean Rank	Sum of Ranks
AreaDensity	2	13	9.69	126.00
	4	8	13.13	105.00
	Total	21		

Table 9.21: Mann Whitney U-test, comparing densities of tools per m^2 between Gravettian and Badegoulian assemblages

Test Statistics[a]

	AreaDensity
Mann-Whitney U	35.000
Wilcoxon W	126.000
Z	-1.232
Asymp. Sig. (2-tailed)	.218
Exact Sig. [2*(1-tailed Sig.)]	.238[b]

a. Grouping Variable: Technoc

b. Not corrected for ties.

Table 9.22: Mann Whitney U-test, comparing densities of tools per m^2 between Gravettian and Badegoulian assemblages

Ranks

	Technoc	N	Mean Rank	Sum of Ranks
AreaDensity	2	13	15.15	197.00
	5	25	21.76	544.00
	Total	38		

Table 9.23: Mann Whitney U-test, comparing densities of tools per m^2 between Gravettian and Magdalenian assemblages

Test Statistics[a]

	AreaDensity
Mann-Whitney U	106.000
Wilcoxon W	197.000
Z	-1.739
Asymp. Sig. (2-tailed)	.082
Exact Sig. [2*(1-tailed Sig.)]	.085[b]

a. Grouping Variable: Technoc

b. Not corrected for ties.

Table 9.24: Mann Whitney U-test, comparing densities of tools per m^2 between Gravettian and Magdalenian assemblages

Ranks

	Technoc	N	Mean Rank	Sum of Ranks
AreaDensity	2	13	8.46	110.00
	6	4	10.75	43.00
	Total	17		

Table 9.25: Mann Whitney U-test, comparing densities of tools per m^2 between Gravettian and Azilian assemblages

Test Statistics[a]

	AreaDensity
Mann-Whitney U	19.000
Wilcoxon W	110.000
Z	-.793
Asymp. Sig. (2-tailed)	.428
Exact Sig. [2*(1-tailed Sig.)]	.477[b]

a. Grouping Variable: Technoc

b. Not corrected for ties.

Table 9.26: Mann Whitney U-test, comparing densities of tools per m^2 between Gravettian and Azilian assemblages

Ranks

	Technoc	N	Mean Rank	Sum of Ranks
AreaDensity	3	7	7.71	54.00
	4	8	8.25	66.00
	Total	15		

Table 9.27: Mann Whitney U-test, comparing densities of tools per m^2 between Soultrean and Badegoulian assemblages

Test Statistics[a]

	AreaDensity
Mann-Whitney U	26.000
Wilcoxon W	54.000
Z	-.231
Asymp. Sig. (2-tailed)	.817
Exact Sig. [2*(1-tailed Sig.)]	.867[b]

a. Grouping Variable: Technoc

b. Not corrected for ties.

Table 9.28: Mann Whitney U-test, comparing densities of tools per m^2 between Solutrean and Badegoulian assemblages

Ranks

	Technoc	N	Mean Rank	Sum of Ranks
AreaDensity	3	7	13.71	96.00
	5	25	17.28	432.00
	Total	32		

Table 9.29: Mann Whitney U-test, comparing densities of tools per m^2 between Soultrean and Magdalenian assemblages

Test Statistics[a]

	AreaDensity
Mann-Whitney U	68.000
Wilcoxon W	96.000
Z	-.889
Asymp. Sig. (2-tailed)	.374
Exact Sig. [2*(1-tailed Sig.)]	.395[b]

a. Grouping Variable: Technoc

b. Not corrected for ties.

Table 9.30: Mann Whitney U-test, comparing densities of tools per m^2 between Solutrean and Magdalenian assemblages

Ranks

	Technoc	N	Mean Rank	Sum of Ranks
AreaDensity	3	7	5.71	40.00
	6	4	6.50	26.00
	Total	11		

Table 9.31: Mann Whitney U-test, comparing densities of tools per m^2 between Soultrean and Azilian assemblages

Test Statistics[a]

	AreaDensity
Mann-Whitney U	12.000
Wilcoxon W	40.000
Z	-.378
Asymp. Sig. (2-tailed)	.705
Exact Sig. [2*(1-tailed Sig.)]	.788[b]

a. Grouping Variable: Technoc

b. Not corrected for ties.

Table 9.32: Mann Whitney U-test, comparing densities of tools per m^2 between Solutrean and Azilian assemblages

Ranks

	Technoc	N	Mean Rank	Sum of Ranks
AreaDensity	4	8	11.88	95.00
	5	25	18.64	466.00
	Total	33		

Table 9.33: Mann Whitney U-test, comparing densities of tools per m^2 between Badegoulian and Magdalenian assemblages

Test Statistics[a]

	AreaDensity
Mann-Whitney U	59.000
Wilcoxon W	95.000
Z	-1.722
Asymp. Sig. (2-tailed)	.085
Exact Sig. [2*(1-tailed Sig.)]	.089[b]

a. Grouping Variable: Technoc

b. Not corrected for ties.

Table 9.34: Mann Whitney U-test, comparing densities of tools per m^2 between Badegoulian and Magdalenian assemblages

Ranks

	Technoc	N	Mean Rank	Sum of Ranks
AreaDensity	4	8	6.75	54.00
	6	4	6.00	24.00
	Total	12		

Table 9.35: Mann Whitney U-test, comparing densities of tools per m^2 between Badegoulian and Azilian assemblages

Test Statistics[a]

	AreaDensity
Mann-Whitney U	14.000
Wilcoxon W	24.000
Z	-.340
Asymp. Sig. (2-tailed)	.734
Exact Sig. [2*(1-tailed Sig.)]	.808[b]

a. Grouping Variable: Technoc

b. Not corrected for ties.

Table 9.36: Mann Whitney U-test, comparing densities of tools per m^2 between Badegoulian and Azilian assemblages

Ranks

	Technoc	N	Mean Rank	Sum of Ranks
AreaDensity	5	25	16.28	407.00
	6	4	7.00	28.00
	Total	29		

Table 9.37: Mann Whitney U-test, comparing densities of tools per m^2 between Magdalenian and Azilian assemblages

Test Statistics[a]

	AreaDensity
Mann-Whitney U	18.000
Wilcoxon W	28.000
Z	-2.024
Asymp. Sig. (2-tailed)	.043
Exact Sig. [2*(1-tailed Sig.)]	.043[b]

a. Grouping Variable: Technoc

b. Not corrected for ties.

Table 9.38: Mann Whitney U-test, comparing densities of tools per m^2 between Magdalenian and Azilian assemblages

Mann Whitney tests on tool densities per m^2

Ranks

	Technoc	N	Mean Rank	Sum of Ranks
AreaTimeDensity	1	21	20.14	423.00
	2	13	13.23	172.00
	Total	34		

Table 9.39: Mann Whitney U-test, comparing densities of tools per m^3 between Aurignacian and Gravettian assemblages

Test Statistics[b]

	AreaTime Density
Mann-Whitney U	81.000
Wilcoxon W	172.000
Z	-1.967
Asymp. Sig. (2-tailed)	.049
Exact Sig. [2*(1-tailed Sig.)]	.050[a]

a. Not corrected for ties.

b. Grouping Variable: Technoc

Table 9.40: Mann Whitney U-test, comparing densities of tools per m^3 between Aurignacian and Gravettian assemblages

Ranks

	Technoc	N	Mean Rank	Sum of Ranks
AreaTimeDensity	1	21	13.67	287.00
	3	5	12.80	64.00
	Total	26		

Table 9.41: Mann Whitney U-test, comparing densities of tools per m^3 between Aurignacian and Solutrean assemblages

Test Statistics[b]

	AreaTime Density
Mann-Whitney U	49.000
Wilcoxon W	64.000
Z	-.228
Asymp. Sig. (2-tailed)	.820
Exact Sig. [2*(1-tailed Sig.)]	.850[a]

a. Not corrected for ties.

b. Grouping Variable: Technoc

Table 9.42: Mann Whitney U-test, comparing densities of tools per m^3 between Aurignacian and Solutrean assemblages

Ranks

	Technoc	N	Mean Rank	Sum of Ranks
AreaTimeDensity	1	21	13.81	290.00
	4	7	16.57	116.00
	Total	28		

Table 9.43: Mann Whitney U-test, comparing densities of tools per m^3 between Aurignacian and Badegoulian assemblages

Test Statistics[b]

	AreaTime Density
Mann-Whitney U	59.000
Wilcoxon W	290.000
Z	-.769
Asymp. Sig. (2-tailed)	.442
Exact Sig. [2*(1-tailed Sig.)]	.466[a]

a. Not corrected for ties.

b. Grouping Variable: Technoc

Table 9.44: Mann Whitney U-test, comparing densities of tools per m^3 between Aurignacian and Badegoulian assemblages

Ranks

	Technoc	N	Mean Rank	Sum of Ranks
AreaTimeDensity	1	21	24.33	511.00
	5	19	16.26	309.00
	Total	40		

Table 9.45: Mann Whitney U-test, comparing densities of tools per m^3 between Aurignacian and Magdalenian assemblages

Test Statistics[b]

	AreaTime Density
Mann-Whitney U	119.000
Wilcoxon W	309.000
Z	-2.182
Asymp. Sig. (2-tailed)	.029
Exact Sig. [2*(1-tailed Sig.)]	.029[a]

a. Not corrected for ties.

b. Grouping Variable: Technoc

Table 9.46: Mann Whitney U-test, comparing densities of tools per m^3 between Aurignacian and Magdalenian assemblages

Ranks

	Technoc	N	Mean Rank	Sum of Ranks
AreaTimeDensity	1	21	14.43	303.00
	6	4	5.50	22.00
	Total	25		

Table 9.47: Mann Whitney U-test, comparing densities of tools per m^3 between Aurignacian and Azilian assemblages

Test Statistics[b]

	AreaTime Density
Mann-Whitney U	12.000
Wilcoxon W	22.000
Z	-2.224
Asymp. Sig. (2-tailed)	.026
Exact Sig. [2*(1-tailed Sig.)]	.025[a]

a. Not corrected for ties.

b. Grouping Variable: Technoc

Table 9.48: Mann Whitney U-test, comparing densities of tools per m^3 between Aurignacian and Azilian assemblages

Ranks

	Technoc	N	Mean Rank	Sum of Ranks
AreaTimeDensity	2	13	8.54	111.00
	3	5	12.00	60.00
	Total	18		

Table 9.49: Mann Whitney U-test, comparing densities of tools per m^3 between Gravettian and Solutrean assemblages

Test Statistics[b]

	AreaTime Density
Mann-Whitney U	20.000
Wilcoxon W	111.000
Z	-1.232
Asymp. Sig. (2-tailed)	.218
Exact Sig. [2*(1-tailed Sig.)]	.246[a]

a. Not corrected for ties.

b. Grouping Variable: Technoc

Table 9.50: Mann Whitney U-test, comparing densities of tools per m^3 between Gravettian and Solutrean assemblages

Ranks

	Technoc	N	Mean Rank	Sum of Ranks
AreaTimeDensity	2	13	8.31	108.00
	4	7	14.57	102.00
	Total	20		

Table 9.51: Mann Whitney U-test, comparing densities of tools per m^3 between Gravettian and Badegoulian assemblages

Test Statistics[b]

	AreaTime Density
Mann-Whitney U	17.000
Wilcoxon W	108.000
Z	-2.258
Asymp. Sig. (2-tailed)	.024
Exact Sig. [2*(1-tailed Sig.)]	.024[a]

a. Not corrected for ties.

b. Grouping Variable: Technoc

Table 9.52: Mann Whitney U-test, comparing densities of tools per m^3 between Gravettian and Badegoulian assemblages

Ranks

	Technoc	N	Mean Rank	Sum of Ranks
AreaTimeDensity	2	13	17.15	223.00
	5	19	16.05	305.00
	Total	32		

Table 9.53: Mann Whitney U-test, comparing densities of tools per m^3 between Gravettian and Magdalenian assemblages

Test Statistics[b]

	AreaTime Density
Mann-Whitney U	115.000
Wilcoxon W	305.000
Z	-.326
Asymp. Sig. (2-tailed)	.744
Exact Sig. [2*(1-tailed Sig.)]	.762[a]

a. Not corrected for ties.

b. Grouping Variable: Technoc

Table 9.54: Mann Whitney U-test, comparing densities of tools per m^3 between Gravettian and Magdalenian assemblages

Ranks

	Technoc	N	Mean Rank	Sum of Ranks
AreaTimeDensity	2	13	9.73	126.50
	6	4	6.63	26.50
	Total	17		

Table 9.55: Mann Whitney U-test, comparing densities of tools per m^3 between Gravettian and Azilian assemblages

Test Statistics[b]

	AreaTime Density
Mann-Whitney U	16.500
Wilcoxon W	26.500
Z	-1.076
Asymp. Sig. (2-tailed)	.282
Exact Sig. [2*(1-tailed Sig.)]	.296[a]

a. Not corrected for ties.

b. Grouping Variable: Technoc

Table 9.56: Mann Whitney U-test, comparing densities of tools per m^3 between Gravettian and Azilian assemblages

Ranks

	Technoc	N	Mean Rank	Sum of Ranks
AreaTimeDensity	3	5	6.00	30.00
	4	7	6.86	48.00
	Total	12		

Table 9.57: Mann Whitney U-test, comparing densities of tools per m^3 between Solutrean and Badegoulian assemblages

Test Statistics[b]

	AreaTime Density
Mann-Whitney U	15.000
Wilcoxon W	30.000
Z	-.406
Asymp. Sig. (2-tailed)	.685
Exact Sig. [2*(1-tailed Sig.)]	.755[a]

a. Not corrected for ties.

b. Grouping Variable: Technoc

Table 9.58: Mann Whitney U-test, comparing densities of tools per m^3 between Solutrean and Badegoulian assemblages

Ranks

	Technoc	N	Mean Rank	Sum of Ranks
AreaTimeDensity	3	5	16.10	80.50
	5	19	11.55	219.50
	Total	24		

Table 9.59: Mann Whitney U-test, comparing densities of tools per m^3 between Solutrean and Magdalenian assemblages

Test Statistics[b]

	AreaTime Density
Mann-Whitney U	29.500
Wilcoxon W	219.500
Z	-1.281
Asymp. Sig. (2-tailed)	.200
Exact Sig. [2*(1-tailed Sig.)]	.208[a]

a. Not corrected for ties.

b. Grouping Variable: Technoc

Table 9.60: Mann Whitney U-test, comparing densities of tools per m^3 between Solutrean and Magdalenian assemblages

Ranks

	Technoc	N	Mean Rank	Sum of Ranks
AreaTimeDensity	3	5	6.20	31.00
	6	4	3.50	14.00
	Total	9		

Table 9.61: Mann Whitney U-test, comparing densities of tools per m^3 between Solutrean and Azilian assemblages

Test Statistics[b]

	AreaTime Density
Mann-Whitney U	4.000
Wilcoxon W	14.000
Z	-1.470
Asymp. Sig. (2-tailed)	.142
Exact Sig. [2*(1-tailed Sig.)]	.190[a]

a. Not corrected for ties.

b. Grouping Variable: Technoc

Table 9.62: Mann Whitney U-test, comparing densities of tools per m^3 between Solutrean and Azilian assemblages

Ranks

	Technoc	N	Mean Rank	Sum of Ranks
AreaTimeDensity	4	7	20.50	143.50
	5	19	10.92	207.50
	Total	26		

Table 9.63: Mann Whitney U-test, comparing densities of tools per m^3 between Badegoulian and Magdalenian assemblages

Test Statistics[b]

	AreaTime Density
Mann-Whitney U	17.500
Wilcoxon W	207.500
Z	-2.834
Asymp. Sig. (2-tailed)	.005
Exact Sig. [2*(1-tailed Sig.)]	.003[a]

a. Not corrected for ties.

b. Grouping Variable: Technoc

Table 9.64: Mann Whitney U-test, comparing densities of tools per m^3 between Badegoulian and Magdalenian assemblages

Ranks

	Technoc	N	Mean Rank	Sum of Ranks
AreaTimeDensity	4	7	7.86	55.00
	6	4	2.75	11.00
	Total	11		

Table 9.65: Mann Whitney U-test, comparing densities of tools per m^3 between Badegoulian and Azilian assemblages

Test Statistics[b]

	AreaTime Density
Mann-Whitney U	1.000
Wilcoxon W	11.000
Z	-2.457
Asymp. Sig. (2-tailed)	.014
Exact Sig. [2*(1-tailed Sig.)]	.012[a]

a. Not corrected for ties.

b. Grouping Variable: Technoc

Table 9.66: Mann Whitney U-test, comparing densities of tools per m^3 between Badegoulian and Azilian assemblages

Ranks

	Technoc	N	Mean Rank	Sum of Ranks
AreaTimeDensity	5	19	13.26	252.00
	6	4	6.00	24.00
	Total	23		

Table 9.67: Mann Whitney U-test, comparing densities of tools per m^3 between Magdalenian and Azilian assemblages

Test Statistics[b]

	AreaTime Density
Mann-Whitney U	14.000
Wilcoxon W	24.000
Z	-1.949
Asymp. Sig. (2-tailed)	.051
Exact Sig. [2*(1-tailed Sig.)]	.054[a]

a. Not corrected for ties.

b. Grouping Variable: Technoc

Table 9.68: Mann Whitney U-test, comparing densities of tools per m^3 between Magdalenian and Azilian assemblages

§ 9.5 Mann Whitney U-tests on Diversity Measures

The following Mann Whitney U-tests were performed to evaluate if there are statistically significant differences in diversity indices (richness and D) between different technocomplexes. Technocomplexes were evaluated in pairs.

Mann Whitney U-tests on Richness by Technocomplex

Ranks

	Technoc	N	Mean Rank	Sum of Ranks
ObsExRich	1.00	56	50.36	2820.00
	2.00	25	20.04	501.00
	Total	81		

Table 9.69: Mann Whitney U-test, comparing Observed-Expected richness values between Aurignacian and Gravettian assemblages

Test Statistics[a]

	ObsExRich
Mann-Whitney U	176.000
Wilcoxon W	501.000
Z	-5.357
Asymp. Sig. (2-tailed)	.000

a. Grouping Variable: Technoc

Table 9.70: Mann Whitney U-test, comparing Observed-Expected richness values between Aurignacian and Gravettian assemblages

Ranks

	Technoc	N	Mean Rank	Sum of Ranks
ObsExRich	1.00	56	37.75	2114.00
	3.00	18	36.72	661.00
	Total	74		

Table 9.71: Mann Whitney U-test, comparing Observed-Expected richness values between Aurignacian and Solutrean assemblages

Test Statistics[a]

	ObsExRich
Mann-Whitney U	490.000
Wilcoxon W	661.000
Z	-.176
Asymp. Sig. (2-tailed)	.860

a. Grouping Variable: Technoc

Table 9.72: Mann Whitney U-test, comparing Observed-Expected richness values between Aurignacian and Solutrean assemblages

Ranks

	Technoc	N	Mean Rank	Sum of Ranks
ObsExRich	1.00	56	31.96	1790.00
	4.00	9	39.44	355.00
	Total	65		

Table 9.73: Mann Whitney U-test, comparing Observed-Expected richness values between Aurignacian and Badegoulian assemblages

Test Statistics[a]

	ObsExRich
Mann-Whitney U	194.000
Wilcoxon W	1790.000
Z	-1.102
Asymp. Sig. (2-tailed)	.271

a. Grouping Variable: Technoc

Table 9.74: Mann Whitney U-test, comparing Observed-Expected richness values between Aurignacian and Badegoulian assemblages

Ranks

	Technoc	N	Mean Rank	Sum of Ranks
ObsExRich	1.00	56	58.04	3250.00
	5.00	60	58.93	3536.00
	Total	116		

Table 9.75: Mann Whitney U-test, comparing Observed-Expected richness values between Aurignacian and Magdalenian assemblages

Test Statistics[a]

	ObsExRich
Mann-Whitney U	1654.000
Wilcoxon W	3250.000
Z	-.144
Asymp. Sig. (2-tailed)	.886

a. Grouping Variable: Technoc

Table 9.76: Mann Whitney U-test, comparing Observed-Expected richness values between Aurignacian and Magdalenian assemblages

Ranks

	Technoc	N	Mean Rank	Sum of Ranks
ObsExRich	1.00	56	32.79	1836.00
	6.00	9	34.33	309.00
	Total	65		

Table 9.77: Mann Whitney U-test, comparing Observed-Expected richness values between Aurignacian and Azilian assemblages

Test Statistics[a]

	ObsExRich
Mann-Whitney U	240.000
Wilcoxon W	1836.000
Z	-.228
Asymp. Sig. (2-tailed)	.820

a. Grouping Variable: Technoc

Table 9.78: Mann Whitney U-test, comparing Observed-Expected richness values between Aurignacian and Azilian assemblages

Ranks

	Technoc	N	Mean Rank	Sum of Ranks
ObsExRich	2.00	25	16.40	410.00
	3.00	18	29.78	536.00
	Total	43		

Table 9.79: Mann Whitney U-test, comparing Observed-Expected richness values between Gravettian and Solutrean assemblages

Test Statistics[a]

	ObsExRich
Mann-Whitney U	85.000
Wilcoxon W	410.000
Z	-3.447
Asymp. Sig. (2-tailed)	.001

a. Grouping Variable: Technoc

Table 9.80: Mann Whitney U-test, comparing Observed-Expected richness values between Gravettian and Solutrean assemblages

Ranks

	Technoc	N	Mean Rank	Sum of Ranks
ObsExRich	2.00	25	13.88	347.00
	4.00	9	27.56	248.00
	Total	34		

Table 9.81: Mann Whitney U-test, comparing Observed-Expected richness values between Gravettian and Badegoulian assemblages

Test Statistics[a]

	ObsExRich
Mann-Whitney U	22.000
Wilcoxon W	347.000
Z	-3.533
Asymp. Sig. (2-tailed)	.000
Exact Sig. [2*(1-tailed Sig.)]	.000[b]

a. Grouping Variable: Technoc

b. Not corrected for ties.

Table 9.82: Mann Whitney U-test, comparing Observed-Expected richness values between Gravettian and Badegoulian assemblages

Ranks

	Technoc	N	Mean Rank	Sum of Ranks
ObsExRich	2.00	25	24.16	604.00
	5.00	60	50.85	3051.00
	Total	85		

Table 9.83: Mann Whitney U-test, comparing Observed-Expected richness values between Gravettian and Magdalenian assemblages

Test Statistics[a]

	ObsExRich
Mann-Whitney U	279.000
Wilcoxon W	604.000
Z	-4.543
Asymp. Sig. (2-tailed)	.000

a. Grouping Variable: Technoc

Table 9.84: Mann Whitney U-test, comparing Observed-Expected richness values between Gravettian and Magdalenian assemblages

Ranks

	Technoc	N	Mean Rank	Sum of Ranks
ObsExRich	2.00	25	14.40	360.00
	6.00	9	26.11	235.00
	Total	34		

Table 9.85: Mann Whitney U-test, comparing Observed-Expected richness values between Gravettian and Azilian assemblages

Test Statistics[a]

	ObsExRich
Mann-Whitney U	35.000
Wilcoxon W	360.000
Z	-3.025
Asymp. Sig. (2-tailed)	.002
Exact Sig. [2*(1-tailed Sig.)]	.002[b]

a. Grouping Variable: Technoc

b. Not corrected for ties.

Table 9.86: Mann Whitney U-test, comparing Observed-Expected richness values between Gravettian and Azilian assemblages

Ranks

	Technoc	N	Mean Rank	Sum of Ranks
ObsExRich	3.00	18	13.06	235.00
	4.00	9	15.89	143.00
	Total	27		

Table 9.87: Mann Whitney U-test, comparing Observed-Expected richness values between Solutrean and Badegoulian assemblages

Test Statistics[a]

	ObsExRich
Mann-Whitney U	64.000
Wilcoxon W	235.000
Z	-.874
Asymp. Sig. (2-tailed)	.382
Exact Sig. [2*(1-tailed Sig.)]	.403[b]

a. Grouping Variable: Technoc

b. Not corrected for ties.

Table 9.88: Mann Whitney U-test, comparing Observed-Expected richness values between Solutrean and Badegoulian assemblages

Ranks

	Technoc	N	Mean Rank	Sum of Ranks
ObsExRich	3.00	18	38.06	685.00
	5.00	60	39.93	2396.00
	Total	78		

Table 9.89: Mann Whitney U-test, comparing Observed-Expected richness values between Solutrean and Magdalenian assemblages

Test Statistics[a]

	ObsExRich
Mann-Whitney U	514.000
Wilcoxon W	685.000
Z	-.308
Asymp. Sig. (2-tailed)	.758

a. Grouping Variable: Technoc

Table 9.90: Mann Whitney U-test, comparing Observed-Expected richness values between Solutrean and Magdalenian assemblages

Ranks

	Technoc	N	Mean Rank	Sum of Ranks
ObsExRich	3.00	18	13.67	246.00
	6.00	9	14.67	132.00
	Total	27		

Table 9.91: Mann Whitney U-test, comparing Observed-Expected richness values between Solutrean and Azilian assemblages

Ranks

	Technoc	N	Mean Rank	Sum of Ranks
ObsExRich	3.00	18	13.67	246.00
	6.00	9	14.67	132.00
	Total	27		

Table 9.92: Mann Whitney U-test, comparing Observed-Expected richness values between Solutrean and Azilian assemblages

Ranks

	Technoc	N	Mean Rank	Sum of Ranks
ObsExRich	4.00	9	39.89	359.00
	5.00	60	34.27	2056.00
	Total	69		

Table 9.93: Mann Whitney U-test, comparing Observed-Expected richness values between Badegoulian and Magdalenian assemblages

Test Statistics[a]

	ObsExRich
Mann-Whitney U	226.000
Wilcoxon W	2056.000
Z	-.784
Asymp. Sig. (2-tailed)	.433

a. Grouping Variable: Technoc

Table 9.94: Mann Whitney U-test, comparing Observed-Expected richness values between Badegoulian and Magdalenian assemblages

Ranks

	Technoc	N	Mean Rank	Sum of Ranks
ObsExRich	4.00	9	10.11	91.00
	6.00	9	8.89	80.00
	Total	18		

Table 9.95: Mann Whitney U-test, comparing Observed-Expected richness values between Badegoulian and Azilian assemblages

Test Statistics[a]

	ObsExRich
Mann-Whitney U	35.000
Wilcoxon W	80.000
Z	-.486
Asymp. Sig. (2-tailed)	.627
Exact Sig. [2*(1-tailed Sig.)]	.666[b]

a. Grouping Variable: Technoc

b. Not corrected for ties.

Table 9.96: Mann Whitney U-test, comparing Observed-Expected richness values between Badegoulian and Azilian assemblages

Ranks

	Technoc	N	Mean Rank	Sum of Ranks
ObsExRich	5.00	60	34.95	2097.00
	6.00	9	35.33	318.00
	Total	69		

Table 9.97: Mann Whitney U-test, comparing Observed-Expected richness values between Magdalenian and Azilian assemblages

Test Statistics[a]

	ObsExRich
Mann-Whitney U	267.000
Wilcoxon W	2097.000
Z	-.053
Asymp. Sig. (2-tailed)	.957

a. Grouping Variable: Technoc

Table 9.98: Mann Whitney U-test, comparing Observed-Expected richness values between Magdalenian and Azilian assemblages

Mann Whitney U-tests comparing Observed-Expected D (heterogeneity values) by technocomplex

Ranks

	Technoc	N	Mean Rank	Sum of Ranks
ObsExD	1.00	56	49.89	2794.00
	2.00	25	21.08	527.00
	Total	81		

Table 9.99: Mann Whitney U-test, comparing Observed-Expected D (heterogeneity) values between Aurignacian and Gravettian assemblages

Test Statistics[a]

	ObsExD
Mann-Whitney U	202.000
Wilcoxon W	527.000
Z	-5.092
Asymp. Sig. (2-tailed)	.000

a. Grouping Variable: Technoc

Table 9.100: Mann Whitney U-test, comparing Observed-Expected D (heterogeneity) values between Aurignacian and Gravettian assemblages

Ranks

	Technoc	N	Mean Rank	Sum of Ranks
ObsExD	1.00	56	38.04	2130.00
	3.00	18	35.83	645.00
	Total	74		

Table 9.101: Mann Whitney U-test, comparing Observed-Expected D (heterogeneity) values between Aurignacian and Solutrean assemblages

Test Statistics[a]

	ObsExD
Mann-Whitney U	474.000
Wilcoxon W	645.000
Z	-.378
Asymp. Sig. (2-tailed)	.705

a. Grouping Variable: Technoc

Table 9.102: Mann Whitney U-test, comparing Observed-Expected D (heterogeneity) values between Aurignacian and Solutrean assemblages

Ranks

	Technoc	N	Mean Rank	Sum of Ranks
ObsExD	1.00	56	32.20	1803.00
	4.00	9	38.00	342.00
	Total	65		

Table 9.103: Mann Whitney U-test, comparing Observed-Expected D (heterogeneity) values between Aurignacian and Badegoulian assemblages

Test Statistics[a]

	ObsExD
Mann-Whitney U	207.000
Wilcoxon W	1803.000
Z	-.855
Asymp. Sig. (2-tailed)	.393

a. Grouping Variable: Technoc

Table 9.104: Mann Whitney U-test, comparing Observed-Expected D (heterogeneity) values between Aurignacian and Badegoulian assemblages

Ranks

	Technoc	N	Mean Rank	Sum of Ranks
ObsExD	1.00	56	44.43	2488.00
	5.00	60	71.63	4298.00
	Total	116		

Table 9.105: Mann Whitney U-test, comparing Observed-Expected D (heterogeneity) values between Aurignacian and Magdalenian assemblages

Test Statistics[a]

	ObsExD
Mann-Whitney U	892.000
Wilcoxon W	2488.000
Z	-4.354
Asymp. Sig. (2-tailed)	.000

a. Grouping Variable: Technoc

Table 9.106: Mann Whitney U-test, comparing Observed-Expected D (heterogeneity) values between Aurignacian and Magdalenian assemblages

Ranks

	Technoc	N	Mean Rank	Sum of Ranks
ObsExD	1.00	56	32.13	1799.00
	6.00	9	38.44	346.00
	Total	65		

Table 9.107: Mann Whitney U-test, comparing Observed-Expected D (heterogeneity) values between Aurignacian and Azilian assemblages

Test Statistics[a]

	ObsExD
Mann-Whitney U	203.000
Wilcoxon W	1799.000
Z	-.931
Asymp. Sig. (2-tailed)	.352

a. Grouping Variable: Technoc

Table 9.108: Mann Whitney U-test, comparing Observed-Expected D (heterogeneity) values between Aurignacian and Azilian assemblages

Ranks

	Technoc	N	Mean Rank	Sum of Ranks
ObsExD	2.00	25	16.84	421.00
	3.00	18	29.17	525.00
	Total	43		

Table 9.109: Mann Whitney U-test, comparing Observed-Expected D (heterogeneity) values between Gravettian and Solutrean assemblages

Test Statistics[a]

	ObsExD
Mann-Whitney U	96.000
Wilcoxon W	421.000
Z	-3.176
Asymp. Sig. (2-tailed)	.001

a. Grouping Variable: Technoc

Table 9.110: Mann Whitney U-test, comparing Observed-Expected D (heterogeneity) values between Gravettian and Solutrean assemblages

Ranks

	Technoc	N	Mean Rank	Sum of Ranks
ObsExD	2.00	25	14.28	357.00
	4.00	9	26.44	238.00
	Total	34		

Table 9.111: Mann Whitney U-test, comparing Observed-Expected D (heterogeneity) values between Gravettian and Badegoulian assemblages

Test Statistics[a]

	ObsExD
Mann-Whitney U	32.000
Wilcoxon W	357.000
Z	-3.142
Asymp. Sig. (2-tailed)	.002
Exact Sig. [2*(1-tailed Sig.)]	.001[b]

a. Grouping Variable: Technoc

b. Not corrected for ties.

Table 9.112: Mann Whitney U-test, comparing Observed-Expected D (heterogeneity) values between Gravettian and Badegoulian assemblages

Ranks

	Technoc	N	Mean Rank	Sum of Ranks
ObsExD	2.00	25	16.44	411.00
	5.00	60	54.07	3244.00
	Total	85		

Table 9.113: Mann Whitney U-test, comparing Observed-Expected D (heterogeneity) values between Gravettian and Magdalenian assemblages

Test Statistics[a]

	ObsExD
Mann-Whitney U	86.000
Wilcoxon W	411.000
Z	-6.404
Asymp. Sig. (2-tailed)	.000

a. Grouping Variable: Technoc

Table 9.114: Mann Whitney U-test, comparing Observed-Expected D (heterogeneity) values between Gravettian and Magdalenian assemblages

Ranks

	Technoc	N	Mean Rank	Sum of Ranks
ObsExD	2.00	25	13.88	347.00
	6.00	9	27.56	248.00
	Total	34		

Table 9.115: Mann Whitney U-test, comparing Observed-Expected D (heterogeneity) values between Gravettian and Azilian assemblages

Test Statistics[a]

	ObsExD
Mann-Whitney U	22.000
Wilcoxon W	347.000
Z	-3.533
Asymp. Sig. (2-tailed)	.000
Exact Sig. [2*(1-tailed Sig.)]	.000[b]

a. Grouping Variable: Technoc

b. Not corrected for ties.

Table 9.116: Mann Whitney U-test, comparing Observed-Expected D (heterogeneity) values between Gravettian and Azilian assemblages

Ranks

	Technoc	N	Mean Rank	Sum of Ranks
ObsExD	3.00	18	13.11	236.00
	4.00	9	15.78	142.00
	Total	27		

Table 9.117: Mann Whitney U-test, comparing Observed-Expected D (heterogeneity) values between Solutrean and Badegoulian assemblages

Test Statistics[a]

	ObsExD
Mann-Whitney U	65.000
Wilcoxon W	236.000
Z	-.823
Asymp. Sig. (2-tailed)	.411
Exact Sig. [2*(1-tailed Sig.)]	.433[b]

a. Grouping Variable: Technoc

b. Not corrected for ties.

Table 9.118: Mann Whitney U-test, comparing Observed-Expected D (heterogeneity) values between Solutrean and Badegoulian assemblages

Ranks

	Technoc	N	Mean Rank	Sum of Ranks
ObsExD	3.00	18	25.61	461.00
	5.00	60	43.67	2620.00
	Total	78		

Table 9.119: Mann Whitney U-test, comparing Observed-Expected D (heterogeneity) values between Solutrean and Magdalenian assemblages

Test Statistics[a]

	ObsExD
Mann-Whitney U	290.000
Wilcoxon W	461.000
Z	-2.965
Asymp. Sig. (2-tailed)	.003

a. Grouping Variable: Technoc

Table 9.120: Mann Whitney U-test, comparing Observed-Expected D (heterogeneity) values between Solutrean and Magdalenian assemblages

Ranks

	Technoc	N	Mean Rank	Sum of Ranks
ObsExD	3.00	18	12.83	231.00
	6.00	9	16.33	147.00
	Total	27		

Table 9.121: Mann Whitney U-test, comparing Observed-Expected D (heterogeneity) values between Solutrean and Azilian assemblages

Test Statistics[a]

	ObsExD
Mann-Whitney U	60.000
Wilcoxon W	231.000
Z	-1.080
Asymp. Sig. (2-tailed)	.280
Exact Sig. [2*(1-tailed Sig.)]	.298[b]

a. Grouping Variable: Technoc

b. Not corrected for ties.

Table 9.122: Mann Whitney U-test, comparing Observed-Expected D (heterogeneity) values between Solutrean and Azilian assemblages

Ranks

	Technoc	N	Mean Rank	Sum of Ranks
ObsExD	4.00	9	26.67	240.00
	5.00	60	36.25	2175.00
	Total	69		

Table 9.123: Mann Whitney U-test, comparing Observed-Expected D (heterogeneity) values between Badegoulian and Magdalenian assemblages

Test Statistics[a]

	ObsExD
Mann-Whitney U	195.000
Wilcoxon W	240.000
Z	-1.336
Asymp. Sig. (2-tailed)	.181

a. Grouping Variable: Technoc

Table 9.124: Mann Whitney U-test, comparing Observed-Expected D (heterogeneity) values between Badegoulian and Magdalenian assemblages

Ranks

	Technoc	N	Mean Rank	Sum of Ranks
ObsExD	4.00	9	9.44	85.00
	6.00	9	9.56	86.00
	Total	18		

Table 9.125: Mann Whitney U-test, comparing Observed-Expected D (heterogeneity) values between Badegoulian and Azilian assemblages

Test Statistics[a]

	ObsExD
Mann-Whitney U	40.000
Wilcoxon W	85.000
Z	-.044
Asymp. Sig. (2-tailed)	.965
Exact Sig. [2*(1-tailed Sig.)]	1.000[b]

a. Grouping Variable: Technoc

b. Not corrected for ties.

Table 9.126: Mann Whitney U-test, comparing Observed-Expected D (heterogeneity) values between Badegoulian and Azilian assemblages

Ranks

	Technoc	N	Mean Rank	Sum of Ranks
ObsExD	5.00	60	36.43	2186.00
	6.00	9	25.44	229.00
	Total	69		

Table 9.127: Mann Whitney U-test, comparing Observed-Expected D (heterogeneity) values between Magdalenian and Azilian assemblages

Test Statistics[a]

	ObsExD
Mann-Whitney U	184.000
Wilcoxon W	229.000
Z	-1.532
Asymp. Sig. (2-tailed)	.125

a. Grouping Variable: Technoc

Table 9.128: Mann Whitney U-test, comparing Observed-Expected D (heterogeneity) values between Magdalenian and Azilian assemblages

Chapter 10

Appendix D

§ 10.1 A Gazeteer of Sites used in this Thesis

This section will provide a brief overview of the main sites used in this study and, where possible, the chronological models built from the available radiocarbon dates in the manner described in Chapter Three, using uniform priors for outlier analysis. Radiocarbon dates are available for a multitude of sites in the region, however not all were suitable for Bayesian modelling; subsequently models are shown only for sites for which models could be built.

10.1.1 Abri Pataud

This classic site is well-documented due to careful excavation by Hallam Movius between 1958 and 1964 (Bricker et al., 1995). A thorough study of the sediments was undertaken by William Farrand (Farrand, 1995). The availability of information, together with the lengthy stratigraphy, makes the site ideal for studying the density of occupation.

The site features a good sequence of Aurignacian, Gravettian, Protomagdalenian and Solutrean and the stratigraphy is illustrated in the following table.

The Abri Pataud is one of the most well dated Palaeolithic sites in France and a

Table 10.1: Stratigraphy of the Abri Pataud

Level	Technocomplex
1	Solutrean
2	Protomagdalenian
3	Périgordian VI
4	Noaillian
5	Middle Périgordian
6	Evolved Aurignacian
7	Intermediate Aurignacian
8	Intermediate Aurignacian
9	Intermediate Aurignacian
10	Intermediate Aurignacian
11	Old Aurignacian
12	Basal Aurignacian
13	Basal Aurignacian
14	Basal Aurignacian

multitude of dates were available for this study. The chronological models created for the site are shown below. Due to the enormous number of dates available for the site, it was necessary to build several models for diffrerent sections of the stratigraphy.

The radiocarbon dates from Abri Pataud levels 5 and 6 could not be modelled, as there was a high level of overlap in dates from both of these levels. This suggests that there may be a degree of mixing between these levels and indeed a 'clearing incident' was observed by the excavators, who commented that the Gravettians occupying Level 5 appeared to have cut into the Aurignacian level beneath it (Bricker et al., 1995).

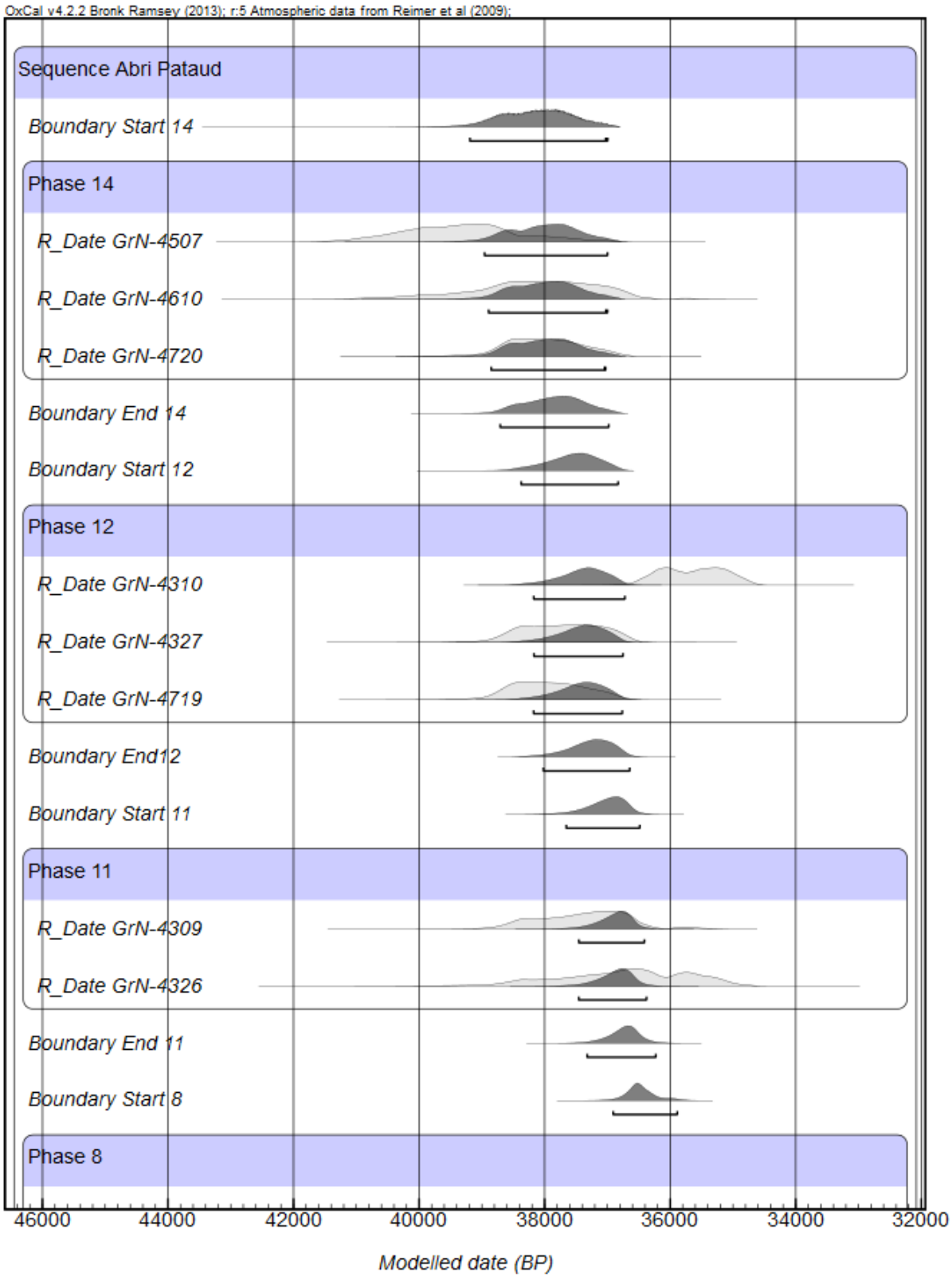

Figure 10.1: Abri Pataud Levels 14 to 8

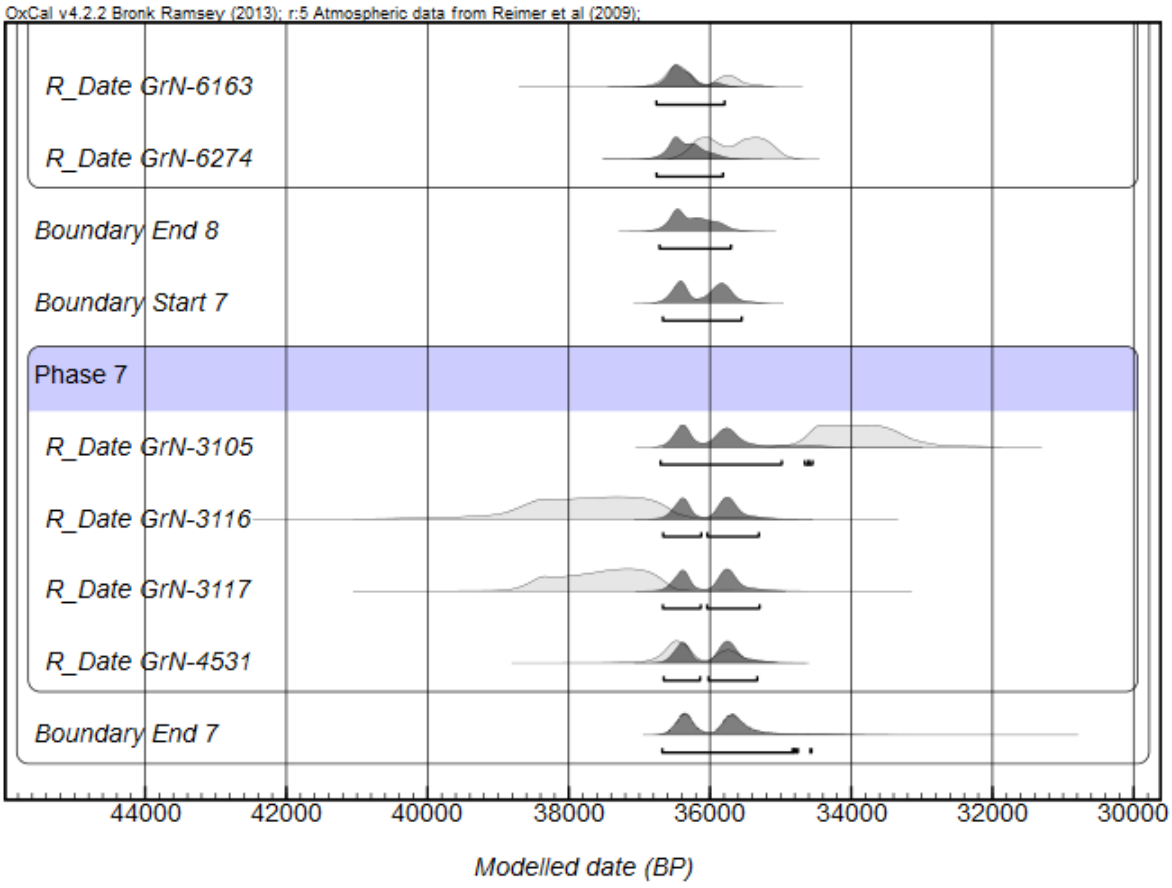

Figure 10.2: Abri Pataud Levels 8 to 7

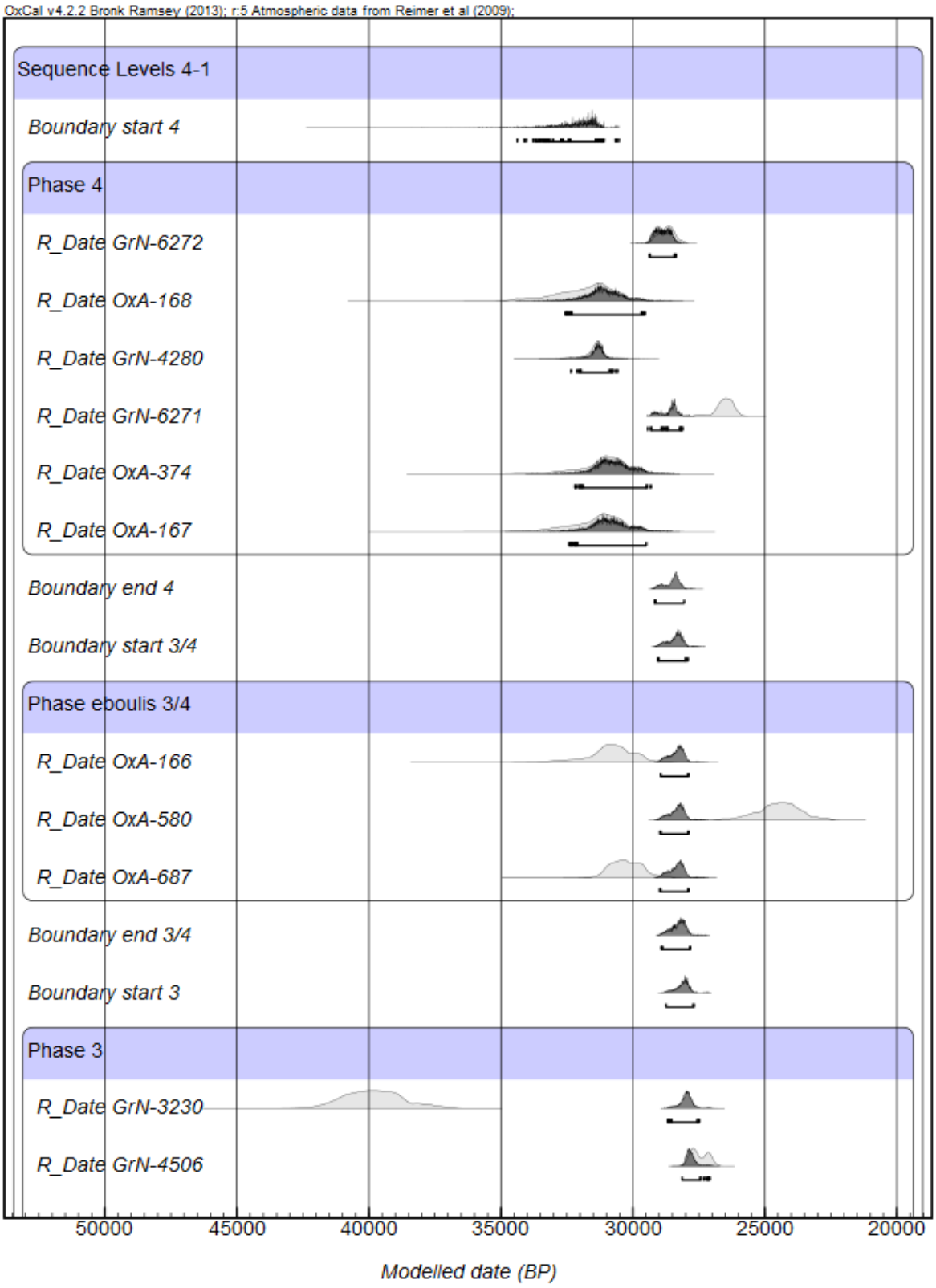

Figure 10.3: Abri Pataud Levels 4 to 3

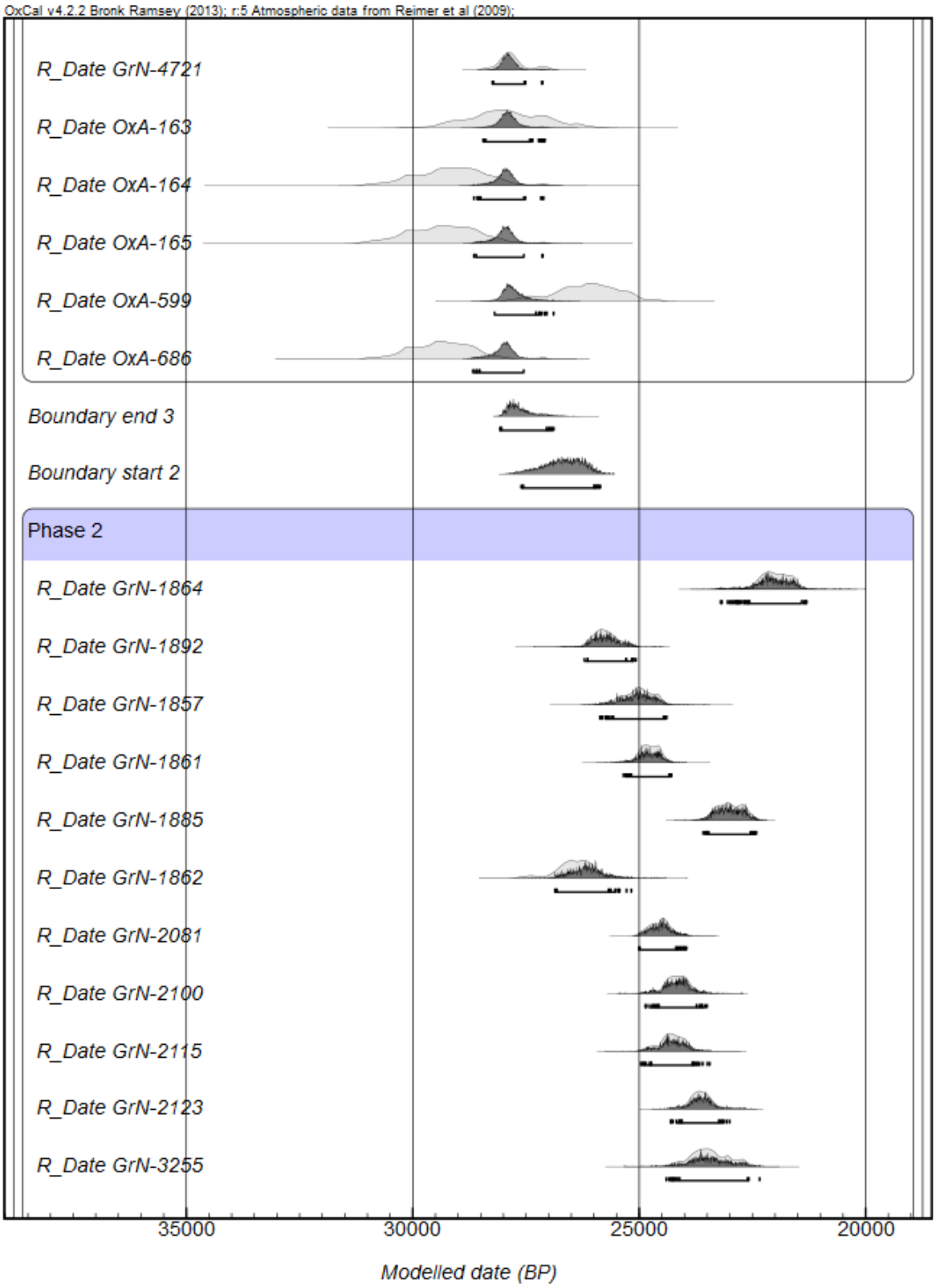

Figure 10.4: Abri Pataud Levels 3 to 2

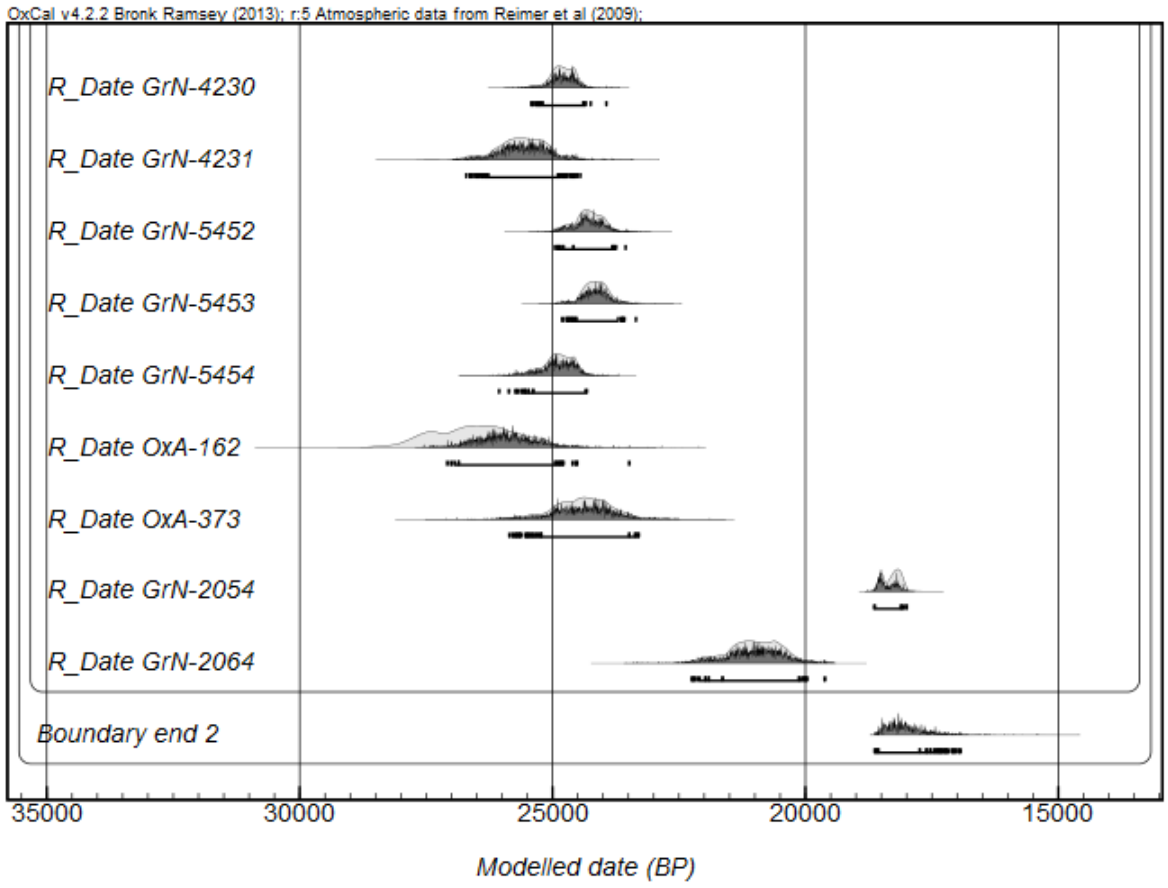

Figure 10.5: Abri Pataud Level 2

10.1.2 Combe Saunière

Located in the Isle Valley, this site features a long sequence of occupation which was described by Geneste and Plisson in the following manner (Plisson and Geneste, 1986):

Table 10.2: Stratigraphy of Combe Saunière

Level	Technocomplex
0	Humus
I	Medieval
II	Sterile
IIIa	Bronze Age
IIIb	Sterile
IIIc	Upper Palaeolithic
IIIe	Indeterminate Industry
IVa	Solutrean
IVb	Solutrean
IVc	Noaillian
V	Noaillian

Due to the large number of dates available for the site, a Bayesian model could be built and the results are shown below.

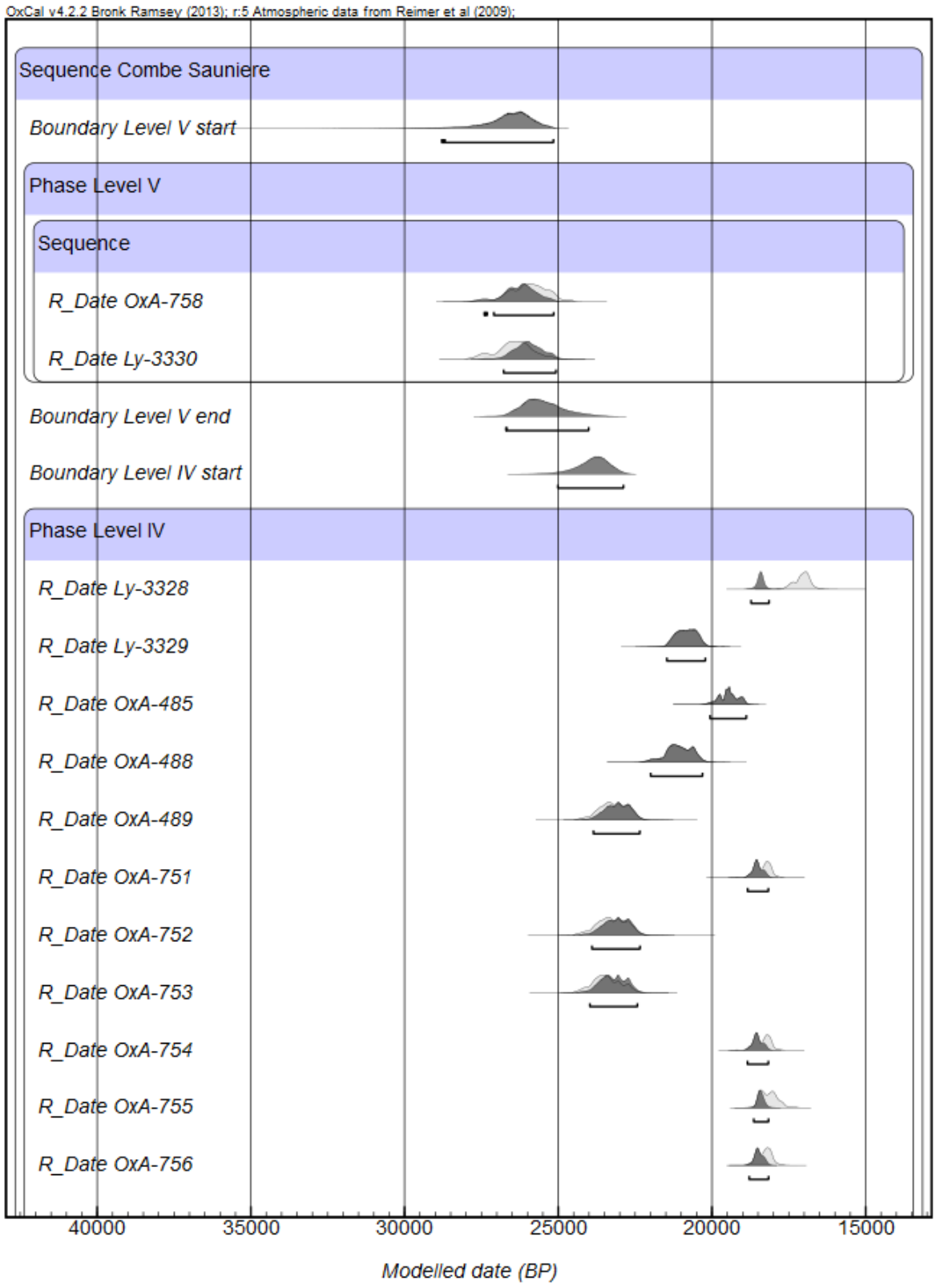

Figure 10.6: Modelled dates from Combe Saunière

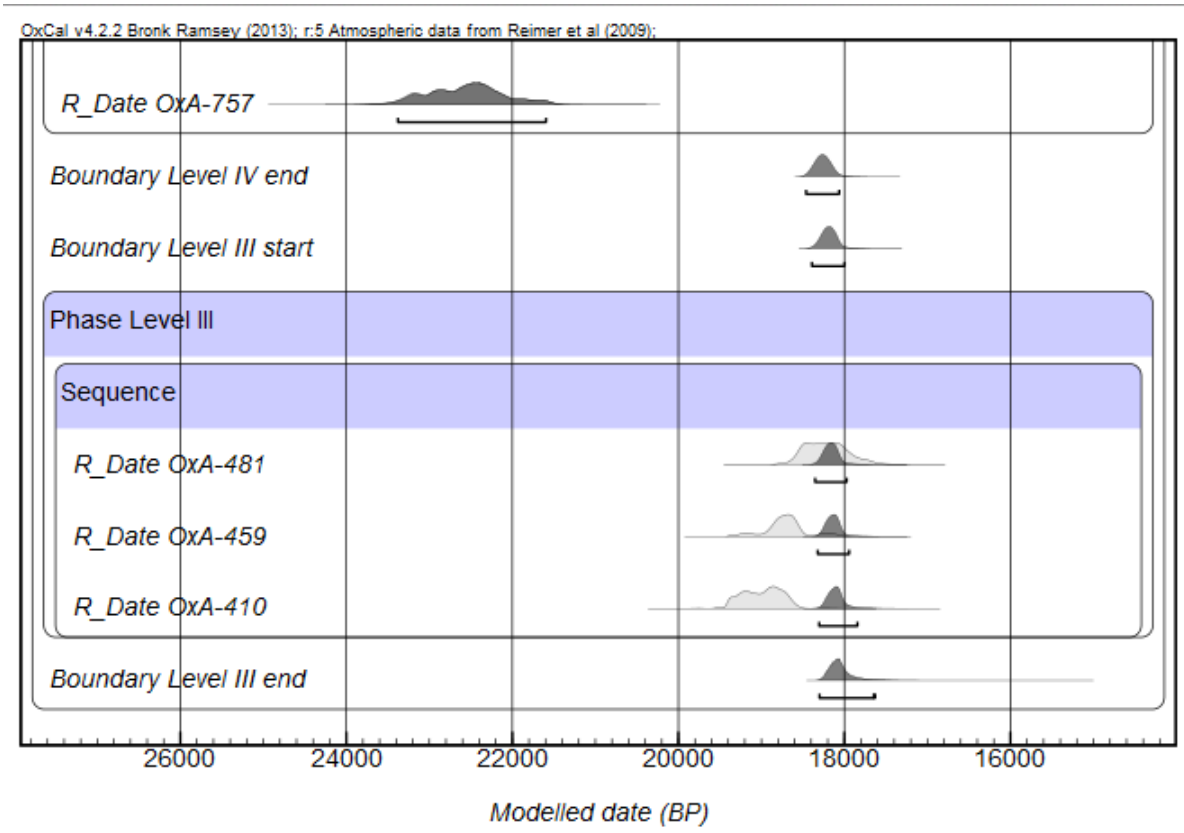

Figure 10.7: Modelled dates from Combe Saunière

10.1.3 Cuzoul de Vers

Excavated by Giraud (Clottes and Giraud, 1996) and (Clottes and Giraud, 1989), this site features a long sequence encompassing Solutrean and Badegoulian, as well as scores of hearths, including a great many stone basins. At the base of the sequence are the Upper Solutrean levels with shouldered points, 31 to 28. The rest of the sequence is Badegoulian (Castel, 2003). The low agreement indices of some dates in the Bayesian model suggests that there is a degree of mixing between levels, although Castel (Castel, 2003) reports that the levels are not disturbed.

10.1.4 La Doue

This site in Corrèze features Final Magdalenian, Sauvettarian, Mesolithic and Neolithic levels. The Magdalenian level revealed 80 tools and three cores, as well as some fragments of osseuse artefacts (Mazière, 1984).

10.1.5 Le Facteur

Aurignacian and Gravettian site first excavated by Peyrony and then Delporte in the 1960s, the stratigraphy encountered by both researchers appears to be markedly different. All radiocarbon dates used to inform the Bayesian model were provenanced from the Delporte excavation.

10.1.6 Faurélie II

This site, excavated in the 1960s by Tixier features several Upper Magdalenian levels, as well as an Azilian level (Bordes, 1970). Six radiocarbon dates were available across two levels and therefore a model could be produced.

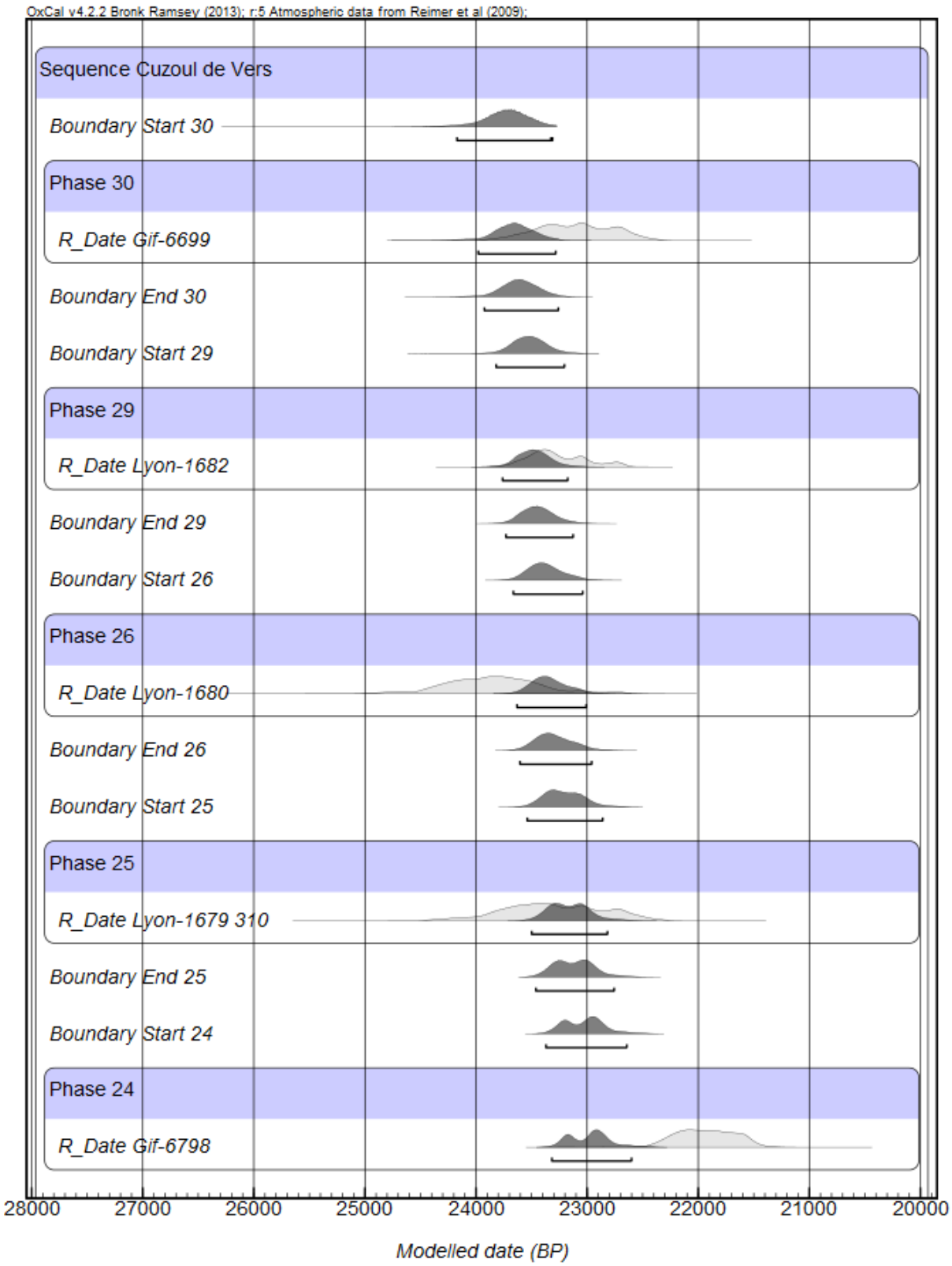

Figure 10.8: Cuzoul de Vers modelled dates

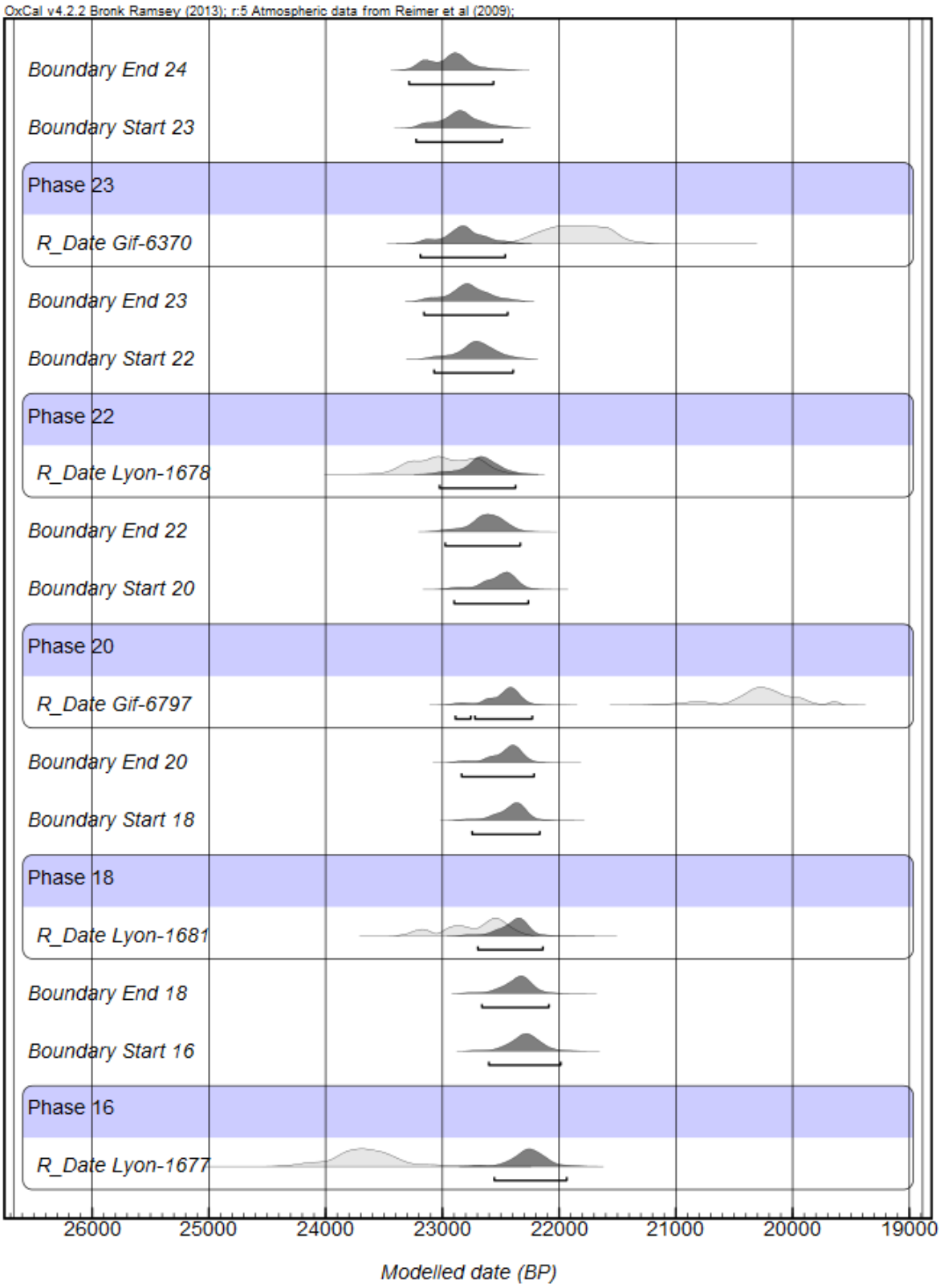

Figure 10.9: Cuzoul de Vers modelled dates

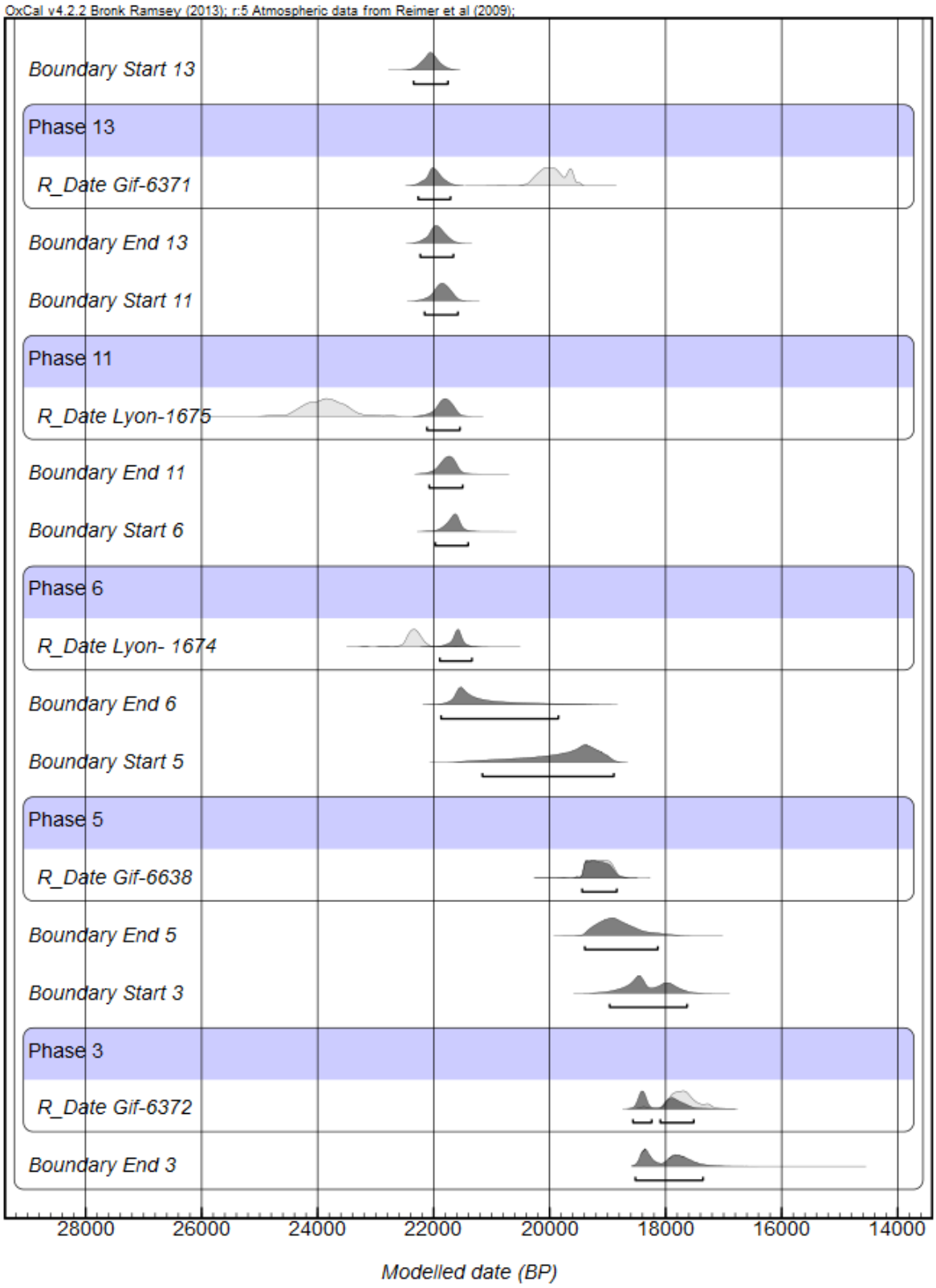

Figure 10.10: Cuzoul de Vers modelled dates

10.1.7 La Ferrassie

One of the most celebrated sites of the Dordogne, La Ferrassie was excavated by Capitan and Peyrony in the early 20th Century and by Delporte in the 1980s (Delporte, 1984). The Delporte excavations revealed a sequence of Aurignacian dates and all available radiocarbon dates originate from these campaigns. Radiocarbon dates with standard deviations over 1000 had to be removed before the model could run. The poor agreement indices of many dates in the upper levels suggests that there is a degree of mixing between these levels. However, for the lower levels, the model suggests stratigraphic integrity.

10.1.8 Flageolet I

Rigaud's 1960s excavations at this site revealed a sequence of Aurignacian and Gravettian industries (Rigaud, 1969). A number of radiocarbon dates have been produced for the site and thus it was possible to produce a Bayesian model.

10.1.9 Flageolet II

This Magdalenian sister site to Flageolet I was excavated by Rigaud from 1966-1967, revealing a sequence of 12 layers (Koetje, 1991). Four radiocarbon dates from two levels at the site are available and are described as 'internally consistent' (Koetje, 1991).

10.1.10 Gandil

This Magdalenian abri is flanked by the sites of Lafaye and Montastruc and has been subject to a programme of excavations by Ladier since the 1980s (Texier, 1997). A good sequence of radiocarbon dates has been published.

10.1.11 Gare de Couze

Magdalenian site excavated by Peyrony, Fitte and then Bordes (Fitte and Sonneville-Bordes, 1962). The site has produced a number of radiocarbon dates, all from samples provenanced from the Bordes excavation.

10.1.12 Grotte XVI

Cave site containing Mousterian and Magdalenian deposits. The Magdalenian deposits are found in a gallery at the back of the cave (Hays, 1998).

10.1.13 Jamblancs

Also known as Jean Blancs and Champs Blancs, this site was excavated on numerous occassions in the 19th Century, but the more recent campaigns by Cleyet-Merle revealed a sequence of Upper Solutrean to Magdalenian III. There are two main sections of the site, the slope deposit and the deposits under the abri (Cretin, 1996). The stratigraphy of both zones appeared sufficiently similar that a single Oxcal model could be built.

10.1.14 Chez Jugie

Also known as Le Bessol, this is predominantly an Azilian and Mesolithic site. The site is divided into high and low areas and was excavated in 1975/76 (Mazière and Raynal, 1977). A number of dates from three levels are available from this site.

10.1.15 Laugerie Haute Est

Occupied continuously from the Gravettian to the Late Magdalenian, this abri site was excavated by Peyrony who observed the following stratigraphy.

Table 10.3: Stratigraphy of Laugerie Haute Est. From Peyrony and Peyrony (1938)

Level	Technocomplex
B	Gravettian
B'	Gravettian
F	Protomagdalenian
H	Lower Solutrean
H'	Middle Solutrean
H"	Upper Solutrean
I	Abrupt retouch
I"	Magdalenian I
I""	Magdalenian II
J	Magdalenian III
K	Magdalenian V

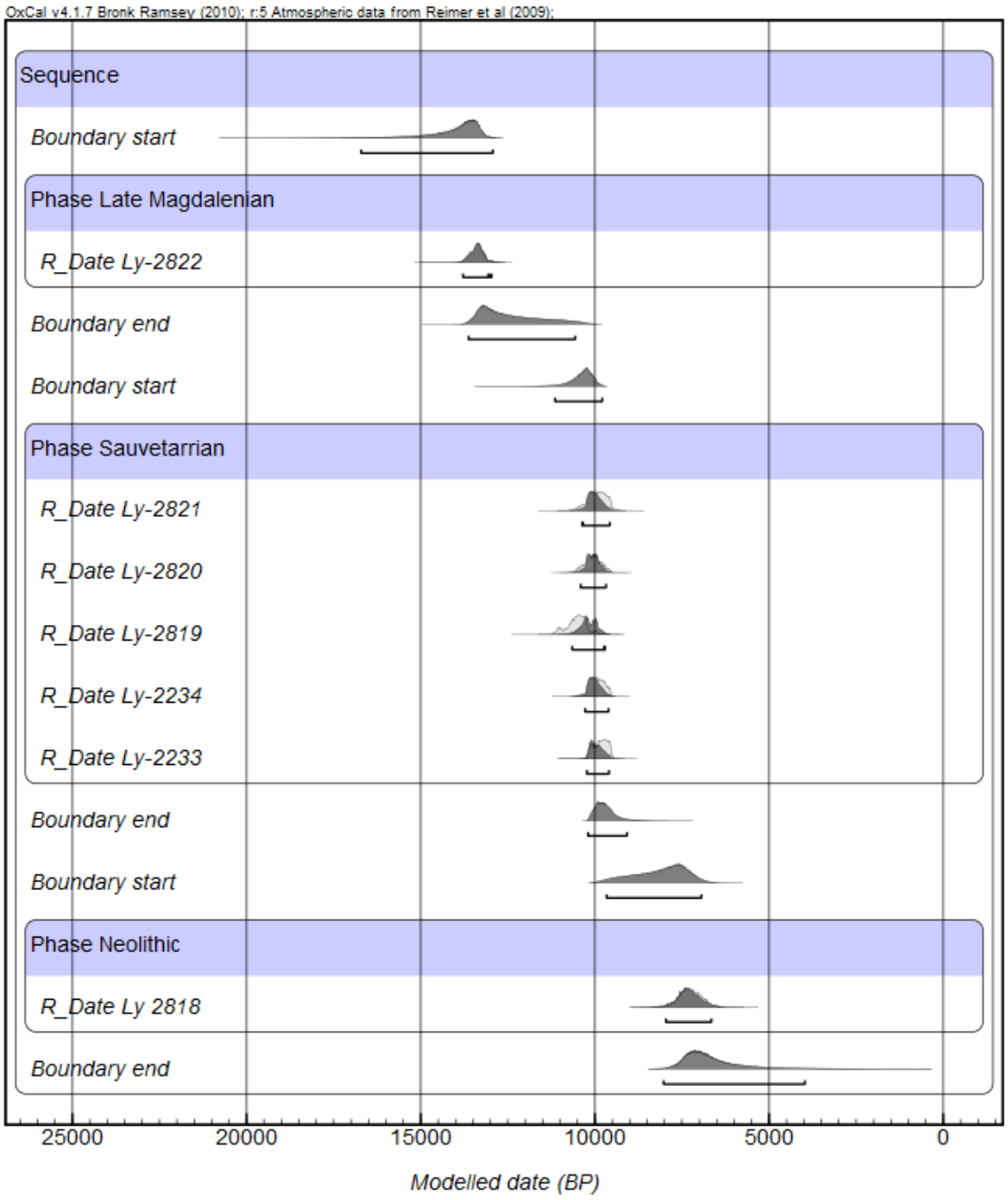

Figure 10.11: La Doue modelled dates

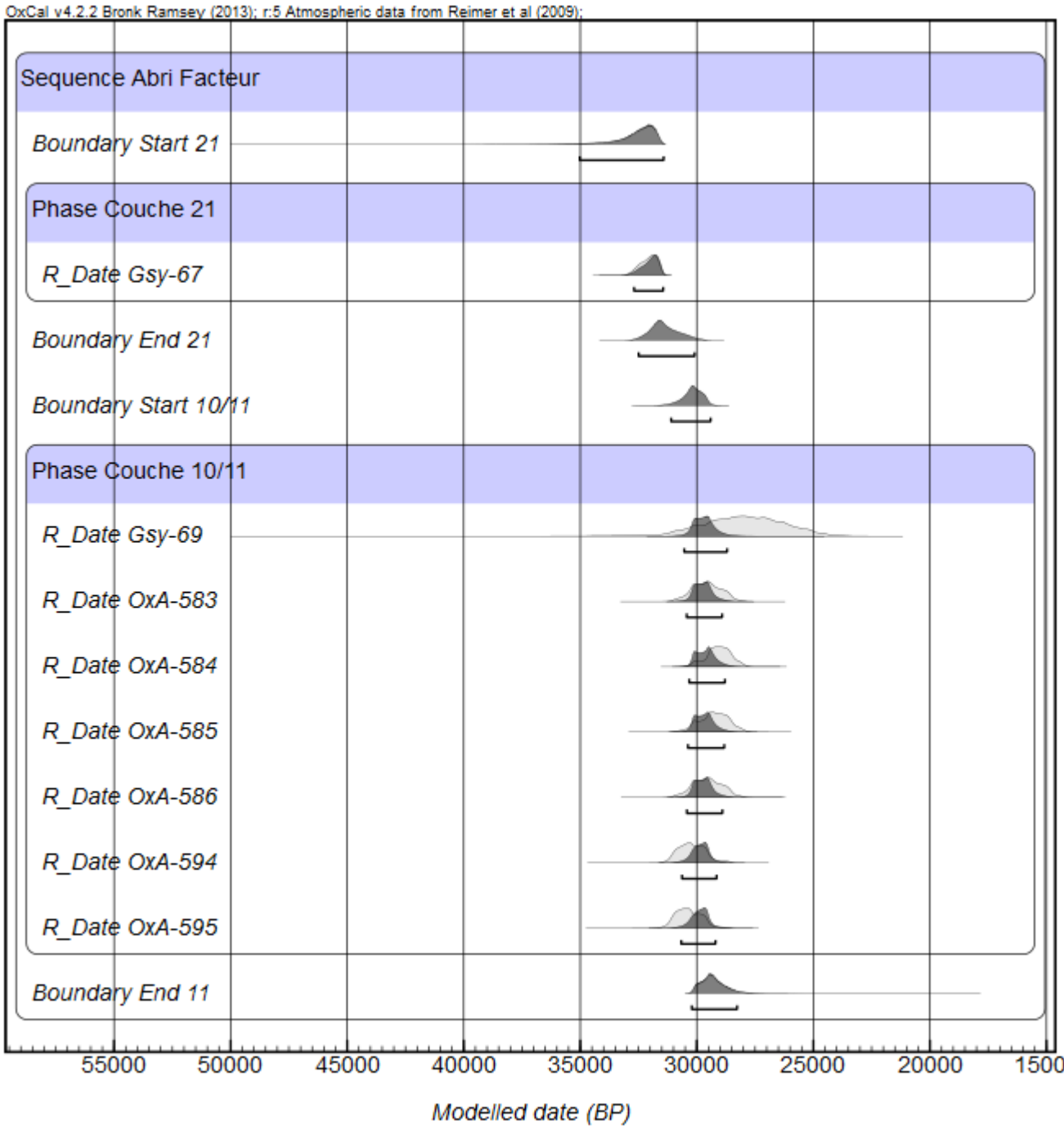

Figure 10.12: Le Facteur modelled dates

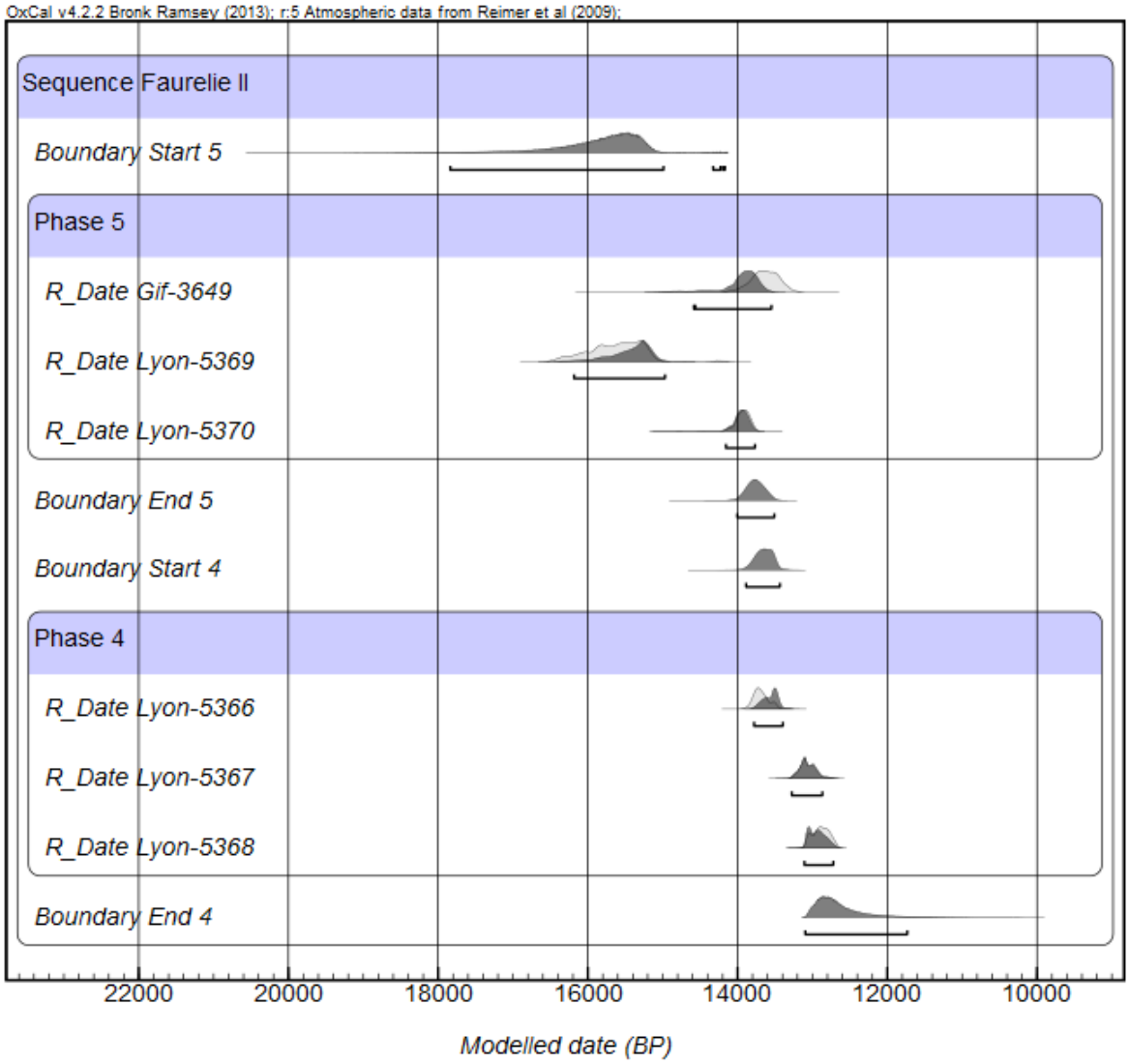

Figure 10.13: Faurelie II modelled dates

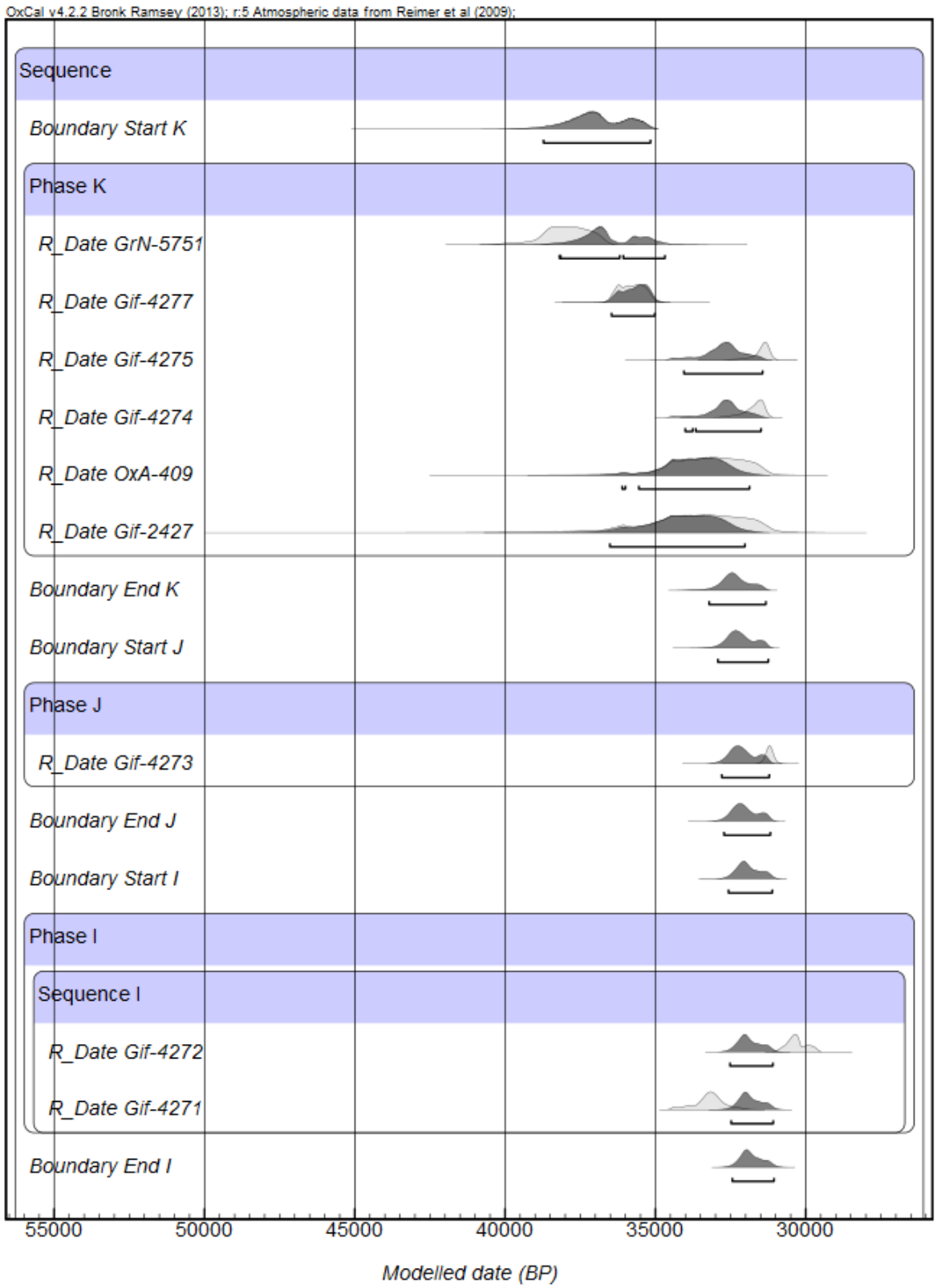

Figure 10.14: La Ferrassie modelled dates

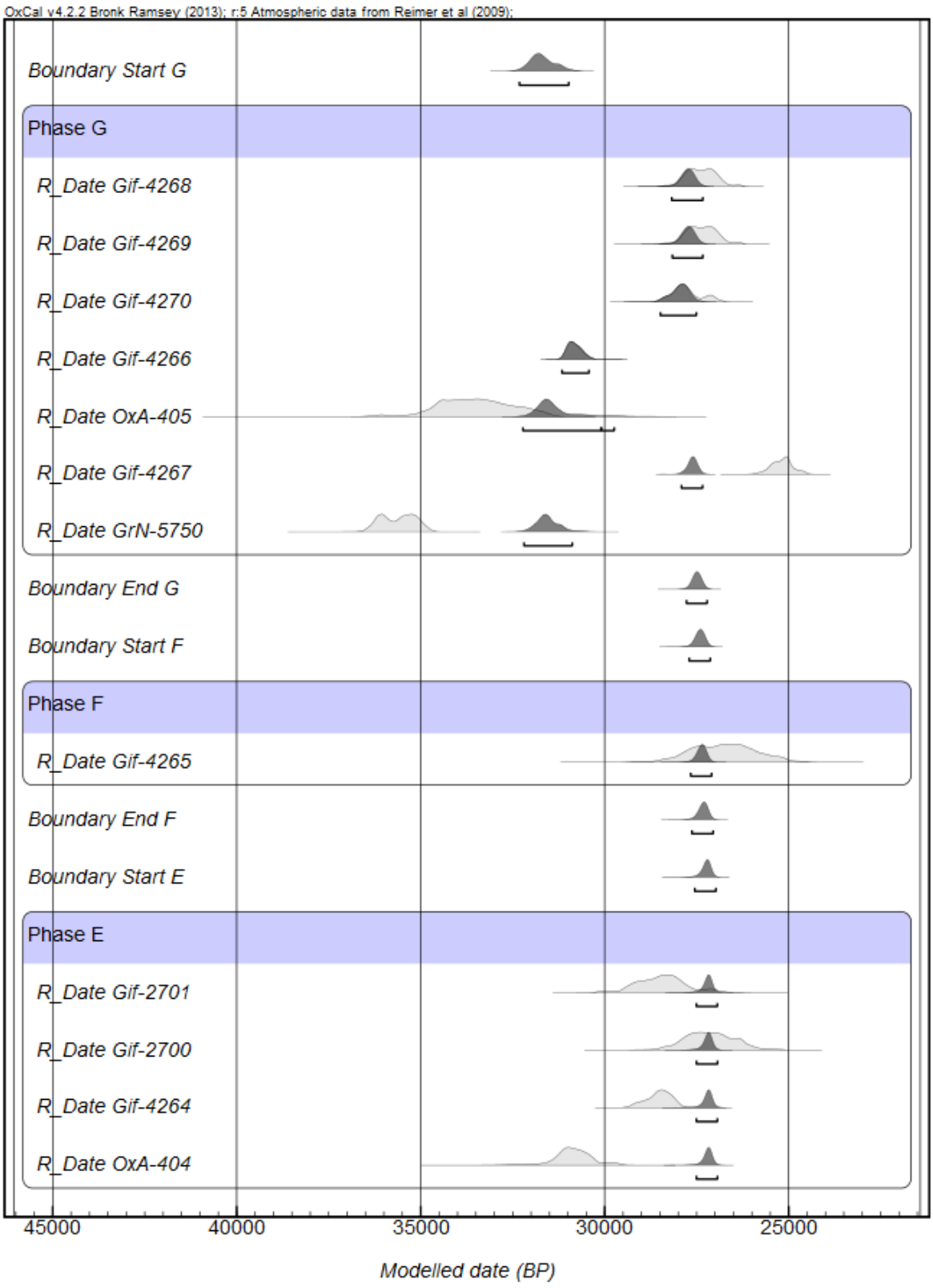

Figure 10.15: La Ferrassie modelled dates

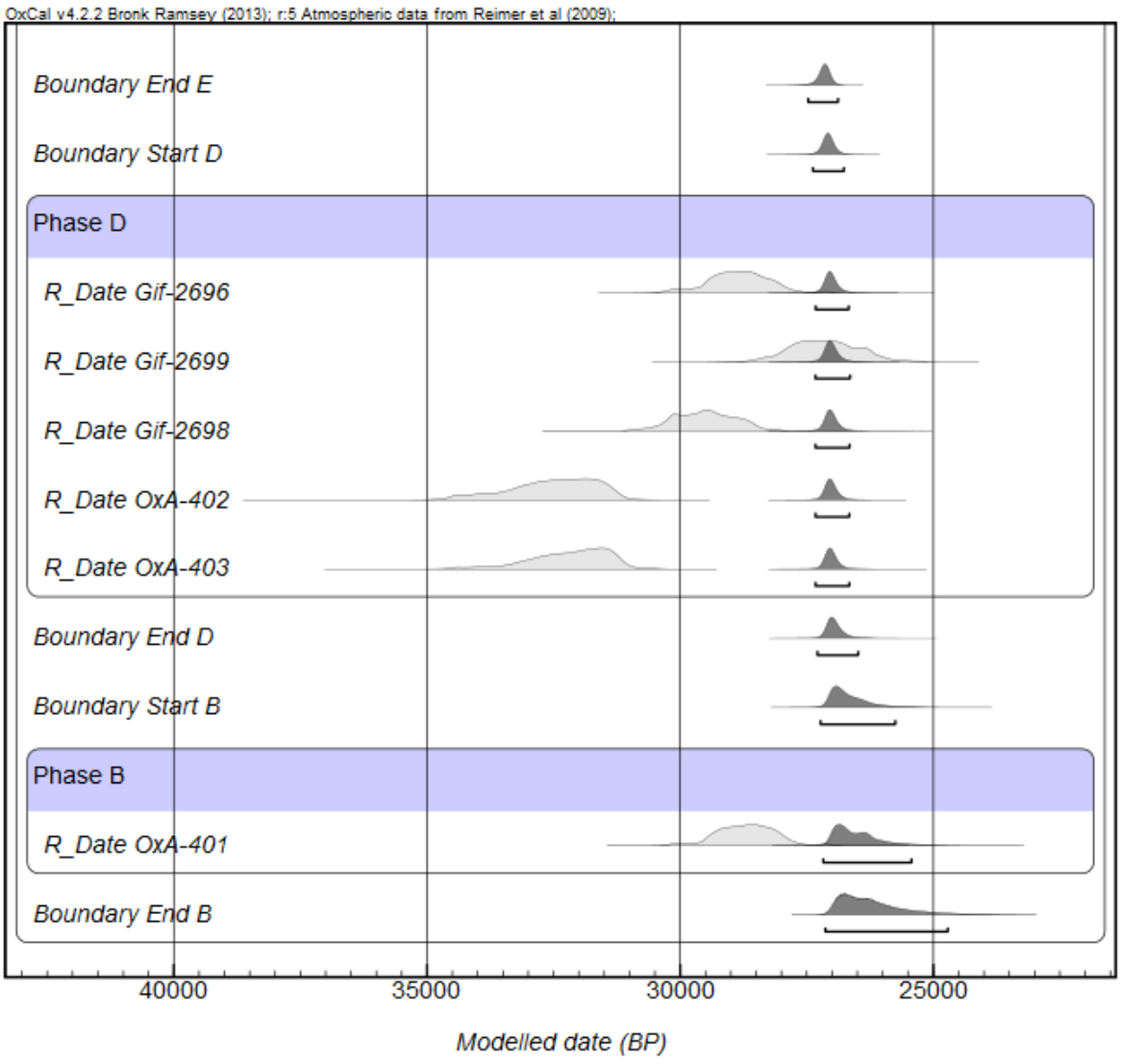

Figure 10.16: La Ferrassie modelled dates

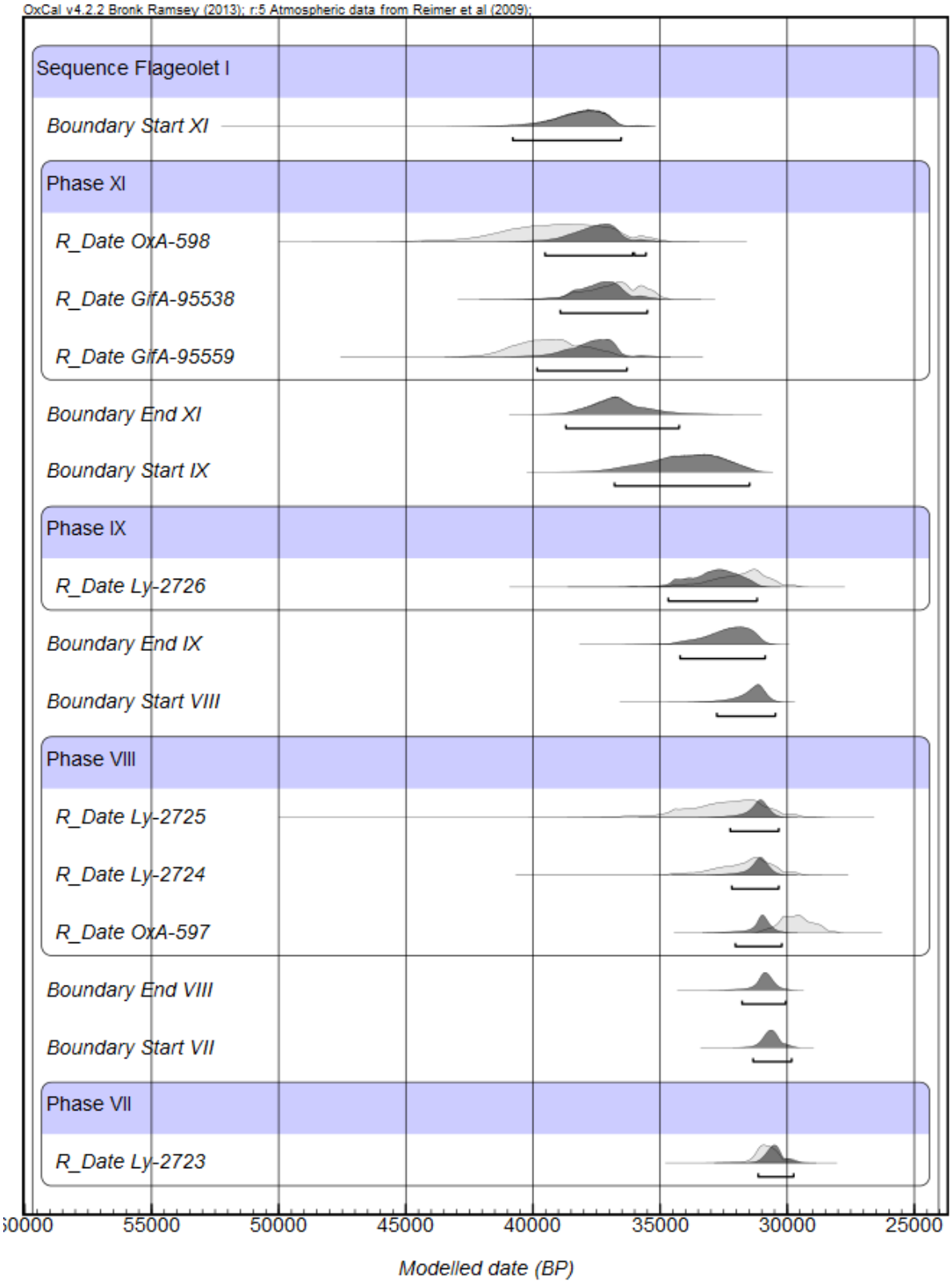

Figure 10.17: Flageolet I modelled radiocarbon dates

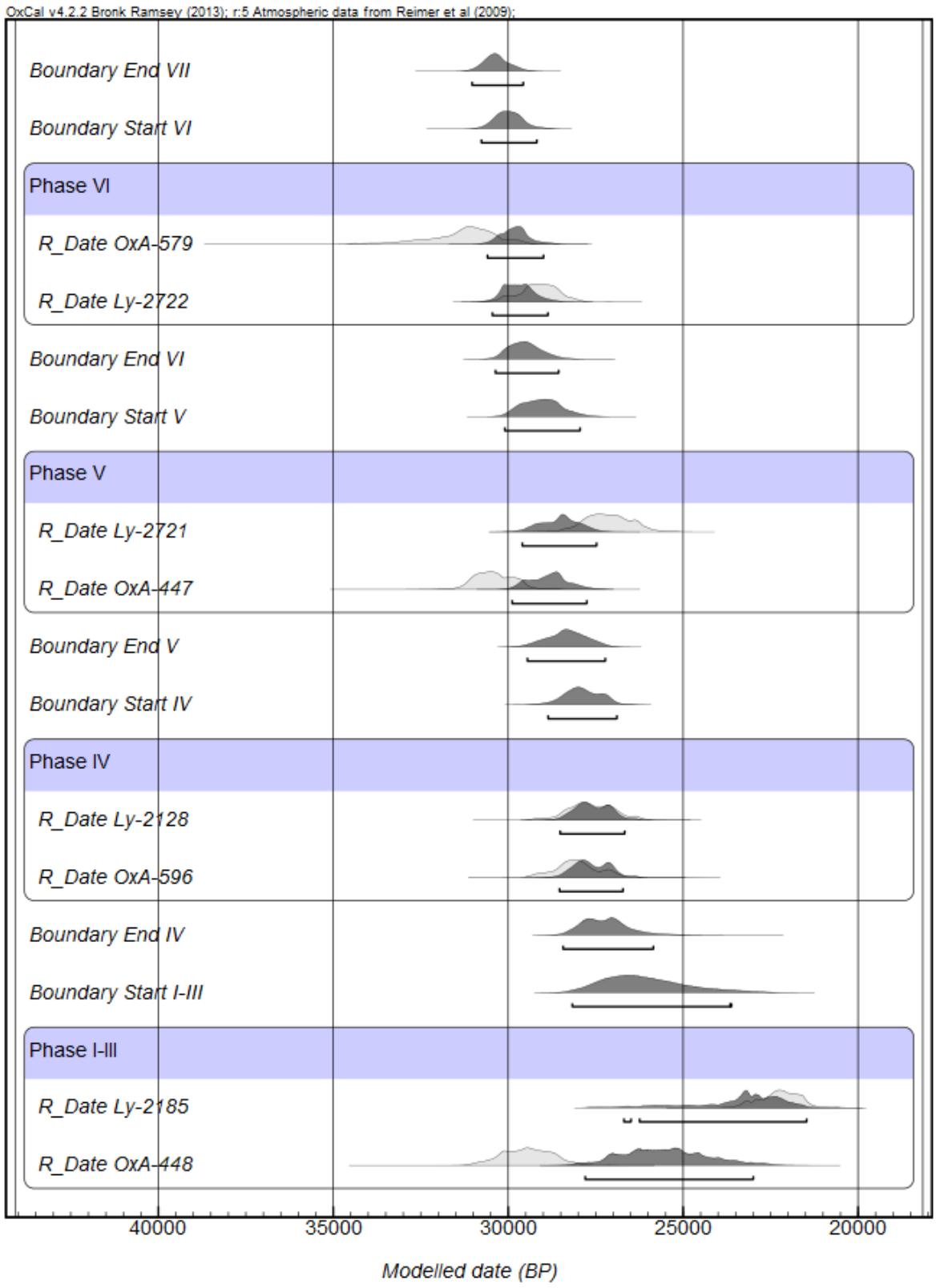

Figure 10.18: Flageolet I modelled radiocarbon dates

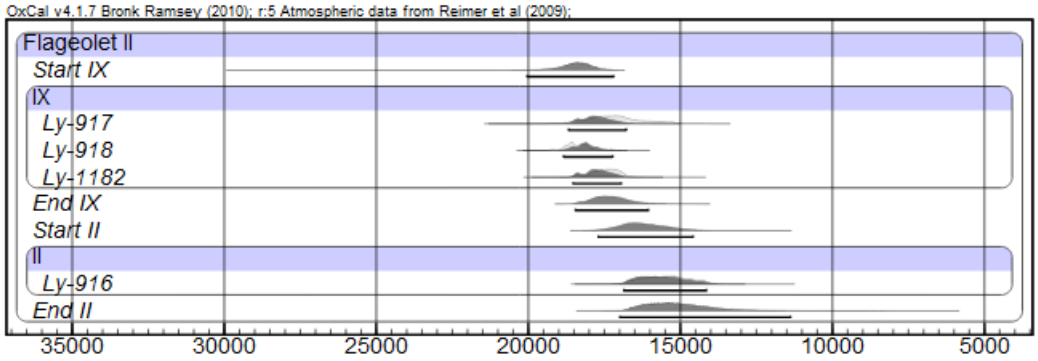

Figure 10.19: Flageolet II modelled radiocarbon dates

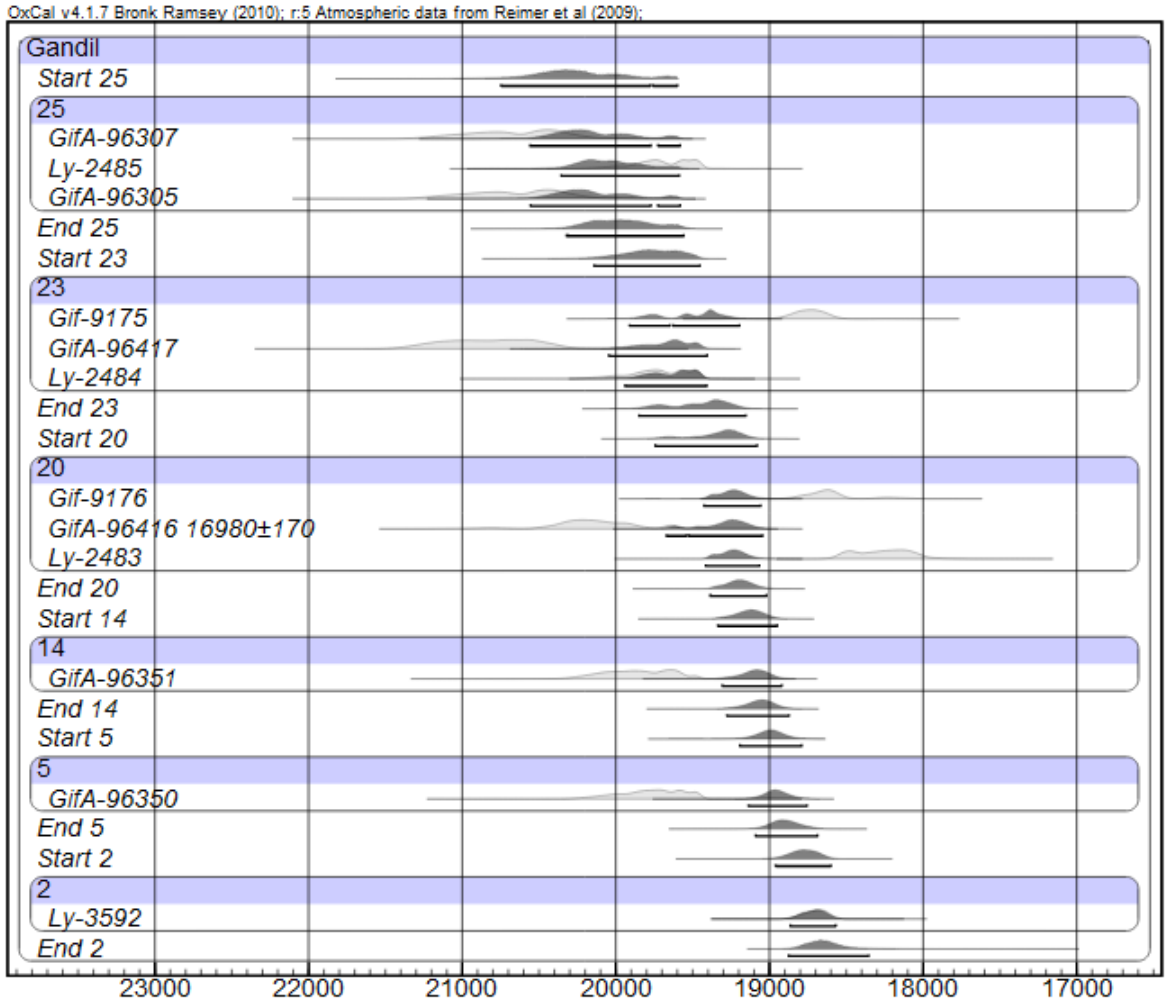

Figure 10.20: Abri Gandil modelled radiocarbon dates

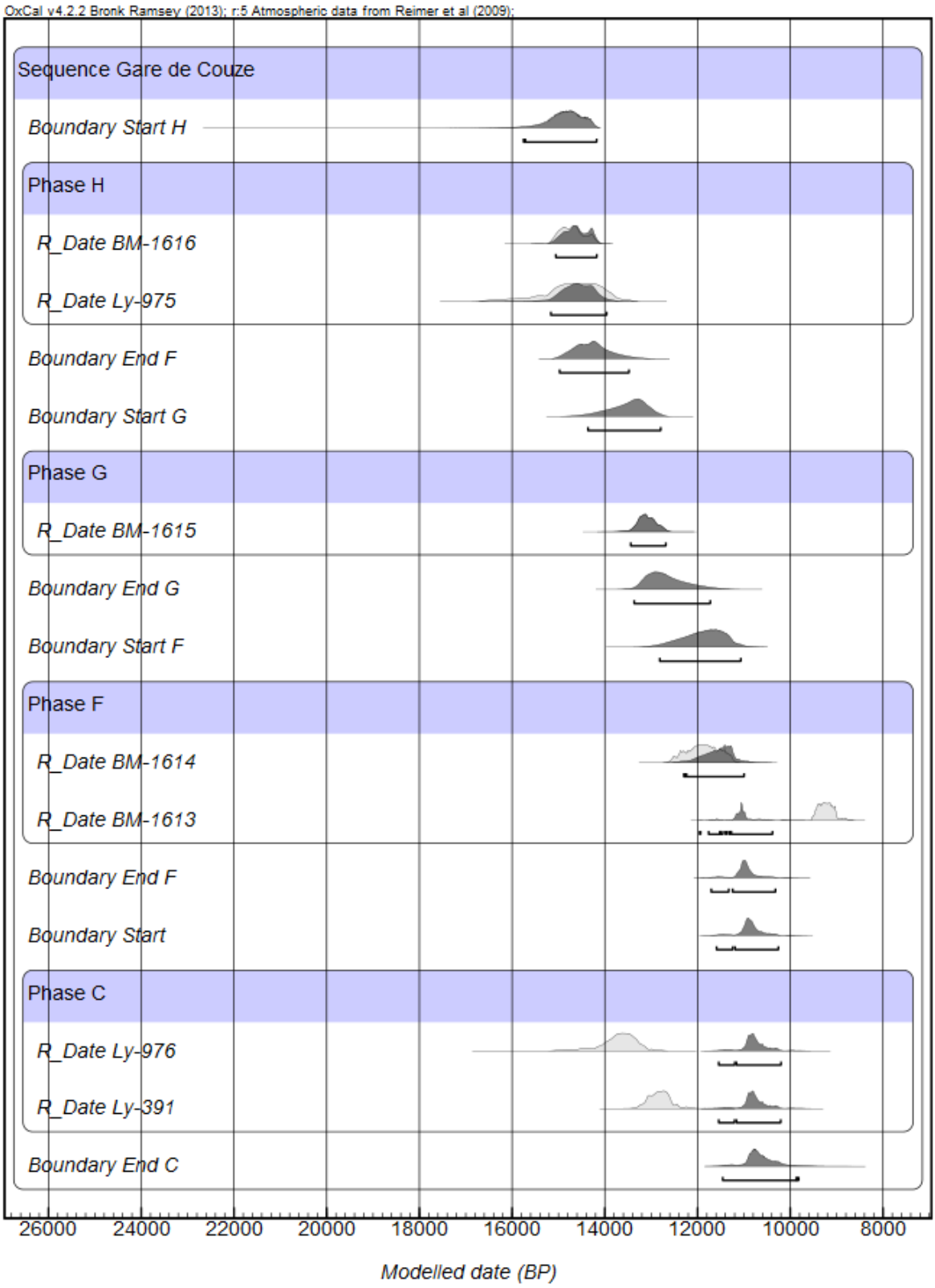

Figure 10.21: Gare de Couze modelled radiocarbon dates

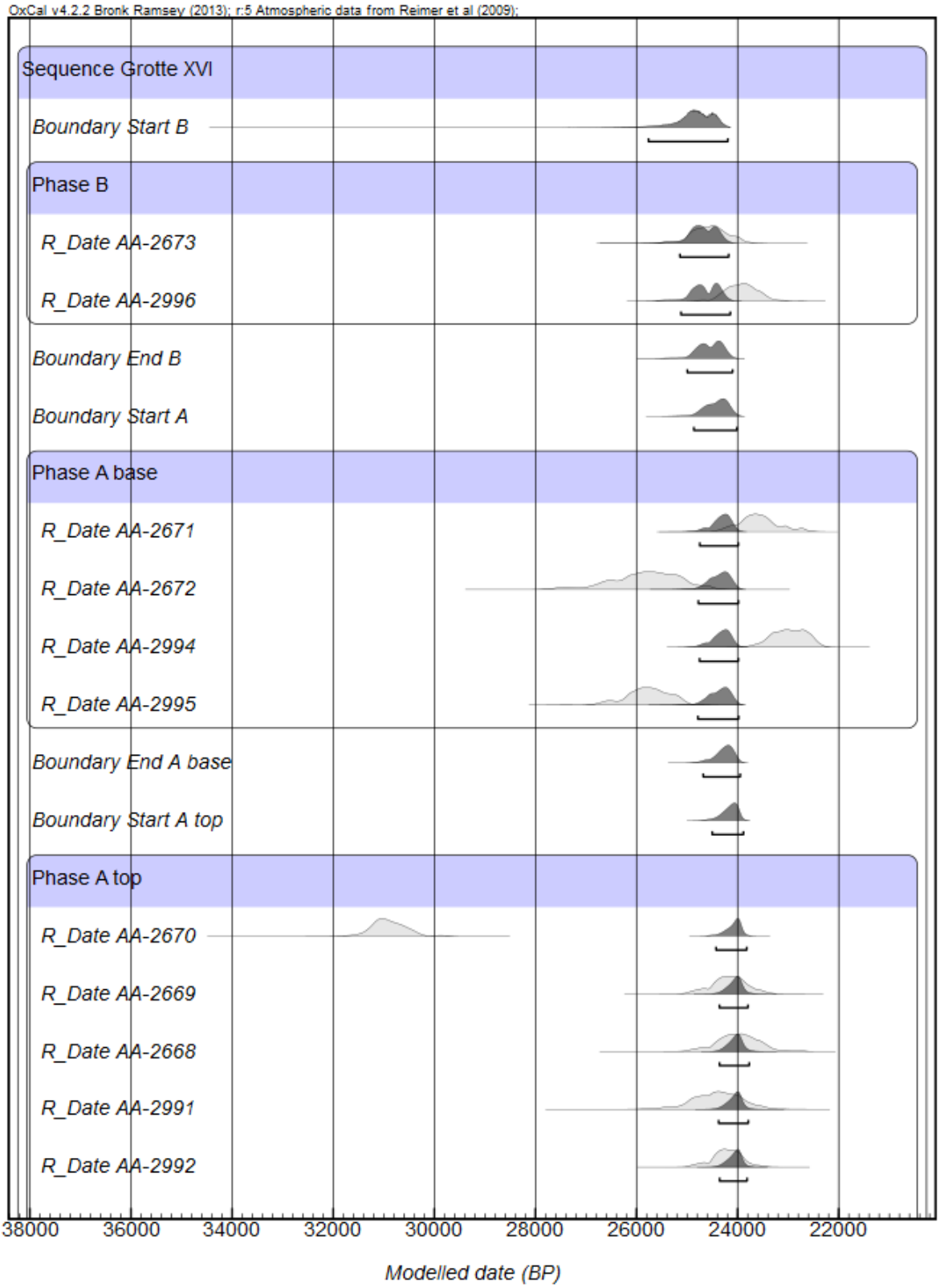

Figure 10.22: Grotte XVI modelled radiocarbon dates

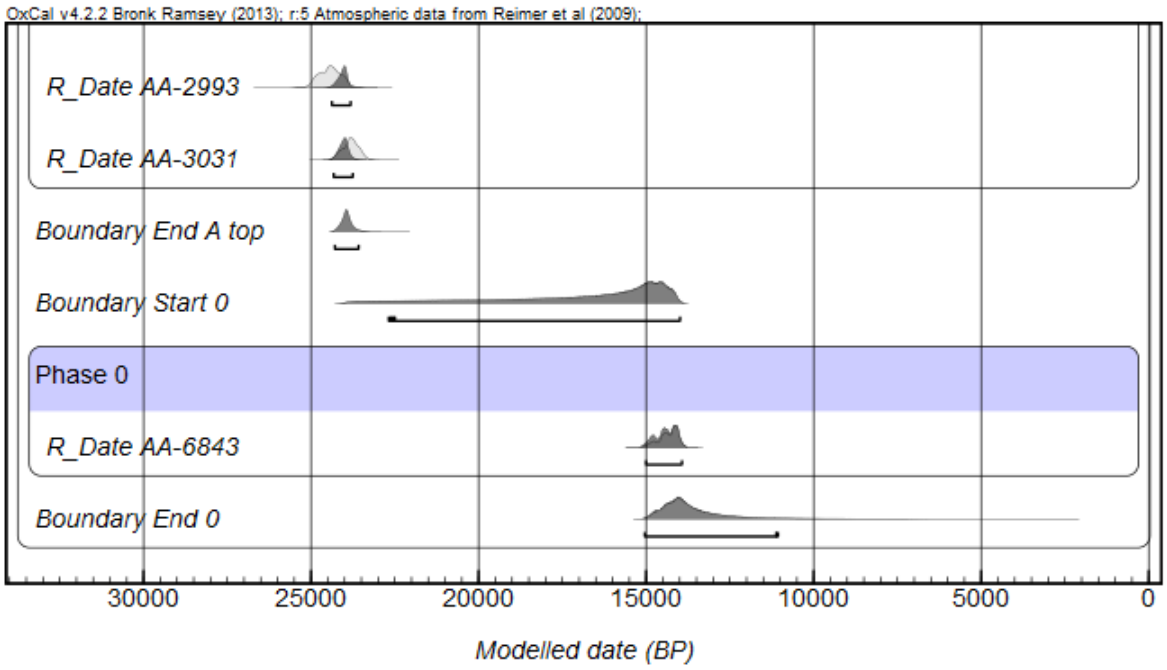

Figure 10.23: Grotte XVI modelled radiocarbon dates

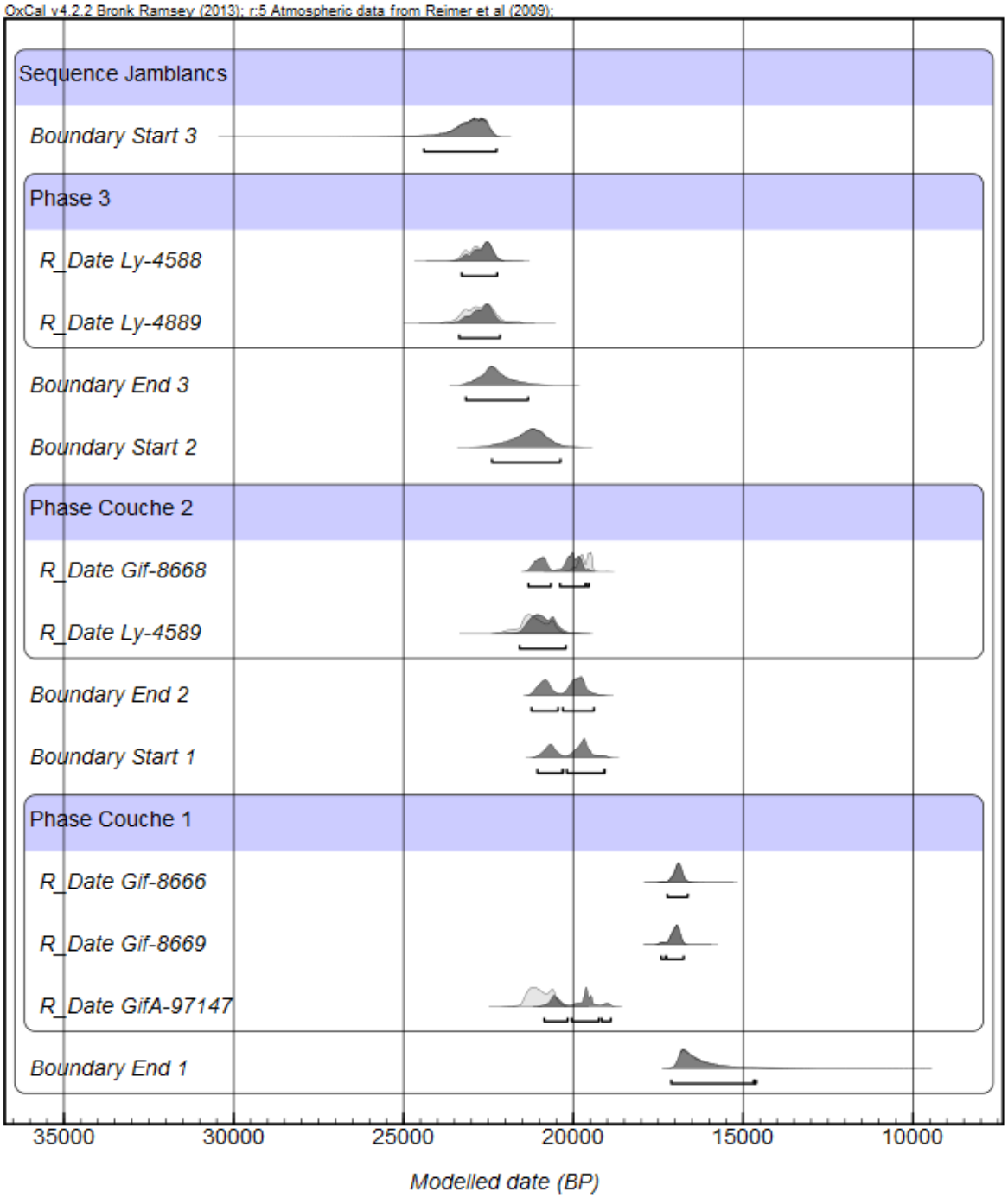

Figure 10.24: Jamblancs modelled dates

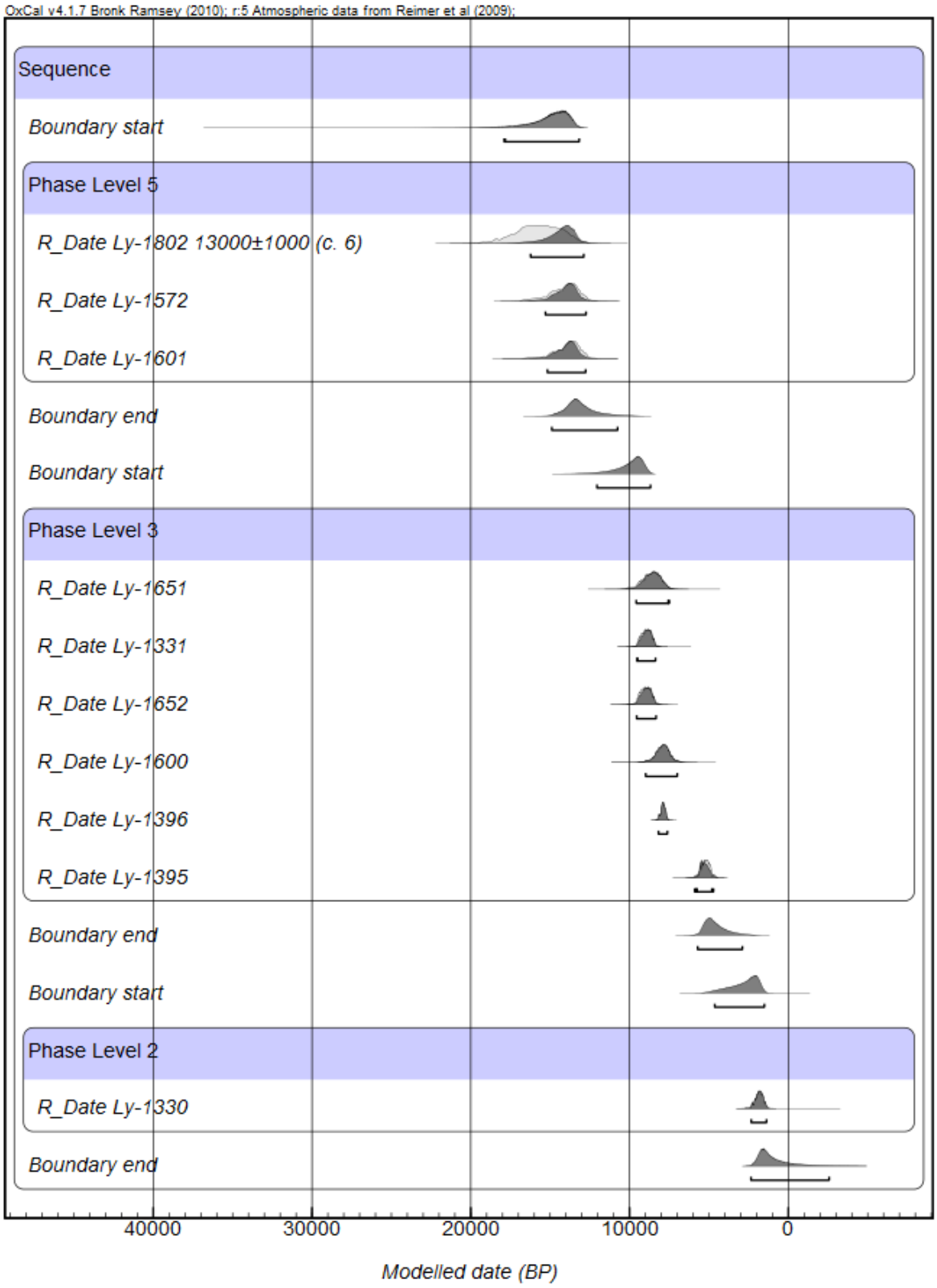

Figure 10.25: Chez Jugie modelled dates

As the many radiocarbon dates available were provenanced from excavations by Guichard and Bordes and it was not possible to match-up the stratigraphy of these two excavations separate models were built. One for the Magdalenian, based on Guichard's excavations and another for the full sequence from Bordes' excavations (Bordes, 1958).

10.1.16 Laugerie Haute Ouest

In contrast to its sister to the east, Laugerie Haute Ouest lacks any Magdalenian levels but has a well-developed Solutrean sequence instead. The stratigraphy has described by Peyrony is as follows:

Table 10.4: Stratigraphy of Laugerie Haute Ouest. From Peyrony and Peyrony (1938)

Level	Technocomplex
B	Gravettian
D	Aurignacian V
G	Protosolutrean
H'	Lower Solutrean
H"	Middle Solutrean
H"'	Upper Solutrean

The later excavation by Bordes observed a similar sequence, although lacking a Gravettian. The model below was developed from radiocarbon dates from the Bordes' excavation.

10.1.17 La Madeleine

Peyrony's excavations at this enormous site on the Vézère led to the subdivision of the Upper Magdalenian into the Magdalenian IV-VI. The site is predominantly an Upper Magdalenian locale, with a small Azilian assemblage. Available radiocarbon dates are from the later excavation by Bouvier (Bouvier, 1973).

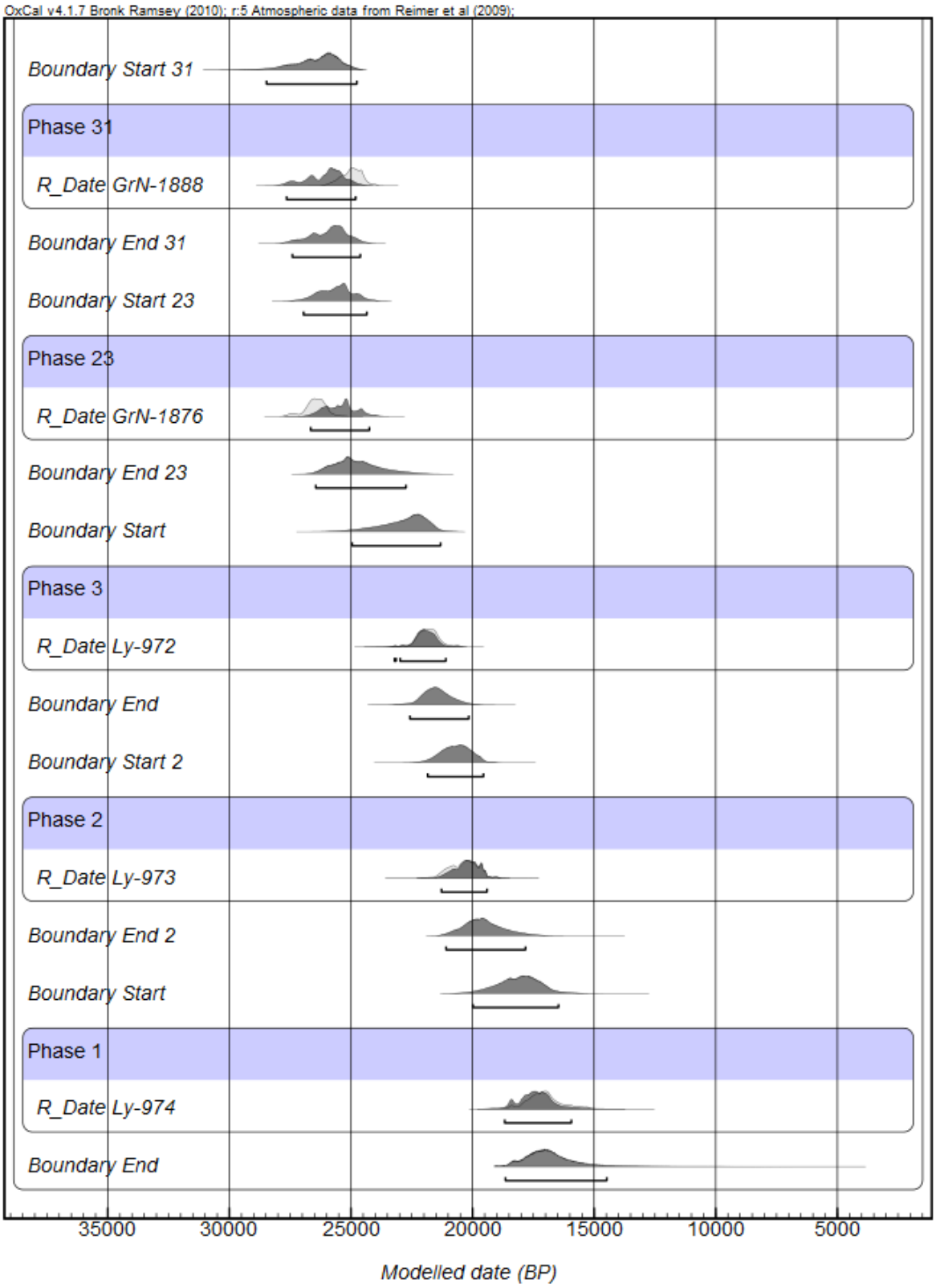

Figure 10.26: Laugerie Haute Est, modelled dates from the excavations of Bordes

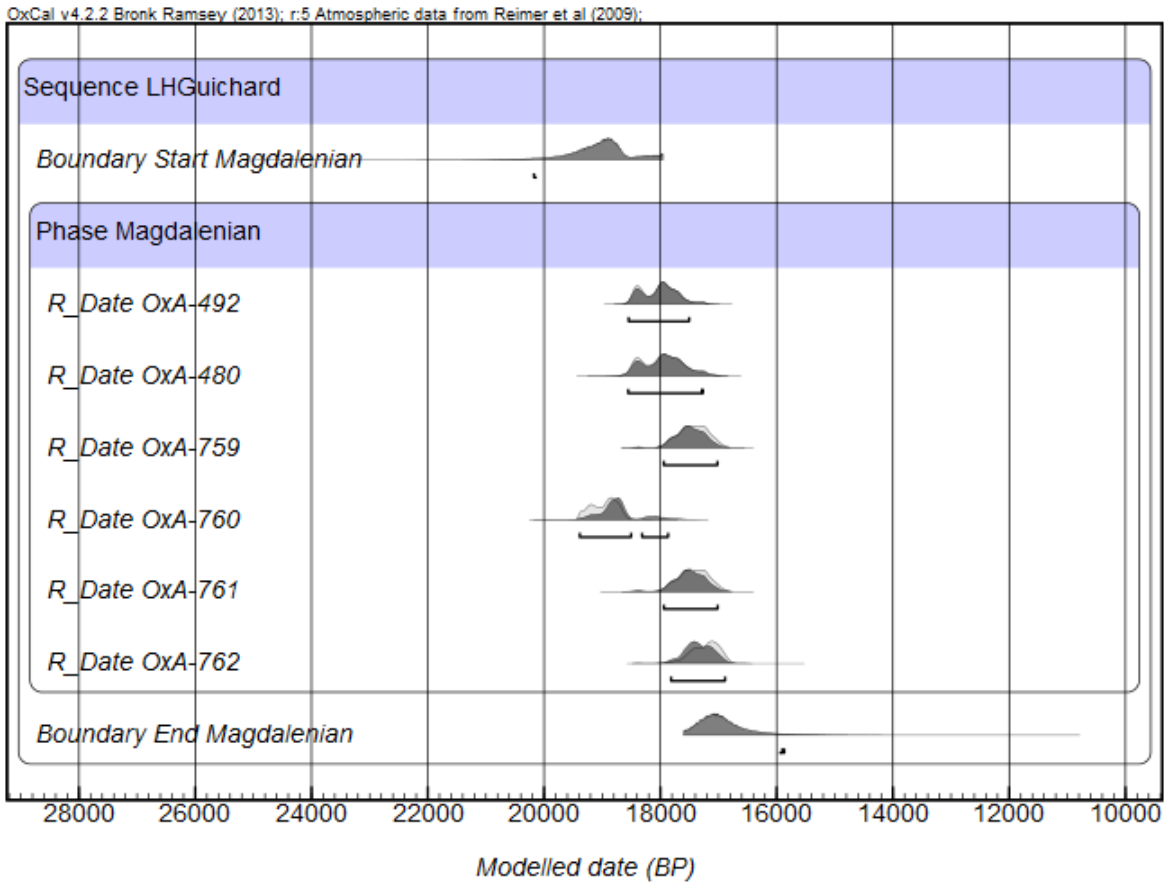

Figure 10.27: Laugerie Haute Est, dates from Guichard

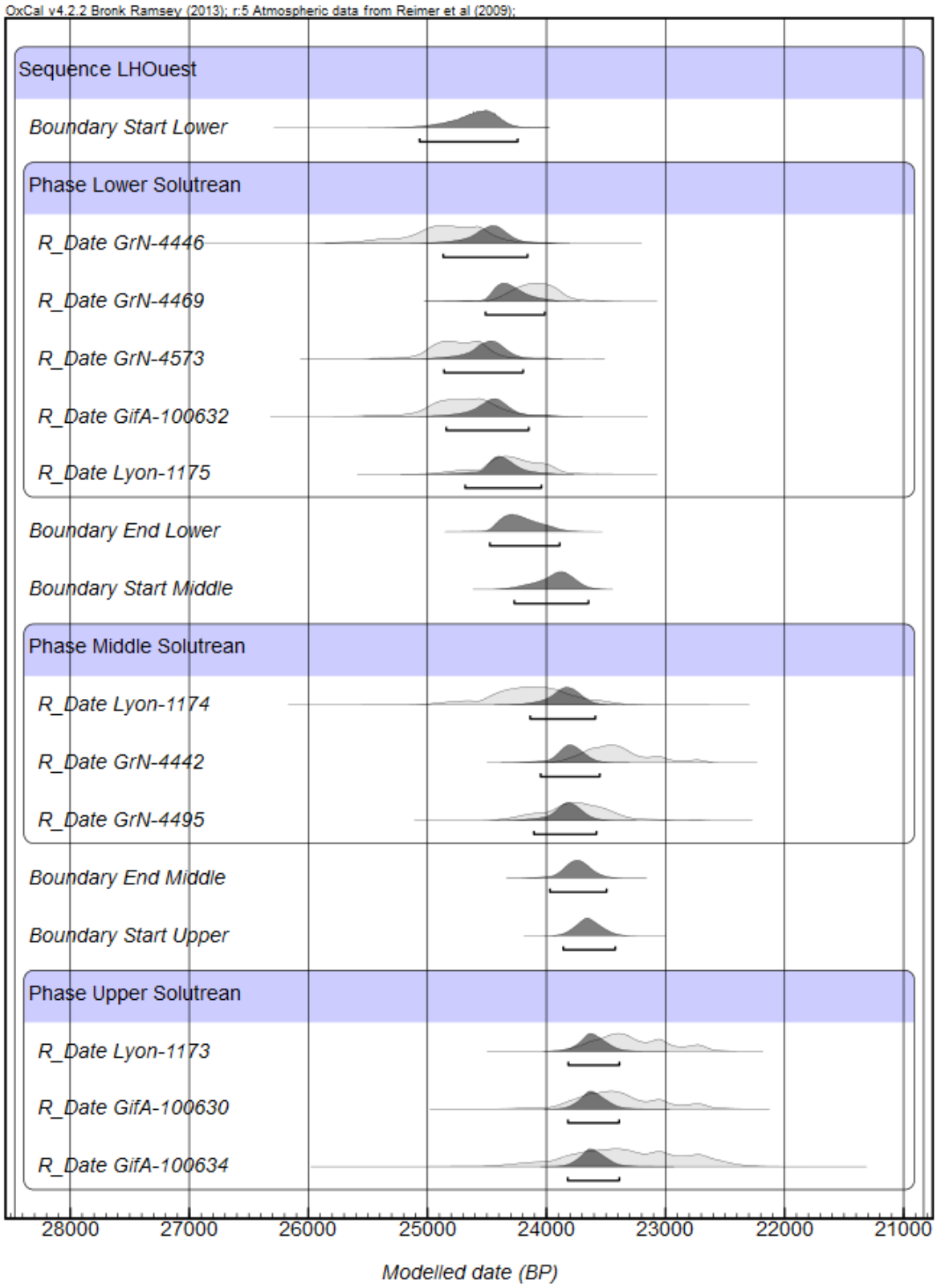

Figure 10.28: Laugerie Haute Ouest modelled dates

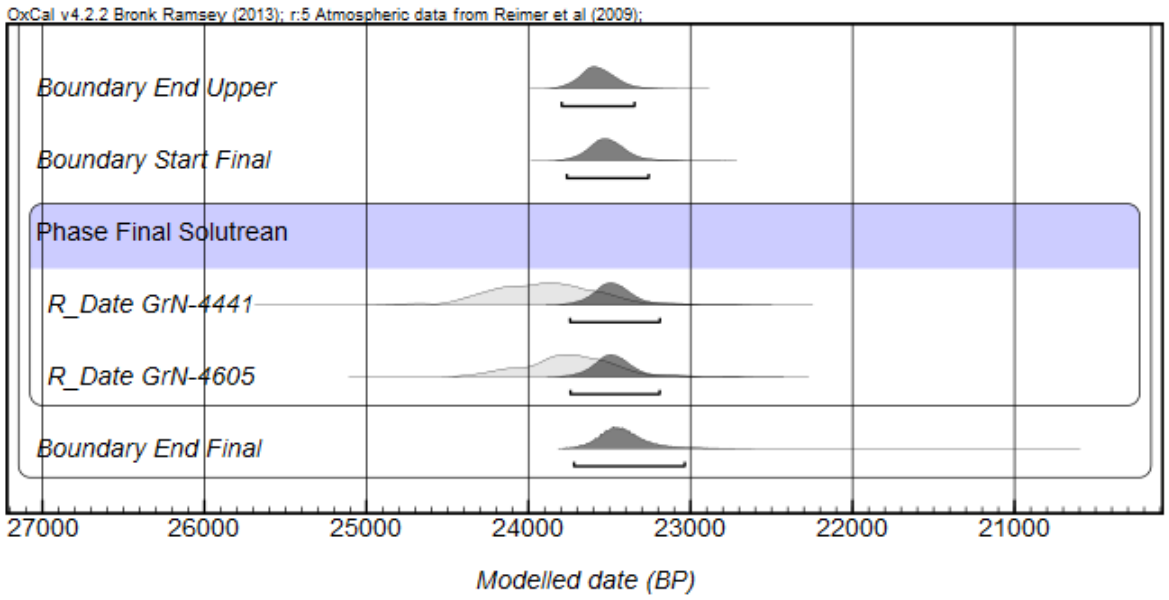

Figure 10.29: Laugerie Haute Ouest modelled dates

10.1.18 Montgaudier

Celebrated portable art site comprised of several shelters; Abri Lartet, Abri Paignon and Abri Gaudry. Abri Lartet contains Mousterian levels, while Abri Paignon has revealed Solutrean, Gravettian and Magdalenian levels. Radiocarbon dates available are provenanced from three levels and modelled dates are shown below.

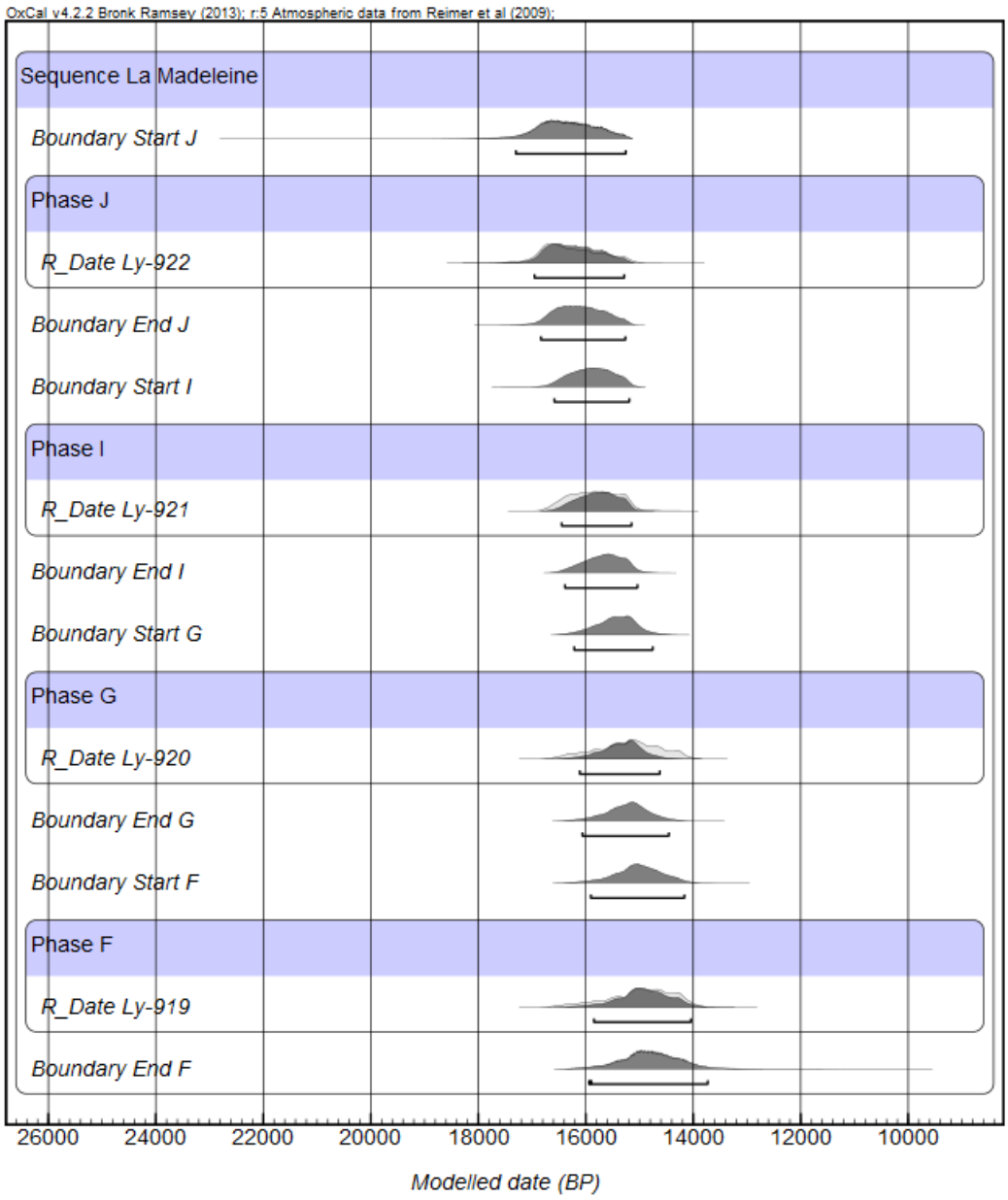

Figure 10.30: La Madeleine modelled dates

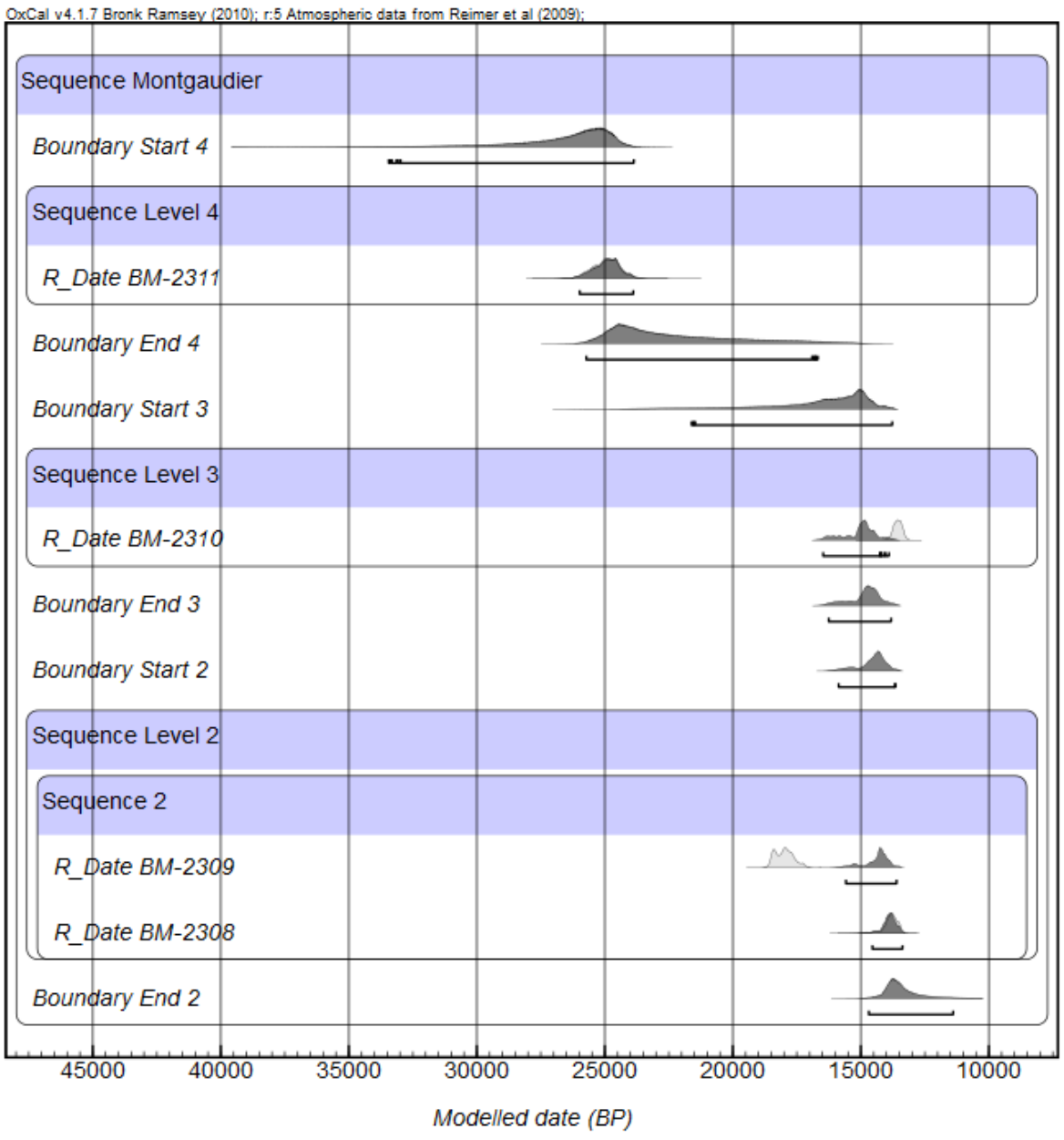

Figure 10.31: Montgaudier modelled dates

10.1.19 Le Morin

A late Magdalenian site containing Magdalenian V and VI assemblages (Lenoir, 1978). Recently dated faunal remains from two levels (Szmidt et al., 2009) were used to construct the model.

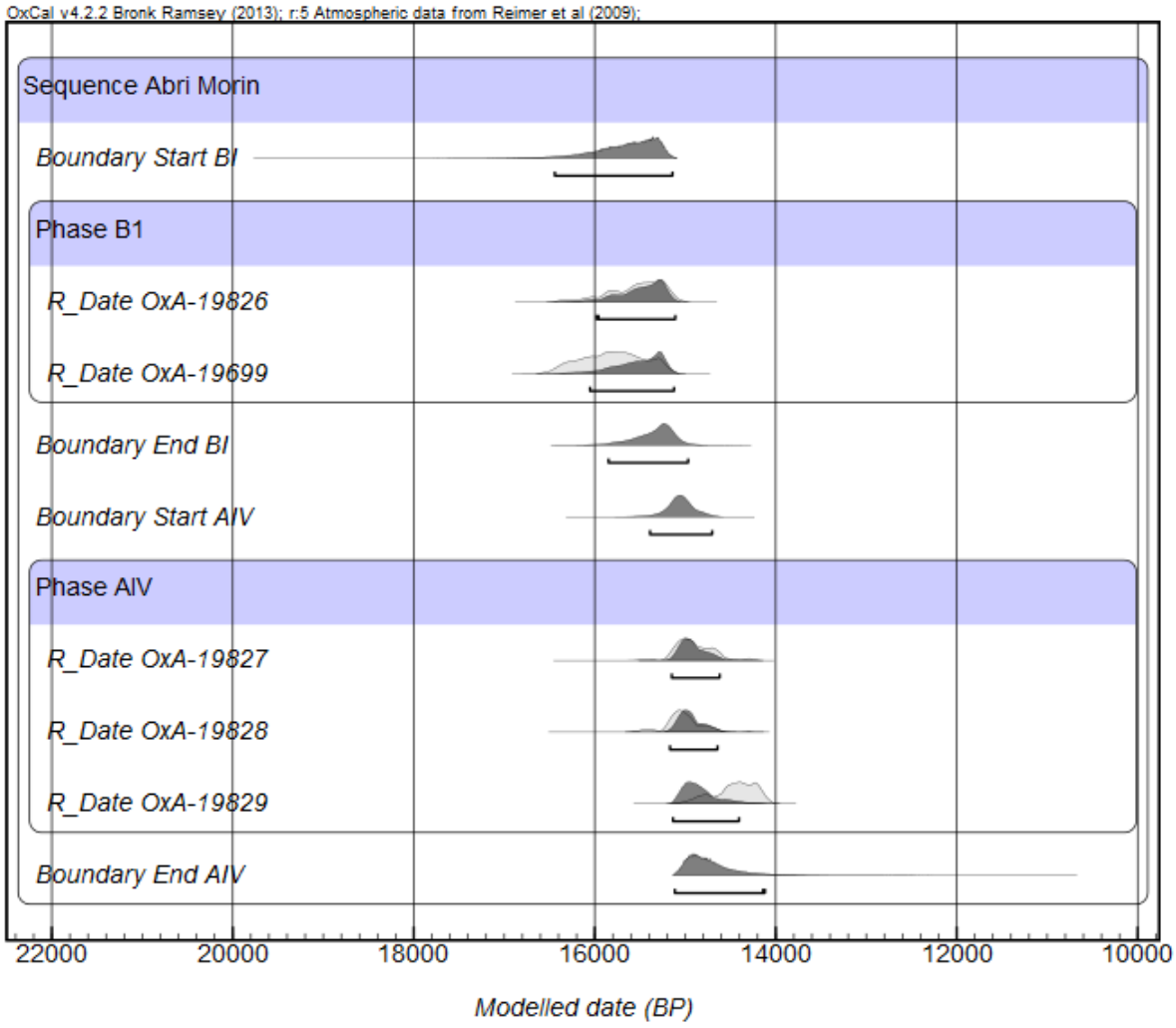

Figure 10.32: Le Morin modelled dates

10.1.20 Moulin du Roc

Also known as Labattut, this site contains a sequence of Magdalenian, Azilian, Sauvettarian and Neolithic. The site has been well studied regarding the transition from Magdalenian to Azilian (Detrain et al., 1996)

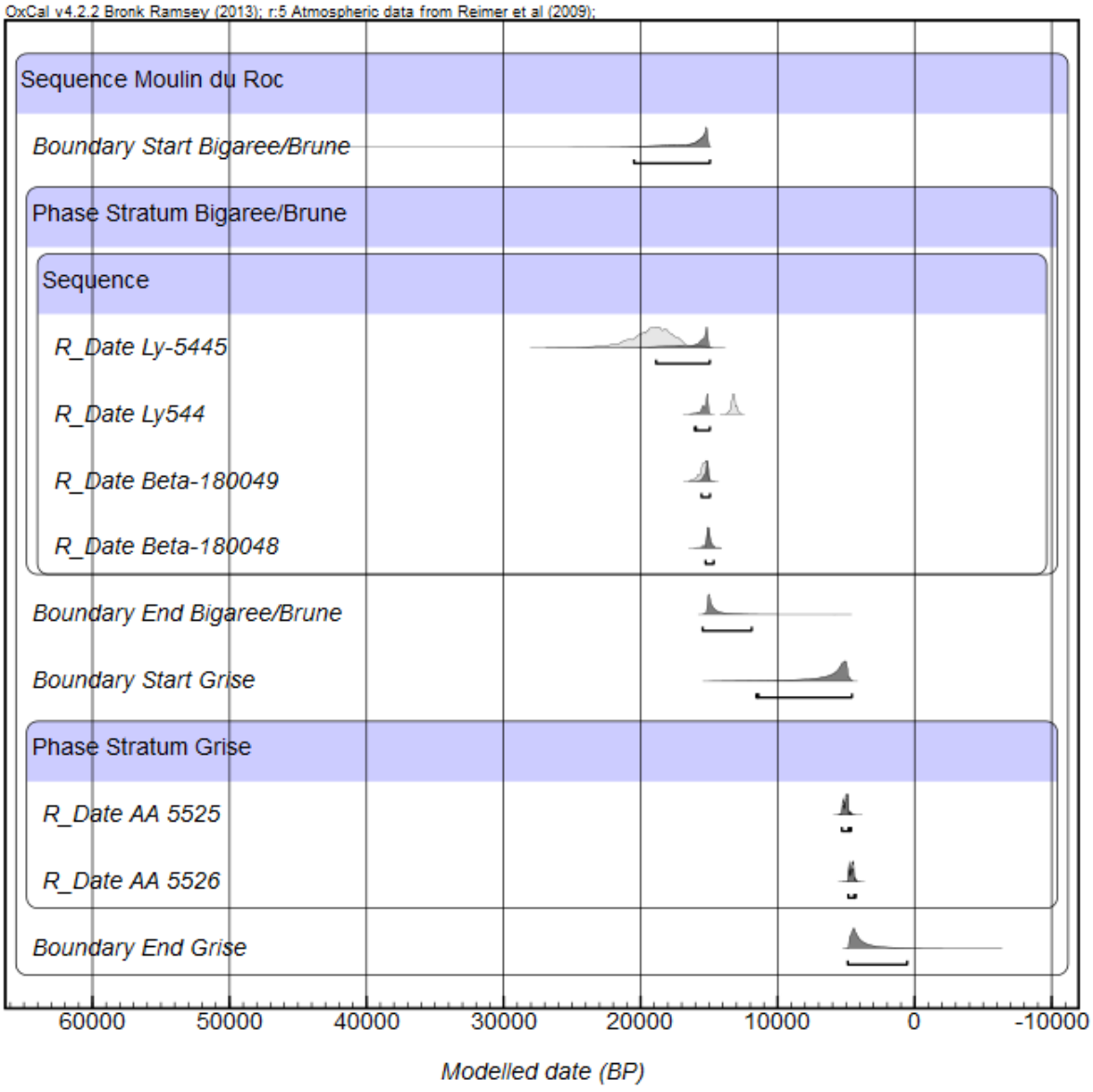

Figure 10.33: Moulin du Roc modelled dates

10.1.21 Pégourié

This vast cave site was excavated by Séronie-Vivien in the 1990s and shows evidence for multiple occupation events from around 24,000 BP up until the Azilian (Séronie-Vivien, 1995). The site is particularly notable for its Badegoulian occupations.

10.1.22 Peyrugues

A good sequence of several Magdalenian and Badegoulian deposits stratified above Solutrean levels is found at this site. The final Magdalenian occupation at the site also revealed some human teeth, both adult and juvenile, alongside an associated perforated shell (Allard and Juillard, 1988). Faunal remains, of reindeer and fish were also abundant.

10.1.23 Le Piage

Excavated by Champagne, who recorded the following stratigraphy (Champagne and Espitalié, 1967)

Table 10.5: Stratigraphy of Le Piage.

Level	Technocomplex
L	Sterile
K	Aurignacian
J	Aurignacian
I	Aurignacian
H	Aurignacian
G-I	Aurignacian
F1	Châtelperronian
F	Aurignacian
C-E	Solutrean and Lower Magdalenian
B	Sterile eboulis
A	Humus

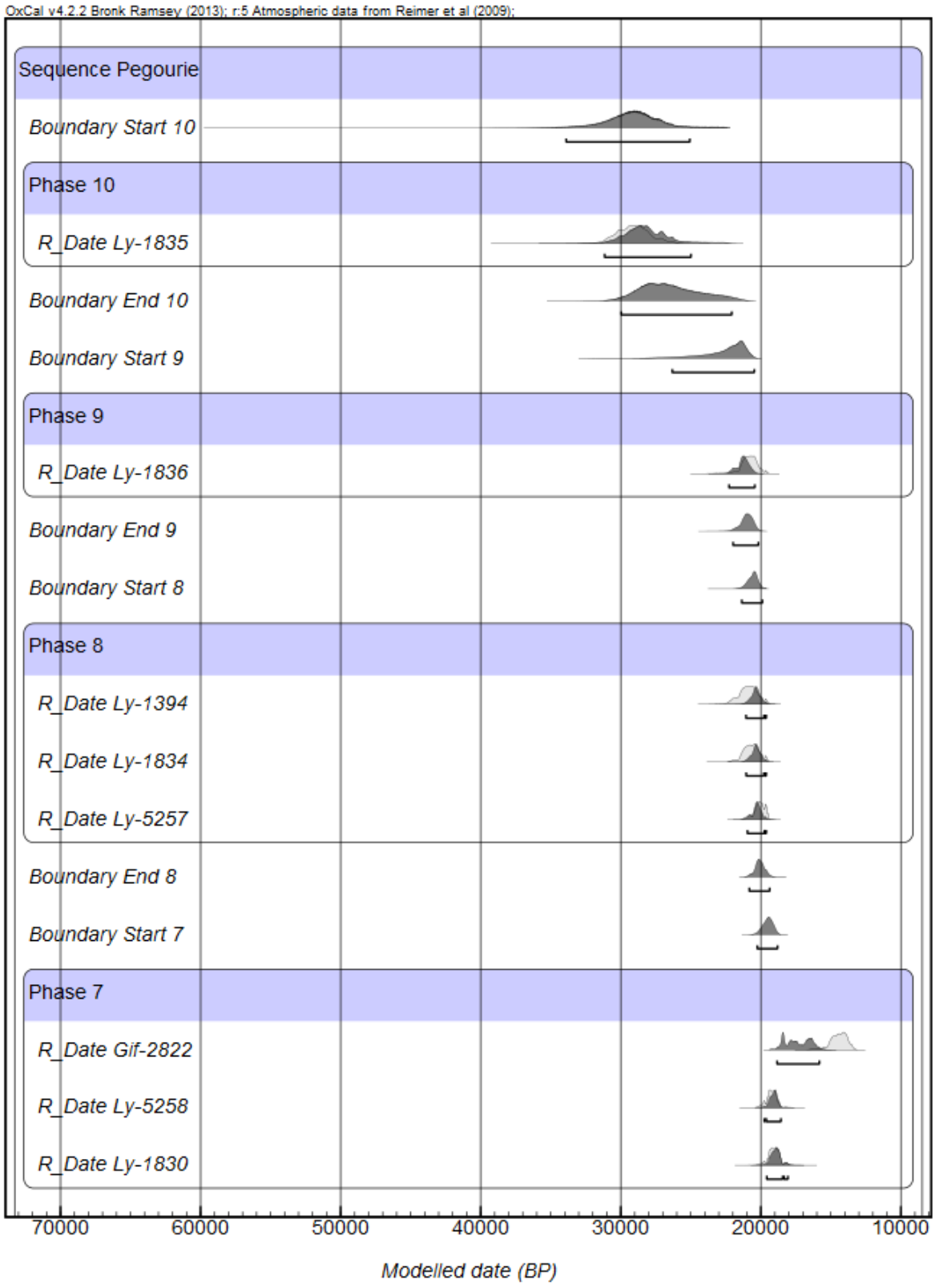

Figure 10.34: Pégourié modelled dates

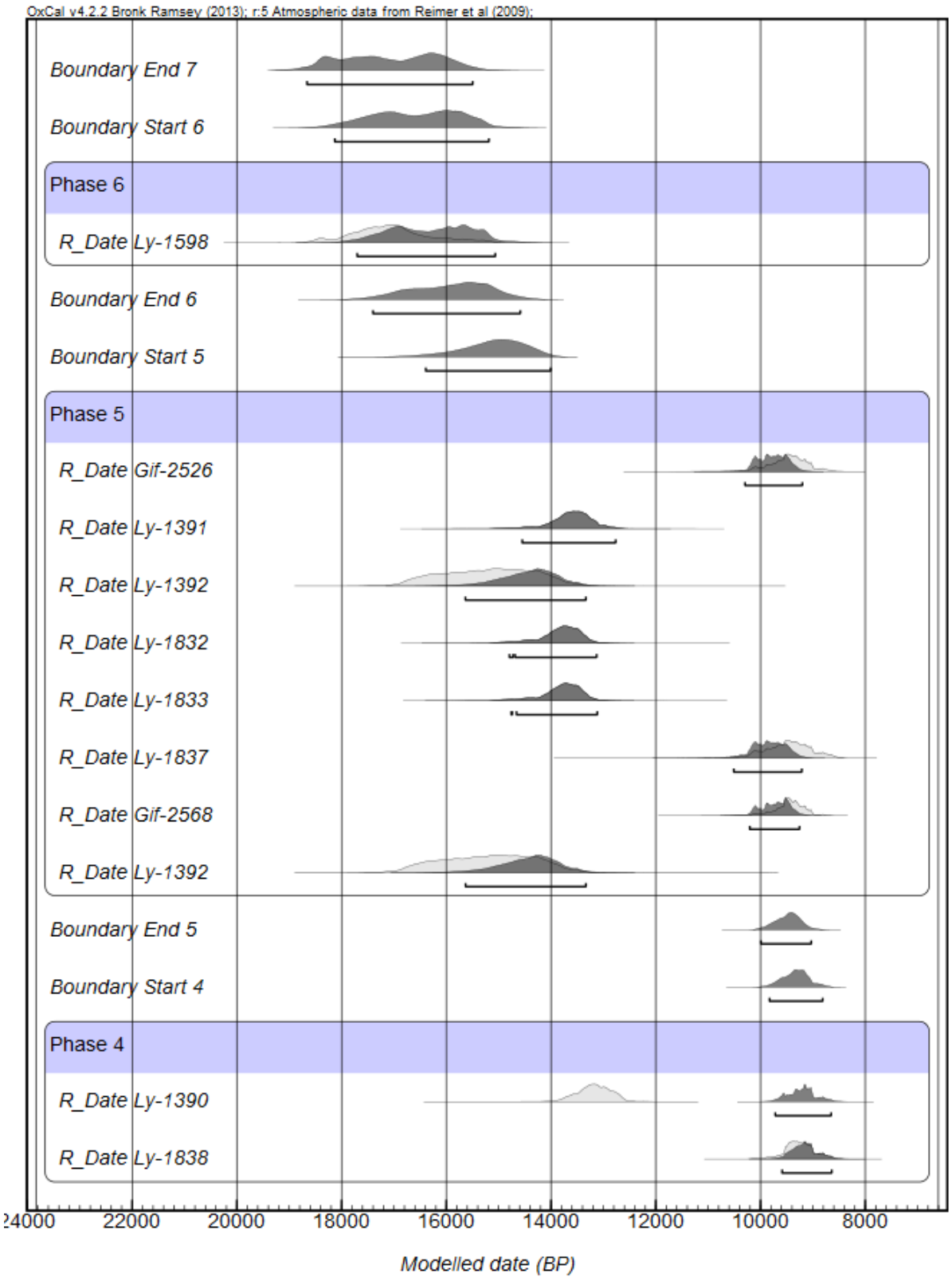

Figure 10.35: Pégourié modelled dates

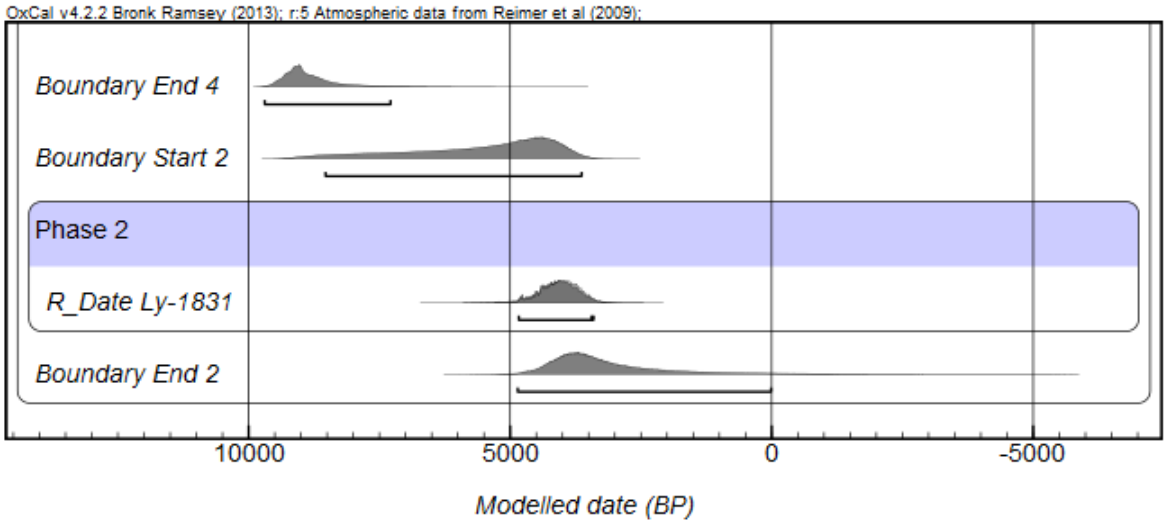

Figure 10.36: Pégourié modelled dates

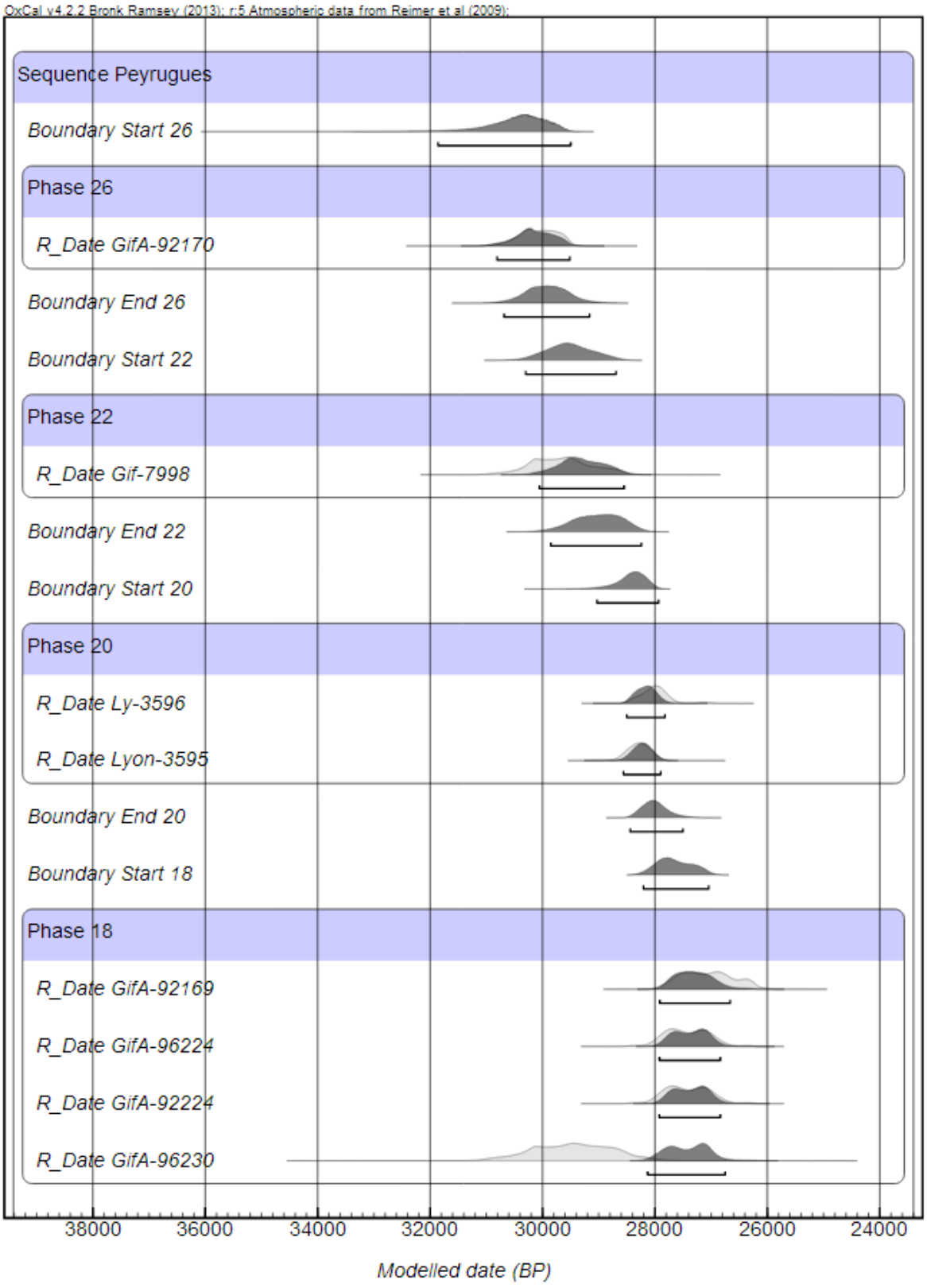

Figure 10.37: Peyrugues modelled dates

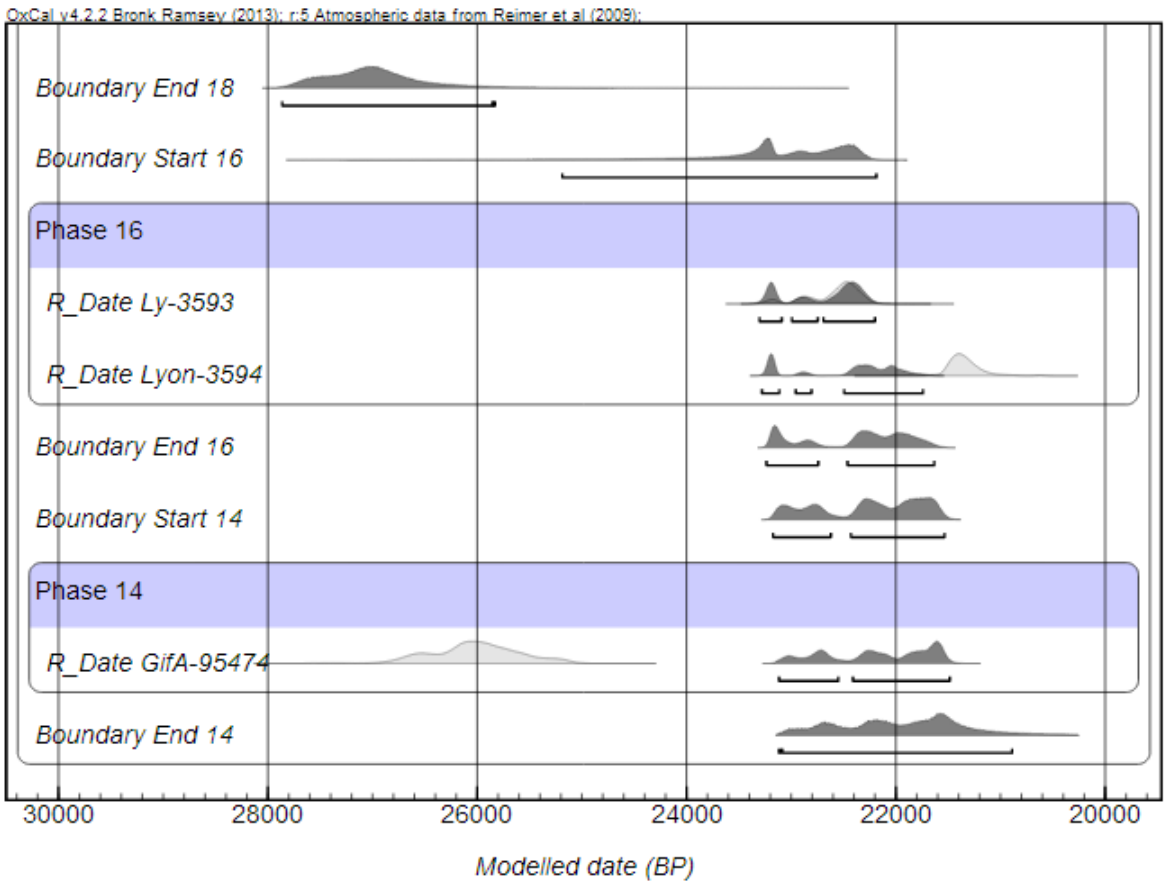

Figure 10.38: Peyrugues modelled dates

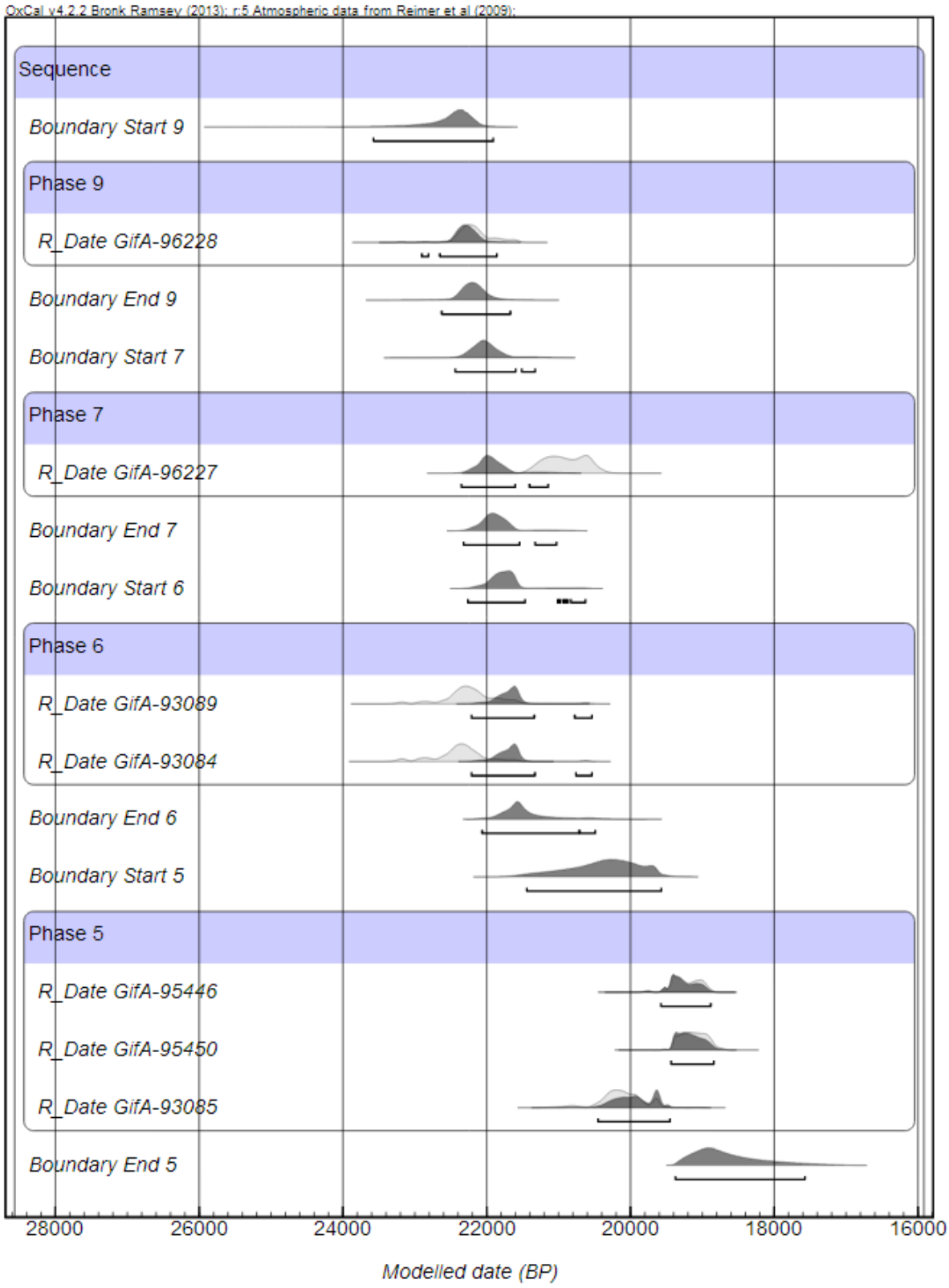

Figure 10.39: Peyrugues modelled dates

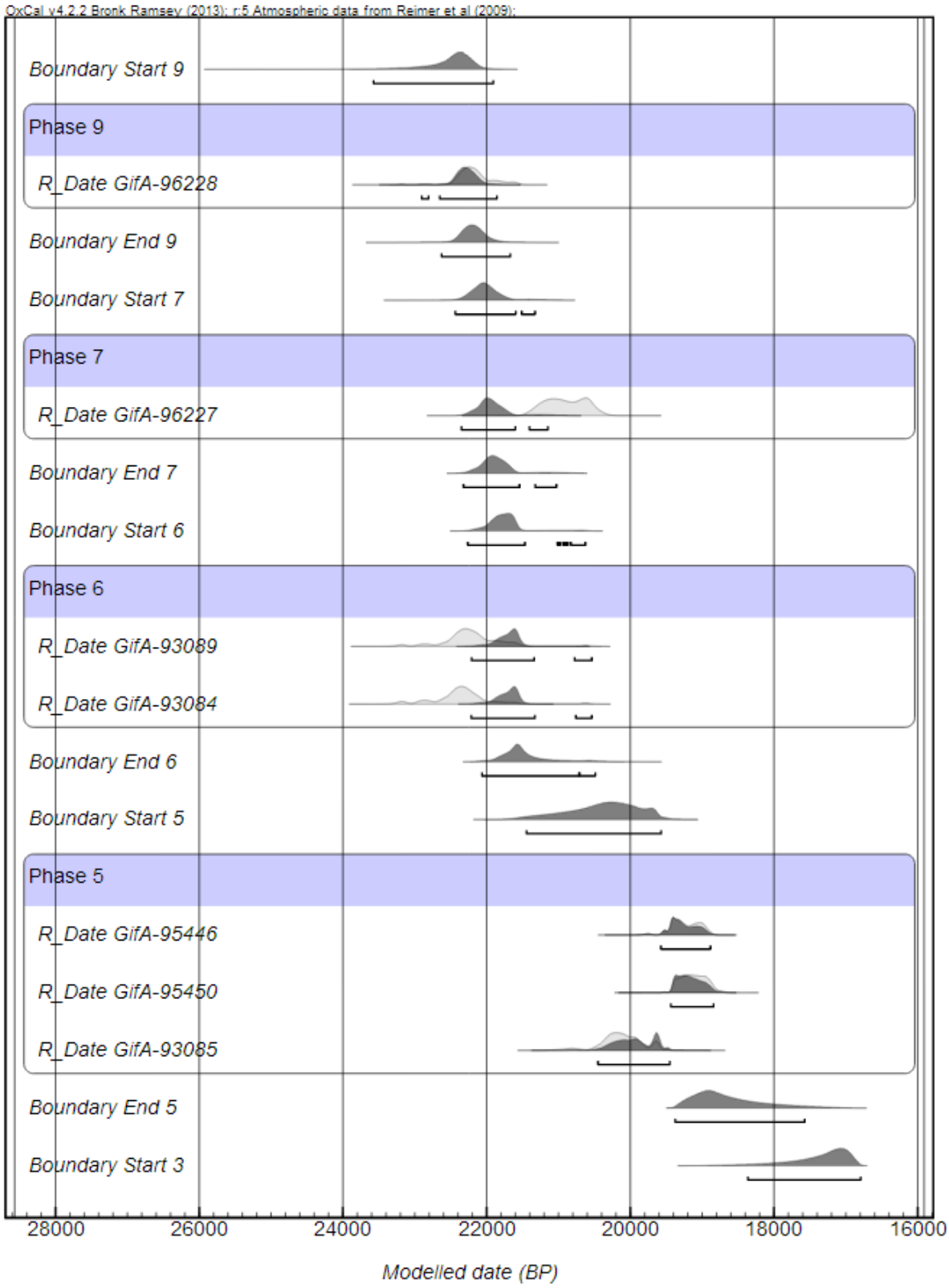

Figure 10.40: Peyrugues modelled dates

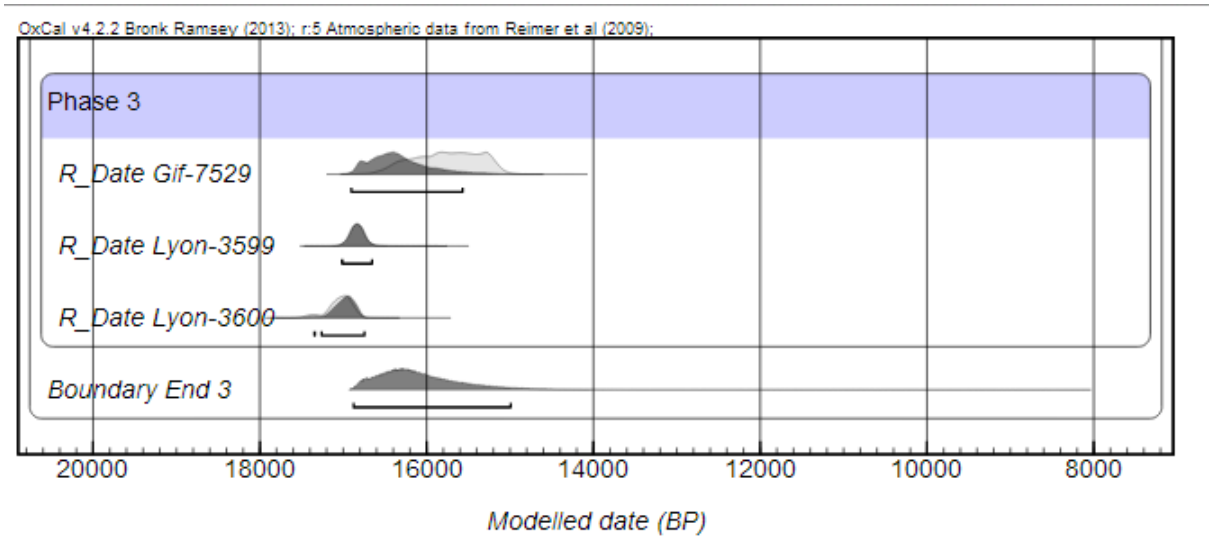

Figure 10.41: Peyrugues modelled dates

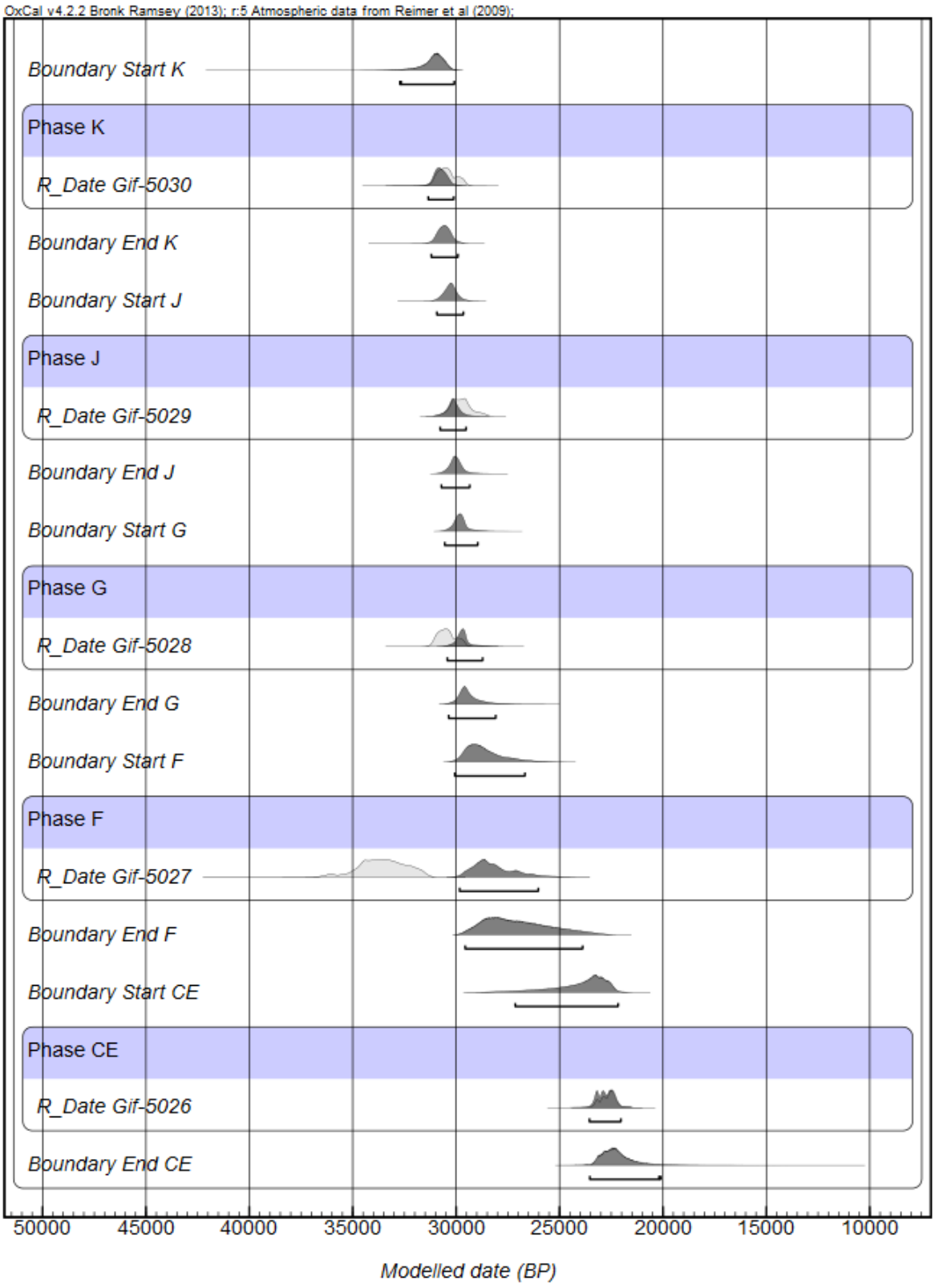

Figure 10.42: Le Piage modelled dates

10.1.24 Le Placard

Large cave in Charent featuring a Robenhausian, three Magdalenian, two Solutrean levels and some Mousterian, with each level separated by a sterile eboulis (Roche, 1965).

10.1.25 Pont d'Ambon

10.1.26 Le Quéroy

Cave site excavated by J. Gomez de Soto from 1972 to 1980, with Pleistocene deposits discovered in 1978 (Tournepiche, 1982). A good stratigraphic sequence encompassing five levels was uncovered, for which several radiocarbon dates, in sequence, are available. Modelled dates from the site are shown below.

10.1.27 La Quina

While this site is most strongly associated with Neanderthals, it is actually two locales, one Mousterian and another Châtelperronian and Aurignacian. We focus here on the latter site.

10.1.28 Renardières

Excavations at this site have revealed a sequence of Middle Palaeolithic, Châtelperronian, Aurignacian, Gravettian, Badegoulian and Magdalenian occupations A second cave nearby contains Bronze Age, Neolithic, Mesolithic and some Palaeolithic levels. (Dujardin, 2001). Radiocarbon dates are available on a number of levels, allowing a Bayesian model to be produced.

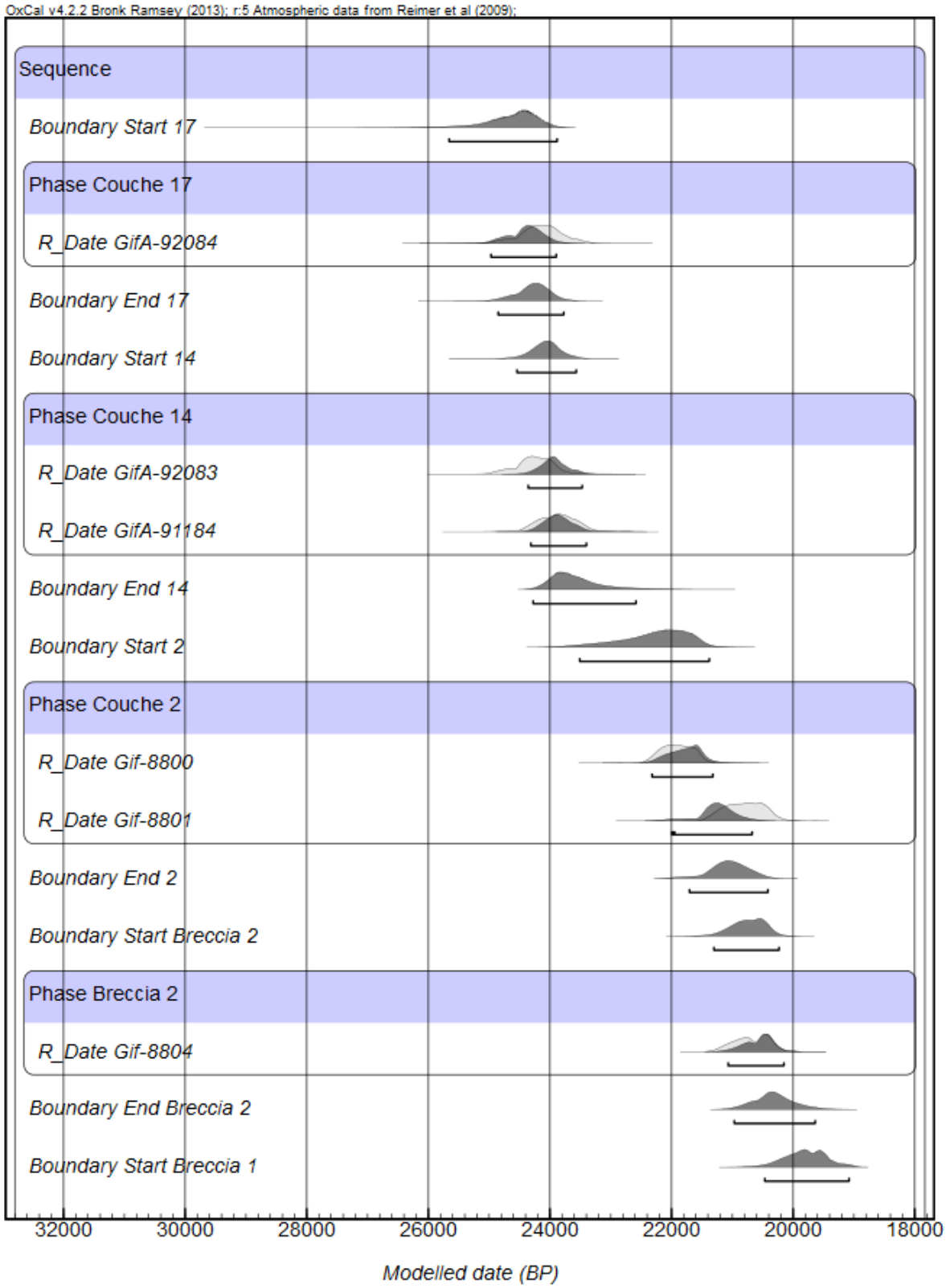

Figure 10.43: Le Placard modelled dates

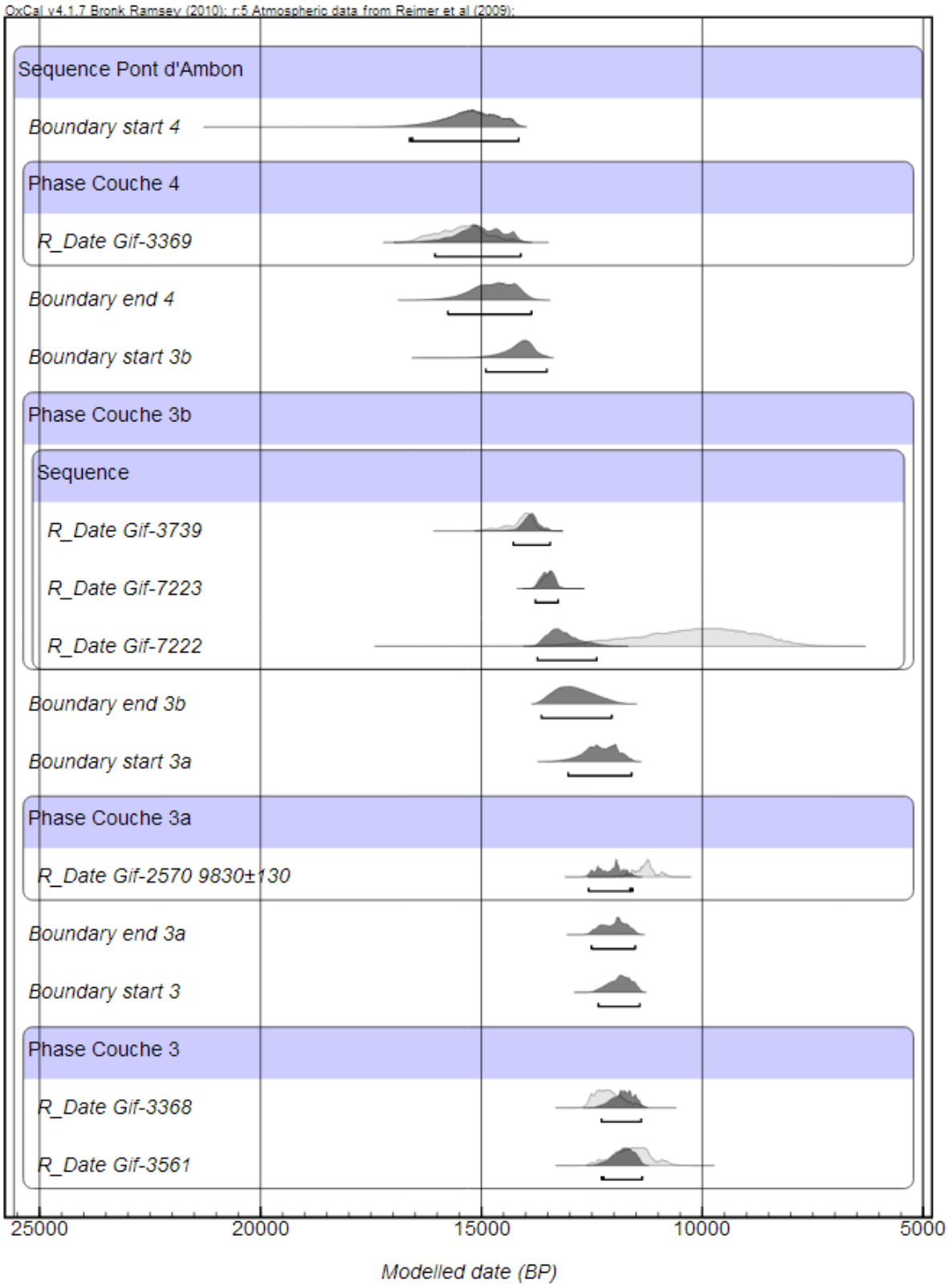

Figure 10.44: Pont d'Ambon modelled dates

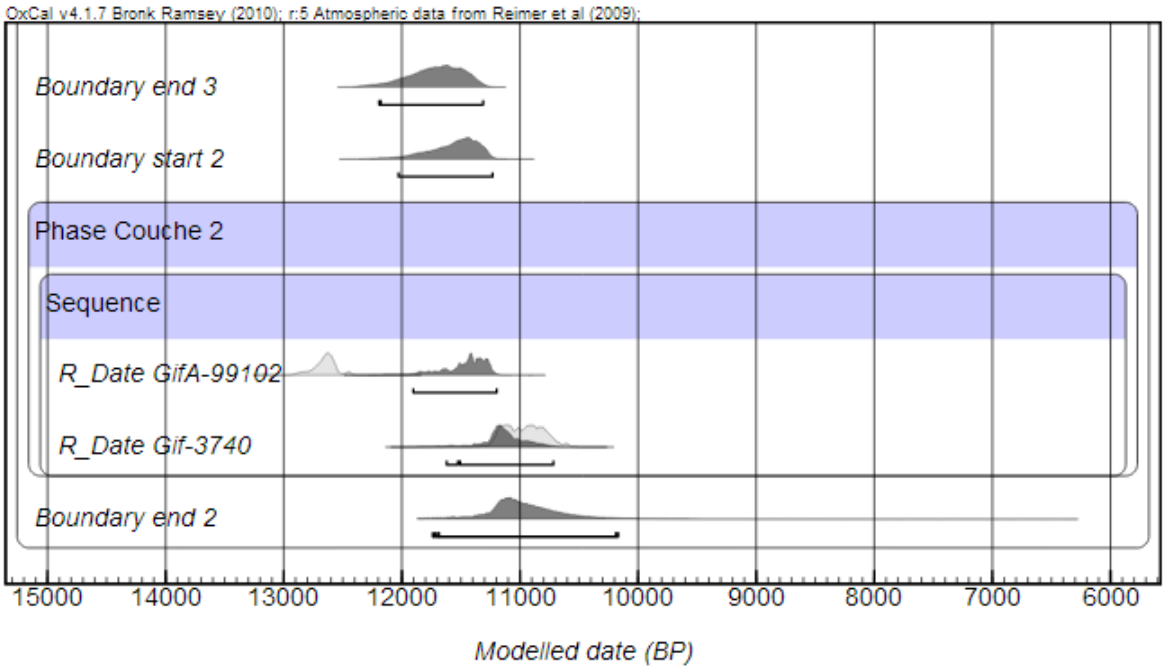

Figure 10.45: Pont d'Ambon modelled dates

10.1.29 Roc de Combe

This cave and abri locale was discovered by Labrot in 1950 and subsequently surveyed. Eight Upper Palaeolithic levels in total are found here, encompassing the Châtelperronian, Aurignacian and Gravettian (Labrot and Bordes, 1964).

10.1.30 Roc de Marcamps

Close to the celebrated cave of Pair-non-Pair and located beside the Dordogne river, this site has been excavated by Ferrier and Maziaud. While there are Neolithic and modern levels, the Upper Palaeolithic at the site is comprised of Magdalenian (Roussot and Ferrier, 1970).

10.1.31 La Rochette

Mousterian, Châtelperronian, Aurignacian and Gravettian sequence recorded by (Delporte, 1962). Human remains uncovered here in the early 20th Century (Hauser, 1911), which have recently been dated to the Gravettian period (Orshiedt, 2002). Unfortunately the dates on the human remains could not be included in the model due to the difficulty in provenancing them to a level.

Table 10.6: Stratigraphy of La Rochette. From Delporte (1962)

Level	Technocomplex
2	Noaillian
3	Aurignacianl
4	Aurignacian
5	Aurignacian
6	Châtelperronian
7	Final Mousterian
8	MTA
9	MTA
10	Charentian Mousterian

10.1.32 Sainte Eulalie

Two large decorated caves in Lot. Much of the literature on the site focusses on the cave art. Excavations in the cave have revealed a stratigraphy containing a sequence of Magdalenian levels (Lorblanchet et al., 1973). Unusually for a cave art site numerous Magdalenian tools have been furnished from excavations here. Many Palaeolithic art sites feature pautry lithic remains, if any.

10.1.33 Saint Germain

Two caves in Gironde beside the Dordogne river. Multiple human remains have been uncovered at the site, beginning with a skeleton in the early twentieth century (Blanchard et al., 1972). Further excavations in the 1960s revealed two additional skeletons

and unfortunately, due to a lack of contextual information, we do not have ages for these human remains. Later excavations by Trécolle uncovered a Magdalenian burial, alongside grave goods (Vanhaeren and d'Errico, 2005). Elaborate burials such as this are rare in the Upper Palaeolithic of Southwest France (Pettitt, 2011). The stratigraphy recorded during the Trécolle excavation runs from lower to Middle Magdalenian. Ultimately we may characterize the site as a Magdalenian cave site, featuring multiple burials.

10.1.34 Sanglier

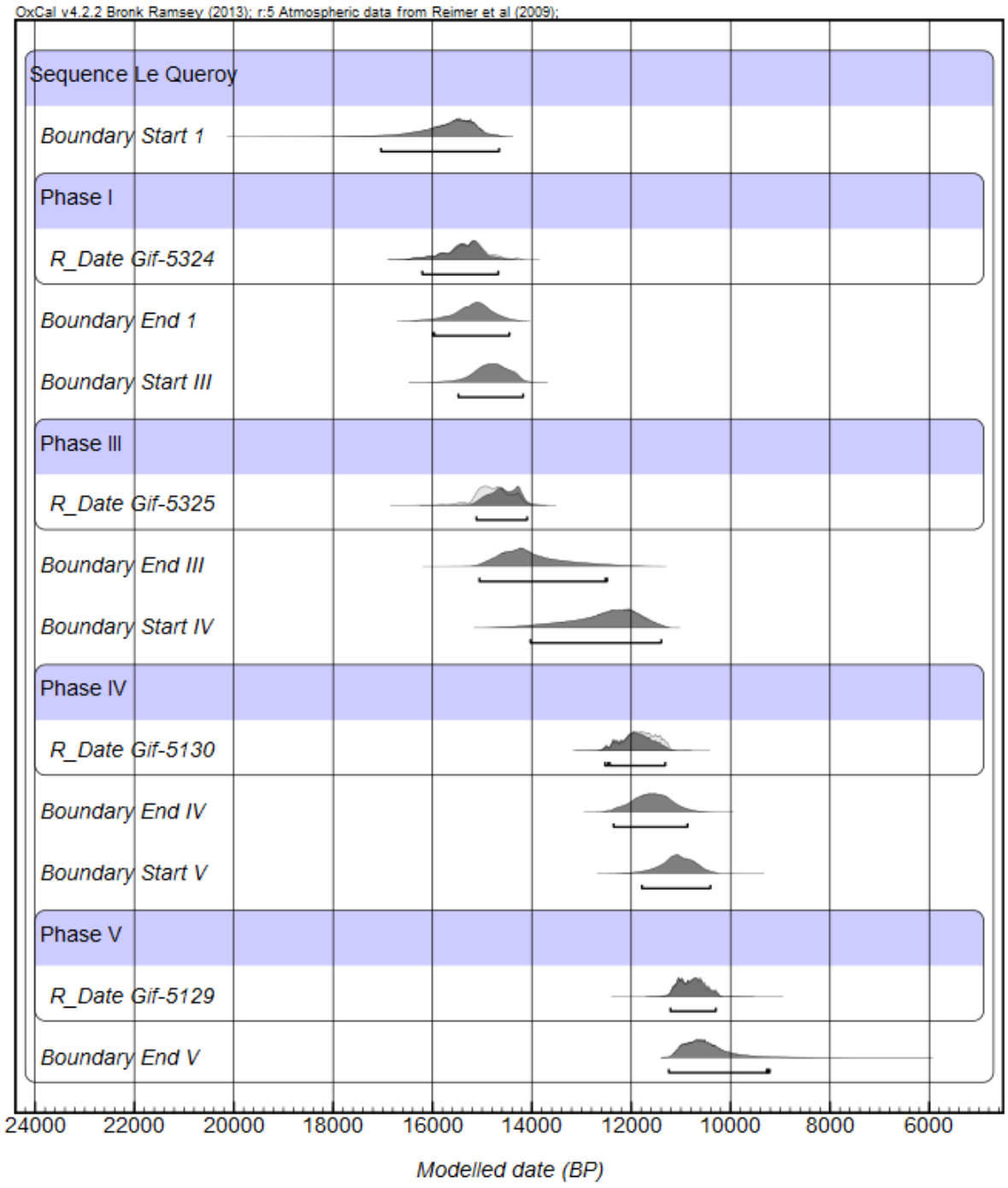

Figure 10.46: Quéroy modelled dates

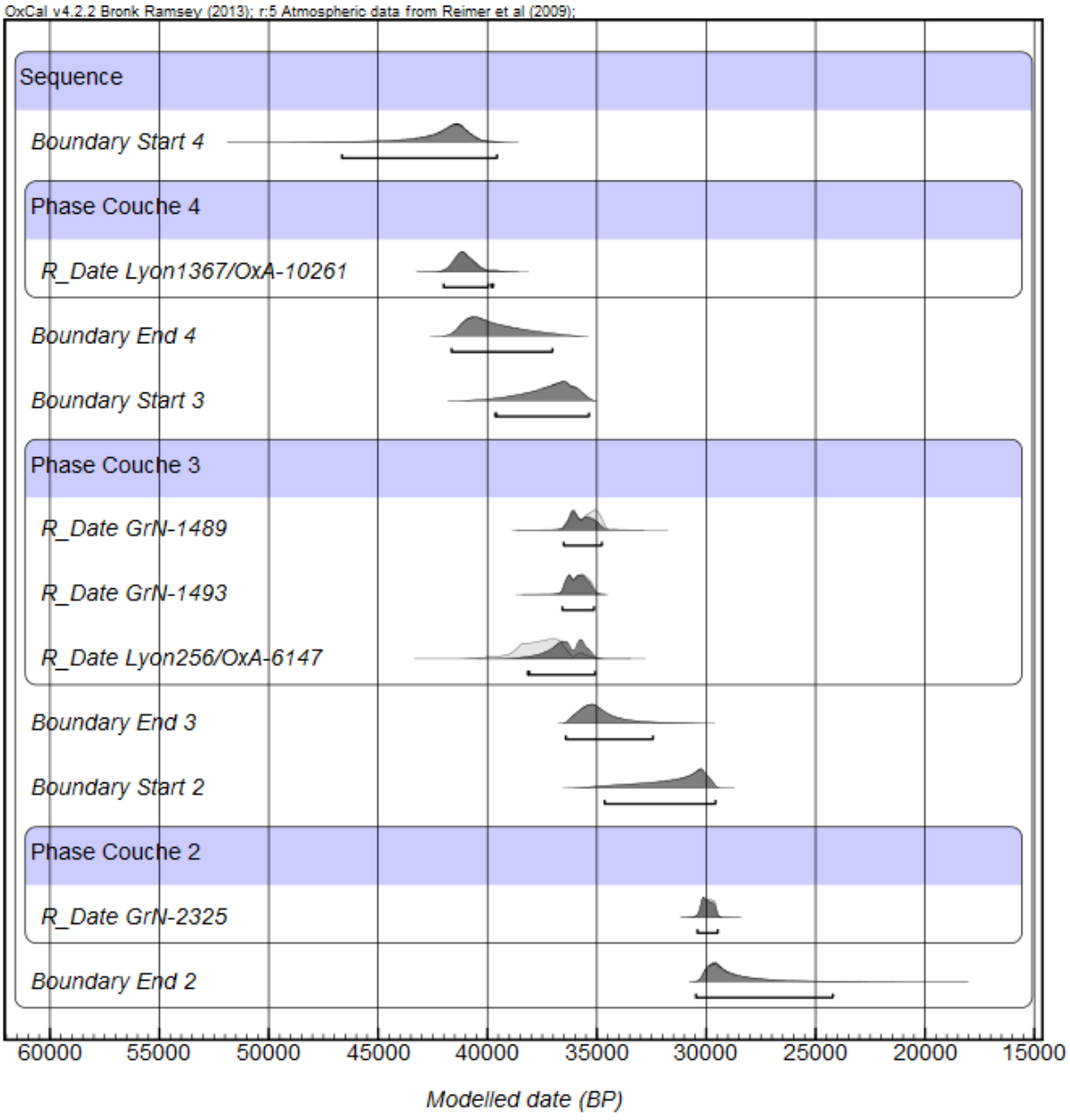

Figure 10.47: La Quina modelled dates

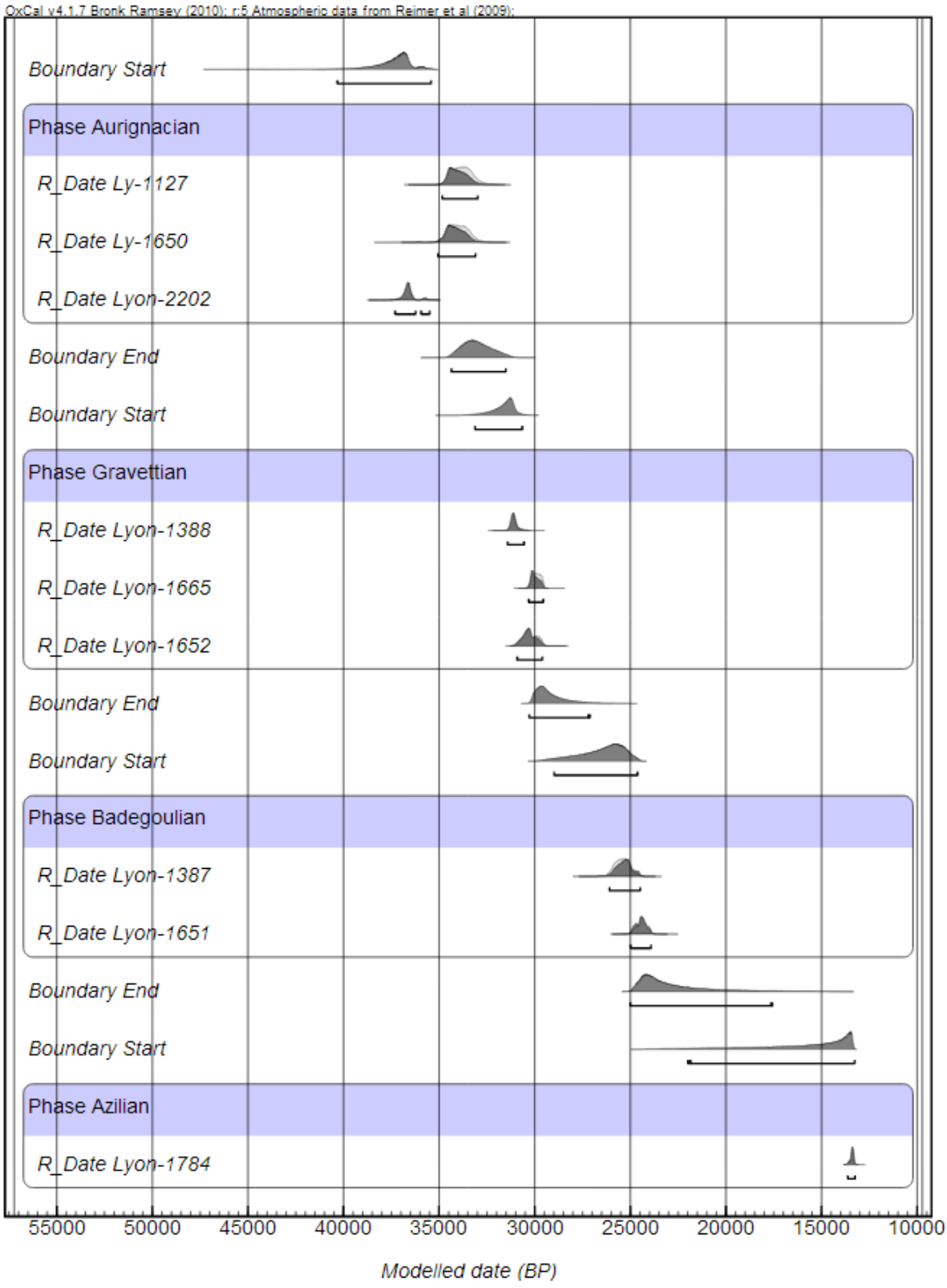

Figure 10.48: Renardieres modelled dates

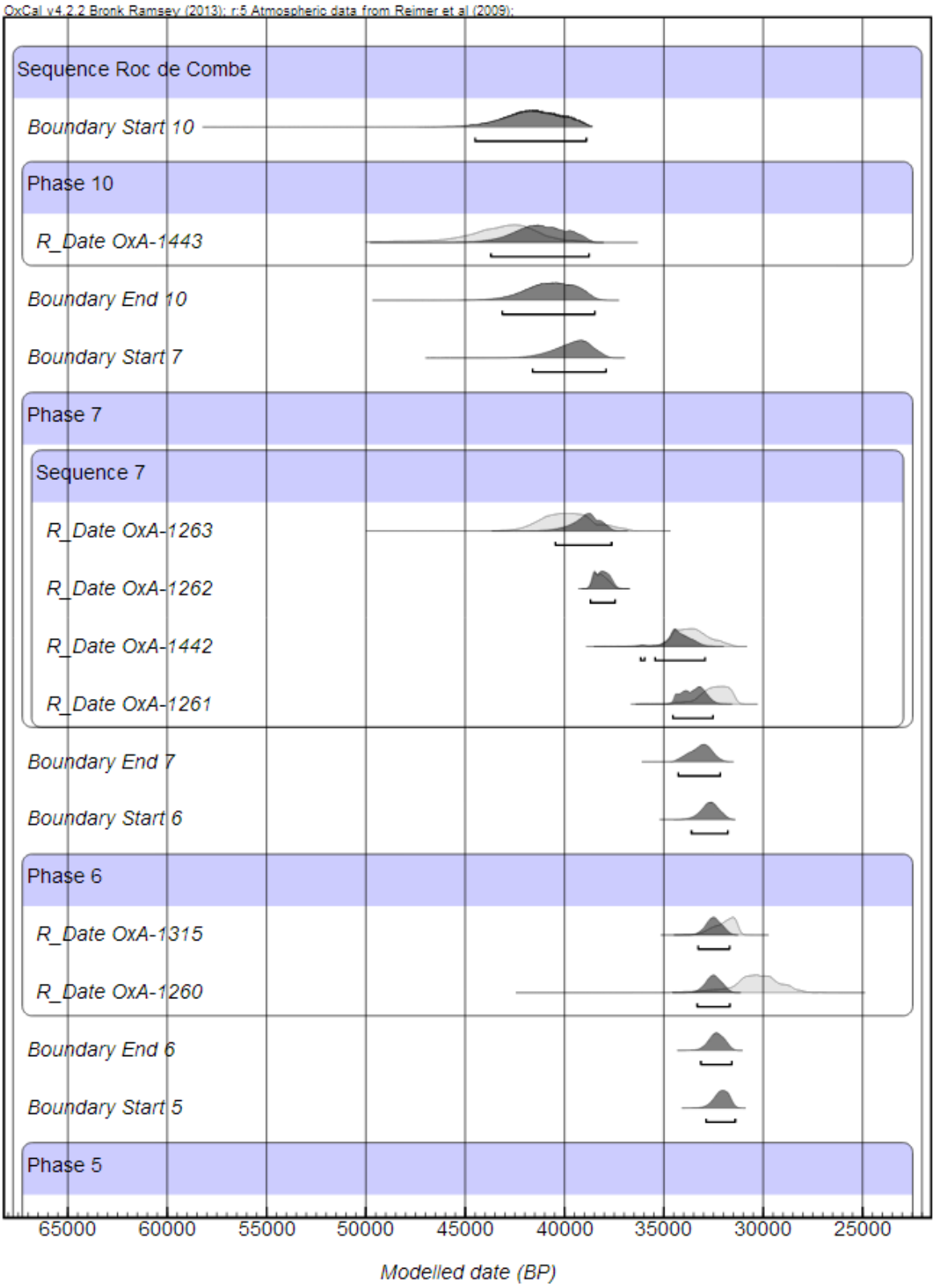

Figure 10.49: Roc de Combe modelled dates

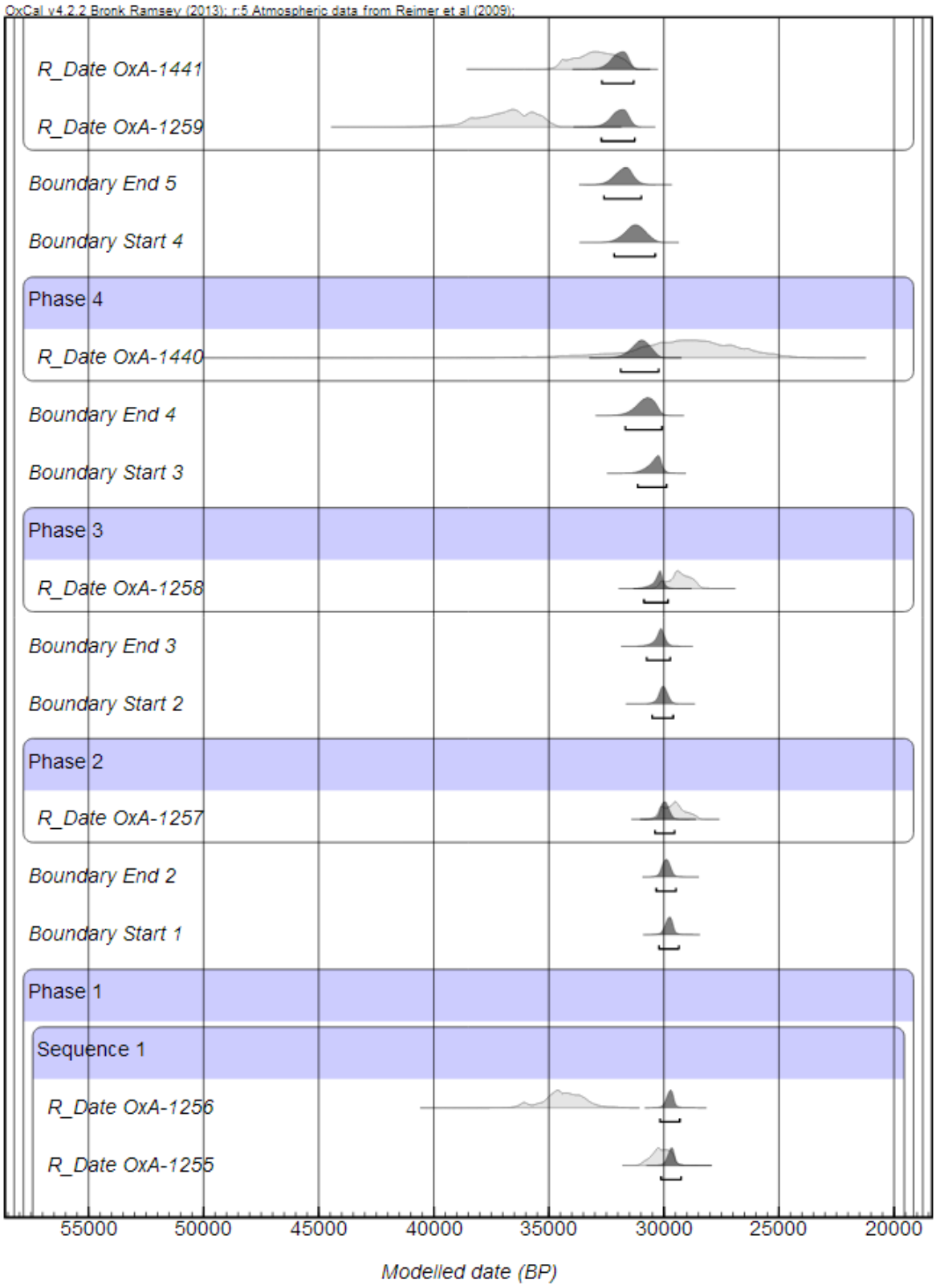

Figure 10.50: Roc de Combe modelled dates

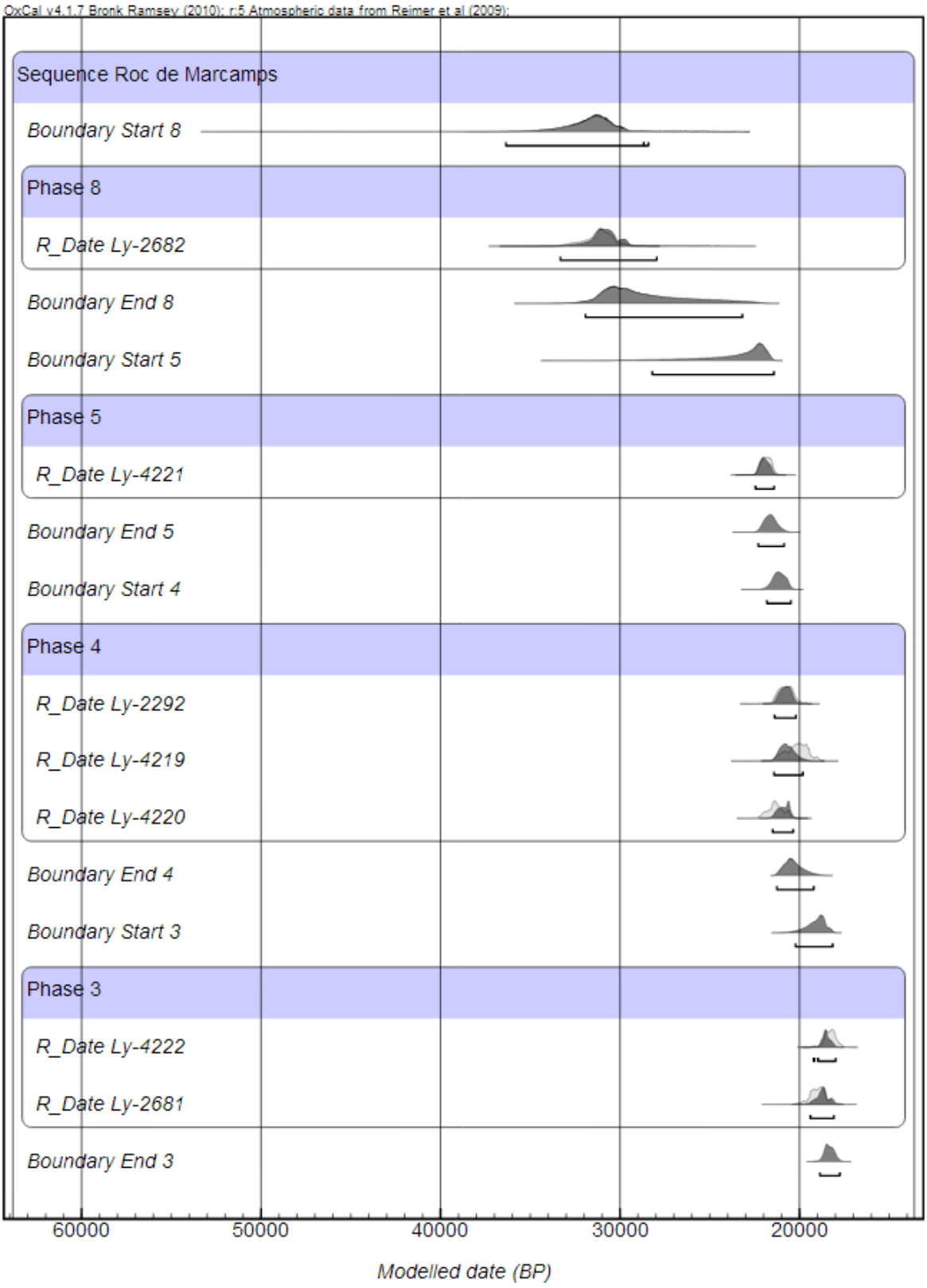

Figure 10.51: Roc de Marcamps modelled dates

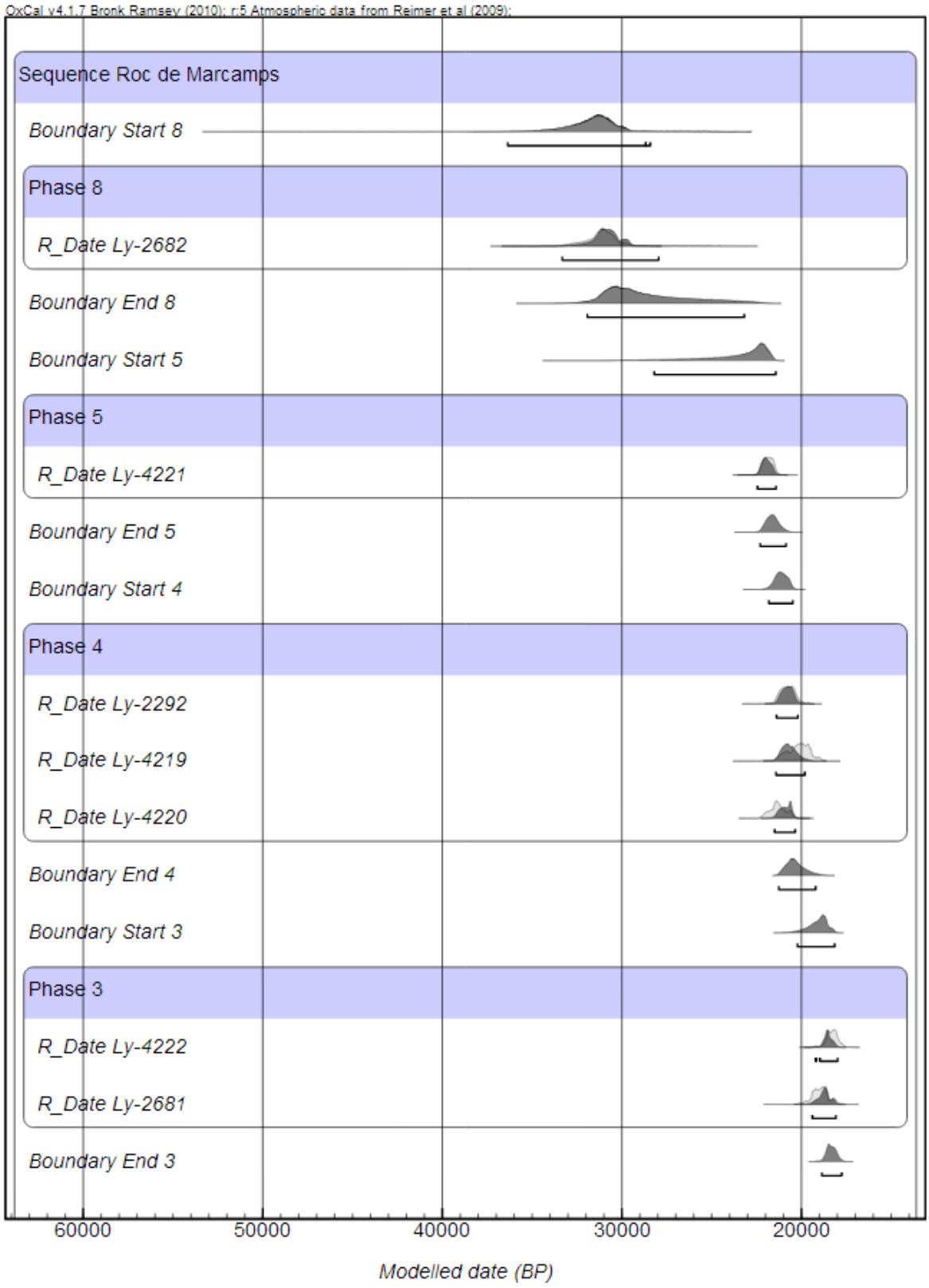

Figure 10.52: Roc de Marcamps modelled dates

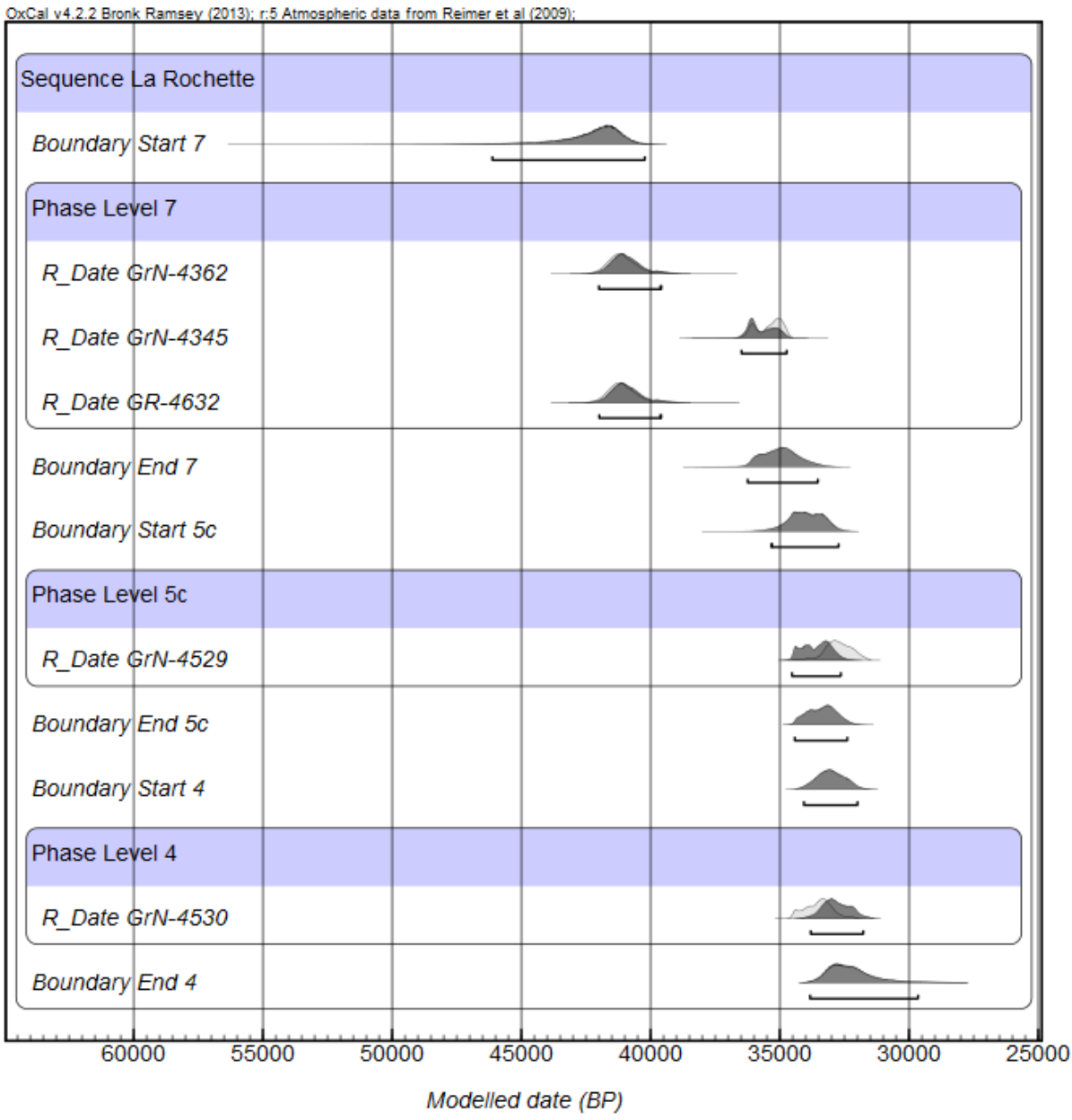

Figure 10.53: La Rochette modelled dates

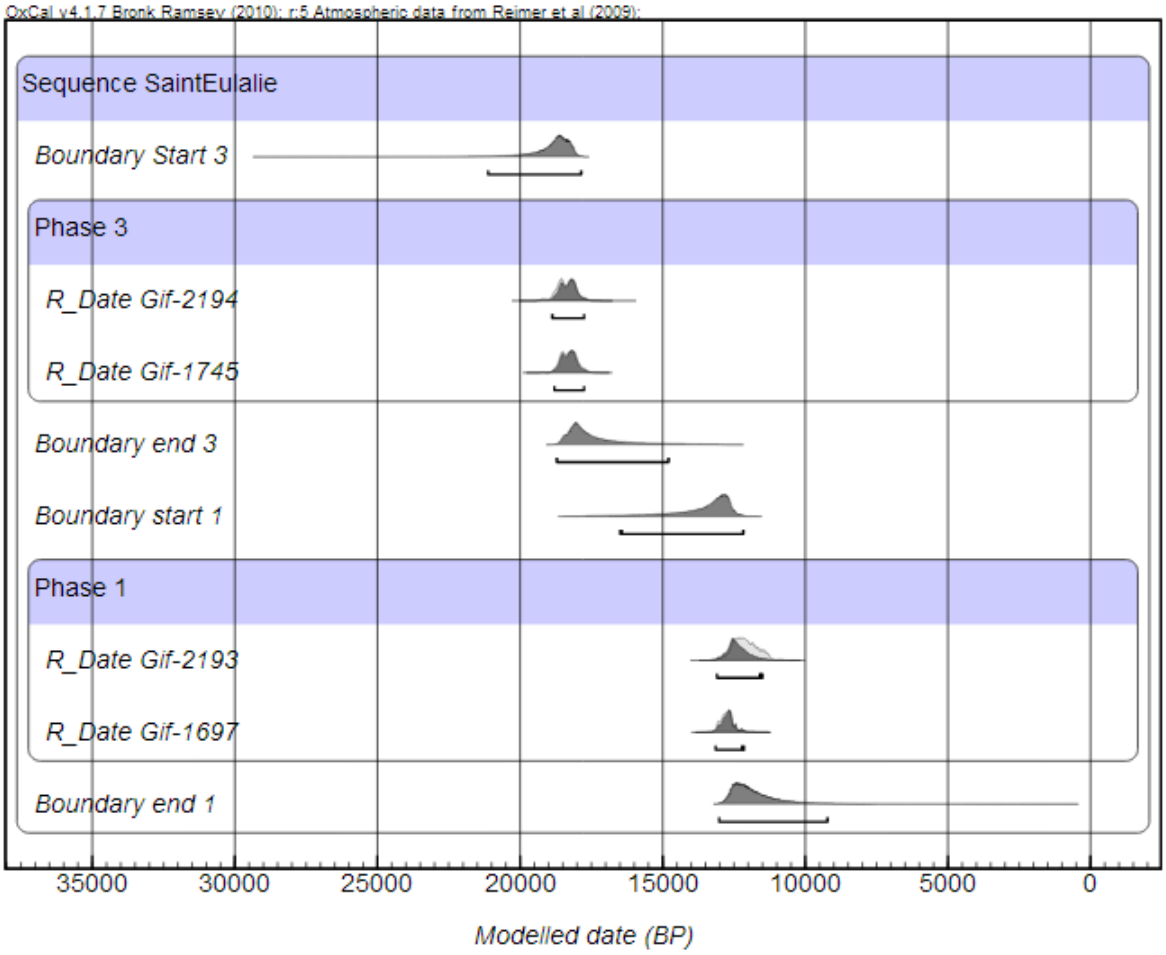

Figure 10.54: Sainte Eulalie modelled dates

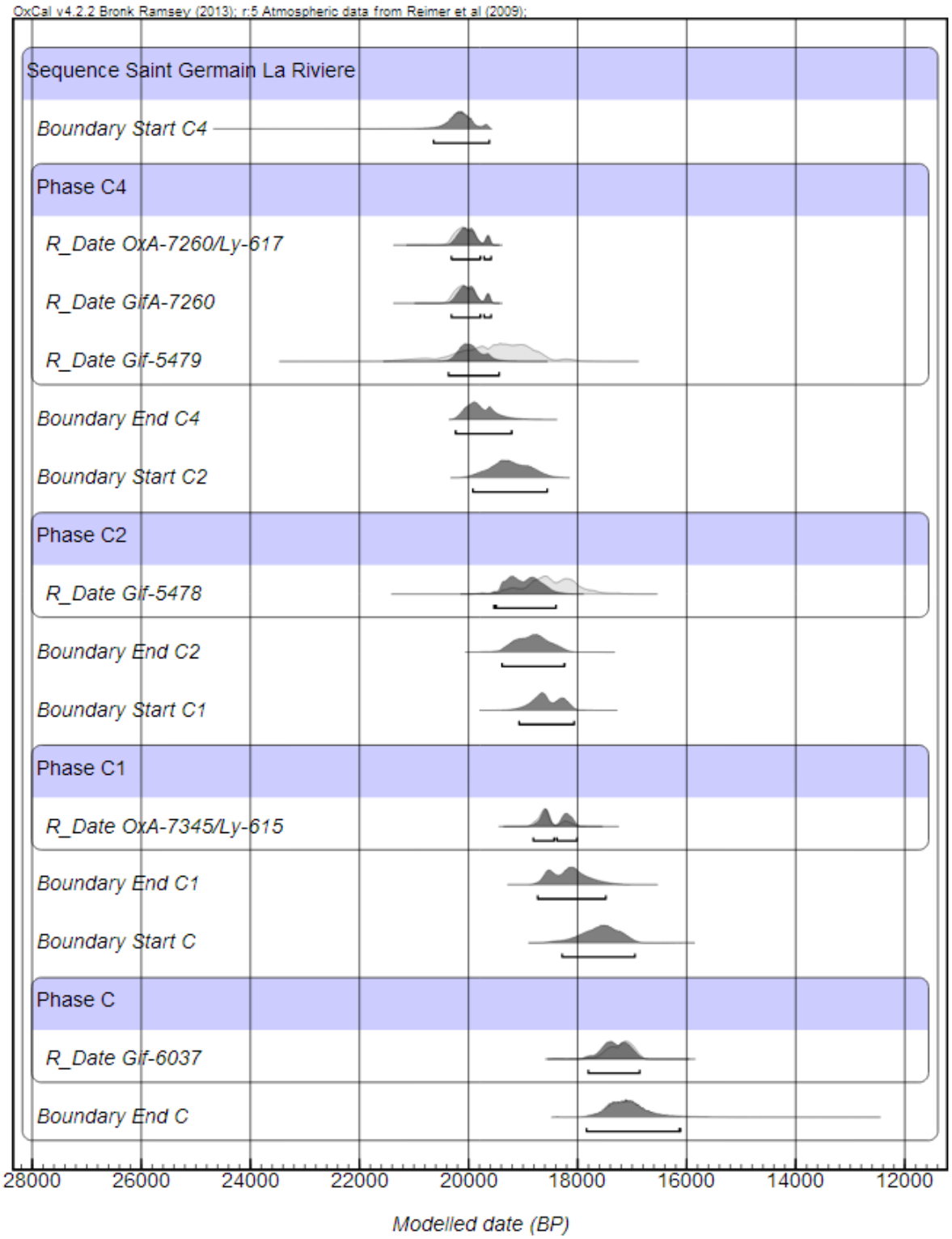

Figure 10.55: Saint Germain modelled dates

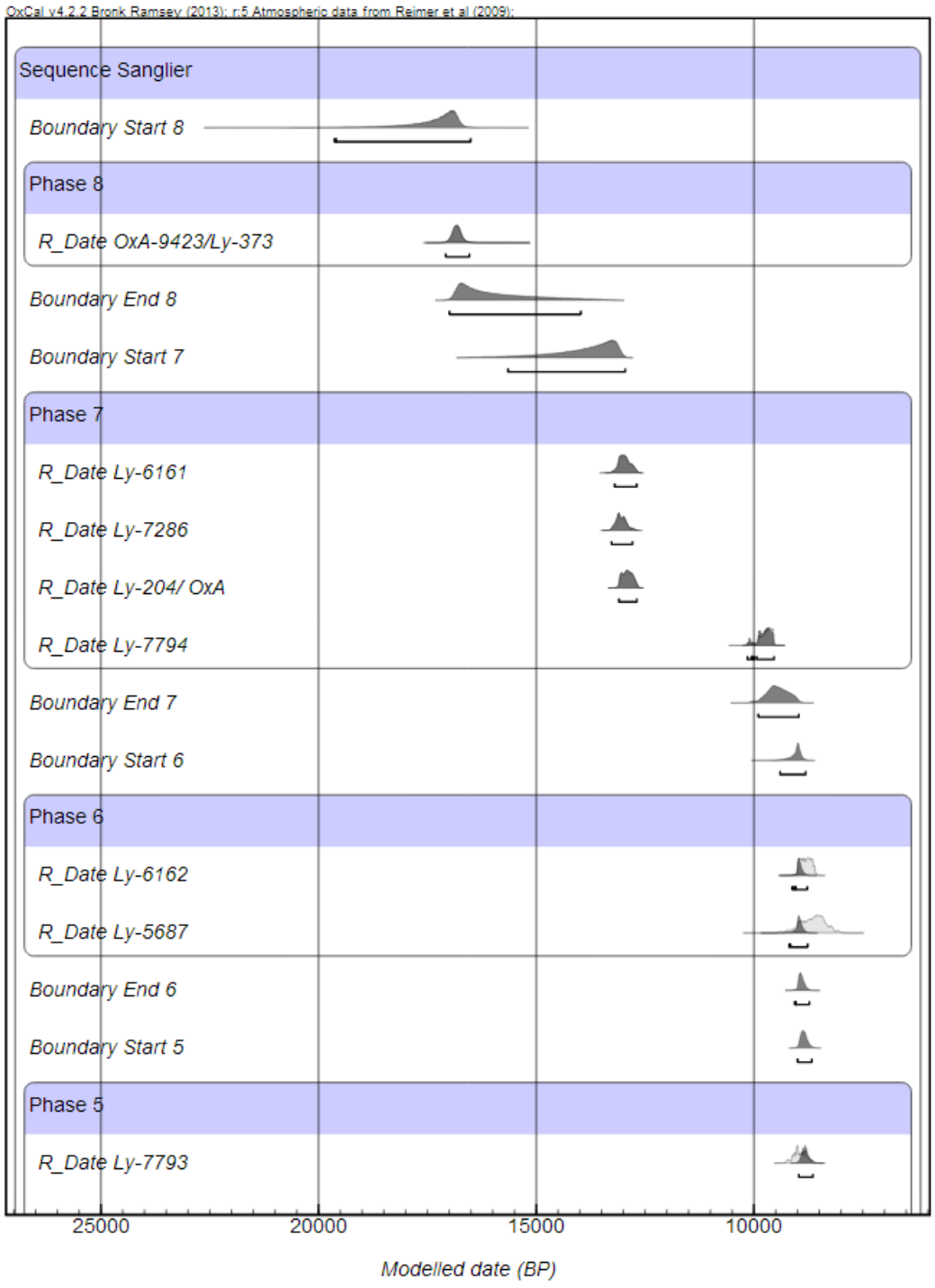

Figure 10.56: Sanglier modelled dates

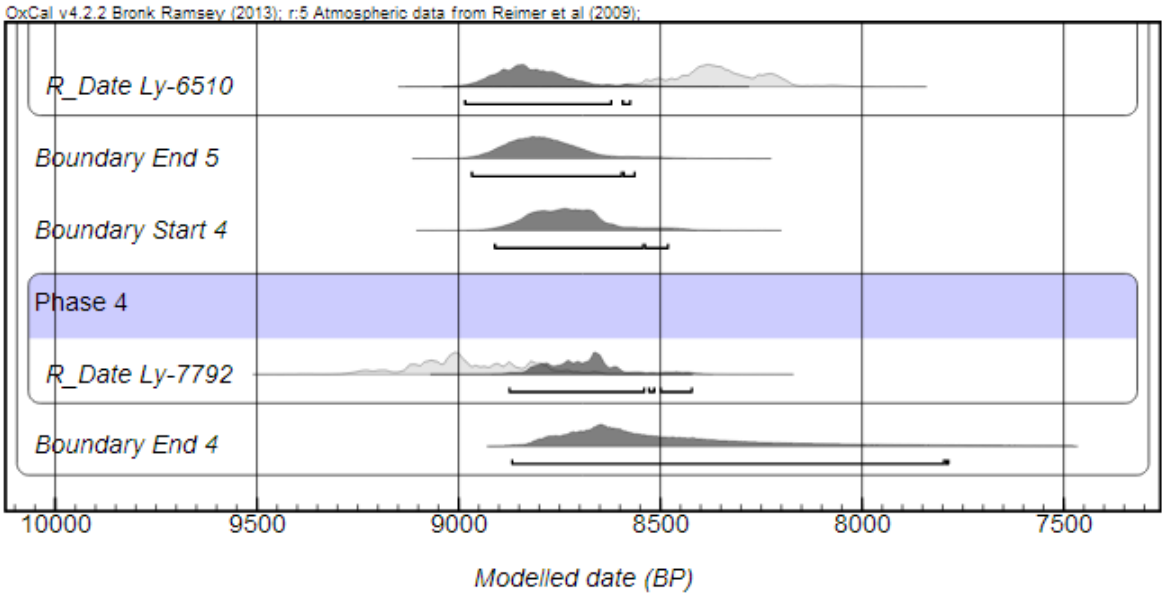

Figure 10.57: Sanglier modelled dates

§ 10.2 Radiocarbon dates used in this thesis

Table 10.7: Modelled radiocarbon dates used in this thesis: Radiocarbon dates that could be built into stratigraphic models. These are dates that occurred in sequences at well dated sites.

Site	Date	Technocomplex
Combe Saunière	Ly-3328 13910+/-230	Magdalenian
Combe Saunière	OxA-751 15190+/-200	Solutrean
Combe Saunière	OxA-753 19630+/-320	Solutrean
Combe Saunière	OxA-755 14890+/-200	Solutrean
Combe Saunière	OxA-756 15120+/-200	Solutrean
Combe Saunière	OxA-757 18860+/-320	Solutrean
Combe Saunière	OxA-459 15480+/-210	Magdalenian
Combe Saunière	OxA-481 14990+/-220	Magdalenian
Combe Saunière	Ly-3330 21940+/-350	Gravettian
Combe Saunière	OxA-758 21640+/-400	Gravettian
Combe Saunière	Ly-3329 17470+/-240	Solutrean
Combe Saunière	OxA-485 16300+/-220	Solutrean
Combe Saunière	OxA-488 17700+/-290	Solutrean
Combe Saunière	OxA-489 19450+/-330	Solutrean
Combe Saunière	OxA-752 19490+/-350	Solutrean
Combe Saunière	OxA-754 15200+/-200	Solutrean
Combe Saunière	OxA-410 15750+/-230	Magdalenian
Flageolet I	Ly-2726 27000+/-1000	Aurignacian
Flageolet I	Ly-2723 26150+/-600	Gravettian
Flageolet I	OxA-596 23250+/-500	Gravettian
Flageolet I	OxA-448 24600+/-700	Gravettian
Flageolet I	OxA-598 33800+/-1800	Aurignacian

Continued on next page

Table 10.7 – continued from previous page

Site	Date	Technocomplex
Flageolet I	GifA-95538 32040+/-850	Aurignacian
Flageolet I	GifA-95559 34300+/-1100	Aurignacian
Flageolet I	Ly-2725 27350+/-1400	Aurignacian
Flageolet I	Ly-2724 26800+/-1000	Aurignacian
Flageolet I	OxA-579 26500+/-900	Gravettian
Flageolet I	Ly-2722 24280+/-500	Gravettian
Flageolet I	Ly-2721 22520+/-500	Gravettian
Flageolet I	OxA-447 25700+/-700	Gravettian
Flageolet I	Ly-2185 18610+/-440	Gravettian
Flageolet II	Ly-917 14110+/-690	Magdalenian
Flageolet II	Ly-918 15250+/-320	Magdalenian
Flageolet II	Ly-1182 14250+/-400	Magdalenian
Flageolet II	Ly-916 12870+/-390	Magdalenian
Gandil	Gif-9176 15380+/-140	Magdalenian
Gandil	Gif-9175 15550+/-140	Magdalenian
Gandil	GifA-96307 17290+/-180	Badegoulian
Gandil	GifA-96351 16700+/-160	
Gandil	GifA-96350 16580+/-160	
Gandil	Ly-2483 15033 +/- 120	Magdalenian
Gandil	Ly-2484 16538 +/- 144	Badegoulian
Gandil	Ly-2485 16507 +/- 144	Badegoulian
Gandil	Ly-3592 15480 +/- 70	
Gandil	GifA-96305 17290 +/- 180	Badegoulian
Gandil	GifA-96416 16980+/-170	
Gandil	GifA-96417 17480+/-180	Magdalenian

Continued on next page

Table 10.7 – continued from previous page

Site	Date	Technocomplex
Gare de Couze	Ly-391 10900+/-230	Magdalenian
Gare de Couze	BM-1616 12540+/-75	Magdalenian
Gare de Couze	BM-1615 11230+/-180	Magdalenian
Gare de Couze	Ly-976 11750+/-310	Magdalenian
Gare de Couze	BM-1613 8260 +/- 130	Magdalenian
Gare de Couze	Ly-975 12430+/-320	Magdalenian
Gare de Couze	BM-1614 10190+/-200	Magdalenian
Grotte XVI	AA-2668 20070 +/- 330	
Grotte XVI	AA-2671 19750 +/- 270	
Grotte XVI	AA-2673 20550 +/- 260	
Grotte XVI	AA-2991 20410 +/- 380	
Grotte XVI	AA-2992 20280 +/- 220	
Grotte XVI	AA-6843 12285+/-100	Magdalenian
Grotte XVI	26340+/-470 (AA2670)	
Grotte XVI	AA-2669 20230 +/- 270	
Grotte XVI	AA-2670 26340 +/- 470	
Grotte XVI	AA-2672 21490 +/- 460	
Grotte XVI	AA-2993 20460 +/- 260	
Grotte XVI	AA-2994 19260 +/- 240	
Grotte XVI	AA-2995 21530 +/- 280	
Grotte XVI	AA-2996 20010 +/- 230	
Jean Blancs	Gif-8666 13790+/-120	Badegoulian
Jean Blancs	Gif-8669 13900+/-110	Badegoulian
Jean Blancs	Ly-4589 17770+/-260	Badegoulian
Jean Blancs	Ly-4889 19010+/-310	Solutrean

Continued on next page

Table 10.7 – continued from previous page

Site	Date	Technocomplex
Jean Blancs	Ly-4588 19010 +/- 210	Badegoulian
Jean Blancs	Gif-8668 16490+/-130	Badegoulian
Jean Blancs	GifA-97147 17650+/-200	Magdalenian
La Doue	Ly-2819 9260+/-200	Sauvetarrian
La Doue	Ly-2822 11520+/-170	Magdalenian
La Doue	Ly-2233 8750+/-150	Sauvetarrian
La Doue	Ly-2234 8880+/-160	Sauvetarrian
La Doue	Ly-2820 8980+/-160	Sauvettarian
La Doue	Ly-2821 8860+/-210	Sauvettarian
La Doue	Ly 2818 6390+/-290	Neolithic
La Faurélie II	Gif-3649 11780+/-180	Magdalenian
La Faurélie II	Lyon-5367 11180 +/- 70	
La Faurélie II	Lyon-5368 11010 +/- 60	
La Faurélie II	Lyon-5369 12980 +/- 80	
La Faurélie II	Lyon-5370 12070 +/- 70	
La Faurélie II	Lyon-5366 11850 +/- 70	
La Ferrassie (Abri)	Gif-4275 27100+/-320	Aurignacian
La Ferrassie (Abri)	Gif-2427 28820+/-1500	Aurignacian
La Ferrassie (Abri)	Gif-4274 27470+/-280	Aurignacian
La Ferrassie (Abri)	Gif-4272 25500+/-25	Aurignacian
La Ferrassie (Abri)	Gif-4266 26100+/-210	Aurignacian
La Ferrassie (Abri)	Gif-4270 23000+/-240	Aurignacian
La Ferrassie (Abri)	GrN-5750 30970+/-395	Aurignacian
La Ferrassie (Abri)	Gif-2701 23580+/-550	Aurignacian
La Ferrassie (Abri)	Gif-4264 23700+/-250	Aurignacian

Continued on next page

Table 10.7 – continued from previous page

Site	Date	Technocomplex
La Ferrassie (Abri)	OxA-402 27900+/-770	Gravettian
La Ferrassie (Abri)	GrN-5751 33220+/-570	Aurignacian
La Ferrassie (Abri)	Gif-4277 31300+/-300	Aurignacian
La Ferrassie (Abri)	OxA-409 28600+/-1050	Aurignacian
La Ferrassie (Abri)	Gif-4273 26750+/-250	Aurignacian
La Ferrassie (Abri)	Gif-4271 28700+/-250	Aurignacian
La Ferrassie (Abri)	OxA-405 29000+/-850	Aurignacian
La Ferrassie (Abri)	Gif-4267 21070+/-170	Aurignacian
La Ferrassie (Abri)	Gif-4268 22700+/-240	Aurignacian
La Ferrassie (Abri)	Gif-4269 23700+/-240	Aurignacian
La Ferrassie (Abri)	Gif-4265 22200+/-650	Aurignacian
La Ferrassie (Abri)	Gif-2696 23960+/-550	Gravettian
La Ferrassie (Abri)	Gif-2698 24650+/-550	Gravettian
La Ferrassie (Abri)	Gif-2699 22520+/-500	Gravettian
La Ferrassie (Abri)	Gif-2700 22520+/-500	Gravettian
La Ferrassie (Abri)	OxA-404 26250+/-620	Gravettian
La Ferrassie (Abri)	OxA-403 27530+/-720	Gravettian
La Madeleine	Ly-922 13440+/-300	Magdalenian
La Madeleine	Ly-921 13070+/-190	Magdalenian
La Madeleine	Ly-920 12750+/-240	Magdalenian
La Madeleine	Ly-919 12640+/-260	Magdalenian
La Quina	Lyon1367/OxA-10261 35950+/-450	Chatelperronian
La Quina	Lyon256/OxA-6147 32650 +/- 850	Aurignacian
La Quina	GrN-1489 30760+/-490	Aurignacian
La Quina	GrN-1493 31400+/-350	Aurignacian

Continued on next page

Table 10.7 – continued from previous page

Site	Date	Technocomplex
La Quina	GrN-2325 25070+/-220	Aurignacian
La Rochette	GrN-4529 28420+/-320	Aurignacian
La Rochette	GrN-4530 28860+/-300	Aurignacian
La Rochette	GrN-4362 36000 +/- 550	Mousterian
La Rochette	GR-4632 36000 +/- 550	Mousterian
La Rochette	GrN-4345 30700 +/- 400	Mousterian
Laugerie Haute	Ly-972 18260+/-360	Badegoulian
Laugerie Haute	Ly-973 17040+/-440	Magdalenian
Laugerie Haute	GrN-4573 20750+/-150	Solutrean
Laugerie Haute	GrN-4446 20810+/-230	Solutrean
Laugerie Haute	GrN-4469 20160+/-100	Solutrean
Laugerie Haute	OxA/Ly-1175 20360+/-160	Solutrean
Laugerie Haute	GrN-4442 19600+/-140	Solutrean
Laugerie Haute	OxA/Ly-1174 20195+/-265	Solutrean
Laugerie Haute	GifA-100630 19600+/-200	Solutrean
Laugerie Haute	GrN-4605 19870+/-190	Solutrean
Laugerie Haute	OxA/Ly-1173 19525+/-155	Solutrean
Laugerie Haute	GrN-1888 20890+/-300	Solutrean
Laugerie Haute	Ly-974 13970+/-480	Magdalenian
Laugerie Haute	GifA-100632 20690+/-210	Solutrean
Laugerie Haute	GrN-4495 19740+/-140	Solutrean
Laugerie Haute	GrN-4441 20000+/-240	Solutrean
Laugerie Haute	GrN-1876 21980+/-250	Gravettian
Laugerie Haute	OxA-492 14770+/-180	Magdalenian
Laugerie Haute	OxA-480 14730+/-250	Magdalenian

Continued on next page

Table 10.7 – continued from previous page

Site	Date	Technocomplex
Laugerie Haute	OxA-759 14320+/-180	Magdalenian
Laugerie Haute	OxA-760 15730+/-200	Magdalenian
Laugerie Haute	OxA-761 14320+/-180	Magdalenian
Laugerie Haute	OxA-762 14100+/-180	Magdalenian
Le Bessol (Chez Jugie)	Ly-1331 8040 +/-260	Sauvettarian
Le Bessol (Chez Jugie)	Ly-1651 7650+/-510	Sauvettarian
Le Bessol (Chez Jugie)	Ly-1652 8080+/-280	Sauvettarian
Le Bessol (Chez Jugie)	Ly-1330 1860+/-200	Le Martinet
Le Bessol (Chez Jugie)	Ly-1395 4540+/-200	Le Martinet
Le Bessol (Chez Jugie)	Ly-1396 7060+/-140	Sauvettarian
Le Bessol (Chez Jugie)	Ly-1600 7010+/-430	Sauvettarian
Le Bessol (Chez Jugie)	Ly-1572 11840+/-580	Azilian
Le Bessol (Chez Jugie)	Ly-1601 11730+/-530	Azilian
Le Bessol (Chez Jugie)	Ly-1802 13000+/-1000	pre-Azilian
Le Cuzoul de Vers	Gif-6370 18300+/-200	Badegoulian
Le Cuzoul de Vers	Gif-6798 18400+/-200	Badegoulian
Le Cuzoul de Vers	Gif-6371 16800+/-170	Magdalenian
Le Cuzoul de Vers	Gif-6797 17050+/-170	Magdalenian
Le Cuzoul de Vers	Lyon-1679 19540 +/- 310	Magdalenian
Le Cuzoul de Vers	Lyon- 1674 18730 +/- 110	Magdalenian
Le Cuzoul de Vers	Lyon-1675 19970 +/- 270	Magdalenian
Le Cuzoul de Vers	Lyon-1677 19800 +/- 190	Magdalenian
Le Cuzoul de Vers	Lyon-1678 19280 +/- 120	Magdalenian
Le Cuzoul de Vers	Lyon-1680 19950 +/- 319	Magdalenian
Le Cuzoul de Vers	Lyon-1681 19020 +/- 110	Magdalenian

Continued on next page

Table 10.7 – continued from previous page

Site	Date	Technocomplex
Le Cuzoul de Vers	Lyon-1682 19510 +/- 110	Magdalenian
Le Cuzoul de Vers	Gif-6699 19400+/-210	Solutrean
Le Cuzoul de Vers	Gif-6372 14560+/-130	Magdalenian
Le Cuzoul de Vers	Gif-6638 15980+/-150	Magdalenian
Le Facteur	OxA-584 24210+/-500	Gravettian
Le Facteur	Gsy-67 27890+/-200	Aurignacian
Le Facteur	Gsy-69 23180+/-1500	Gravettian
Le Facteur	OxA-583 24720+/-600	Gravettian
Le Facteur	OxA-585 24400+/-600	Gravettian
Le Facteur	OxA-586 24690+/-600	Gravettian
Le Facteur	OxA-594 25450+/-650	Gravettian
Le Facteur	OxA-595 25630+/-650	Gravettian
Le Morin	OxA-19699 13065+/-60	Magdalenian
Le Morin	OxA-19826 12945+/-50	Magdalenian
Le Morin	OxA-19827 12630+/-60	Magdalenian
Le Morin	OxA-19828 12690+/-60	Magdalenian
Le Morin	OxA-19829 12380+/-55	Magdalenian
Le Moulin du Roc	AA 5526 4050 +/- 80	Neolithic
Le Moulin du Roc	AA-5525 4390 +/- 100	Neolithic
Le Moulin du Roc	Ly-5444 11340+/-170	Magdalenian
Le Moulin du Roc	Ly-5445 15600+/-1200	Magdalenian
Le Moulin du Roc	Beta-180049 12890 +/- 50	Magdalenian
Le Moulin du Roc	Beta-180048 12700 +/- 50	Magdalenian
Le Piage	Gif-5030 25700+/-500	Aurignacian
Le Piage	Gif-5027 29000+/-1000	Aurignacian

Continued on next page

Table 10.7 – continued from previous page

Site	Date	Technocomplex
Le Piage	Gif-5026 18900+/-250	Solutrean
Le Piage	Gif-5029 24900+/-450	Aurignacian
Le Piage	Gif-5028 25700+/-500	Aurignacian
Le Placard	Gif-8800 18370+/-200	Badegoulian
Le Placard	GifA-91184 19970+/-250	Solutrean
Le Placard	GifA-92083 20310+/-220	Solutrean
Le Placard	Gif-8803 16300+/-190	Magdalenian
Le Placard	Gif-8804 17320+/-160	Badegoulian
Le Placard	Gif-8801 17440+/-200	Badegoulian
Le Placard	GifA-92084 20210+/-260	Solutrean
Le Pont d'Ambon	Gif-2570 9830+/-130	Magdalenian
Le Pont d'Ambon	Gif-3739 12130+/-160	Azilian
Le Pont d'Ambon	Gif-7222 8750+/-1000	Azilian
Le Pont d'Ambon	Gif-3369 12840+/-220	Magdalenian
Le Pont d'Ambon	Gif-3368 10350+/-190	Azilian
Le Pont d'Ambon	Gif-3561 9990+/-250	Azilian
Le Pont d'Ambon	Gif-7223 11600+/-120	Azilian
Le Pont d'Ambon	Gif-3740 9640+/-120	Azilian
Le Pont d'Ambon	GifA-99102 10730+/-100	Mesolithic
Le Quéroy	Gif-5129 9460+/-170	Azilian
Le Quéroy	Gif-5130 10150+/-180	
Le Quéroy	Gif-5325 12590+/-140	
Le Quéroy	Gif-5324 12800+/-140	
Les Peyrugues	GifA-92169 22400+/-280	Gravettian
Les Peyrugues	Gif-7998 24800+/-500	Gravettian

Continued on next page

Table 10.7 – continued from previous page

Site	Date	Technocomplex
Les Peyrugues	GifA-96230 24590 +/- 700	Protomag
Les Peyrugues	Lyon-3594 17890 +/- 100	Gravettian
Les Peyrugues	GifA-95474 21700 +/- 250	Solutrean
Les Peyrugues	Lyon-3595 23520 +/- 180	Gravettian
Les Peyrugues	GifA-92170 25270 +/- 320	Gravettian
Les Peyrugues	Ly-3593 18910 +/- 110	Gravettian
Les Peyrugues	Ly-3596 23150 +/- 170	Gravettian
Les Peyrugues	GifA-92224 22750 +/- 250	Protomag
Les Peyrugues	Gif-7529 13020 +/- 140	Magdalenain
Les Peyrugues	GifA-92168 20290+/-230	Solutrean
Les Peyrugues	Lyon-3599 13700 +/- 60	Magdalenian
Les Peyrugues	Lyon-3600 13960 +/- 100	Magdalenian
Les Peyrugues	GifA-96224 22750 +/- 250	Gravettian
Les Peyrugues	GifA-95446 16140 +/- 150	Badegoulian
Les Peyrugues	GifA-95450 15940 +/- 150	Badegoulian
Les Peyrugues	GifA-93085 16960 +/- 190	Badegoulian
Les Peyrugues	GifA-96227 17560 +/- 160	Badegoulian
Les Peyrugues	GifA-96228 18600 +/- 140	Badegoulian
Les Peyrugues	GifA-92166 19310 +/- 210	Solutrean
Les Peyrugues	GifA-92167 19410 +/- 210	Solutrean
Les Peyrugues	GifA-93089 18660 +/- 210	Badegoulian
Les Peyrugues	GifA-93084 18740 +/- 200	Badegoulian
Les Peyrugues	GifA-96225 19410 +/- 200	Solutrean
Les Peyrugues	GifA-95460 20910 +/- 220	Solutrean
Les Peyrugues	GifA-91419 19970 +/- 210	Solutrean

Continued on next page

Table 10.7 – continued from previous page

Site	Date	Technocomplex
Les Peyrugues	GifA-95461 20110 +/- 210	Solutrean
Les Peyrugues	GifA-91410 20400 +/- 220	Solutrean
Les Peyrugues	GifA-91186 20410 +/- 280	Solutrean
Les Peyrugues	GifA-91427 20470 +/- 290	Solutrean
Les Peyrugues	GifA-91417 20750 +/- 240	Solutrean
Les Renardières	Ly-1650/GrA-? 29440+/-490	Aurignacian
Les Renardières	Lyon-1388 26600 +/- 240	Gravettian
Les Renardières	Lyon-1652 25460 +/- 310	Gravettian
Les Renardières	Lyon-2202 32170 +/- 220	Aurignacian
Les Renardières	Ly-1127/OxA-? 29200+/-450	Aurignacian
Les Renardières	Lyon-1387 21270 +/- 280	Badegoulian
Les Renardières	Lyon-1665 25065 +/- 135	Gravettian
Les Renardières	Lyon-1651 20430 +/- 180	Badegoulian
Les Renardières	Lyon-1784 11550 +/- 70	Azilian
Montgaudier	BM-2308 11930 +/- 190	Magdalenian
Montgaudier	BM-2309 14770 +/- 270	Magdalenian
Montgaudier	BM-2310 11690 +/- 170	Magdalenian
Montgaudier	BM-2311 20870 +/- 370	
Montgaudier	BM-1911 11450+/-70	Magdalenian
Montgaudier	BM-1912 12180+/-130	Magdalenian
Pégourié	Ly-1834 17320+/-420	Badegoulian
Pégourié	Gif-2568 8450+/-190	Azilian
Pégourié	Ly-1392 12690+/-530	Azilian
Pégourié	Ly-1598 13980+/-510	Azilian
Pégourié	Ly-1832 11870+/-290	Azilian

Continued on next page

Table 10.7 – continued from previous page

Site	Date	Technocomplex
Pégourié	Ly-1391 11680+/-330	Azilian
Pégourié	Ly-1833 11850+/-280	Azilian
Pégourié	Ly-1837 8450+/-310	Azilian
Pégourié	Ly-1838 8310+/-220	Azilian
Pégourié	Ly-1830 15830+/-400	Magdalenian
Pégourié	Ly-1835 24200+/-1100	Gravettian
Pégourié	Ly-1836 17420+/-390	Magdalenian
Pégourié	Ly-1394 17490+/-520	Badegoulian
Pégourié	Ly-5257 16890+/-300	Badegoulian
Pégourié	Gif-2822 12250+/-350	Azilian
Pégourié	Ly-1390 11290+/-320	Azilian
Pégourié	Ly-5258 16090+/-320	Azilian
Pataud	OxA-580 20400+/-600	Gravettian
Pataud	GrN-4610 33300+/-760	Aurignacian
Pataud	GrN-4720 33330+/-410	Aurignacian
Pataud	GrN-4309 32600+/-550	Aurignacian
Pataud	GrN-6163 31800+/-280	Aurignacian
Pataud	GrN-6274 31080+/-290	Aurignacian
Pataud	GrN-3105 29300+/-450	Aurignacian
Pataud	GrN-3116 32900+/-700	Aurignacian
Pataud	GrN-3117 32800+/-450	Aurignacian
Pataud	GrN-6273 28510+/-280	Aurignacian
Pataud	OxA-582 24340+/-700	Aurignacian
Pataud	Ly-100 23800+/-800	Gravettian
Pataud	Ly-300 22000+/-1000	Gravettian

Continued on next page

Table 10.7 – continued from previous page

Site	Date	Technocomplex
Pataud	GrN-4631 21780+/-215	Gravettian
Pataud	GrN-4634 28150+/-225	Gravettian
Pataud	Gx-1369 26720+/-460	Gravettian
Pataud	Gx-1370 27545+/-320	Gravettian
Pataud	Gx-1371 25815+/-330	Gravettian
Pataud	W-151 23600+/-800	Gravettian
Pataud	OxA-374 26300+/-900	Gravettian
Pataud	OxA-166 26100+/-900	Gravettian
Pataud	OxA-687 25500+/-700	Gravettian
Pataud	GrN-3230 34760+/-1000	Gravettian
Pataud	GrN-4721 23010+/-170	Gravettian
Pataud	OxA-163 23180+/-670	Gravettian
Pataud	OxA-599 21740+/-450	Gravettian
Pataud	OxA-686 24500+/-600	Gravettian
Pataud	GrN-1885 19300+/-170	Gravettian
Pataud	GrN-2115 20340+/-200	Gravettian
Pataud	OxA-162 22000+/-600	Gravettian
Pataud	OxA-373 20400+/-450	Gravettian
Pataud	GrN-4507 34250+/-675	Aurignacian
Pataud	GrN-4310 31000+/-500	Aurignacian
Pataud	GrN-4327 33000+/-500	Aurignacian
Pataud	GrN-4719 33260+/-425	Aurignacian
Pataud	GrN-4326 32000+/-800	Aurignacian
Pataud	GrN-4531 31800+/-310	Aurignacian
Pataud	OxA-689 26600+/-800	Aurignacian

Continued on next page

Table 10.7 – continued from previous page

Site	Date	Technocomplex
Pataud	OxA-690 26600+/-800	Aurignacian
Pataud	GrN-4477 26600+/-200	Gravettian
Pataud	GrN-4662 27660+/-260	Gravettian
Pataud	GrN-5009 23350+/-170	Gravettian
Pataud	Gx-1372 26340+/-450	Gravettian
Pataud	OxA-169 28400+/-1100	Gravettian
Pataud	W-191 24000+/-1000	Gravettian
Pataud	OxA-168 26900+/-1000	Gravettian
Pataud	GrN-4280 27060+/-370	Gravettian
Pataud	GrN-6271 22040+/-175	Gravettian
Pataud	OxA-167 26500+/-980	Gravettian
Pataud	GrN-1864 18470+/-280	Gravettian
Pataud	GrN-1892 21540+/-160	Gravettian
Pataud	GrN-4506 22780+/-140	Gravettian
Pataud	OxA-164 24250+/-750	Gravettian
Pataud	OxA-165 24440+/-740	Gravettian
Pataud	GrN-1857 20960+/-220	Gravettian
Pataud	GrN-1861 20780+/-170	Gravettian
Pataud	GrN-1862 21940+/-250	Gravettian
Pataud	GrN-2081 20540+/-140	Gravettian
Pataud	GrN-2100 20240+/-200	Gravettian
Pataud	GrN-2123 19780+/-170	Gravettian
Pataud	GrN-3255 19650+/-300	Gravettian
Pataud	GrN-4230 20810+/-170	Gravettian
Pataud	GrN-4231 21380+/-340	Gravettian

Continued on next page

Table 10.7 – continued from previous page

Site	Date	Technocomplex
Pataud	GrN-5452 20350+/-200	Gravettian
Pataud	GrN-5453 20230+/-190	Gravettian
Pataud	GrN-5454 20860+/-215	Gravettian
Pataud	GrN-2064 17605 +/- 420	Gravettian
Pataud	GrN-6272 23870+/-180	Gravettian
Pataud	GrN-2054 15080 +/- 100	Gravettian
Pille Bourse (Saint Germain la Rivière)	Gif-5479 16200+/-600	Magdalenian
Pille Bourse (Saint Germain la Rivière)	OxA-7260/Ly-617 16890+/-130	Magdalenian
Pille Bourse (Saint Germain la Rivière)	Gif-5478 15300+/-410	Magdalenian
Pille Bourse (Saint Germain la Rivière)	Gif-7345/Ly-615 15330+/-150	Magdalenian
Roc de Combe	OxA-1254 32000 +/- 1000	Gravettian
Roc de Combe	OxA-1255 25300 +/- 400	Gravettian
Roc de Combe	OxA-1256 29800 +/- 750	Gravettian
Roc de Combe	OxA-1257 24700 +/- 400	Gravettian
Roc de Combe	OxA-1258 24500 +/- 400	Gravettian
Roc de Combe	OxA-1440 24000 +/- 1900	Gravettian
Roc de Combe	OxA-1259 32000 +/- 1000	Aurignacian
Roc de Combe	OxA-1260 25500 +/- 1200	Aurignacian
Roc de Combe	OxA-1315 27500+/-500	Aurignacian
Roc de Combe	OxA-1261 28000+/-550	Aurignacian
Roc de Combe	OxA-1442 29100 +/-700	Aurignacian
Roc de Combe	OxA-1443 38000+/-2000	Chatelperronian
Roc de Combe	OxA-1263 34800+/-1200	Aurignacian
Roc de Combe	OxA-1262 33400+/-1100	Aurignacian
Roc de Combe	OxA-1441 28500+/-700	Aurignacian

Continued on next page

Table 10.7 – continued from previous page

Site	Date	Technocomplex
Roc de Marcamps	Ly-2682 26520+/-830	Aurignacian
Roc de Marcamps	Ly-4219 16840+/-520	Aurignacian
Roc de Marcamps	Ly-4220 17880+/-280	Magdalenian
Roc de Marcamps	Ly-4221 18290+/-230	Magdalenian
Roc de Marcamps	Ly-2680 13570+/-420	Magdalenian
Roc de Marcamps	Ly-4222 15070+/-270	Magdalenian
Roc de Marcamps	Ly-2292 17410+/-310	Magdalenian
Roc de Marcamps	Ly-2290 14200+/-190	Magdalenian
Roc de Marcamps	Ly-2291 14910+/-240	Magdalenian
Roc de Marcamps	Ly-2681 15700+/-450	Magdalenian
Saint Germain la Rivière	Gif-6037 14100+/- 160	Magdalenian
Saint Germain la Rivière	GifA-7260 16890 +/- 130	Magdalenian
Sainte Eulalie	Gif-2194 15200+/-300	Magdalenian
Sainte Eulalie	Gif-1745 15100+/-270	Magdalenian
Sainte Eulalie	Gif-1697 10830+/-200	Magdalenian
Sainte Eulalie	Gif-2193 10400+/-300	Magdalenian
Sanglier	OxA-9423/Ly-373 13700+/-90	Magdalenian
Sanglier	Ly-6161 11100+/-100	Azilian
Sanglier	Ly-7286 11180+/-80	Azilian
Sanglier	Ly-204/ OxA 11025+/-70	Azilian
Sanglier	Ly-6162 7943+/-76	Sauvettarian
Sanglier	Ly-7792 8075+/-75	Sauvettarian
Sanglier	Ly-7793 8065+/-80	Sauvettarian
Sanglier	Ly-5687 7753+/-235	Sauvettarian
Sanglier	Ly-6510 7557+/-104	Sauvettarian

Continued on next page

Table 10.7 – continued from previous page

Site	Date	Technocomplex
Sanglier	Ly-7794 8710+/-75	Mesolithic

Table 10.8: Unmodelled radiocarbon dates used in this thesis: Radiocarbon dates that could be built into stratigraphic models. These are dates that occurred in sequences at well dated sites.

Site	Date	Technocomplex
Montgaudier	BM-1913 18050+/-230	Magdalenian
Montgaudier	BM-1914 18180+/-1070	Magdalenian
Montgaudier	BM-2307 18090 +/- 650	Magdalenian
Andreé Ragout	GrN-4677 12890+/-140	Badegoulian
Andreé Ragout	GrN-4693 9490+/-90	Badegoulian
Le Placard	Gif-8802 18470+/-300	Solutrean
Les Garennes	Beta-216141 27110+/-210	Gravettian
Les Garennes	Beta-216142 26790+/-190	Gravettian
La Roche a Pierrot	Ly-2193 22960+/-840	Chatelperronian
La Roche a Pierrot	Ly-2192 21100+/-540	Protoaurignacian
Moulin de Laguenay (La Poissiere)	Ly-18015 26770+/-380	Gravettian
Jean Blancs	Gif-8667 14850+/-130	Badegoulian
Limeuil	Gif-8040 11720+/-110	Badegoulian
Combe Saunière	OxA-486 22100+/-440	Hiatus

Continued on next page

Table 10.8 – continued from previous page

Site	Date	Technocomplex
Combe Saunière	OxA-487 10140+/-120	Hiatus
Gabillou	GifA-95583 17180+/-170	Badegoulian
Flageolet I	OxA-597 24800+/-600	Aurignacian
Combarelles	Ly-3201 11380+/-210	Magdalenian
Cro le Biscop	Ly-3392 18510+/-470	Chatelperronian
Cro Magnon	Beta-157439 27680+/-270	Aurignacian
Laugerie Basse	GifA-94204 15700+/-150	Magdalenian
Les Marseilles	Gif-5386 12500+/-250	Magdalenian
Les Marseilles	Gif-5387 13850+/-160	Magdalenian
Pataud	GrN-5012 26050+/-310	Gravettian
Pataud	GrN-6392 22730+/-160	Gravettian
Lascaux	GrN-1182 8510+/-100	Magdalenian
Lascaux	GrN-1514 8060+/-75	Magdalenian
Lascaux	GrN-1632 17190+/-140	Magdalenian
Lascaux	GrN-3184 9070+/-90	Magdalenian

Continued on next page

Table 10.8 – continued from previous page

Site	Date	Technocomplex
Lascaux	Ly-1196 7510+/-650	Magdalenian
Lascaux	Ly-1197 8660+/-360	Magdalenian
Lascaux	Sa-102 16100+/-500	Magdalenian
La Rochette	GifA-95455 1610+/-80	Aurignacian
Caminade	GifA-97185 37200+/-1500	Aurignacian
La Ferrassie (Abri)	Gif-2428 15180+/-130	Aurignacian
Castanet	GifA-97312 34800+/-1100	Aurignacian
La Madeleine	GifA-95457 10190+/-100	Magdalenian
Roc de Marcamps	Ly-3148 11910+/-230	
Beauregard	Ly-2700 12370+/-220	Magdalenian
Lespaux	Ly-3308 10580+/-210	Gravettian
Gandil	Ly-3591 16060 +/- 80	
Montgaudier	BM-2307 18090 +/- 650	Magdalenian
Chaire-à-Calvin	Ly-1998 15440+/-440	Magdalenian
Chaire-à-Calvin	OxA-12053(LYON-2098) 16 020 +/- 80	

Continued on next page

Table 10.8 – continued from previous page

Site	Date	Technocomplex
Roc de Sers	Gif-3609 19230+/-300	
Roc de Sers	Gif A-97329 17090+/-160	Solutrean
Le Placard	Gif-8962 19680+/-180	Badegoulian
Les Garennes	Beta-216143 28520+/-230	Gravettian
Le Raysse (Fouillade)	Ly-2783 23630+/-480	Aurignacian
Le Raysse (Fouillade)	Ly-2782 25000+/-660	Gravettian
Puyjarrige	Ly-2279 19310+/-790	Aurignacian
Esclauzur (Esclauzure)	Ly-361 14540+/-300	Magdalenian
Moulin de Laguenay (La Poissiere)	Ly-360 11330 +/- 480	
La Truffiere	Beta 156643 25120+/-120	
La Truffiere (Cussac)	Beta 156644 15750+/-50	
Combe Saunière	OxA-482 26290+/-800	Magdalenian
Combe Saunière	OxA-768 14260+/-200	Magdalenian
Combe Saunière	OxA-770 14770+/-200	Magdalenian
Combe Saunière	OxA-6507 34000+/-850	Aurignacian

Continued on next page

Table 10.8 – continued from previous page

Site	Date	Technocomplex
Combe Saunière	OxA-6503 35900+/-1100	Chatelperronian
Combe Saunière	OxA-6503 38100+/-1000	Chatelperronian
Combe Saunière	OxA-6504 33000+/-900	Chatelperronian
Combarelles	Ly-3202 13680+/-210	Magdalenian
Commarque	Ly-2154 13370+/-340	Magdalenian
Commarque	Ly-2355 12760+/-200	Magdalenian
Pataud	OxA-688 19700+/-350	Aurignacian
Pataud	GrN-6390 26330+/-230	Gravettian
Pataud	GrN-6391 22670+/-160	Gravettian
Vignaud	Ly-3761 24220+/-360	Aurignacian
Lascaux	C-406 15516+/-900	Magdalenian
Lascaux	GifA-95582 18600+/-190	Magdalenian
Caminade	GifA-97186 35400+/-1100	Aurignacian
Caminade	GifA-97187 34140+/-990	Aurignacian
Caminade	GrN-1491 29100+/-300	Aurignacian

Continued on next page

Table 10.8 – continued from previous page

Site	Date	Technocomplex
Castanet	GifA-97313 35200+/-1100	Aurignacian
Camiac	Ly-1104 35100+/-2000	Early Upper Pal
Moulin Neuf	Ly-2352 13570+/-260	Magdalenian
Roc de Combe	Gif-6304 23900+/-330	Gravettian
Pégourié	Ly-3851 8390+/-690	Azilian
Combe Cullier (Crozo Gentillo)	Ly-978 15030+/-330	Magdalenian
Graves	Gif-3518 9900+/-180	Azilian
Graves	Gif-7340 11360+/-120	
Les Fieux	Gif-1807 9450+/-190	Sauvettarian
Les Fieux	Gif-4281 9060+/-190	Sauvettarian
Roc de Cave	GifA-95048 11210+/-140	
Borie del Rey	Ly-1402 9870+/-320	Azilian
Borie del Rey	Ly-1401 10350+/-340	Azilian
Le Martinet	Ly-1605 12600+/-1100	Magdalenian
Le Martinet	Ly-5069 14100+/-240	Magdalenian

Continued on next page

Table 10.8 – continued from previous page

Site	Date	Technocomplex
Roc Allan	7625+/-80	Mesolithic
Roc Allan	Ly-4545 8160+/-90	Mesolithic
La Magdeleine La Plaine	Ly-1109 11180+/-300	
La Magdeleine La Plaine	GifA-96345 13680+/-130	Magdalenian
Le Courbet (les Forges)	Ly-1175 10110+/-440	Azilian
Le Courbet (les Forges)	BM-302 11750+/-300	Magdalenian
Le Courbet (les Forges)	BM-303 11110+/-160	Magdalenian
Le Courbet (les Forges)	GifA-90169 13400+/-260	Magdalenian
Le Courbet (les Forges)	GifA-90170 13490+/-260	Magdalenian
Le Courbet (les Forges)	GifA-97311 13380+/-120	Magdalenian
Le Castellas	Ly-2251 26550+/-700	
Grotte XVI	GifA-94201 29710 +/- 510	Aurignacian
Laugerie Haute	GifA-100631 19550+/-340	
Vidon	Ly-2701 14000+/-350	Magdalenian
Le Morin	Gif-2105 10480+/-200	Magdalenian

Continued on next page

Table 10.8 – continued from previous page

Site	Date	Technocomplex
Fongaban	Ly-977 14300+/-680	Magdalenian
Pille Bourse (Saint Germain la Rivière)	GifA-95456 15780+/-200	Magdalenian
Pille Bourse (Saint Germain la Rivière)	Ly-614 15510+/-120	Magdalenian
Pille Bourse (Saint Germain la Rivière)	Ly-614 31300 +/- 1800	
Jaurias (Bisqueytan)	Ly-3730 13580+/-140	Magdalenian
Jaurias (Bisqueytan)	Gd-2693 13500+/-200	
Jaurias (Bisqueytan)	Gd-2697 14660+/-200	
Lespaux	Ly-3307 17450+/-780	Gravettian
Moulin Neuf	Ly-2275 14280+/-440	Magdalenian
Moulin Neuf	Ly-2699 13380+/-250	Magdalenian
Conduché	Ly-2693 12040+/-160	Magdalenian
Pech de Cavaniès	Ly-1717 12150+/-60	
Les Peyrugues	GifA-95447 17660 +/- 160	Badegoulian
La Bergerie de Saint Géry	20000+/-300	
Pégourié	Ly-3852 12160+/-200	Azilian

Continued on next page

Table 10.8 – continued from previous page

Site	Date	Technocomplex
Pégourié	Ly-3932 8050+/-120	Azilian
Pégourié	Ly-3933 10710+/-290	Azilian
Gandil	Gif A-92385 16950+/-360	Magdalenian
Gandil	Gif A-93238 16070+/-160	Magdalenian
La Plantade	GifA-94184 14020+/-140	Magdalenian
La Plantade	GifA-94185 15890+/-160	Magdalenian
La Plantade	GifA-96326 12740+/-120	Magdalenian
Lafaye	GifA-95047 15290+/-150	Magdalenian
Montastruc	BM-304 12070+/-180	Magdalenian
Montastruc	GifA-963346 13020+/-130	Magdalenian
Fontalès	GifA 96327 13140+/-120	Azilian
Les Eyzies	BM-2285 11600+/-380	Magdalenian
Les Eyzies	BM-2286 12590+/-980	Magdalenian

Bibliography

A. Achilli, C. Rengo, C. Magri, V. Battaglia, S. Olivieri, R. Scozzari, F. Cruciani, M. Zeviani, E. Briem, V. Carelli, P. Moral, J-M. Dugoujon, U. Roostalu, E-L. Loogväli, T. Kivisild, H-J. Bandelt, M. Richards, R. Villems, A.S. Santachiara-Benerecetti, O. Semino, and A. Torroni. The Molecular Dissection of mtDNA Haplogroup H Confirms that the Franco-Cantabrian Glacial Refuge was a Major Source for the European Gene Pool. *American Journal of Human Genetics*, 75:910–18, 2005.

M. Allard and F. Juillard. Le Paléolithique Supérieur de l'abri des Peyrugues, à Orniac (Lot). *Bulletin de la Societé Meridionale de Spéléologie et Préhistoire*, XXVIII:33–43, 1988.

A.J. Ammerman and L.L. Cavalli-Sforza. *The Neolithic Transition and the Genetics of Populations in Europe*. Princeton University Press: Princeton, 1984.

K.K. Andersen, A. Svensson, S.J. Johnsen, S.O. Rasmussen, M. Bigler, R. Röthlisberger, U. Ruth, M.L. Siggaard-Andersen, J.P. Steffensen, D. Dahl-Jensen, B.M. Vinther, and H.B. Clausen. The Greenland Ice Core Chronology 2005, 1542 ka. Part 1: Constructing the Time Scale. *Quaternary Science Reviews*, 25(23-24): 3246 – 3257, 2006.

J.R. Arnold and W.F. Libby. Age Determinations by Radiocarbon Content: Checks with Samples of Known Age. *Science*, 110:678–680, 1949.

J.R. Arnold and W.F. Libby. Radiocarbon Dates. *Science*, 113:111–120, 1951.

J. E. Aura, V. Villaverde, M.G. Morales, C.G. Sainz, J. Zilhão, and L.G. Straus. The Pleistocene-Holocene Transition in the Iberian Peninsula: Continuity and Change in Human Adaptations. *Quaternary International*, 49/50:87–103, 1998.

W.E. Banks. Eco-cultural Niches of the Badegoulian: Unravelling Links between Cultural Adaptation and Ecology during the Last Glacial Maximum in France. *Journal of Anthropological Archaeology*, 30:359–374, 2011.

E. Barron, T.H. van Andel, and D. Pollard. Glacial Environments II: Reconstructing the Climate of Europe in the Last Glaciation. In T.H. van Andel and W. Davis, editors, *Neanderthals and Modern Humans in the European Landscape during the Last Glaciation: Archaeological Results of the Stage 3 Project*, pages 57–78. Cambridge: Cambridge University Press, McDonald Institute Monographs, 2003.

C. M. Barton and A. E. Cohen G.A. Clark. Art as Information: Explaining Upper Palaeolithic Art in Western Europe. *World Archaeology*, 26(2):185–207, 1994.

M.J. Baxter, C.C. Beardah, and R.V.S. Wright. Some Archaeological Applications of Kernel Density Estimates. *Journal of Archaeological Science*, 24(4):347 – 354, 1997.

A. Bayliss. Rolling Out Revolution: Using Radiocarbon Dating in Archaeology. *Radiocarbon*, 51:123–147, 2009.

L. Binford. *Constructing Frames of Reference: An Analytical Method for Archaeological Theory Building Using Hunter-Gatherer and Environmental Data Sets.* Berkeley: University of California Press, 2001.

L.R. Binford. Willow Smoke and Dogs' Tails: Hunter-Gatherer Settlement Systems and Archaeological Site Formation. *American Antiquity*, 45(1):4–20, 1980.

J.B. Birdsell. Some Environmental and Cultural Factors Influencing the Structuring of Australian Aboriginal Populations. *American Society of Naturalists*, 87(834):171–207, 1953.

P.G. Blackwell and C.E. Buck. The Late Glacial Human Reoccupation of North-Western Europe: New Approaches to Space-Time Modelling. *Antiquity*, 77(296): 232–240, 2003.

R. Blanchard, D. Peyrony, and H.V. Vallois. *Le Gisement et le Squelette de Saint-Germain-la-Rivière*. Paris:Masson, 1972.

S.P.E. Blockley, C.S. Lane, M. Hardiman, S.O. Rasmussen, I.K. Seierstad, J.P. Steffensen, A. Svensson, A.F. Lotter, C.S.M. Turney, C. Bronk Ramsey, and INTIMATE members. Synchronisation of Palaeoenvironmental Records Over the Last 60,000 years, and an Extended INTIMATE Event Stratigraphy to 48,000 b2k. *Quaternary Science Reviews*, (36):2–10, 2012.

P.T. Bobrowsky and B.F. Ball. The Theory and Mechanics of Ecological Diversity in Archaeology. In R.D. Leonard and G.T. Jones, editors, *Quantifying Diversity in Archaeology*, pages 4–12. Cambridge: Cambridge University Press, 1989.

J-P. Bocquet-Appel. Personal communication, 2010.

J-P. Bocquet-Appel and P-Y. Demars. Neanderthal contraction and modern human colonization in Europe. *Antiquity*, 74:544–52, 2000.

J-P. Bocquet-Appel and A. Truffeau. Technological Responses of Neanderthals to Macroclimatic Variations (240,000 - 40,000 BP). In J. Steele and S. Shennan, editors, *Human Biology: The International Journal of Population Genetics and Anthropology*, pages 287–308. American Association of Anthropological Genetics, 2009.

J-P. Bocquet-Appel, P-Y. Demars, L. Noiret, and D. Dobrowsky. Estimates of Upper Palaeolithic Meta-population Size in Europe from Archaeological Data. *Journal of Archaeological Science*, 32:1656–1668, 2005.

M.A. Boden. What is creativity? In S. Mithen, editor, *Creativity in Human Evolution and Prehistory*, pages 22–60. London: Routledge, 1998.

F. Bordes. Nouvelles Fouilles à Laugerie-Haute Est: Premiers Resultants. *l'Anthropologie*, 62:205–244, 1958.

F. Bordes. Circonscription d'Aquitaine. *Gallia préhistoire*, 13(13–2):485–511, 1970.

F. Bordes and D. de Sonneville-Bordes. The Significance of Variability in Palaeolithic Assemblages. *World Archaeology*, 2:61–73, 1970.

E. Boserup. *The Conditions of Agricultural Growth.* London: Allen and Unwin, 1965.

J. Bouchud. Étude de la faune de l'Abri Pataud. In H. Movius, editor, *Excavation of the Abri Pataud, Les Eyzies (Dordogne)*, pages 69–153. Cambridge: Peabody Museum, Harvard University, 1975.

J.M. Bouvier. Nouvelle Diagnose Stratigraphique du Gisement Éponyme de La Madeleine (Tursac, Dordogne). *Académie des Sciences Paris*, 277:26–28, 1973.

M. Brennan. *Health and Disease in the Middle and Upper Palaeolithic of Southwestern France. A Bioarchaeological Study.* PhD thesis, New York: New York University, 1991.

H.M. Bricker, A.S. Brooks, B. Clay, and N. David. Les Fouilles de H.L. Movius Jr. à l'abri Pataud: Génèralités. In H.M. Bricker, editor, *Le Paléolithique Superièur de l'Abri Pataud (Dordogne): Les Fouilles de H.L. Movius Jr.*, pages 11–29. Paris: Document d'Archaeologie Francçais 50, 1995.

James A. Brown. Long-Term Trends to Sedentism and the Emergence of Complexity in the American Midwest. In T.D. Price and James A. Brown, editors, *Prehistoric Hunter-Gatherers: The Emergence of Cultural Complexity*, pages 201–231. Orlando: Academic Press, 1985.

B. Buchanan, M. Collard, and K. Edinborough. Paleoindian Demography and the Extraterrestrial Impact Hypothesis. *Proceedings of the National Academy of Sciences*, 105(33):1651–11654, 2008.

C.E. Buck, W.G. Cavanagh, and C.D. Litton. *Bayesian Approach to Interpreting Archaeological Data*. Chester: John Wiley and Sons, 1996.

R. Burleigh, M. Leese, and M. Tite. An Intercomparison of Some AMS and Small Gas Counter Laboratories. *Radiocarbon*, 28(2A):571–577, 1986.

W.J. Burroughs. *Climate Change in Prehistory*. Cambridge: Cambridge University Press, 2005.

A. Leroi-Gourhan. Translated by A. Michelson. The Religion of the Caves: Magic or Metaphysics? *October Magazine*, 37:6, 1986.

R.L. Cann, M. Stoneking, and A.C. Wilson. Mitochondrial DNA and Human Evolution. *Nature*, 325(6099):31–36, 1987.

J-C Castel. Économie de Chasse et d'Exploitation de l'Animal au Cuzoul de Vers (Lot) au Solutréen et au Badegoulian. *Bulletin de la Société Préhistorique Française*, 100 (1):41–65, 2003.

L.L. Cavalli-Sforza and M.W. Feldman. *Cultural Transmission and Evolution: A Quantitative Approach*. Princeton: Princeton University Press, 1981.

A. Chamberlain. *Demography in Archaeology*. Cambridge University Press: Cambridge, 2006.

F. Champagne and R. Espitalié. La Stratigraphie du Piage. Note Préliminaire. *Bulletin de la Société Préhistorique Française*, 64(1):29–34, 1967.

F. Champagne and R. Espitalié. *Le Piage, Site Préhistorique du Lot*. Paris: Mémoires de la Société Préhistorique Francaise Tome 15, 1981.

R.C. Chiverrell, R.C. Thorndycraft, and T.O. Hoffmann. Cumulative Probability Functions and their Role in Evaluating the Chronology of Geomorphological Events during the Holocene. *Journal of Quaternary Science*, 26(1):76–85, 2011.

P.U. Clark, A.S. Dyke, J.D. Shakun, A.E. Carlson, J. Clark, B. Wohlfarth, J.X. Mitrovica, S.W. Hostetler, and A.M. McCabe. The Last Glacial Maximum. *Science*, 325 (5941):710–714, 2009.

J. Clottes and J-P. Giraud. Le Gisement Préhistoriques du Cuzoul (Vers, Lot). *Quercy Recherche*, 65/66:82–91, 1989.

J. Clottes and J-P. Giraud. Solutréens et Badegouliens au Cuzoul de Vers (Lot). In *La vie préhistoriques*, pages 256–261. Paris: Faton, Dijon, et Société Préhistorique Francaise, 1996.

M.N. Cohen. *The Food Crisis in Prehistory: Overpopulation and the Origins of Agriculture*. New Haven : Yale University Press, 1979.

M. Collard, K. Edinborough, S. Shennan, and M.G. Thomas. Radiocarbon Evidence Indicates that Migrants Introduced Farming to Britain. *Journal of Archaeological Science*, 37(4):866 – 870, 2010.

C. Collins. A Palaeodemographic Investigation into Upper Palaeolithic Population Dynamics in Southwest France. Master's thesis, Cambridge University, 2008.

N.J. Conard, P.M. Grootes, and F.H. Smith. Unexpectedly Recent Dates for Human Remains from Vogelherd. *Nature*, 430:198–201, 2004.

M. Conkey. The Identification of Prehistoric Hunter-Gatherer Aggregation Sites: The Case of Altamira. *Current Anthropology*, 21:609–30, 1980.

H. Craig. Carbon 13 in Plants and the Relationships between Carbon 13 and Carbon 14 Variations in Nature. *The Journal of Geology*, 62:115–149, 1954.

C. Cretin. Vers une Nouvelle Perception du Badegoulien des Jamblancs: Premiers Éléments Techno-Économiques. *Paléo*, 8:243–268, 1996.

M-T. Cuzange, E. Delque-Kolic, T. Goslar, P.M. Grootes, T. Higham, E. Kaltnecker, M-J. Nadeau, C. Oberlin, M. Paterne, J. van der Plicht, C.B. Ramsey, H. Valladas,

J. Clottes, and J-M. Geneste. Radiocarbon Intercomparison Program for Chauvet Cave. *Radiocarbon*, 49(2):339–347, 2007.

W. Dansgaard, S.J. Johnsen, H.B. Clausen, D. Dahl-Jensen, N.S. Gundestrup, C.U. Hammer, C.S. Hvidberg, J.P. Steffensen, A.E. Sveinbjornsdottir, J. Jouzel, and G. Bond. Evidence for General Instability of Past Climate from a 250-kyr Ice-Core Record. *Nature*, 364:218–220, 1993.

NGRIP dating group. *Greenland Ice Core Chronology 2005 (GICC05) 60,000 Year, 20 Year Resolution*. NOAA/NGDC Paleoclimatology Program, Boulder CO, 2008.

N. David and H.M. Bricker. Perigordian and Noaillian in the Greater Périgord. In O. Soffer, editor, *The Pleistocene Old World: Regional Perspectives*, pages 237–250. New York: Plenum, 1987.

N.C. David. On Upper Palaeolithic Society, Ecology and Technological Change: The Noaillian Case. In C. Renfrew, editor, *The Explanation of Culture Change*, pages 277–303. Duckworth: London, 1973.

D. de Sonneville-Bordes. *Le Paléolithique Supérieur en Périgord*. Bordeaux: Delmas, 1960.

D. de Sonneville-Bordes. Les industries du Roc-de-Combe (Lot). Périgordien et Aurignacien. *Bulletin Préhistoire du Sud-Ouest*, 9:121–161, 2002.

H. Delporte. Le Gisement Paléolithique de la Rochette (Commune de Saint-Léon-sur-Vézère, Dordogne). *Gallia préhistoire*, 5(1):1–22, 1962.

H. Delporte. Les niveaux Aurignaciens de La Rochette. *Bulletin de la Societé d'études et de Recherches Préhistoriques*, 13:1–24, 1964.

H. Delporte. Étude générale, industrie, et statuette. *Gallie préhistoire*, 11:1–112, 1968.

H. Delporte, editor. *Le Grand Abri de la Ferrassie: Fouilles 1968-1973*. Éditions

du Laboratoire de Paléontologie Humaine et de Préhistoire. Études Quaternaires, Géologie, Paléontologie, Préhistoire, Mémoire no. 7, 1984.

P-Y. Demars. Démographie et Occupation de l'Espace au Paléolithique Supérieur et au Mésolithique en France. *Préhistoire Européenne*, 8:3–26, 1996.

P-Y. Demars. Les Rapports de l'Homme et du Mileu dans le Nord de l'Aquitaine au Paléolithique Supérieur l'Implantation des Habitats. *Bulletin Préhistoire du Sud-Ouest, Nouvelles Études*, 5(1):13–30, 1998.

P-Y. Demars and P. Laurent. *Types d'Outils Lithiques du Paléolithique Supérieur en Europe*. Paris: Éditions de CNRS, 1992.

L. Detrain, M. Guillon, B. Kervazo, S. Madelaine, A. Morala, and A. Turq. Le Moulin du Roc à Saint-Chamassy (Dordogne). Résultats Préliminaire. *Bulletin de la Société Préhistorique Française*, 93(1):43–48, 1996.

J. Diamond. The worst mistake in the history of the human race. *Discover Magazine*, May:64–66, 1987.

J. Diamond. *Guns, Germs and Steel: A Short History of Everybody for the Last 13,000 years*. London: Vintage, 1997.

M. Douglas. Population Control in Primitive Groups. *The British Journal of Sociology*, 17(3):263–273, 1966.

V. Dujardin. Les Pins, les Renardières (Niveaux Paléolithiques). Fouille Programmée Pluriannuelle 2000-2002. Rapport Intermédiaire. 2001.

R.I.M. Dunbar. Neocortex Size as a Constraint on Group Size in Primates. *Journal of Human Evolution*, 22(6):469–493, 1989.

R.G. Fairbanks, R.A. Mortlock, T-C. Chiu, L. Cao, A. Kaplan, T.P. Guilderson, T.W. Fairbanks, A.L. Bloom, P.M. Grootes, and M-J. Nadeau. Radiocarbon Calibration

Curves Spanning 0-50,000 BP based on $^{230}Th/^{234}U/^{238}U$ and ^{14}C Dates on Pristine Corals. *Quaternary Science Reviews*, 24:1781–1796, 2005.

R. Farbstein. Technologies of Art: A Critical Reassessment of Pavlovian Art and Society, Using *Châine Opératoire* Method and Theory. *Current Anthropology*, 52(3): 401–432, 2011.

W. Farrand. Etude Sédimentologique du Remplissage de l'Abri Pataud. In H.M. Bricker, editor, *Le Paléolithique Supérieur de l'Abri Pataud (Dordogne): Les Fouilles de H.L. Movius Jr*, pages 31–65. Paris: Documents d'Archeologie Francais 50, 1995.

P. Fitte and D. Sonneville-Bordes. Le Magdalénien VI de la Gare de Couze, Commune de Lalinde (Dordogne). *l'Anthropologie*, 66:216–246, 1962.

Ø. Flagstad and K. H. Røed. Refugial Origins of Reindeer *Rangifer tarandus* Inferred from Mitochondrial DNA Sequences. *Evolution*, 2003.

K. Flannery. Origins and Ecological Effects of Early Domestication in Iran and the Near East. In P.J. Ucko and G.W. Dimbleby, editors, *The Domestication and Exploitation of Plants and Animals*, pages 73–100. Chicago:Aldine, 1969.

C. Fourloubey. Badegoulien et Premiers Temps du Magdalénien. Un Essai de Clarification à l'aide d'un Exemple, la Vallée de l'Isle en Périgord. *Paléo*, 10:185–209, 1998.

S J Gale and P G Hoare. The Stratigraphic Status of the Anthropocene. *The Holocene*, 2012. doi: 10.1177/0959683612449764.

C. Gamble. *The Palaeolithic Settlement of Europe*. Cambridge: Cambridge University Press, 1986.

C. Gamble. *The Palaeolithic Societies of Europe*. Cambridge University Press : Cambridge, 2002.

C. Gamble, W. Davies, P. Pettitt, L. Hazelwood, and M. Richards. Archaeological and Genetic Foundations of the European Population during the Late Glacial: Implications for 'Agricultural Thinking'. *Cambridge Archaeological Journal*, 15(2):193–223, 2005.

N.H.H. Graburn and B.S. Strong. *Circumpolar Peoples: An Anthropological Perspective*. Goodyear: California, 1973.

B. Gravina, P. Mellars, and C. Bronk Ramsey. Radiocarbon Dating of Interstratified Neanderthal and Early Modern Human Occupations at the Chatelperronian Type-Site. *Nature*, 438:51–56, 2005.

M.. Grove. A Spatio-Temporal Kernel Method for Mapping Changes in Prehistoric Land-Use Patterns. *Archaeometry*, 53(5):1012–1030, 2011.

J. Halverson, L.H. Abrahamian, K.M. Adams, P.G. Bahn, L.T. Black, W. Davis, R. Frost, R. Layton, D. Lewis-Williams, A.M. Llamazares, P. Maynard, and D. Stenhouse. Art for Art's Sake in the Paleolithic. *Current Anthropology*, 28:63–89, 1987.

H.C. Harpending, M.A. Batzer, M. Gurven, L.B. Jorde, A.R. Rogers, and S.T. Sherry. Genetic Traces of Ancient Demography. *Proceedings of the National Academy of Sciences*, 95:1961–1967, 1998.

O. Hauser. *Le Périgord Préhistorique: Guide pour les Excursions dans les Vallées de la Vézère et de la Dordogne et pour l'Étude de leur Stations Préhistoriques*. 1911.

B. Hayden, B. Chisholm, and H.P. Schwarz. Fishing and Foraging: Marine Resources in the Upper Palaeolithic of France. In O. Soffer, editor, *The Pleistocene Old World: Regional Perspectives*, pages 279–291. New York: Plenum, 1987.

M. Hays. *A Functional Analysis of the Magdalenian Lithic Assemblage from Grotte XVI (Dordogne, France)*. PhD thesis, University of Tennessee, 1998.

J. Henrich. Demography and Cultural Evolution. How Adaptive Cultural Processes can Produce Maladaptive Losses: The Tasmanian Case. *American Antiquity*, 69(2): 197–214, 2004.

J. Henrich. The Evolution of Innovation-Enhancing Institutions. In M. J. O'Brien and S.J. Shennan, editors, *Innovation in Cultural Systems: Contributions from Evolutionary Anthropology*, pages 99–120. Cambridge: MIT Press, 2010.

D.O. Henry. Preagricultural Sedentism: The Natufian Example. In T.D. Price and J.A. Brown, editors, *Prehistoric Hunter-Gatherers: The Emergence of Cultural Complexity*, pages 365–384. Orlando: Academic Press, 1985.

G. Hewitt. The Genetic Legacy of the Quaternary Ice Ages. *Nature*, 405:907–913, 2000.

B.S. Hewlett and L.L. Cavalli-Sforza. Cultural Transmission Among Aka Pygmies. *American Anthropologist*, 88(4):922–934, 1986.

T. Higham. Personal communication, 2010.

T. Higham, R. Jacobi, M. Julien, F. David, L. Basell, R. Wood, W. Davies, and C.B. Ramsey. Chronology of the Grotte du Renne (France) and implications for the context of ornaments and human remains within the Chatelperronian. *Proceedings of the National Academy of Science*, 107(47):20234–20239, 2010.

T. Higham, T. Compton, C. Stringer, R. Jacobi, B. Shapiro, E. Trinkhaus, B. Chandler, F. Gröning, C. Collins, S. Hillson, P. O'Higgins, C. Fitzgerald, and M. Fagan. The Earliest Evidence for Anatomically Modern Humans in Northwestern Europe. *Nature*, 479:521–524, 2011a.

T. Higham, R. Jacobi, L. Basell, C. Bronk Ramsey, L. Chiotti, and R. Nespoulet. Precision Dating of the Palaeolithic: A New Radiocarbon Chronology for the Abri Pataud (France), a Key Aurignacian Sequence. *Journal of Human Evolution*, 61: 549–563, 2011b.

T.F.G. Higham, R.M. Jacobi, and C. Bronk Ramsey. AMS Radiocarbon Dating of Ancient Bone using Ultrafiltration. *Radiocarbon*, 48(2):179–195, 2006.

M. Jochim. Palaeolithic Cave Art in Ecological Perspective. In G. Bailey, editor, *Hunter-Gatherer Economy in Prehistory*, pages 212–219. Cambridge: Cambridge University Press, 1983.

M. Jochim. Late Pleistocene Refugia in Europe. In O. Soffer, editor, *The Pleistocene Old World: Regional Perspectives*, pages 317–333. New York: Plenum Press, 1987.

M.A. Jochim. *Hunter-Gatherer Landscape: Southwest Germany in the Late Paléolithic and Mesolithic*. New York: Plenum, 1998.

M.A. Jochim. The Upper Palaeolithic. In S. Milisauskas, editor, *European Prehistory: A Survey*, pages 55–114. New York: Plenum, 2002.

E.L. Jones. Subsistence Change, Landscape Use, and Changing Site Elevation at the Pleistocene-Holocene Transition in the Dordogne of Southwest France. *Journal of Archaeological Science*, 34:344–353, 2007.

G. Judkins, M. Smith, and E. Keys. Determinism within Human-Environment Research and the Rediscovery of Environmental Causation. *The Geographical Journal*, 174:1, 2008.

M. Julien. Les Harpons Magdaléniens. *Gallia Préhistoire*, XVIIe supplément, 1982.

L.H. Keeley. Hunter-Gatherer Economic Complexity and 'Population Pressure': A Cross-Cultural Analysis. *Journal of Anthropological Archaeology*, 7:373–411, 1988.

C.D. Keeling. The Suess Effect: ^{13}Carbon-^{14}Carbon Interrelations. *Environment International*, 2:229–300, 1979.

K.W. Kintigh. Sample Size, Significance, and Measures of Diversity. In R.D. Leonard and G.T. Jones, editors, *Quantifying diversity in archaeology*, pages 25–36. Cambridge: Cambridge University Press, 1989.

T.A. Koetje. Simulated Archaeological Levels and the Analysis of Le Flagéolet II, the Dordogne, France. *Journal of Field Archaeology*, 18(2):187–198, 1991.

J. Labrot and F. Bordes. La Stratigraphie du Gisement de Roc de Combe (Lot) et ses Implications. *Bulletin de la Société preéhistorique française. Études et travaux*, 64 (H-S):15–28, 1964.

E. Larsen, H.P. Sejrup, S.J. Johnsen, and K.L. Knudsen. Do Greenland Ice Cores Reflect NW European Interglacial Climate Variations? *Quaternary Research*, 43: 125–132, 1995.

D.O. Larson. Innovation, Replicative Behaviour, and Evolvability: Contributions from Neuroscience and Human Decision-Making Theory. In M.J. O'Brien and S.J. Shennan, editors, *Innovation in Cultural Systems: Contributions from Evolutionary Anthropology*, pages 69–80. 2010.

H. Laville and J-P. Rigaud. The Perigordian V Industries in Périgord: Typological Variations, Stratigraphy and Relative Chronology. *World Archaeology*, 4(3):330–338, 1973.

H. Laville, J-P Rigaud, and James Sackett. *Rock Shelters of the Périgord: Geological Stratigraphy and Archaeological Sucession*. London: Academic Press, 1980.

R.B. Lee and I. DeVore. *Man the Hunter*. Chicago: Aldine, 1968.

M. Lenoir. Les Grattoirs-Burins du Morin et du Roc de Marcamps (Gironde). *Bulletin de la Société Préhistorique Française*, 75(3):73–82, 1978.

D. Lewis-Williams. *The Mind in the Cave*. London: Thames and Hudson, 2002.

W.F. Libby. Atmospheric Helium Three and Radiocarbon from Cosmic Radiation. *Physical Review*, 69(11–12):671–672, 1946.

M. Lorblanchet, F. Delpech, P. Renault, and C. Andrieux. La Grotte de Sainte-Eulalie à Espagnac (Lot). *Gallia préhistoire*, 16(16–2):233–325, 1973.

T.R. Malthus. *An Essay on the Principle of Population*. Dent, 1798.

F.W. Marlowe. Hunter-gatherers and human evolution. *Evolutionary Anthropology*, 14: 54–67, 2005.

G. Mazière. Abri de la Doue: Commune de Saint-Cernin-de-Larche (Corrèze). Etat des Recherches. *Bulletin de la Société d'Anthropologie du Sud-Ouest*, XIX(1):41–55, 1984.

G. Mazière and J-P. Raynal. Gisement de 'Chez Jugie' près Cosnac (corrèze): Campagne de Fouilles 1976. *Société des Lettres, Sciences et Arts de la Correèze*, LXXX: 29–41, 1977.

P. Mellars. The Character of the Middle-Upper Palaeolithic Transition in South-West France. In C. Renfrew, editor, *The explanation of culture change: Models in prehistory*, pages 255–276. London: Duckworth, 1973.

P. Mellars. The Ecological Basis of Social Complexity in the Upper Palaeolithic of Southwest France. In T.D. Price and J.A. Brown, editors, *Prehistoric Hunter-Gatherers: The Emergence of Social Complexity*, pages 271–297. Orlando: Academic Press, 1985.

P. Mellars. *The Neanderthal Legacy: An Archaeological Perspective of Western Europe*. Princeton: Princeton University Press, 1995.

P. Mellars and J.C. French. Tenfold Population Increase in Western Europe at the Neanderthal-to-Modern Human Transition. *Science*, 333(6042):623–627, 2011.

P.A. Mellars. The Impossible Coincidence. a Single-Species Model for the Origins of Modern Human Behavior in Europe. *Evolutionary Anthropology: Issues, News, and Reviews*, 14(1):12–27, 2005.

P.A. Mellars. Archaeology and the Dispersal of Modern Humans in Europe: Deconstructing the Aurignacian. *Evolutionary Anthropology*, 2006.

G. Miller. Sexual Selection for Cultural Displays. In R. Dunbar, C. Knight, and C. Power, editors, *The Evolution of Culture: An Interdisciplinary View*, pages 71–91. Edinburgh: Edinburgh University Press, 1999.

S.J. Mithen. *Thoughtful Foragers: A Study of Prehistoric Decision Making*. Cambridge: Cambridge University Press, 1990.

H. L. Movius. *Excavation of the Abri Pataud Les Eyzies (Dordogne)*. Harvard: Peabody Museum of Archaeology and Ethnology, 1975.

L. Nagaoka. Using Diversity Indices to Measure Changes in Prey Choice at the Shag River Mouth Site, Southern New Zealand. *International Journal of Osteoarchaeology*, 11:101–111, 2001.

R. Naroll. Floor area and settlement population. *American Antiquity*, 27:587–589, 1962.

M.J. O'Brien, J. Darwent, and R. Lee Lyman. Cladistics is Useful for Reconstructing Archaeological Phylogenies: Palaeoindian Points from the Southeastern United States. *Journal of Archaeological Science*, 28:1115–1136, 2001.

I.U. Olsson. Radiocarbon Dating History: Early Days, Questions, and Problems Met. *Radiocarbon*, 51(1):1–43, 2009.

J. Orshiedt. Datation d'un Vestige Humain Provenant de la Rochette (Saint Léon-sur-Vézère, Dordogne) par la Méthode du Carbone 14 en Spectrométrie de Masse. *Paléo*, 14:239–240, 2002.

L. Pereira, M. Richards, A. Goios, A. Alonso, C. Albarran, O. Garcia, D.M. Behar, M. Golge, J. Hatina, L. Al-Gazali, D.G. Bradley, V. Macauley, and A. Amorim. High-resolution mtDNA Evidence for the Late-Glacial Resettlement of Europe from an Iberian Refuge. *Genome Research*, 15:19–24, 2005.

P. Pettitt. *The Palaeolithic Origins of Human Burial*. Abingdon: Routledge, 2011.

P. Pettitt, W. Davies, C.S. Gamble, and M.B. Richards. Palaeolithic Radiocarbon Chronology: Quantifying our Confidence Beyond Two Half-Lives. *Journal of Archaeological Science*, 30(12):1685–1693, 2003.

D. Peyrony. Les Industries Aurignaciennes dans le Bassin de la Vézère. *Bulletin de la Société Préhistorique Française*, 30:543–559, 1933.

D. Peyrony. La Ferrassie (Moustérien, Périgordien, Aurignacien). *La Préhistoire*, III: 1–92, 1934.

D. Peyrony and E. Peyrony. *Laugerie Haute près des Eyzies (Dordogne)*. Paris: Masson, Archives de l'Institut de Paléontologie humaine, No. 19, 1938.

A. Pike-Tay, V. Cabrera Valdés, and F. Bernaldo de Quirós. Seasonal Variations of the Middle-Upper Palaeolithic Transition at El Castillo, Cueva Morín and El Pendo (Cantabria, Spain). *Journal of Human Evolution*, 36:283–317, 1999.

H. Plisson and J-M. Geneste. Le Solutréen de la Grotte de Combe Saunière I (Dordogne): Premère Approche Palethnologique. *Gallia Préhistoire*, 29:9–27, 1986.

A. Powell, S. Shennan, and M.G. Thomas. Late Pleistocene Demography and the Appearance of Modern Human Behavior. *Science*, 324:1298–1301, 2009.

A. Powell, S.J. Shennan, and M.G. Thomas. Demography and Variation in the Accumulation of Culturally Inherited Skills. In M.J. O'Brien and S.J. Shennan, editors, *Innovation in Cultural Systems: Contributions from Evolutionary Anthropology*, pages 137–160. Cambridge: MIT press, 2010.

T.D. Price. The Mesolithic of western Europe. *Journal of World Prehistory*, 1(3): 225–305, 1987.

C. Bronk Ramsey. Combination of dates, oxcal online manual, 2005a. URL `c14.arch.ox.ac.uk/oxcal3/archl`.

C. Bronk Ramsey. Radiocarbon calibration and analysis of stratigraphy: The oxcal programme. *Radiocarbon*, 37(2):425–430, 2005b.

C. Bronk Ramsey. Dealing with outliers and offsets in radiocarbon dating. *Radiocarbon*, 51(3):1023–1045, 2009a.

C. Bronk Ramsey. Bayesian analysis of radiocarbon dates. *Radiocarbon*, 51:337–360, 2009b.

D.E. Reich and D.B. Goldstein. Genetic Evidence for a Paleolithic Human Population Expansion in Africa. *Proceedings of National Academy of Science*, 95:8119–8123, 1998.

P.J. Reimer, M.G.L. Baillie, E. Bard, A. Bayliss, J.W. Beck, P.G. Blackwell, C. Bronk Ramsey, C.E. Buck, G.S. Burr, R.L. Edwards, M. Friedrich, P.M. Grootes, T.P. Guilderson, I. Hajdas, T.J. Heaton, A.G. Hogg, K.A. Highen, K.F. Kaiser, B. Kromer, F.G. McCormac, S.W. Manning, R.W. Reimer, D.A. Richards, J.R. Southon, S. Talamo, C.S.M. Turney, J. van der Plicht, and C.E. Weyhenmeyer. Intcal09 and Marine09 Radiocarbon Calibration Curves, 0-50,000 Years Cal BP . *Radiocarbon*, 51(4):1111–1150, 2009.

C. Renard. Continuity or Discontinuity in the Late Glacial Maximum of South-Western Europe: the Formation of the Solutrean in France. *World Archaeology*, 43(4):726–743, 2011.

C. Renfrew. The Sapient Behaviour Paradox: How to Test for Potential? In P. Mellars and K. Gibson, editors, *Modelling the Early Human Mind*. Cambridge: Cambridge University Press, 1996.

C. Renfrew. All the King's Horses: Assessing Cognitive Maps in Later Prehistoric Europe. In S. Mithen, editor, *Creativity in Human Evolution and Prehistory*, pages 260–284. London: Routledge, 1998.

M. Richards, H. Corte-Real, P. Forster, V. Macauley, H. Wilkinson-Herbots, A. Demaine, S. Papiha, R. Hedges, H-J. Bandelt, and B. Sykes. Paleolithic and Neolithic Lineages in the European Mitochondrial Gene Pool. *American Journal of Human Genetics*, 59:185–203, 1996.

M.P. Richards and E. Trinkaus. Isotopic Evidence for the Diets of European Neanderthals and Early Modern Humans. *Proceedings of the National Academy of Sciences*, 106(38):16034–16039, 2009.

M.P. Richards, P.B. Pettitt, M.C. Stiner, and E. Trinkaus. Stable Isotope Evidence for Increasing Dietary Breadth in the European Mid-Upper Palaeolithic. *Proceedings of the National Academy of Sciences*, 98(11):6528–6532, 2001.

M.P. Richards, R. Jacobi, J. Cook, P.B. Pettitt, and C.B. Stringer. Isotope Evidence for the Intensive use of Marine Foods by Late Upper Palaeolithic humans. *Journal of Human Evolution*, 49:390–394, 2005.

P.J. Richerson, R. Boyd, and R.L. Bettinger. Cultural Innovations and Demographic Change. In J. Steele and S. Shennan, editors, *Human Biology: International Journal of Population Genetics and Anthropology*, pages 211–235. American Association of Anthropological Genetics, 2009.

J.W. Rick. Dates as Data: An Examination of the Peruvian Preceramic Radiocarbon Record. *American Antiquity*, 52(1):55–73, 1987.

J-P. Rigaud. Note Preliminaire de la Stratigraphie du Gisement du 'Flageolet I' (Commune de Bezenac, Dordogne). *Bulletin de la Sociétè Prehistorique Française*, 66(3): 73–75, 1969.

J-P. Rigaud. Étude préliminaire des industries magdaléniennes de l'abri du Flageolet II, commune de Bézenac (Dordogne). *Bulletin de la Société préhistorique francaise. Comptes rendus des séances mensuelles*, 67:456–474, 1970.

J-P. Rigaud. Human adaptation to the climatic deterioration of the last Pleniglacial in southwestern France (30,000-20,000). In Wil Roebroeks, M. Mussi, J. Svoboda, and O. Soffer, editors, *Hunters of the Golden Age: The Mid Upper Palaeolithic of Eurasia 30,000-20,000 BP*, pages 325–336. Leiden: University of Leiden, 2000.

J-P. Rigaud. Les industries lithiques du Gravettian du nord de l'Aquitaine dans leur cadre chronologique. *Paléo*, 20:149–166, 2008.

J-P. Rigaud and J.F. Simek. 'Arms too short to box with God': Problems and Prospects for Palaeolithic Prehistory in Dordogne, France. In O.Soffer, editor, *The Pleistocene Old World: Regional Perspectives*, pages 47–62. New York and London: Plenum Press, 1987.

J. Roche. La Grotte du Placard. *Bulletin de l'Association française pout l'étude du quaternaire*, 2(2-3-4):245–250, 1965.

A.R. Rogers. Genetic Evidence for a Pleistocene Population Explosion. *Evolution*, 4: 608–615, 1995.

D. Román and V. Villaverde. The Magdalenian Harpoons from the Iberian Mediterranean, based on Pieces from Cova de les Cendres (Teulada-Moraira, Valencian Region). *Quaternary International*, 2012.

A. Roussot and J. Ferrier. Le Roc deMarcamps (Gironde) : Quelques Nouvelles Observations. *Bulletin de la Société Preéhistorique Française*, 67(H–S):293–303, 1970.

P. Rowly-Conwy. Sedentary Hunters: The Ertebølle Example. In G. Bailey, editor, *Hunter-Gatherer Economy in Prehistory: A European Perspective*, pages 111–126. Cambridge: Cambridge University Press, 1983.

K. Rozanski, W. Stichler, R. Gonfiantini, E.M. Scott, R.P. Beukens, B. Kromer, and J. van der Plicht. The IAEA ^{14}C intercomparison exercise 1990. *Radiocarbon*, 34(3): 506–519, 1992.

B. Sadier, J-J. Delannoy, L. Benedetti, D. Bourles, S. Jaillet, J-M. Geneste, A-E. Lebatard, and M. Arnold. Further constraints on the Chauvet cave artwork elaboration. *Proceedings of the National Academy of Sciences*, 2012. doi: 10.1073/pnas.1118593109.

K. Sbonius. Introduction to Issues in Demography and Survey. In J. Bintliff and K. Sbonius, editors, *Reconstructing Past Population Trends in Mediterranean Europe*, pages 170–204. Oxbow: Oxford, 1999.

E.M. Scott. Part 2: The Third International Radiocarbon Intercomparison (TIRI). *Radiocarbon*, 45(2):293–328, 2003a.

E.M. Scott. Section 3: Preliminary Analysis of the Results. *Radiocarbon*, 45(2):159–174, 2003b.

M-R. Séronie-Vivien. *La Grotte de Pégourié (Caniac-du-Causse, Lot).* Association Préhistoire Quercinoise, 1995.

S. Shennan. Demography and Cultural Innovation: a Model and its Implications for the Emergence of Modern Human Culture. *Cambridge Archaeological Journal*, 11 (1):5–16, 2000.

S. Shennan and K. Edinborough. Prehistoric Population History: from the Late Glacial to the Late Neolithic in Central Europe . *Journal of Archaeological Science*, 34:1339–1345, 2007.

P.E.L. Smith. *Le Solutréen en France.* Publications de l'institut de l'université de Bordeaux: Bordeaux, 1966.

P.E.L. Smith. Changes in population pressure in archaeological explanation. *World Archaeology*, 4(1):5–18, 1972.

O. Soffer. Upper Palaeolithic Connubia, Refugia, and the Archaeological Record from Eastern Europe. In O. Soffer, editor, *The Pleistocene Old World: Regional Perspectives*, pages 333–348. New York: Plenum Press, 1987.

O. Soffer. Gravettian Technologies in Social Contexts. In W. Roebroeks, M. Mussi, J. Svoboda, and O. Soffer, editors, *Hunters of the Golden Age: The Mid Upper Palaeolithic of Eurasia 30,000-20,000 BP*, pages 59–76. Leiden: University of Leiden, 2000.

R.S. Sommer and A. Nadachowski. Glacial Refugia of Mammals in Europe: Evidence from Fossil Records. *Mammal Review*, 36:251–265, 2006.

P. Spikins. Autism, the Integration of 'Difference' and the Origins of Modern Human Behaviour. *Cambridge Archaeological Journal*, 19:179–201, 2009.

M. Spriggs. The Dating of the Island Southeast Asian Neolithic: An Attempt at Chronometric Hygiene and Linguistic Correlation. *Antiquity*, 63:587–613, 1989.

M. Spriggs and A. Anderson. Late Colonisation of East Polynesia. *Antiquity*, 67: 200–217, 1993.

Mary C. Stiner and Natalie D. Munro. Approaches to Prehistoric Diet Breadth, Demography, and Prey Ranking Systems in Time and Space. *Journal of Archaeological Method and Theory*, 9(2):181–214, 2002.

M.C. Stiner, N.D. Munro, and T.A. Surovell. The Tortoise and the Hare: Small-Game Use, the Broad-Spectrum Revolution, and Paleolithic Demography. *Current Anthropology*, 41(1):39–79, 2000.

L.G. Straus. Southwest Europe at the Last Glacial Maximum. *Current Anthropology*, 32(2):189–199, 1991a.

L.G. Straus. Human Geography of the Late Upper Palaeolithic in Western Europe: Present State of the Question. *Journal of Anthropological Research*, 47(2):259–278, 1991b.

T. A. Surovell, J.B. Finley, G. M. Smith, P. J. Brantingham, and R. Kelly. Correcting Temporal Frequency Distributions for Taphonomic Bias. *Journal of Archaeological Science*, 36(8):1715 – 1724, 2009.

T.A. Surovell and P.J. Brantingham. A Note on the Use of Temporal Frequency Distributions in Studies of Prehistoric Demography. *Journal of Archaeological Science*, 34:1868–1877, 2007.

C. Szmidt, V. Laroulandie, M. Dachary, M. Langlais, and S. Costamagnos. Harfang Rene et Cerf : Nouvelles Dates ^{14}C par SMA du Magdalenian Supérieur du Bassin Aquitain au Morin (Gironde) et Bourrouilla (Pyrénées-Atlantiques). *Bulletin de la Société Préhistorique Française*, 106(3):583–587, 2009.

P. Taberlet, L. Fumagalli, A-G. Wust-Saucy, and J-F. Cosson. Comparative Phylogeography and Postglacial Colonization Routes in Europe. *Molecular Evolution*, 7: 453–464, 1998.

M. Tallavaara, P. Pesonen, and M. Oinonen. Prehistoric Population History in Eastern Fennoscandia. *Journal of Archaeological Science*, 37(2):251 – 260, 2010.

R.E. Taylor. *Radiocarbon Dating: An Archaeological Perspective*. London: Academic Press, 1987.

J. Tehrani and M. Collard. Investigating Cultural Evolution through Biological Phylogenetic Analyses of Turkmen Textiles. *Journal of Anthropolological Archaeology*, 4 (2):443–463, 2002.

I. Tëmkin and N. Eldridge. Phylogenetics and Material Cultural Evolution. *Current Anthropology*, 48(1):146–153, 2007.

J-P. Texier. Les dépots du site Magdalénien de Gandil à Bruniquel (Tarn-et-Garonne): dynamique sédimentaire, signification paléoenvironmentale, lithostratigraphique et implications archéologiques. *Paléo*, 9:263–277, 1997.

R. Torrence. Time Budgeting and Hunter-Gatherer Technology. In G. Bailey, editor, *Hunter-Gatherer Economy in Prehistory: A European Perspective*, pages 11–22. Cambridge: Cambridge University Press, 1983.

J-F. Tournepiche. Le Gisement Paléontologique Würmien de la Grotte du Quéroy (Charente). *Bulletin de la Société Préhistorique Française*, 79(4):99, 1982.

H. Valladas, N. Tisnérat-Laborde, H. Cachier, M. Arnold, F. Bernaldo de Quirós, V. Cabrera-Valdés, J. Clottes, J. Courtin, J.J. Fortea-Pérez, and C. Gonzáles-Sainz. Radiocarbon AMS Dates for Palaeolithic Cave Paintings. *Radiocarbon*, 43:977, 2001.

T.H. van Andel and W.D. Davies, editors. *Neanderthals and Modern Humans in the European Landscape of the Last Glaciation: Archaeological Results of the Stage 3 Project*. Cambridge: Cambridge University Press, McDonald Institute Monographs, 2003.

T.H. van Andel, W. Davies, B. Weninger, and O. Joris. Archaeological Dates as Proxies for the Spatial and Temporal Human Presence in Europe: a Discourse on the Method. In T.H. van Andel and W. Davis, editors, *Neanderthals and Modern Humans in the European Landscape during the Last Glaciation: Archaeological Results of the Stage Three Project*, pages 21–30. Cambridge: Cambridge University Press, McDonald Institute Monographs, 2003.

M. Vanhaeren and F. d'Errico. Grave Goods from the Saint-Germain-la-Rivière Burial: Evidence for Social Inequality in the Upper Palaeolithic. *Journal of Anthropological Archaeology*, 24(2):117–134, 2005.

M. Vanhaeren and F. d'Errico. Aurignacian Ethno-linguistic Geography of Europe Revealed by Personal Ornaments. *Journal of Archaeological Science*, 33:1105–1128, 2006.

H.T. Waterbolk. Working with Radiocarbon Dates. *Proceedings of the Prehistoric Society*, 37:15–33, 1971.

E. Weiss, W. Wetterstrom, D. Nadel, and O. Bar-Yosef. The broad spectrum revisited: Evidence from plant remains. *Proceedings of the National Academy of Sciences*, 101: 9551–9555, 2009.

R. White. *Upper Palaeolithic Land Use in the Périgord*. BAR International Series 253. Oxford: BAR, 1985.

R. White. Glimpses of Long-Term Shifts in Late Paleolithic Land Use in the Périgord. In O. Soffer, editor, *The Pleistocene Old World: Regional Perspectives*, pages 263–277. New York: Plenum, 1987.

A.N. Williams. The use of summed radiocarbon probability distributions in archaeology: A review of methods. *Journal of Archaeological Science*, 39:578–589, 2012.

H.M. Wobst. The Archaeo-Ethnology of Hunter-Gatherers or the Tyranny of the Ethnographic Record in Archaeology. *American Antiquity*, 43(2):303–309, 1978.

M. Wobst. Boundary Conditions for Palaeolithic Social Systems: A Simulation Approach. *American Antiquity*, 39(2):147–178, 1974.

G. Woillard. Grand Pile Peat Bog: a Continuous Pollen Record for the Last 140,000 Years. *Quaternary Research*, 9:1–21, 1978.

J. Zilhao, F. d'Errico, J-G. Bordes, A. Lenoble, J-P Texier, and J-P. Rigaud. Analysis of Aurignacian Interstratification at the Chatelperronian Type Site and the Implications for the Behavioral Modernity of Neanderthals. *Proceedings of the National Academy of Science*, 103(33):12643–12648, 2006.

E.B.W. Zubrow. Carrying Capacity and Dynamic Equilibrium in the Prehistoric Southwest. *American Antiquity*, 36(2):127–138, 1971.